

Semi-Rigid Action in Steel Frames

by

Ishtiaque Ahmed

B.Sc., M.Sc.

Thesis Submitted to the University of Sheffield
for the degree of Doctor of Philosophy

The University of Sheffield
Department of Civil and Structural Engineering
August 1992

To my parents

Contents

1	Introduction	1
1.1	General Introduction	1
1.2	Objectives and Scope of the Present Study	3
1.3	Outline of the Thesis	5
2	Literature Review	8
2.1	Introduction	8
2.2	Joint Behaviour and its Representation	9
2.3	Methods of Analysis of Semi-Rigid Frames	10
2.3.1	Modification of the Conventional Methods	11
2.3.2	Computer Analysis of Semi-Rigidly Connected Plane Frames	11
2.4	Behaviour of Members with Semi-Rigid Joints	15
2.5	Design Methods	20
2.5.1	Design of Braced Frames	20
2.5.2	Design of Unbraced Frames	21
2.5.3	Column Design: The Effective Length Approach	21
2.6	Concluding Remarks	27

3	Finite Element Formulation and the Computer Program	36
3.1	Introduction	36
3.2	Formulation of the Semi-Rigid Element	37
3.2.1	Shape Function	38
3.2.2	Strain-Displacement Relationship	40
3.2.3	Element Stiffness Matrix	42
3.3	Evaluation of Sectional Properties	43
3.3.1	Elastic Section	43
3.3.2	Inelastic Section: Spread of Yield	44
3.4	Stress-Strain Relationship	45
3.5	Inclusion of Initial Imperfection	47
3.5.1	Inclusion of Residual Stress	47
3.5.2	Inclusion of Geometric Imperfection	50
3.6	Modelling of the Connection Behaviour	52
3.6.1	Unloading and Reloading of Connection Under Monotonic Loading	52
3.6.2	Connection Behaviour Under Cyclic Loading	53
3.6.3	Connection Offset Effect	54
3.7	Computer Program	55
3.7.1	General Layout of the Program	55
3.7.2	Computing Technique	58
4	Verification of the Computer Program in Non-Sway Mode	77
4.1	Introduction	77
4.2	Load Deflection Analysis	78

4.2.1	Load-Deflection Response of a Perfect and Imperfect System	78
4.2.2	Effect of Increment Size in a Load Deflection Analysis . . .	80
4.3	Behaviour Under Uniformly Distributed Load	81
4.4	Comparison With Full Scale Frame Tests	82
4.4.1	Description of the Test Frames	82
4.4.2	Comparison of the Test Result with the Prediction of the Present Program	85
4.4.3	Limitation of the Comparison	90
4.5	Concluding Remarks	92
5	Verification of the Computer Program in Sway Mode	108
5.1	Introduction	108
5.2	Description of Frame Tests	109
5.2.1	General	109
5.2.2	Choice of Tests for Comparison/Validation Purpose	111
5.3	Analytical Modelling of the Test Frames	111
5.4	Modelling of the Connection Behaviour	112
5.4.1	Connection Data	114
5.5	Comparison of the Test Results and the Analytical Predictions . .	115
5.5.1	Comparison with the Result of Test 1	116
5.5.2	Comparison with the Result of Test 6	118
5.5.3	Comparison with the Result of Test 9	120
5.5.4	Comparison with the Result of Test 10	121
5.6	General Discussion on the Comparison	124
5.7	General Observations for Frames Under Cyclic Loading	125

5.8	Concluding Remarks	126
6	Behaviour of Semi-Rigid Steel Frames	152
6.1	Introduction	152
6.2	Scope of the Parametric Study	153
6.2.1	Connection Details	153
6.2.2	Geometric Dimensions	154
6.2.3	Load Combinations	155
6.2.4	Imperfections	156
6.2.5	Material Properties	156
6.3	Influence of Connection Stiffness on the Behaviour of Frames . . .	157
6.3.1	General	157
6.3.2	Ultimate Capacity of Semi-Rigid Frame	157
6.3.3	Flexible End Moment and Its Distribution to Column Ends	164
6.4	Connection Rotation at Failure	169
6.5	Moment Shedding and the Effect of Initial Geometric Imperfection	171
6.6	Conclusion	177
7	Simplified Design Approach for Non-Sway Semi-Rigid Frames	216
7.1	Introduction	216
7.2	Semi-Rigid Connection Behaviour: Implications for Design	217
7.2.1	General	217
7.2.2	Connection $M-\phi$ Relationship	218
7.2.3	Present State of Information	220
7.2.4	Reliability of Connection Response and Its Implication . .	224

7.2.5	Simplified Representation of the Connection Response: Linearization of the $M-\phi$ Relationship	226
7.2.6	Limitation of the Secant Stiffness Approach	228
7.2.7	Classifying the Joint as Semi-Rigid	229
7.3	Semi-Rigid Action in Non-Sway Frames: Simplified Approach . .	229
7.3.1	General	229
7.3.2	Basis for Semi-Rigid Design	230
7.4	Conclusions	247
8	Conclusions and Recommendations	279
8.1	Summary of Conclusions	280
8.2	Recommendations for Future Work	284
	References	288
	Appendices	303
A	Additional Details of Comparisons with SUF Tests	303
B	Worked Design Examples	309

List of Figures

Chapter 1

- Figure 1.1** *Moment-rotation characteristic of beam-to-column connections: (a) extended end plate; (b) flush end plate; (c) seat and web cleats; (d) flange cleats (e) web cleats.*
- Figure 1.2** *Effect of end restraint on moments and deflections for elastic response.*

Chapter 2

- Figure 2.1** *The beam-joint model for various force components.*
- Figure 2.2** *Various representations of the joint behaviour.*
- Figure 2.3** *Semi-rigid beam-joint element by Cosenza [22].*
- Figure 2.4** *Semi-rigid beam-joint element by Chen and Lui [28].*
- Figure 2.5** *Limited column-subassemblage considered by Rifai [12].*
- Figure 2.6** *Effect of connection stiffness on frame strength [35].*
- Figure 2.7** *Flexibly connected frame analysed by Simitses et al [50].*
- Figure 2.8** *Effective beam stiffness with semi-rigid joints [54].*
- Figure 2.9** *Determination of column effective length [40].*
- Figure 2.10** *Measure of joint stiffness in Driscoll's method [63].*

Chapter 3

- Figure 3.1(a)** *Element degrees of freedom.*
- Figure 3.1(b)** *Deformed shape of a semi-rigidly connected beam-column element.*
- Figure 3.2** *Dividing the cross-section for calculating the properties of the section.*
- Figure 3.3** *Idealised stress-strain relationship of the material.*
- Figure 3.4** *Parabolic distribution of residual stress.*
- Figure 3.5** *Linear pattern of residual stress.*
- Figure 3.6** *Rectangular pattern of residual stress.*

Figure 3.7	<i>Possible local imperfection types.</i>
Figure 3.8	<i>Global geometrical imperfection for frames.</i>
Figure 3.9	<i>Combination of local and global geometrical imperfections.</i>
Figure 3.10	<i>Loading-unloading characteristics of flexible connections.</i>
Figure 3.11	<i>Simplified unloading model for connection.</i>
Figure 3.12	<i>Actual joint versus analytical model.</i>
Figure 3.13	<i>Effect of connection offset [12].</i>
Figure 3.14	<i>Joint offset model [12].</i>
Figure 3.15	<i>Flow-chart for the computer program.</i>
Figure 3.16	<i>Local and global nodal displacements.</i>
Figure 3.17	<i>Newton-Raphson procedure.</i>

Chapter 4

Figure 4.1(a)	<i>Pinned portal used to generate load-deflection response for the column.</i>
Figure 4.1(b)	<i>Load-deflection behaviour of geometrically perfect and imperfect, concentrically loaded column of figure 4.1(a).</i>
Figure 4.1(c)	<i>Pin-ended idealized column with geometric imperfection.</i>
Figure 4.2(a)	<i>Effect of number of load increments in simple incremental technique [85].</i>
Figure 4.2(b)	<i>Effect of increment size in the iterative incremental analyses.</i>
Figure 4.3(a)	<i>Portal frame considered for comparison of the response of the present program with that of the computer program INSTAF [86].</i>
Figure 4.3(b)	<i>Comparison of the load-deflection response for rigid portal of figure 4.3(a).</i>
Figure 4.3(c)	<i>Comparison of the load-deflection response for pinned portal of figure 4.3(a).</i>
Figure 4.4(a)	<i>Description of test frame SUF1.</i>
Figure 4.4(b)	<i>Description of test frame SUF2.</i>
Figure 4.5(a)	<i>Frame bracing locations (in-plane).</i>
Figure 4.5(b)	<i>Frame nomenclature.</i>
Figure 4.6(a)	<i>Initial shape of SUF1.</i>
Figure 4.6(b)	<i>Initial shape of SUF2.</i>
Figure 4.7	<i>$M-\phi$ behaviour of the connections used in the frame tests.</i>
Figure 4.8	<i>Comparison of the beam load-deflection response for SUF1.</i>
Figure 4.9	<i>Comparison of the column (C-7) load-deflection response for SUF1.</i>
Figure 4.10	<i>Comparison of the bending moments around the frame for SUF1.</i>
Figure 4.11	<i>Comparison of the beam load-deflection response for SUF2.</i>
Figure 4.12	<i>Comparison of the load-deflection responses of columns (C1 and C5) for SUF2.</i>
Figure 4.13	<i>Comparison of the bending moments around the frame for SUF2.</i>

Chapter 5

- Figure 5.1** *One-storey frame details.*
- Figure 5.2** *Two-storey frame details.*
- Figure 5.3(a)** *Support arrangement at the column foot.*
- Figure 5.3(b)** *Beam-to-column connections.*
- Figure 5.4** *Trilinear parameters for 1/2 inch connections [89].*
- Figure 5.5** *Trilinear parameters for 1/4 inch connections [89].*
- Figure 5.6** *Finite element idealization for one-storey frame.*
- Figure 5.7** *Finite element idealization for two-storey frame.*
- Figure 5.8** *Load reversal technique.*
- Figure 5.9** *Moncarz's connection trilinearization model [90].*
- Figure 5.10** *M- ϕ hysteresis exhibiting connection model assumptions [80].*
- Figure 5.11** *Analytical connection representation.*
- Figure 5.12** *Connection model response to a general loading history [80].*
- Figure 5.13** *Comparison of the predicted and measured response [80].*
- Figure 5.14** *Comparison of Marley's 1/2 inch connection results with the trilinearized representation of M- ϕ characteristics.*
- Figure 5.15** *Comparison of Marley's 1/4 inch connection results with the trilinearized representation of M- ϕ characteristics.*
- Figure 5.16** *Test load-displacement curve for test-1 [89].*
- Figure 5.17** *Load-deflection response as predicted from the present program for test-1.*
- Figure 5.18** *Comparison of the measured and predicted load-deflection response for the initial four cycles of test-1.*
- Figure 5.19** *Test load-displacement curve for test-6 [89].*
- Figure 5.20** *Load-deflection response as predicted from the present program for test-6.*
- Figure 5.21** *Enlarged plot for the predicted load-deflection response of 5 initial cycles in test-6.*
- Figure 5.22** *Test load-displacement curve for first storey of test-9 [89].*
- Figure 5.23** *Test load-displacement curve for second storey of test-9 [89].*
- Figure 5.24** *Predicted load-deflection response for the first storey of test-9 frame.*
- Figure 5.25** *Predicted load-deflection response for the second storey of test-9 frame.*
- Figure 5.26** *Comparison of the predicted and measured load-deflection response for different cycles of test-9.*
- Figure 5.27** *Comparison of the predicted and measured load-deflection response for the second storey of test-10.*
- Figure 5.28** *Comparison of the predicted and measured load-deflection response for the first storey of test-10.*

- Figure 5.29** *Test load-displacement curve for the first storey of test-10 [89].*
- Figure 5.30** *Test load-displacement curve for the second storey of test-10 [89].*
- Figure 5.31** *Comparison of the first storey load-deflection response between the test result and the analytical prediction assuming the parameters of table 5.3.*
- Figure 5.32** *Comparison of the second storey load-deflection response between the test result and the analytical prediction assuming the parameters of table 5.3.*

Chapter 6

- Figure 6.1** *Moment-rotation relationship of the three connections considered.*
- Figure 6.2** *Frame geometry and designation of the members.*
- Figure 6.3** *Loading types used in the parametric study.*
- Figure 6.4** *Initial geometric imperfections in the column.*
- Figure 6.5** *Column strength curves for two different patterns of residual stress [93].*
- Figure 6.6** *Residual stress pattern used in the study.*
- Figure 6.7** *Frame strength for different conditions (type-A loading).*
- Figure 6.8** *Internal force distribution in column C6 at the end of beam loading phase (ie end of sequence 2).*
- Figure 6.9** *Effect of the presence of residual stress on degradation of stiffness and moment.*
- Figure 6.10** *Effect of imperfection on frame strength for different connection types (type-A loading).*
- Figure 6.11** *Variation of frame strength for different connection types (type-B loading).*
- Figure 6.12** *Variation of frame strength for different connection types (type-D loading).*
- Figure 6.13** *Variation of frame strength for different connection types (type-C loading).*
- Figure 6.14** *Variation of beam moments for frame with flange cleat connections (storey height = 3.6 m).*
- Figure 6.15** *Variation of beam moments for frame with FEP connections (storey height = 3.6 m).*
- Figure 6.16** *Variation of beam moments for frame with EEP connections (storey height = 3.6 m).*
- Figure 6.17** *Influence of relative beam-column connection stiffness on the development of column moment (moment at the end of col. C6 at the end of beam loading phase are shown).*
- Figure 6.18** *Column (C6) end moment for the last three load stages in the*

- sequence-2 (connection type FC).
- Figure 6.19** Column (C6) end moment for the last three load stages in the sequence-2 (connection type FEP).
- Figure 6.20** Column (C6) end moment for the last three load stages in the sequence-2 (connection type EEP).
- Figure 6.21** Effect of connection-stiffness on column moment.
- Figure 6.22** Distribution of beam end moments to columns for flange cleat connection (3.6m storey height).
- Figure 6.23** Deformed shape of the column.
- Figure 6.24** Distribution of beam end moments to the columns for flush end plate connection (3.6m storey height).
- Figure 6.25** Distribution of beam end moments to columns for extended end plate connection (3.6m storey height).
- Figure 6.26** Development of connection rotation with applied load for flange cleat connection.
- Figure 6.27** Development of connection rotation with applied load for flush end plate connection.
- Figure 6.28** Development of connection rotation with applied load for extended end plate connection.
- Figure 6.29(a)** Geometry and loading of Poggi et al's subassemblage [95].
- Figure 6.29(b)** Response of the subassemblage of figure 6.29(a) [95].
- Figure 6.30(a)** Portal frame analysed by Chen [96].
- Figure 6.30(b)** Connection $M - \phi$ behaviour used by Chen [96].
- Figure 6.31(a)** Response of the non-sway frame of figure 6.30(a) for case-1 loading [96].
- Figure 6.31(b)** Response of the non-sway frame of figure 6.30(a) for case-2 loading [96].
- Figure 6.32(a)** Geometry and loading of Chen's frame [96].
- Figure 6.32(b)** Results of study by Chen [96].
- Figure 6.33** Column subassemblage and connection characteristics used by Rifai [97].
- Figure 6.34(a)** Variation of column end moment with column axial load for subassemblage of figure 6.33 – axial column load only [97].
- Figure 6.34(b)** Variation of column end moment with column axial load for subassemblage of figure 6.33 – beam loads present [97].
- Figure 6.35** Column (C6) end moment for different load cases.
- Figure 6.36** Column (C6) end moment for different load cases.
- Figure 6.37** Moment at the centre of column C6.
- Figure 6.38** Moment at the centre of column C6.
- Figure 6.39** Column deformation pattern due to various loading condition.
- Figure 6.40** Loading pattern for tables 6.6 and 6.7.

Chapter 7

- Figure 7.1** Connection moment and rotation.
- Figure 7.2** M – ϕ relationships for connections of tables 7.1 and 7.2.
- Figure 7.3(a)** Available M – ϕ data for flange cleat connections.
- Figure 7.3(b)** Available M – ϕ data for flush end plate connections.
- Figure 7.3(c)** Available M – ϕ data for extended end plate connections.
- Figure 7.4** M – ϕ relationship for the four flange cleat connection of table 7.2.
- Figure 7.5** M – ϕ relationship for the two flange cleat connection of table 7.3.
- Figure 7.6** Range of variation observed in replicated connection test results [110].
- Figure 7.7** Effect of 10% shift in M – ϕ characteristic on beam response [8].
- Figure 7.8** Frame considered for parametric study.
- Figure 7.9(a)** I-shaped subassembly used for column strength determination.
- Figure 7.9(b)** Connection M – ϕ behaviour considered for the subassembly of figure 7.9(a).
- Figure 7.9(c)** Column strength curve for the different connections of figure 7.9(b).
- Figure 7.10** Observation of the semi-rigid moment for a given rotation when using the linear initial tangent stiffness.
- Figure 7.11** Variation of estimated response by a beam line approach for a nonlinear connection M – ϕ behaviour and the linear initial tangent stiffness approximation.
- Figure 7.12** Secant stiffness based on fixed rotation level.
- Figure 7.13** The beam line concept.
- Figure 7.14** Secant stiffnesses based on beam-line.
- Figure 7.15** Semi-rigid connection to different support arrangements.
- Figure 7.16** Secant stiffness representation of the connection ‘B’ and ‘C’ – based on beam line.
- Figure 7.17** Effect of using a secant linear representation of the nonlinear connection behaviour for connection B of figure 7.16.
- Figure 7.18** Effect of using a secant linear representation of the nonlinear connection behaviour for connection C of figure 7.16.
- Figure 7.19** Effect of beam-column-connection stiffness on the effectiveness of semi-rigid behaviour.
- Figure 7.20** Effect of beam-column-connection stiffness on the effectiveness of semi-rigid behaviour.
- Figure 7.21** Effect of beam-column-connection stiffness on the effectiveness of semi-rigid behaviour.
- Figure 7.22** Beam deformation for different support conditions.
- Figure 7.23(a)** Nomenclatures for slope-deflection equation.
- Figure 7.23(b)** Rigid frame joint behaviour for the calculation of δ_{rigid} .
- Figure 7.24** I-shaped subassembly tested by Davison [57].

- Figure 7.25** *CRC column strength curve [93].*
Figure 7.26 *Beam mechanism for semi-rigidly connected beam.*

Chapter 8

- Figure 8.1** *Design chart format for semi-rigid beams.*

Appendix B

- Figure B.1** *Frame considered for example 1.*
Figure B.2 *Bending moment diagram for example 1.*
Figure B.3 *Bending moment diagram for example 2.*
Figure B.4 *Frame considered for example 3.*
Figure B.5 *Bending moment diagram for example 3.*
Figure B.6 *Bending moment diagram for example 4.*

List of Tables

Chapter 2

Table 2.1 *Methods of modelling connection $M-\phi$ data.*

Table 2.2 *Influence of slenderness ratio and residual stress on the effectiveness of end restraint.*

Chapter 3

Table 3.1 *Mode shapes for elements with rigid and semi-rigid ends.*

Chapter 4

Table 4.1 *Comparison of the additional column failure loads for SUF1.*

Table 4.2 *Comparison of the additional column failure loads for SUF2.*

Chapter 5

Table 5.1 *Summary of the tests conducted by Stelmack [89]*

Table 5.2 *Comparison of the controlling deflections between the result of test-6 and the prediction of the present program for the first 5 cycles.*

Table 5.3 *Parameters for the trial models for test-10.*

Chapter 6

Table 6.1 *Range of geometric parameters considered.*

Table 6.2 *Percentage of cases (stage-1) for different levels of failure rotation.*

Table 6.3 *Percentage of cases (stage-2) for different levels of failure rotation.*

Table 6.4 *Percentage of cases (stage-3: 6.0 m beam span) for different levels of*

- failure rotation.
- Table 6.5** *Percentage of cases (stage-3: 7.0 m beam span) for different levels of failure rotation.*
- Table 6.6** *Change of beam and column end moment due to application of column load in the external column.*
- Table 6.7** *Change of beam and column end moment due to application of column load in the central column.*

Chapter 7

- Table 7.1** *Details of FEP and EEP connections shown in figure 7.2.*
- Table 7.2** *Details of flange cleat connections shown in figure 7.2.*
- Table 7.3** *Details of flange cleat connections from reference [108]*
- Table 7.4** *Available connection test results.*
- Table 7.5** *Effect of variation of connection stiffness.*
- Table 7.6** *Member serial sizes and properties used in the analysis.*
- Table 7.7** *Connection stiffness values for the different connections used in analysis.*
- Table 7.8** *Comparison of the secant stiffness values with the tangent stiffness of the nonlinear connection at different load levels.*
- Table 7.9** *Effect of using a linear secant representation of the nonlinear connection $M-\phi$ behaviour.*
- Table 7.10** *Effect of beam and column stiffness in influencing the effectiveness of the connection restraint at working load level (5.0 m span).*
- Table 7.11** *Variation of restraint at different storey levels.*
- Table 7.12** *Prediction of the serviceability deflection.*
- Table 7.13** *Comparison of the test load with the predicted load [57].*
- Table 7.14** *Comparison of the subassembly test load [57] with the predicted load by G-factor approach using k_j^{10} connection stiffness.*
- Table 7.15** *Comparison of the subassembly test load [57] with the predicted load by BS 5950 effective length chart using k_j^{10} connection stiffness.*
- Table 7.16** *Comparison of the frame test load (major axis) [32] with the predicted load by G-factor approach using k_j^{10} connection stiffness.*
- Table 7.17** *Comparison of the frame test load (major axis) [32] with the predicted load by BS 5950 effective length chart using k_j^{10} connection stiffness.*
- Table 7.18** *Comparison of the frame test load (minor axis) [32] with the predicted load by G-factor approach using k_j^{10} connection stiffness.*
- Table 7.19** *Comparison of the frame test load (minor axis) [32] with the predicted load by BS 5950 effective length chart using k_j^{10} connection stiffness.*

Appendix A

- Table A.1** *Loading history in the beams of the test SUF1 [32].*
- Table A.2** *Loading history in the beams of the test SUF2 [32].*
- Table A.3** *Loading history in the beams of the analytical model of SUF1 and SUF2 (B-1 is only for SUF2).*
- Table A.4** *Sectional properties of the members of the test frame [32].*
- Table A.5** *Material properties of the members of the test frames [32].*

ACKNOWLEDGEMENT

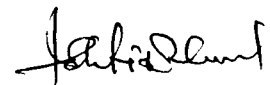
The author wishes to express his sincere indebtedness to Dr. P. A. Kirby, Senior Lecturer in the Department of Civil & Structural Engineering, University of Sheffield, for his continuous guidance, valuable suggestions and affectionate encouragement throughout this study. Thanks are also expressed to the members of the staff in the department for their help and cooperation at different stages.

The author is grateful to the Association of Commonwealth Universities for providing him with the award of a Commonwealth scholarship, which enabled him to conduct this study.

I am indebted to my parents for their understanding, patience and blessings. Finally, truly unbounded thanks are due to Dolly, my wife, and Ishrat, my daughter, for their love and patience which provided me great encouragement to accomplish this study.

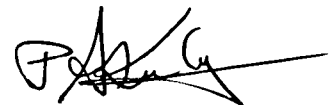
DECLARATION

Except where specific reference has been made to the work of others the work embodied in this thesis is the result of investigation carried out by the author. No part of this thesis has been submitted to any university or other educational establishment for a degree, diploma or other qualification.



Ishtiaque Ahmed

Candidate



Dr. P.A. Kirby

Supervisor

Notation

A	<i>Area of the cross-section</i>
ΔA	<i>Area of the sub-element in the cross-section</i>
A_f	<i>Area of the flange of an I section</i>
A_w	<i>Area of the web of an I section</i>
B	<i>Width of the section</i>
C_{j1}, C_{j2}	<i>Connection stiffnesses at ends 1 and 2 of a beam element</i>
D	<i>Depth of the section</i>
E	<i>Young's modulus of elasticity of steel</i>
F_1, F_2	<i>Applied vertical load in load sequence 1 and 2 respectively</i>
G	<i>AISC G-factor for determining column effective length for rigid frame</i>
G_r	<i>Modified G-factor for determining column effective length for semi-rigid frame</i>
h	<i>Height of a storey</i>
H	<i>Overall height of a frame</i>
I	<i>Second moment of area of a section</i>
I_b, I_c	<i>Second moment of area of a beam and a column section respectively</i>
k_b	<i>Rotational stiffness of a beam</i>
k_c	<i>Rotational stiffness of a column</i>
k_e	<i>Effective length factor</i>
k_j	<i>Linear rotational stiffness of a connection</i>
k_j^{10}	<i>Secant stiffness of a connection based on 10 m rad rotation.</i>
k_0	<i>Initial rotational stiffness of the connection</i>
k_1, k_2, k_3	<i>Rotational stiffnesses in a trilinearized representation of the connection</i>
L	<i>Length of an element or member</i>
L_b	<i>Length of a beam</i>
L_c	<i>Length of a column</i>
M	<i>Moment</i>
M_b	<i>Bending moment at the end of a beam</i>
M_{bl}, M_{br}	<i>Bending moment at the end of a left hand and a right hand beam of any joint</i>
M_c	<i>Connection moment capacity</i>
M_{cu}, M_{cl}	<i>Bending moment at the upper and lower column at a joint</i>
M_E	<i>Beam end moment</i>
M_F	<i>Fixed end moment</i>
M_F^i, M_F^e	<i>Fixed end moment for internal and external end respectively</i>
M_p	<i>Plastic moment capacity of a beam</i>
M_{pc}	<i>Plastic moment capacity of a column</i>
M_{pl}	<i>Connection proportional limit moment</i>
M_r	<i>Beam end moment for rigid frame</i>
M_{sr}	<i>Beam end moment for semi-rigid frame</i>
M_Y	<i>Connection yielding moment</i>

$M-\phi$	Moment-rotation characteristic
N_1 to N_6	Shape functions for the semi-rigid element
\overline{N}_1 to \overline{N}_6	Shape functions for the rigid element
P	Applied vertical load
P_{cr}	Critical load
Q	Applied vertical load
q	Intensity of uniformly distributed load
r	Radius of gyration of the column
T_w	Web thickness
T_f	Flange thickness
u, v	Displacement components in a general point
v_0	Initial displacement at the free end of member
w	Intensity of uniformly distributed load
W	Total uniformly distributed load on a beam

Greek Symbols

α	Angle between the local and global axes
σ	Stress
σ_y	Yield stress
σ_f	Residual stress at the flange tip
σ_{fw}	Residual stress at the junction of the web and flange
σ_w	Residual stress at the web
δ_0	Initial deflection at a specified location in the member.
ε	Strain at a cross section
ϕ	Rotation of connection
θ_j	Rotation of connection
θ_{j1}	Rotation of connection at the beam end 1
θ_{jab}	Rotation of connection at end 'b' due to mode shape 'a'
ψ	Lean angle for global imperfection

Matrices and Vectors

$[B]$	Strain displacement matrix
$[D]$	Elasticity matrix
$[K_E]$	Elastic stiffness matrix based on small deflection theory
$[K_G]$	Geometrical stiffness matrix which depends on the level of axial force

	<i>of the element</i>
$[K_L]$	<i>Large displacement stiffness matrix which depends on the displaced shape of the element</i>
$[K_T]$	<i>Tangential stiffness matrix</i>
$[N]$	<i>Shape function matrix</i>
$\{P_0\}$	<i>Imaginary set of forces simulating initial deflections</i>
$\{\delta\}$	<i>Displacement vector</i>
$\{\delta^*\}$	<i>Initial nodal displacement vector</i>

Abbreviations

<i>AISC</i>	<i>American Institute of Steel Construction</i>
<i>BRE</i>	<i>Building Research Establishment</i>
<i>BS</i>	<i>British Standard</i>
<i>CRC</i>	<i>Column Research Council</i>
<i>EEP</i>	<i>Extended end plate connection</i>
<i>FC</i>	<i>Flange cleat connection</i>
<i>FEP</i>	<i>Flush end plate connection</i>
<i>PR</i>	<i>Partially restrained</i>
<i>SUF1, SUF2</i>	<i>Sheffield University Frames 1 and 2 respectively</i>
<i>cm</i>	<i>Centi metre</i>
<i>kN</i>	<i>Kilo Newton</i>
<i>kip</i>	<i>4.4482 kN</i>
<i>m</i>	<i>Metre</i>
<i>mm</i>	<i>Milli metre</i>
<i>m rad</i>	<i>Milli radian</i>

SUMMARY

This research work is aimed at the development of simplified methods for the design of semi-rigid steel frames. It is now widely appreciated that if the inherent stiffnesses possessed by the commonly used beam-to-column connections can be included in the design practice, the resulting structure will be more economical compared to those designed using the conventional 'simple' or 'rigid' frame assumption.

Keeping the above objective in mind, an existing finite element computer program dealing with a column subassemblage has been modified to facilitate a behavioural study of flexibly connected steel frames. This ultimate strength analysis program has the following features:

1. Includes material nonlinearity (including gradual spread of yield over the cross section).
2. Includes geometric nonlinearity (initial stress and initial strain effects)
3. Full connection nonlinearity is taken into account
4. Initial member imperfections (both material and geometric) are considered
5. Includes cyclic loading-unloading behaviour of connections

The prediction of this program has been validated against available analytical and experimental results. The results of two non-sway full scale frame tests and four sway frame tests loaded cyclically, have been simulated. Good agreement have been found between the test result and predicted behaviour.

After the necessary validation, this program has been used for a limited parametric study and general conclusions regarding the behaviour of non-sway flexibly connected frames have been made. The main obstacles in the development of a semi-rigid design method have been identified. Observations from the case studies have been collated with the findings of other researchers to develop simplified methods to incorporate the semi-rigid joint action in the design of non-sway semi-rigid frames. Examples have been worked and the results compared with those obtained from rigorous analyses to demonstrate the validity of the simplified approach.

Finally, general conclusions have been made and recommendations for further research work have been put forward.

Chapter 1

Introduction

1.1 General Introduction

Many multistorey steel frame structures are designed on the assumption that the connections operate in shear only. Although there is a general consensus that many of these simple shear joints have the ability to transmit significant moments, this ability is seldom utilised in design. The reason for this is the absence of specific guide-lines and design aids to permit continuity of these so called simple connections to be incorporated in design.

The leading codes of practice [1,2] recognize three basic types of beam-to-column connections. Two of these types are the commonly designated 'rigid frame' and 'simple frame' construction and the third is the 'semi-rigid frame' (partially restrained) which assumes that connections between beams and columns possess a dependable and known moment capacity and are intermediate in degree between the rigidity of the rigid frame and the flexibility of the simple frame.

The assumption that the so called simple beam-column connections are incapable of transmitting moments is not a realistic one [3,4,5]. All common forms of beam-to-column connection possess some degree of rotational stiffness. Figure 1.1 presents the moment-rotation characteristics of some common beam-to-column connections. The true response of an ideal rigid and an ideal pin connection would coincide with the vertical and the horizontal axis respectively of figure 1.1. The actual response of any practical connection would be in between these two extremes — and would be more appropriately categorized as semi-rigid.

Figure 1.2 illustrates the effect of end restraint on the behaviour of the member under uniformly distributed load. In simple design, the beam would be designed to carry a moment of $wl^2/8$ at its midspan. If it were perfectly fixed at ends, the design moment would be $wl^2/12$ at the supports. For a semi-rigid connection, the end and span moments are somewhat in between these conditions. Depending on the stiffness of the connection, the reduction in the midspan moment below the simply supported value can lead to useful savings in beam weight. Furthermore, the ratio of the midspan deflection for simply supported and fully fixed beams is 5:1 (see figure 1.2) indicating that the potential for reductions in deflection as a result of semi-rigid action is greater than that in design moments. This is particularly important since serviceability rather than strength is often the controlling limit state. Similar economies are also achievable in the case of columns, because of better end restraint. It has been claimed [3] that weight savings of more than 11 percent can be achieved in the case of columns alone if realistic connection stiffness is considered in design; savings as high as 20 percent in the case of beams in frames are also demonstrated [6]. Similar economies have also been established elsewhere [7,8,9]. It should be emphasized that these are net savings, since no change in construction practices is required. However, the sav-

ings due to the use of lighter member in case of a rigid frame design are sometimes offset by the requirement for the complete joint rigidity. With a comprehensive semi-rigid design approach the same joint as that used for simple design can be utilized, the benefits arising because some allowance is made for the restraining moment at the end of the beams which would otherwise have been neglected in simple design. The research to explore the behaviour of flexible connections was started in early twentieth century when Wilson and Moore [10] first investigated the response of riveted connections. To date, many researchers have contributed to a better understanding of connection restraint and its influence on the behaviour of beam and column frames. However, detailed dependable methods for designing beams and columns with semi-rigid joints are still not available in the leading codes of practice. To realise the potential structural economies of including the beneficial effects of semi-rigid construction, design guide-lines suitable for straightforward use by engineers are required.

1.2 Objectives and Scope of the Present Study

The main aim of this research work is to produce simplified design guide-lines for the semi-rigid construction. Fundamental to the fulfilment of this objective is the availability of well coded analysis programs or other tools capable of modelling the physical problem in an efficient and accurate way so as to enable a systematic study to be conducted. Such tools should ideally be able to handle the various sources of nonlinearities, imperfections and a wide range of loading conditions. A reasonably high level of confidence in predicting the physical behaviour is an essential prerequisite which must also be satisfied. This can be achieved by substantiating the predicted behaviour against the experimental evidence.

At the University of Sheffield, a finite element computer program was developed by Jones [11] to investigate the in-plane behaviour of a non-sway isolated column with its ends connected to infinitely rigid supports by means of flexible connections. Rifai [12] later developed a computer program to include the effect of beam flexibility for the analysis of non-sway column subassemblages – subjected only to loads parallel to the column. The subassemblage in this case consists of one column and four beams with provision for semi-rigid joints at both the ends of the column. Material and geometric nonlinearities were included in the formulation and geometric as well as material imperfections were catered for. The use of limited subassemblages to study the response of individual members of the frame was arguably popular because of the economic advantages in modelling the problem and the capabilities of readily available computers at that time. However, the interaction of a number of local and global parameters may sometimes vitiate the subassemblage method to reflect the true behaviour of the overall frame action. The other program available in Sheffield to analyse flexibly connected frames was SERVAR, developed by Poggi [13] in Milan, Italy. This finite element program can analyse any skeletal structure with flexible connections. Though it is a well coded program, it has following limitations:

1. The nonlinear terms in the strain-displacement relationship have been neglected.
2. Neither geometric nor material imperfections can be taken into consideration.
3. Column bending about major axis only was considered.
4. A piecewise linear representation of the connection moment-rotation behaviour was assumed.

Recognising the suitability of Rifai's formulation it was decided to implement it for the analysis of two dimensional behaviour of flexibly connected steel frames in order to meet the objectives stated in the preceding paragraph.

The resulting finite element analysis program permits the prediction of the deformation history and the ultimate load(s) under a set of proportional, patterned or cyclic loads both in non-sway and sway modes. The analysis is based on a tangent stiffness formulation of a beam element with three degrees of freedom per node. Deterioration of the strength and stiffness of the material, connections and frame under increasing load are all catered for by using an incremental Newton-Raphson iterative procedure. Material and geometric imperfections both at local and global level, can be considered. Different constitutive relations such as elastic, elastic-plastic with or without strain-hardening can be used.

The response of this program has been validated against the results of two non-sway full scale frame tests under monotonic loading and four frame tests in a cyclically loaded sway condition. A limited parametric study has been conducted and general conclusions regarding the behaviour of flexibly connected frames have been made. Observations made from this study, together with those of other researchers, have been collated to aid the development of simplified method of semi-rigid frame design.

1.3 Outline of the Thesis

Each of the individual chapters in this thesis is concerned with a specific area and is presented sequentially to the achievement of the stated objectives of this research work. A brief description of the contents of each chapter follows:

Chapter 2 presents a review of the related research work in the field of semi-rigid frames. Emphasis was given to the analytical work and to the development of design methods.

In chapter 3, the basic formulation of the analytical model has been described. Implementation of the various aspects of the program are also discussed.

The validation in the non-sway mode is presented in chapter 4. Comparisons with established analytical, numerical and experimental results are made.

Chapter 5 describes the implementation of an algorithm of connection behaviour in a cyclic sway mode. Validation of the program under cyclic lateral load history is shown in this chapter by comparing predictions against four half-scale test results.

In chapter 6, a behavioural study of flexible frames has been presented for a range of controlling parameters. The various implications for the semi-rigid design are identified.

It has been already mentioned that the main objective of this study was to develop methods of semi-rigid design which could be utilised by the practising engineers. To this aim, chapter 7 provides some simplified approaches to the semi-rigid frame design in the non-sway situation.

Finally chapter 8 summarizes the general conclusions from this study and also identifies the topics which warrant further investigation for a decisive conclusion to be reached. In order to facilitate fellow researchers, these aspects have been collated in this final chapter as recommendations for future studies.

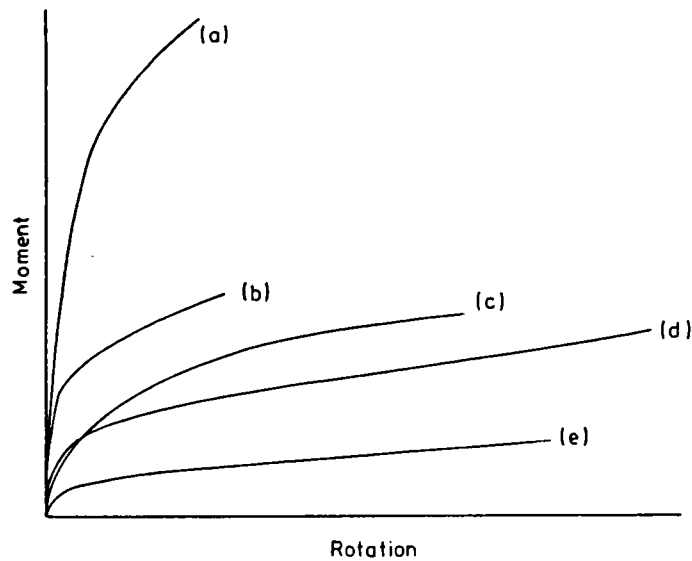


Figure 1.1 Moment-rotation characteristic of beam-to-column connections: (a) extended end plate; (b) flush end plate; (c) seat and web cleats; (d) flange cleats (e) web cleats.

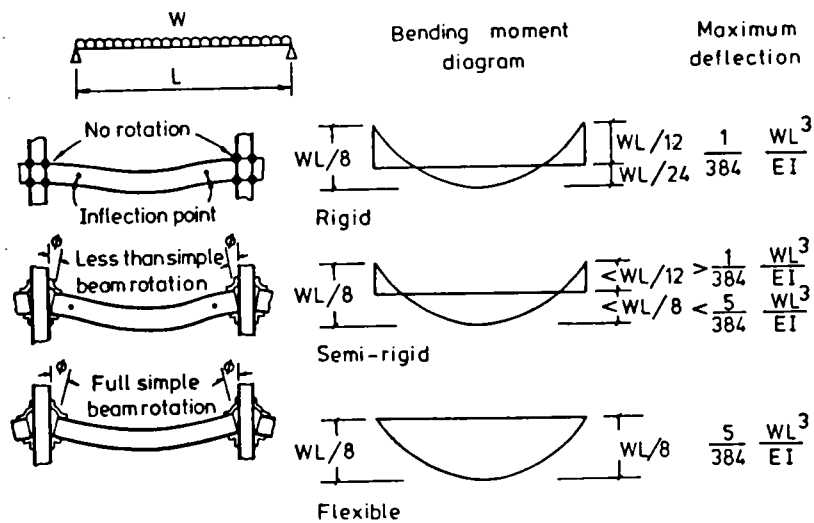


Figure 1.2 Effect of end restraint on moments and deflections for elastic response.

Chapter 2

Literature Review

2.1 Introduction

The true behaviour of structural frames lies between the two extreme cases of joint response; the first being pinned, commonly referred to as ‘simple construction’ and the second is rigid leading to ‘continuous construction’. Considerable research over the years has shown clearly that actual joints exhibit characteristics over a wide spectrum between these two extremes. Structural frames with such joint behaviour are classified under the heading of semi-rigid. In this chapter a brief review of the previous work on semi-rigid joints, with particular emphasis on the resulting member behaviour due to semi-rigid action, will be made. The discussion in this chapter will be grouped into the following four categories:

1. Joint behaviour and its representation
2. Methods of analysis of semi-rigid frames

3. Behaviour of members with semi-rigid joints

4. Design methods

2.2 Joint Behaviour and its Representation

Numerous investigations into the behaviour of beam-to-column connections have been reported during the past sixty years or so. The flexural behaviour of a connection is best represented by the relationship between M , the moment transmitted through the connection, and ϕ , the relative rotation of the two members fastened by the connection. Most of the popular forms of connections such as web cleats, flush end plates, extended end plates etc. show a nonlinear relationship of M - ϕ over virtually the whole range [14]. In order to include the effect of a semi-rigid connection in analysis, it is important to model the connection M - ϕ behaviour mathematically so that a reasonable estimate of the rotational stiffness of the connection at any level of moment can be made.

Attempts to model connection moment-rotation response mathematically have been made by different researchers. These are summarized in tabular form in table 2.1 [15], which also includes the relative advantages and disadvantages of each model. It appears that the cubic B-spline represents the experimental data points of connection M - ϕ relationship most closely and provides the rotational stiffness at any level of load most accurately. Jones [11] pointed out that the polynomial representation may lead to erroneous slope of the M - ϕ curve, which is of utmost importance in any analysis.

In addition to the approach which seeks to mathematically represent

the experimentally obtained connection behaviour (the $M-\phi$ relationship), attempts have also been made to develop methods for the prediction of $M-\phi$ curves. Such attempts include the use of simplified analytical, behavioural or mechanical models to full numerical models using a finite element approach.

Nethercot and Zandonini [16] provide an in-depth summary of all such methods currently available. It has, however, been observed that the ability to predict the moment-rotation curve with good accuracy is rather limited. This situation, coupled with the fact that test data for the full range of connection parameters are not usually readily available to the designer, presents a severe handicap for semi-rigid frame design to become a viable design alternative. Thus further research is needed in the near future to bridge this gap.

2.3 Methods of Analysis of Semi-Rigid Frames

Although joint behaviour has long been recognised as an important parameter influencing frame response, the traditional concept of frame analysis by either pin or rigid joint assumptions still dominates design practice. As mentioned earlier, although the leading codes of practice recognize the possibility of semi-rigid action in frames, along with the two idealized extreme cases of pin and fully rigid connections, simplified methods of analysing frames with such semi-rigid connections are still not available to the designer. The subject has been under investigation by many researchers in the recent past. Attempts to include semi-rigid joint action in the analysis include a wide range of work; from modification of traditional methods of analysis of rigid frames to the formulation of classical finite element models. A brief review of this work is made in the following sections.

2.3.1 Modification of the Conventional Methods

As long ago as 1942, the slope deflection equations were used to represent members with semi-rigid joints at ends by modifying the co-efficients of the usual rigid case [17]. The procedure is otherwise the same as the conventional slope deflection method. The modified moment distribution method also follows the same procedure as the conventional one, with the only difference being that different distribution and carry over factors are used with semi-fixed end moments. The other basic methods like the Method of Three Moments and the Deformeter Methods have also been modified to take account of the semi-rigid nature of the beam-column connections and are described in detail in the reference.

In all of these modifications a linear connection stiffness was assumed, which is taken as the initial slope of the connection $M-\phi$ curve. Considering the very nonlinear nature of the $M-\phi$ curve, this simplification, however, remains a formidable shortcoming.

2.3.2 Computer Analysis of Semi-Rigidly Connected Plane Frames

The application of computers has made it possible to represent the joint behaviour in a more refined and accurate manner. Most approaches to the analysis of semi-rigid frames have been developed with one or other of the two basic philosophies: i) by introducing one or more discrete spring elements [18,19,20,21,22] to simulate the joint response (see figure 2.1). Each of these springs can be assigned a predetermined force-displacement relation representing the axial, shear and flex-

ural behaviour of the joint. Any type of constitutive law can, in principle, be assumed: linear elastic, nonlinear elastic or inelastic (see figure 2.2). However, research studies have shown that, for rectilinear frames, flexural behaviour of the joint is the most significant one.

ii] by directly modifying the member stiffness relationships to account for the partial rotational restraining effect of the connections [23,24,25,26].

The former approach has the disadvantage that the total number of degrees of freedom required to model the deformed configuration of the structure increases significantly. These approaches, because of their dependence on the availability of computers, are more suitable for an academic setting than day-to-day design office practice. The main features of some of the important developments in the recent years are discussed here.

Ackroyd [18] developed a computer program for the analysis of flexibly connected steel frames. Based on a secant stiffness formulation, this development accounts for both material and geometric nonlinearities including loading and unloading capabilities of nonlinear connection $M-\phi$ behaviour.

Cosenza, De Luca and Failla [22] also developed a computer program which utilizes the stiffness method of analysis and includes second order effects. Semi-rigid joints were modelled as extra elements consisting of short rigid segments and springs with axial, shear and rotational stiffnesses (see figure 2.3). Many alternative approaches for representing the connection $M-\phi$ relationship have been considered. The behaviour of multistorey flexibly connected frames has been studied using this program and it was concluded that the use of stiffer connections increases the critical load for the frame.

Anderson and Lok[27] developed a method of analysis to incorporate

the influence of connection flexibility into the analysis of plane frames. Second order effects were considered in this elastic analysis procedure. In the analysis the rotations at any connections except real pins are initially assumed to be zero. Using conventional rigid frame analysis, the displacement and rotations are calculated and hence the member end reactions are obtained using slope deflection equations. Connection $M-\phi$ characteristics are then used to assess connection rotations and these are used to amend the applied load vector. Using this new vector of applied loads, a new vector of displacements and thus new member end reactions are obtained. The procedure is repeated until the convergence is achieved. The stiffness matrix at each iteration is kept unchanged and thus a saving in computer time is achieved.

Chen and Lui [28] employed the stiffness method in which the element matrices were derived on the basis that an element with two semi-rigid joints at its ends is treated as a sub-structure. The sub-structure consists of three sub-elements : two joint elements and one beam-column element (see figure 2.4). Stability functions derived by Chen [20] were used to account for the presence of axial forces in the beam-column elements and an incremental iterative type of analysis was used. The $M-\phi$ data for the connections were represented by an exponential function.

Poggi and Zandonini [29] report the development of a program [13] by modifying the program developed by Corradi and Poggi [30] to include the effect of semi-rigid joints. In this program $M-\phi$ data for the connection was modelled by a series of straight lines. It is based on small deflection theory —which obviously affects its performance for the analysis of flexibly connected sway frames, where the occurrence of large displacements is commonly encountered. This analysis

program includes neither material nor geometrical imperfections and is capable of handling column bending about the major axis only.

Lee [23] developed a large-displacement inelastic formulation based on the secant stiffness approach for the limit load analysis of planar frames with partially restrained connections. It has been claimed that, as opposed to the tangent stiffness approach, the use of a secant stiffness approach allows the use of an increment size large enough to limit the required number of iteration cycles for convergence. The analytical approach is based on the slope-deflection method in which the equilibrium equations are written with respect to the deformed shape of the structure [31] and involves the use of stability functions to reflect the effect of member axial forces exactly.

Jones [11] developed a computer program to trace the load deflection behaviour of an isolated column with semi-rigid joints up to its failure load. This finite element program includes both geometric and material nonlinearities. The column was assumed to be connected to infinitely rigid beams through semi-rigid joints (ie beam stiffness were not included). A nonlinear $M-\phi$ relationship was utilised. Jones was the first to use the B-spline technique to model the connection $M-\phi$ relationship. He concluded that even the most flexible connections may improve the buckling load of the column considerably.

Following Jones' work, Rifai [12] developed a program to analyse a beam-column subassembly (figure 2.5). This finite element formulation again considers both geometric and material nonlinearities; the influence of residual stresses and geometric imperfections is included. This program can only handle subassemblies of the fixed shape shown in figure 2.5. He concluded that the stiffness of the beam and the performance of the joint stiffness both influ-

ence the restraint for the column. The accuracy of the program was verified by experimental work undertaken by Davison [32].

Anderson et al [33] extended a computer program originally developed by Majid and Anderson [34] and based on the matrix-displacement method of analysis to include the effect of semi-rigid connections which are treated as elastic hinges. The nonlinear $M-\phi$ curve is idealised as piece-wise linear relations and successive estimates are made of the secant stiffness of each connection as the iteration proceeds.

The methods of analysis mentioned here are only a few selected from a much higher number of available techniques which vary in their level of refinement and in their capability to simulate full physical behaviour accurately.

2.4 Behaviour of Members with Semi-Rigid Joints

Numerous studies on the behaviour of members with semi-rigid joints have been carried out throughout the world. Only a selective mention is made here to demonstrate how frame behaviour is affected by connection flexibility.

Ackroyd and Gerstle [35] studied a range of realistic building frames to determine the effects of nonlinear beam-to-column connections and inelastic member instability. Simple subassemblages from the frames were analyzed by computer, and the results were represented in terms of two non-dimensional parameters, Ψ and p , as shown in figure 2.6. The following conclusions were drawn from study:

1. Excess connection stiffness, can in exceptional cases, cause a reduction in the ultimate capacity of the flexibly connected steel frames due to premature column yielding due to gravity moments.
2. The parameter Ψ appears to be a reliable index for determining the susceptibility of a frame to increases or decreases in the factor of safety against collapse due to changes in connection stiffness, where Ψ is given by:

$$\Psi = \frac{I_G}{I_c} \frac{\ell}{h} \frac{P_2 \ell}{M_w + Qh} \frac{k_0}{\frac{EI_G}{t}} \left(\frac{r}{h}\right)^2 \quad (2.1)$$

where,

Ψ = non – dimensional structure/ loading parameter

E = Young's modulus of elasticity

I_c & I_G = moment of inertia of the column and the girder respectively

M_w = column top wind moment on subassemblage

P_1 = ultimate vertical load acting at top of each column

P_2 = ultimate girder mid – span load on subassemblage

Q = column top wind shear on subassemblage

h = storey height

r = radius of gyration of the column

k_0 = initial tangent stiffness of flexible connection

ℓ = bay span

and

$$p = \text{non – dimensional frame capacity} = \frac{(P_1 + 0.5P_2)}{P_{cr}}, \text{ where } P_{cr} = \frac{\pi^2 EI_c}{h^2}$$

Gerstle [36] studied frame behaviour under both gravity and combined gravity plus wind loading with flexible connections. He concluded that girder

design moments are highly sensitive to connection flexibility and column moments are much less dependent on connection behaviour. AISC type-2 analysis (simple framing/ wind connection method) consistently overestimates girder moments, and underestimates column moments.

Shen and Lu [37] studied the behaviour of end restrained columns. The analysis considers nonlinear material properties, loading, unloading and reloading of yielded fibres, both geometrical and material imperfections and load eccentricities. The following important conclusions have been drawn from their study:

1. Initial crookedness reduces the strength of the column and this reduction is maximum for a $\lambda = 1.2$, where λ is defined as $\lambda = \frac{L}{r} \times \frac{1}{\pi} \sqrt{\frac{\sigma_y}{E}}$
2. The band width of the column curves decrease as the end restraint increases and the maximum difference between the curves (ie. the maximum band width) occurs at λ value of about 0.9. This observation obviates, however, the necessity for multiple column curves as suggested by SSRC, provided that end restraint is taken into account.

Sugimoto and Chen [38] conducted an analytical study of the behaviour and strength of symmetrically loaded wide-flange steel columns with small end restraint by means of an approximate deflection method using a bi-linear representation of test data for the moment-rotation relationship for the beam-to-column connections. They showed that their results were in good agreement with the test results of Berquist [39] and the analytical prediction of Jones et al [40] whose model is based on a B-spline representation of connection $M-\phi$ relationship. It was also observed that at or near the maximum load, P_{max} , the rotational stiffness factor of the end restraint, R_k , lies in the linear elastic range for cases with

slenderness ratio (l/r) between 20 to 120, while it is in the plastic range for l/r between 140 to 160. From the results of this study it was reported that the effect of end restraint is more pronounced in weak axis bending than in strong axis bending.

Gerstle [41] studied flexible frame behaviour by analysing a number of subassemblages representing critical portions of typical unbraced multistorey steel frames. He concluded from his study that connection stiffness would generally lead to an increase in frame strength. However, he also noticed that for long span frames only a few storey high, the over-stiff connection might result in a reduction in frame strength.

Davison et al [42] used a finite element program [13] which resulted in good agreement with experimental observations [43,44,45] of the behaviour of partially restrained full scale non-sway steel frames. From their study, the following important conclusions were drawn:

1. Load carrying capacity of the frame increases as the joint stiffness increases but, after a certain critical value of the joint stiffness, it has virtually no effect.
2. Even with the use of modestly stiff connections, a significant reduction in column effective length occurs.
3. The effective length of a column is not only dependent on particular type of beam-to-column connection; it depends on the location of the column as well as the loading pattern.

Jones et al [46] report that, with the use of semi-rigid joints, the max-

imum strength of slender columns are significantly increased, however for more stocky columns this increase is less significant. In other words the strength raising effect of end restraint depends on the relative stiffness of the connection and the column. Table 2.2 shows some aspects of the results presented by Jones and later discussed by Ackroyd et al [47]. It is evident that the presence of residual stress significantly influences the effect of end restraint as does the relative stiffness of the connection to column. It is also evident that the effect of end restraint on the realistic column is to raise the strength by a relatively small amount (eg. 9% as shown in table 2.2). It was observed in their study that a codified method of estimating column strength could lead to erratic predictions.

Razzaq and Chang [48] studied the behaviour of isolated columns with partial end restraint and initial imperfections. This finite difference approach considers a linear pattern of residual stress distribution and elastic-perfectly-plastic material behaviour. Both linear and bi-linear $M-\phi$ relationships of the connection have been modelled. Based on a limited parametric study it was concluded that the end-restraint has a considerable influence on the behaviour of crooked columns. The influence is however, more pronounced when both initial crookedness and residual stresses are present together.

Vinnakota [49] used a finite difference approach to study the problem of an isolated column with end restraint. The analysis uses a linear, bi-linear or tri-linear representation of connection $M-\phi$ data and allows geometric imperfections to be included. He constructed column strength curves for end restraint columns and suggested the following formula for the effective length factor

$$k_e = \frac{\pi^2 + 2\bar{\alpha}}{\pi^2 + 4\bar{\alpha}} \quad (2.2)$$

where $\bar{\alpha} = \frac{C_j}{EI}$, where C_j is the linear connection stiffness.

Simitzes and Vlahinos [50] analysed the two bar L shaped flexibly connected frame shown in Figure 2.7. Both linear and nonlinear representations of $M-\phi$ data were considered. The nonlinear relationship was modelled by using a cubic polynomial and an incremental type of analysis was employed to tackle nonlinearity in $M-\phi$ relations. An increasing capacity of the beam column assembly was reported with an increase in connection stiffness. It was also reported that both column slenderness and the nonlinearity of $M-\phi$ relationship of the connection do not significantly affect the critical load.

2.5 Design Methods

Despite the fact that considerable progress has already been achieved in understanding the influence of semi-rigid joints on the behaviour of members, simplified tools for the realistic quantification of this influence are yet to be developed. However, a brief review of the various suggestions for the design of members with semi-rigid joint so far evolved, are made here.

2.5.1 Design of Braced Frames

In this section the available methods for the design of braced frames with semi-rigid connections are reviewed. Plastic design methods are already well established and explained in reference [51]. So far as the elastic designs are concerned, there are two alternative approaches to semi-rigid design in the British Structural Steel Design Code [1]. The first is rather empirical, in which a conservative

nominal allowance is made for the stiffness of the connections by a limited redistribution of moment. In the second approach, the stiffness is represented by $M-\phi$ relationships based on experimental evidence. These relationships are taken into account during analysis and the frame's components are sized on the basis of the resulting moments and forces. Both approaches are delineated in reference [51], indicating their relative advantages and disadvantages.

2.5.2 Design of Unbraced Frames

When a frame is unbraced it has been an established practice in some countries to rely on the stiffness of practical connections to provide resistance to wind, even though such restraint is ignored under gravity load. The resulting procedure is known as the Wind Connection Method. Ackroyd and Gerstle [52] have studied the results of frame analysis with realistic account being taken of the behaviour of semi-rigid connections under both gravity and wind loading. Anderson et al [51] observed that further studies should be carried out to provide guidance on the extent to which sway deflections calculated by wind connection method are likely to underestimate those given by exact analysis accounting for the flexibilities expected from the actual connections. Such studies require sophisticated tools capable of modelling physical problems efficiently.

2.5.3 Column Design: The Effective Length Approach

The modern tendency of designing individual components of a frame makes the effective length approach a very popular one, so far as the design of columns is concerned. Various codes [1,2] provide charts and nomographs for estimating the

effective length of a column, considering the restraint provided by the surrounding members in a rigid frame. Satisfactorily accurate methods of determining effective lengths of columns in semi-rigid frames are yet to evolve — although the restraining effect of the semi-rigid joint results in an increased capacity of the column is a very well established fact.

Wood [53] developed a method of estimating the effective lengths of columns in a framework. Although his work mainly refers to rigid frames he indicated the effects of semi-rigid joints as well. Referring to the work of Baker [54], Wood [53] provides a formula for the effective stiffness of a beam with semi-rigid connections:

$$k'_b = k_b \left(\frac{1 + \frac{3\alpha}{2}}{1 + 4\alpha + 3\alpha^2} \right) \quad (2.3)$$

where $\alpha = 0.5 \left(\frac{k_b}{k_j} \right)$

k_b is the beam stiffness with fixed joints

k_j is the initial joint stiffness

and k'_b is the modified beam stiffness due to semi-rigid connection.

The value of α typically ranges from 1.0 to 2.5, suggesting $\alpha = 5$ for a very flexible light joint, $\alpha = 1.0$ for a fairly stiff joint and $\alpha = 0$ for an infinitely rigid joint. Figure 2.8 shows the effect of α upon k'_b . For high values of α (low values of k_j), $k'_b = k_b$, implying that for light flexible connections, the connection stiffness dominates and the far end condition is not important [55]

Taylor [55] tried to link the effective lengths of a column to both beam sizes and the level of joint stiffness. The effective length factor was defined as $k_e = (1 - e_1 - e_2)$ where e_1 and e_2 relate to the degree of restraint at each end of the column and are defined by

$$e = \left(\frac{0.25 \sum k_b}{0.6 \sum k_c + \sum k_b} \right) \quad (2.4)$$

He developed this approach specifically for the case of top and bottom cleat connections, assuming cleat sizes (and thus joint stiffnesses) to be proportional to the beam's elastic section modulus Z_b , to fix the ratio of joint stiffness to beam stiffness, leading to

$$e = \left(\frac{0.25 \sum Z_b}{250 \sum k_c + \sum k_b} \right) \not\approx 0.15 \quad (2.5)$$

Assuming very stiff beams, Jones et al [40] suggested specific values of effective length factor for some commonly used connection types. For example, 0.75 for web cleats and 0.55 for end plate joints. However in realistic situations such specified values have little significance since actual end restraint for the column depends on many factors like relative beam-to-connection stiffness, axis of bending [56,57], slenderness ratio etc.

Lui and Chen [58] report that the effective length factor k_e with a flexible connection can be obtained as follows:

$$k_e = 1 - 0.017\alpha > 0.60 \quad (2.6)$$

where $\alpha = \frac{C}{M_{pc}}$

C =initial connection stiffness

M_{pc} = plastic moment capacity of the column.

Galambos [59] suggested that the influence of realistic beams should also be taken into account while considering the restraint provided through the connections to the column. He defined the relative rotational stiffness C^* as

$$C^* = \frac{\frac{2EI_b}{L_b}}{\left(1 + \frac{2EI_b}{CL_b}\right)} \quad (2.7)$$

$(2EI_b)/L_b$ is the beam stiffness for the beams bent in single curvature with equal

and opposite end rotations which is the most conservative condition; for other real situation more appropriate beam stiffnesses may be used.

Introducing beam flexibility the Lui and Chen equation (Eq. no. 2.6) can be rewritten as

$$k_e = 1.0 - 0.017\alpha^* > 0.60 \quad (2.8)$$

where $\alpha^* = \frac{C^*}{M_{pc}}$

However, the method is workable only if the column has the same framing arrangement both at the top and the bottom joints, a case which may not be true in practice.

Bjorhovde [3] gave a detailed account for determining the effective length factor for a column in a real frame taking column buckling into consideration. He modified the SSRC G-factor [60] approach (which is meant for rigid frames) in order to apply it for the semi-rigid frame case. Instead of computing

$$G \text{ as } \frac{\sum \left(\frac{EI_c}{L_c} \right)}{\sum \left(\frac{EI_b}{L_b} \right)} \quad (2.9)$$

he suggested that a reduced value of G as

$$G_r = \frac{\sum \left(\frac{EI_c}{L_c} \right)}{C^*} \quad (2.10)$$

Although G_r is based on the initial slope of the $M-\phi$ relationship, Bjorhovde suggested that the resistance of the beam for which connection goes on loading as the column buckles should be neglected. Thus, with G_r factor known at the top and bottom joint, the alignment chart of reference[60] can be used directly to find the effective length factor.

Bjorhovde's method can be used for the inelastic case by considering the suggestions made by Yura [61]. However, Nethercot and Chen [15] have

expressed the need for confirmation of the intuitive approach of including beam flexibility as suggested in equation 2.7 above.

Davison et al [57] applied the principle detailed after Bjorhovde [3] in the preceding paragraph to the results of their subassemblage tests. Satisfactory agreement between the test load and predicted capacity of the column had been reported, although they cautioned that a more detailed investigation is required before adopting it for the purpose of design.

Jones et al [40] suggested a graphical procedure for determining the effective length which uses the strength curve for two columns – one pin-ended and the other semi-rigid jointed (figure 2.9). The length on the pin-ended curve which gives the same strength as the failure load of the end restrained column is defined as the effective length for the latter column. This method has been applied by Sugimoto and Chen [38]. The approach seems sensible but requires the column curve with the given end restraint to be available beforehand. Of course it is not clear from reference [40] whether the column curve for the pin ended column is based on the assumption of a perfect column or whether it has similar imperfections as that considered in the case of restrained column (ie the column in question). Chapuis [56] introduced the concept of crooked effective length $k_{crooked}$, in which he used the same approach as Jones [40] but in this case the pin-ended column curve with which he compared the result of the restrained column possesses the same degree of imperfection.

De Falco and Marino [62] suggested a modification of the girder stiffness to include the effect of a semi-rigid connection and thus to enable the alignment chart of reference [60] to be used. However, the procedure is based on initial connection stiffness and the assumed boundary conditions for this development

did not comply with those used in the development of the alignment chart. As a result of this Driscoll [63] refined and extended the above approach. Utilizing the matrix force method, he developed the force-displacement relationship of a beam with semi-rigid joints at the ends. The rotational stiffness of the joint was represented by the initial connection slope. Finally he developed with the modified beam stiffness factor for the beams having semi-rigid connections at the ends. If both the ends of beam have the same connection stiffness (ie $K_B=K_A$) then the relative stiffness (I/L) of the beam can be written as:

Case I: For use in general frame analysis:

$$k'_b = \left(\frac{3}{4(K_B + 1) - (K_B + 1)} \right) \times \frac{I}{L}. \quad (2.11)$$

Case II: For use in the G-factor approach in the sway case:

$$k'_b = \left(\frac{1}{2K_B + 1} \right) \times \frac{I}{L} \quad (2.12)$$

Case III: For use in the G-factor approach in the non-sway case:

$$k'_b = \left(\frac{3}{2K_B + 3} \right) \times \frac{I}{L} \quad (2.13)$$

where $K_B = K_A = 3Z\left(\frac{EI}{L}\right)$

and $\frac{1}{Z}$ is the initial connection stiffness (see figure 2.10).

Driscoll [63] himself recognizes the shortcomings of using the initial connection stiffness to represent the semi-rigid connection considering the highly nonlinear nature of many $M-\phi$ relationships.

All of the approaches mentioned above (except that of Jones) have one thing in common — that is they are all based on the initial slope of the connection $M-\phi$ curve and are therefore less satisfactory for the determination of

the true maximum strength of partially restrained columns. Reference [15] also observes that the use of initial connection stiffness is correct for a bifurcation type of buckling approach but, for a real column, the end deformation will occur prior to the attainment of the maximum load — indicating a decrease in connection stiffness. Therefore, it is questionable whether the effective length factors based on consideration of elastic buckling (as in the G- factor approach) are truly representative of the restraining effects provided to real columns.

2.6 Concluding Remarks

The foregoing discussion presents an overall picture of the state of semi-rigid design to date. Clearly, the production of simplified design tools are an essential prerequisite, yet to be met, before it can be accepted as a viable design method by the wider engineering community. Such simplified design tools will emerge as a result of systematic study into the behaviour of semi-rigid frames. In order to enable such studies to be made, well validated computer programs which can model physical problems accurately are an essential research tool.

The computer programs described in section 2.2, may help to serve this purpose but these programs have different levels of refinement in simulating the physical behaviour in real structures. Various sources of nonlinearities and member imperfections are the important consideration that any formulation should ideally be able to cater for in an efficient way. Reference [51] expressed expectations of developing highly refined approaches that would make possible a proper investigation of the behaviour of semi-rigid construction.

Type of Model	Reference	Year	Advantages	Disadvantages
1.Linear	Baker Rathbun	1933	1. Simple to use. 2. Stiffness matrix only requires initial modification.	Inaccurate at high rotation values
2.Bi-linear	Lionberger & Weaver Romstad & Subramanian	1969 1970	1. Simple to use. 2. Curve follows M- ϕ curve more closely than linear model.	Inaccurate at some rotation values
3.Polynomial	Sommer Frye & Morris	1970 1975	Produce a close approximation to shape of M- ϕ data	1. Can produce inaccurate (even negative) connection stiffness 2. Nonlinear, hence requires iterative evaluation.
4.Cubic B-Spline	Jones,Kirby & Nethercot	1980	1. Produces a very close approximation to M- ϕ data shape 2. Produces accurate value of connection stiffness.	1. Nonlinear, hence requires iterative evaluation. 2. Requires special numerical procedure for evaluation.

Table 2.1 Methods of modelling connection M- ϕ data [15].

Slenderness ratio	Residual stress	Increase in strength ^a
100	none	56%
75	none	21%
75	considered	09%

^aIncrease in column strength is due to the end restraint provided by a T-stub connection, w.r.t. a pin-ended column.

Table 2.2 Influence of slenderness ratio and residual stress on the effectiveness of end restraint [46].

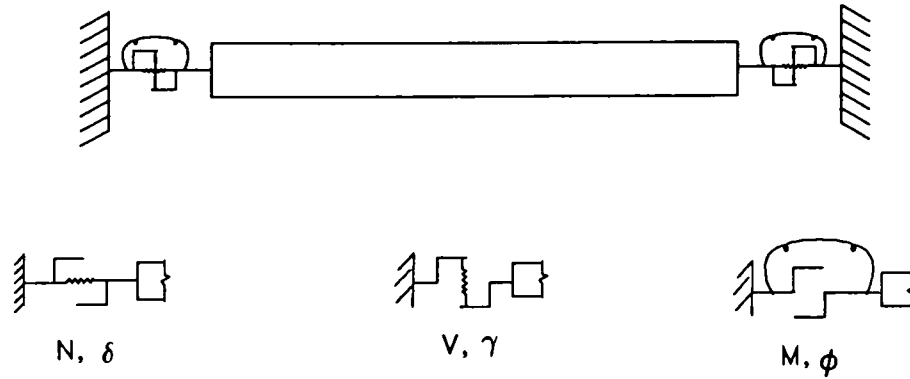


Figure 2.1 The beam-joint model for various force components.

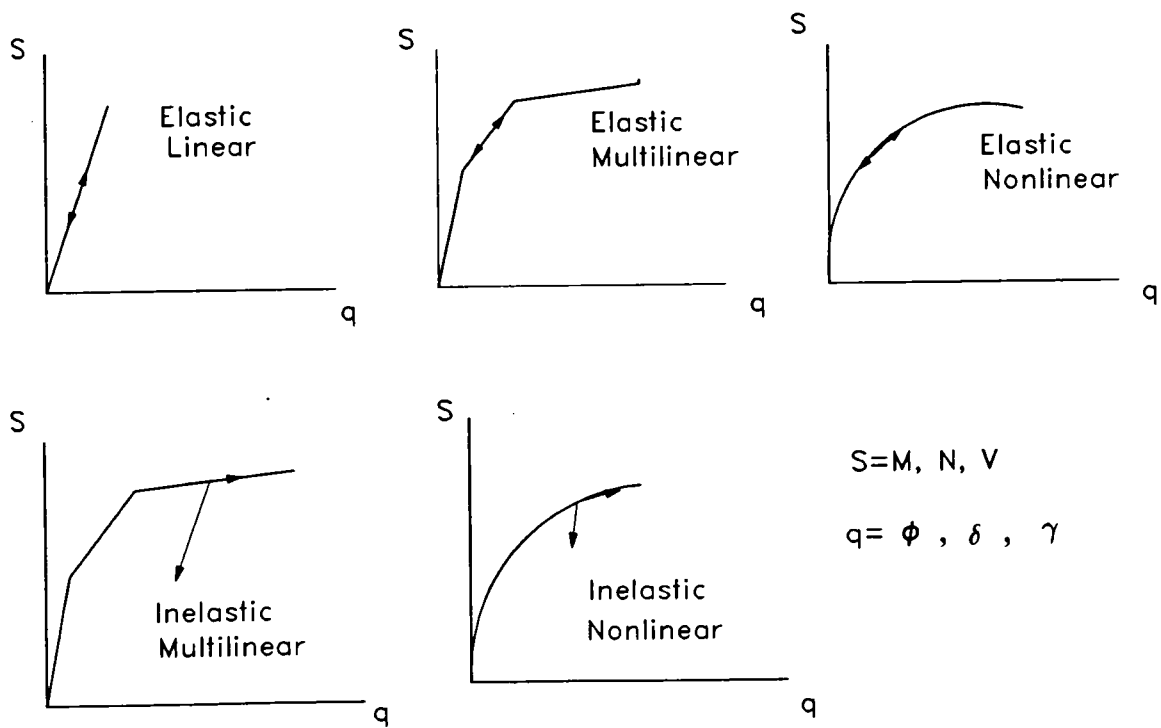


Figure 2.2 Various representations of the joint behaviour.

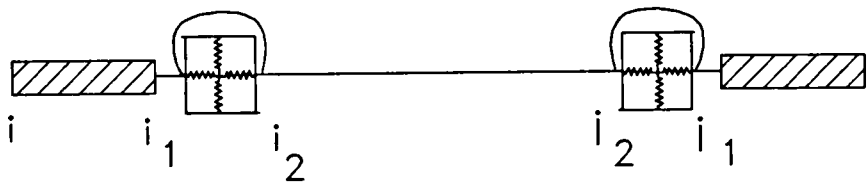


Figure 2.3 Semi-rigid beam-joint element by Cosenza [22].

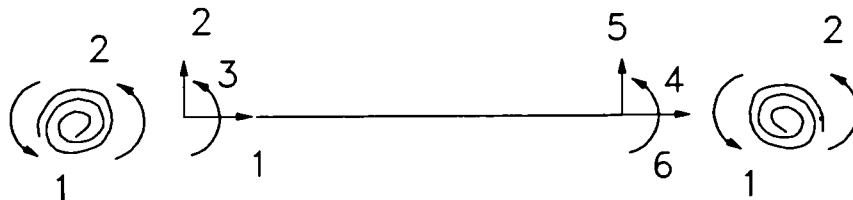


Figure 2.4 Semi-rigid beam-joint element by Chen and Lui [28].

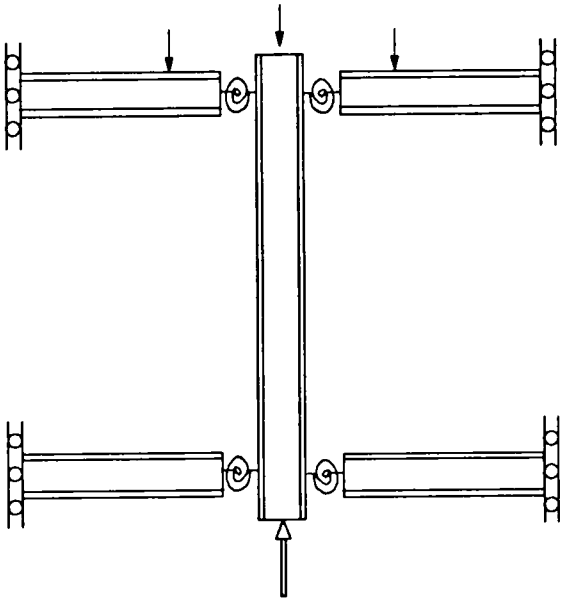


Figure 2.5 Limited column-subassemblage considered by Rifai [12].

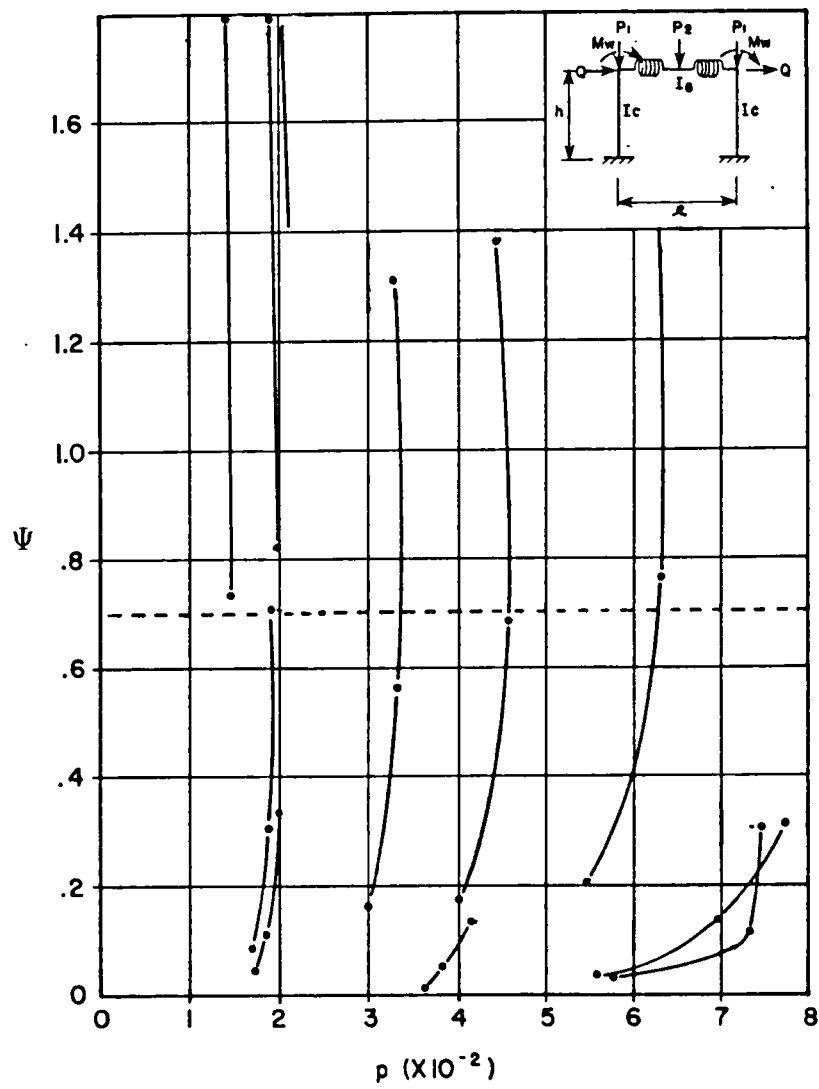


Figure 2.6 Effect of connection stiffness on frame strength [35].

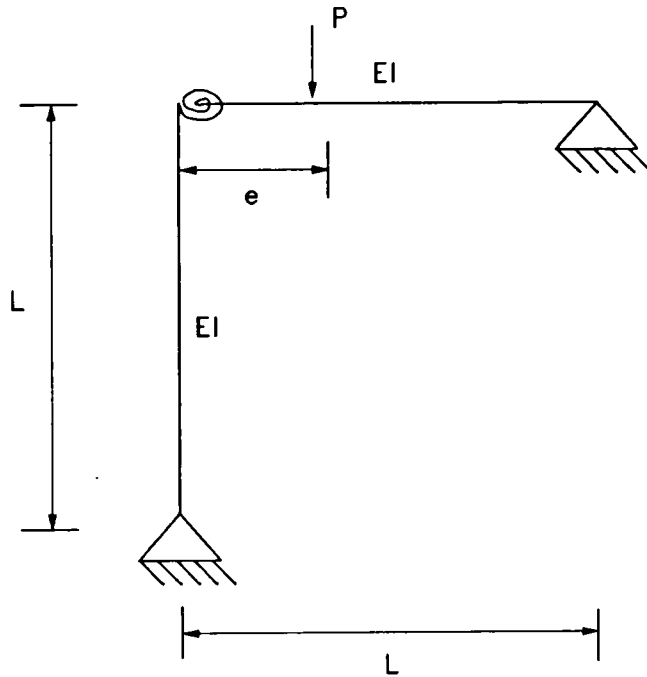


Figure 2.7 Flexibly connected frame analysed by Simitse et al [50]

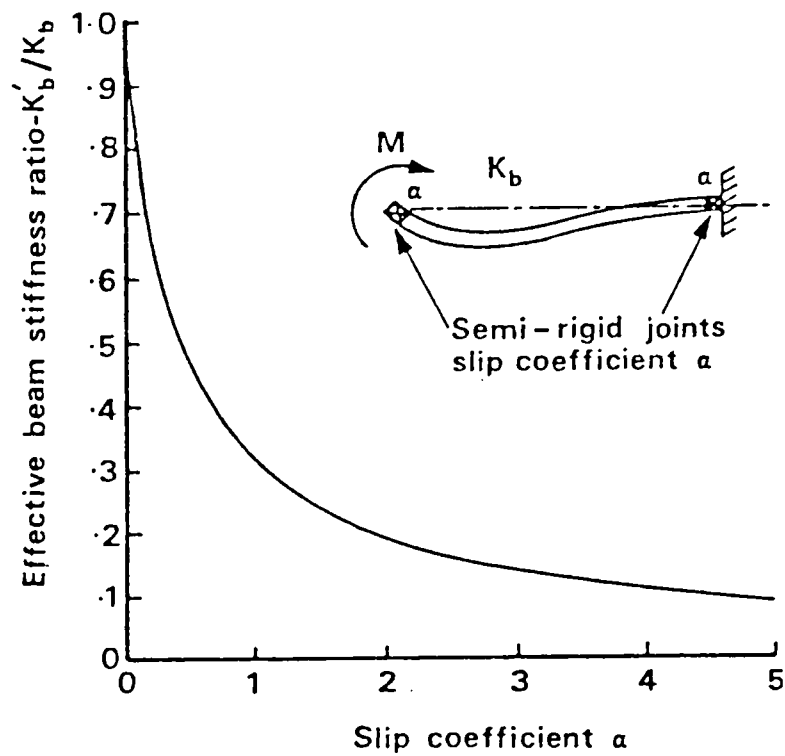


Figure 2.8 Effective beam stiffness with semi-rigid joints [54].

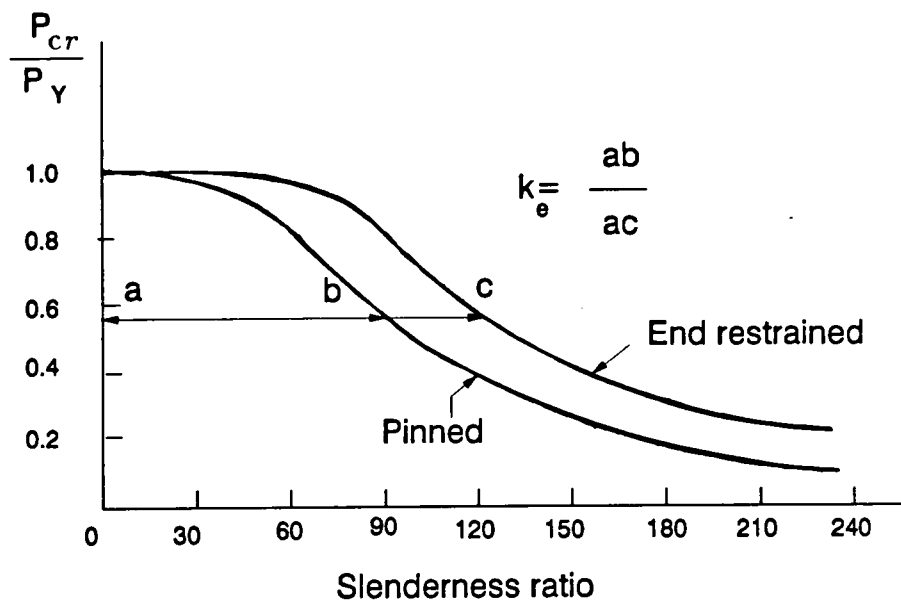


Figure 2.9 Determination of column effective length [40].

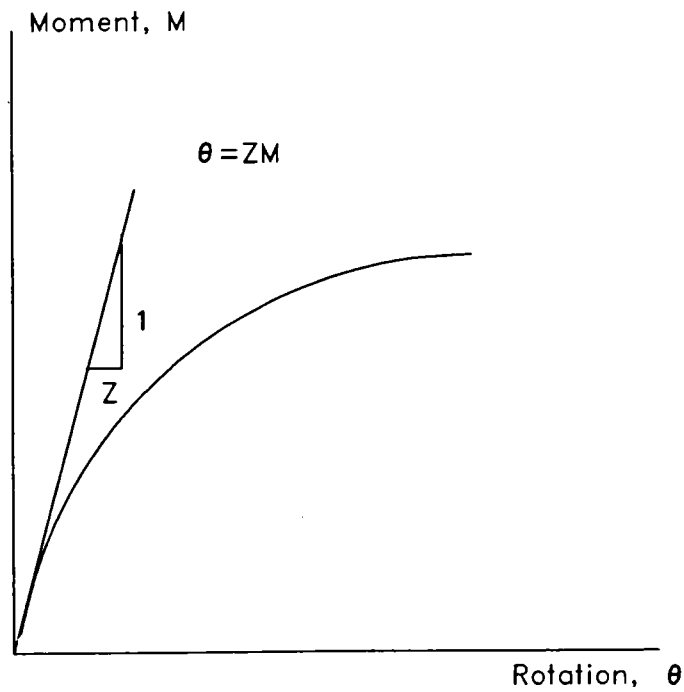


Figure 2.10 Measure of joint stiffness in Driscoll's method [63].

Chapter 3

Finite Element Formulation and the Computer Program

3.1 Introduction

The success of the finite element method in solving various physical problems has resulted in its widespread use in structural problems. Although the analysis of structures by the finite element method has become fairly common due to the abundance of computers in the design offices, the major drawback lies in the simplifying assumptions that are almost certainly have to be made in any such computer model. Such assumptions normally include idealised behaviour which is the basis of most of the available formulations. One of the important idealisations commonly made in the analysis of structural frames relates to the behaviour of the connections which are usually taken either as either perfectly hinged or rigidly fixed. However, as mentioned earlier, the realistic behaviour of the connection

is semi-rigid and its inclusion in the analysis and design is advantageous in the sense of reliability and economy of construction.

As already mentioned in the previous chapter, the effect of semi-rigid connections on member stiffness can be accounted for in two ways. One is to represent the connection stiffness by introducing discrete elements at the ends of the member in the form of springs with flexural, shear and axial stiffness; the other is to modify directly the member stiffness relationships to account for the partial rotational restraining effect of the connections. The latter has the advantage that the total number of degrees of freedom required to model the deformed configuration of the structure decreases significantly when compared to the former, if all the connections of a large structure are of a semi-rigid nature.

Rifai [12] derived shape functions for a beam-column element having semi-rigid connections at its ends. He then implemented that formulation in the analysis of a semi-rigid limited column subassemblage as described in chapter 2. The author has extended this program to cope with the analysis of a full frame. Detailed features of this program will be discussed later in this chapter. In the next section a brief account of the formulation of the semi-rigid beam element is presented.

3.2 Formulation of the Semi-Rigid Element

The beam-column element proposed by Rifai [12] has three degrees of freedom associated with each node giving a total of six degrees of freedom per element (see figure 3.1(a)). This prismatic element has, in general, two semi-rigid joints at its ends. Elastic behaviour is assumed although the effect of loss of stiffness

due to initiation and spread of yield is dealt with in an approximate method and will be discussed later in this chapter.

3.2.1 Shape Function

Figure 3.1(b) shows the deformed configuration of a typical element with semi-rigid end connections. The presence of the semi-rigid joints at nodes 1 and 2 will cause these nodes to have two rotations at each location; one is just to the left and the other is just to the right of the node. The difference between these two rotations is the rotation of the connection θ_j . Thus referring to figure 3.1(b), if θ_1 is the rotation of the column centre line and $\bar{\theta}_1$ is the rotation of the beam end at node 1, then $\theta_{j1} = \theta_1 - \bar{\theta}_1$ is the rotation of the beam caused by the flexibility of the connection.

Written in terms of nodal displacements, the displacement of a general point on the element can be expressed as:

$$\begin{Bmatrix} u \\ v \end{Bmatrix} = \begin{bmatrix} N_1 & 0 & 0 & N_2 & 0 & 0 \\ 0 & N_3 & N_4 & 0 & N_5 & N_6 \end{bmatrix} \begin{Bmatrix} u_1 \\ v_1 \\ \theta_1 \\ u_2 \\ v_2 \\ \theta_2 \end{Bmatrix} \quad (3.1)$$

where N_1 to N_6 are the shape functions of the element. The shape functions N_1 to N_6 are defined in table 3.1, together with their rigid element counterparts, \bar{N}_1 to \bar{N}_6 . With the substitution of the appropriate expressions for \bar{N}_1 to \bar{N}_6 , the shape functions N_1 to N_6 for a beam-column element with semi-rigid joint at its end are obtained as [12]:

$$N_1 = 1 - r \quad (3.2)$$

$$N_2 = r \quad (3.3)$$

$$N_3 = 1 - \theta_{j31}Lr - (3 - 2\theta_{j31}L)r^2 + (2 - \theta_{j31}L - \theta_{j32}L)r^3 \quad (3.4)$$

$$N_4 = L[(1 - \theta_{j41}r - (2 - 2\theta_{j41} - \theta_{j42})r^2 + (1 - \theta_{j41} - \theta_{j42})r^3] \quad (3.5)$$

$$N_5 = \theta_{j51}Lr + (3 - 2\theta_{j51}L - L\theta_{j52})r^2 - (2 - \theta_{j51}L - \theta_{j52}L)r^3 \quad (3.6)$$

and

$$N_6 = L[-\theta_{j61}r - (1 - 2\theta_{j61} - \theta_{j62})r^2 + (1 - \theta_{j61} - \theta_{j62})r^3] \quad (3.7)$$

Now referring to mode shape 3 of table 3.1 the slope-deflection equation may be used to write the following relationships:-

$$M_1 = \frac{2EI}{L}(-2\theta_{j31} - \theta_{j32} + \frac{3}{L}) = C_{j1}\theta_{j31} \quad (3.8)$$

$$M_2 = \frac{2EI}{L}(-\theta_{j31} - 2\theta_{j32} + \frac{3}{L}) = C_{j2}\theta_{j32} \quad (3.9)$$

where C_{j1} and C_{j2} are the connection stiffnesses at node 1 and node 2 respectively and $\frac{EI}{L}$ is, as usual, a measure of flexural stiffness for the element. Solving these two equations for θ_{j31} and θ_{j32} , the following may be obtained:

$$\theta_{j31} = \frac{A_1 B_1}{H} \quad (3.10)$$

$$\theta_{j32} = \frac{A_1 B_2}{H} \quad (3.11)$$

Writing similar relations as in equation nos 3.8 and 3.9 for mode shapes 4, 5, and 6 the following relationships can be obtained:

$$\theta_{j41} = \frac{A_2 B_3}{H} \quad (3.12)$$

$$\theta_{j42} = \frac{A_2 C_{j1}}{2H} \quad (3.13)$$

$$\theta_{j51} = \theta_{j31} \quad (3.14)$$

$$\theta_{j52} = \theta_{j32} \quad (3.15)$$

$$\theta_{j61} = \frac{A_2 C_{j2}}{2H} \quad (3.16)$$

$$\theta_{j62} = \frac{A_2 B_4}{H} \quad (3.17)$$

where,

$$A_1 = \frac{6EI}{L^2} \quad A_2 = \frac{4EI}{L}$$

$$B_1 = \frac{2EI}{L} + C_{j2} \quad B_2 = \frac{2EI}{L} + C_{j1}$$

$$B_3 = \frac{3EI}{L} + C_{j2} \quad B_4 = \frac{3EI}{L} + C_{j1}$$

$$\text{and } H = \frac{L}{2} A_1 A_2 + A_2 (C_{j1} + C_{j2}) + C_{j1} C_{j2}$$

3.2.2 Strain-Displacement Relationship

The average strains at a cross section can be written as:

$$\varepsilon = \left[- \left(\frac{du}{dx} + \frac{1}{2} \left(\frac{dv}{dx} \right)^2 \right), - \frac{d^2 v}{dx^2} \right]^T \quad (3.18)$$

In the above expression, the axial component of the strain contains a nonlinear term, which arises due to the elongation of the element caused by the deflection v . Now strain, ε , can be written as

$$\varepsilon = \varepsilon_0 + \varepsilon_L \quad (3.19)$$

where ε_0 is the linear component of the strain and ε_L is the nonlinear one.

Hence, it can be shown that [64]

$$\begin{aligned} \varepsilon_0 &= \left\{ \begin{array}{c} -\frac{du}{dx} \\ -\frac{d^2 v}{dx^2} \end{array} \right\} \\ &= - \left\{ \begin{array}{c} \frac{d}{dx} \\ \frac{d^2}{dx^2} \end{array} \right\} \left\{ \begin{array}{c} u \\ v \end{array} \right\} \end{aligned}$$

$$\begin{aligned}
 &= - \left\{ \begin{array}{c} \frac{d}{dx} \\ \frac{d^2}{dx^2} \end{array} \right\} \left[\begin{array}{cccccc} N_1 & 0 & 0 & N_2 & 0 & 0 \\ 0 & N_3 & N_4 & 0 & N_5 & N_6 \end{array} \right] \left\{ \begin{array}{c} u_1 \\ v_1 \\ \theta_1 \\ u_2 \\ v_2 \\ \theta_2 \end{array} \right\} \\
 &= - \left[\begin{array}{cccccc} \frac{dN_1}{dx} & 0 & 0 & \frac{dN_2}{dx} & 0 & 0 \\ 0 & \frac{d^2N_3}{dx^2} & \frac{d^2N_4}{dx^2} & 0 & \frac{d^2N_5}{dx^2} & \frac{d^2N_6}{dx^2} \end{array} \right] \left\{ \begin{array}{c} u_1 \\ v_1 \\ \theta_1 \\ u_2 \\ v_2 \\ \theta_2 \end{array} \right\} \\
 &= [B_0] \delta^e \tag{3.20}
 \end{aligned}$$

and

$$\varepsilon_L = -\frac{1}{2} \left\{ \begin{array}{c} \left(\frac{dv}{dx} \right)^2 \\ 0 \end{array} \right\}$$

It can be shown [64] that,

$$d\varepsilon_L = -\frac{dv}{dx} \left[\begin{array}{cccccc} 0 & \frac{dN_3}{dx} & \frac{dN_4}{dx} & 0 & \frac{dN_5}{dx} & \frac{dN_6}{dx} \\ 0 & 0 & 0 & 0 & 0 & 0 \end{array} \right] d\{\delta^e\} \tag{3.21}$$

$$d\varepsilon_L = [B_L] d\{\delta^e\} \tag{3.22}$$

Thus the two components of the strain displacement matrix [B] are identified as [B₀] and [B_L].

Once the strains are evaluated, the stresses may be obtained as

$$\sigma = [D] \{\varepsilon\} \tag{3.23}$$

where $\sigma = [F^p \ F^b]^T$ in which F^p and F^b denote force components in in-plane axial force and bending respectively.

SHEPHERD
UNIVERSITY
LIBRARY

and

$$[D] = \begin{bmatrix} D^p & 0 \\ 0 & D^b \end{bmatrix}$$

D^p and D^b are the in-plane and bending components of the elasticity matrix $[D]$. The $[D]$ matrix is assumed to be constant but the effect of yielding is taken into account in an approximate manner which will be discussed later in section 3.3.2.

3.2.3 Element Stiffness Matrix

Following the standard procedure described by Zienkiewicz et al [64], the tangential stiffness matrix for the element is derived [12] as :

$$[K_T] = \int_0^L [B]^T [D] [B] dx + \int_0^L \frac{d[B]^T}{d\delta^e} \sigma dx + (N_{j1}^T C_{j1} N_{j1} + N_{j2}^T C_{j2} N_{j2}) \quad (3.24)$$

where,

$$N_{j1} = \left[0 \quad \frac{dN_3}{dx} \quad -1 + \frac{dN_4}{dx} \quad 0 \quad \frac{dN_5}{dx} \quad \frac{dN_6}{dx} \right]$$

$$N_{j2} = \left[0 \quad \frac{dN_3}{dx} \quad \frac{dN_4}{dx} \quad 0 \quad \frac{dN_5}{dx} \quad -1 + \frac{dN_6}{dx} \right]$$

and C_{j1}, C_{j2} are the stiffnesses of the connection at the ends 1 and 2 of the element.

Now recognizing from equation nos. 3.19, 3.20 and 3.21 that

$$[B] = [B_0] + [B_L] \quad (3.25)$$

the above expression for the tangential stiffness matrix may be written as:

$$[K_T] = [K_E] + [K_G] + [K_L] \quad (3.26)$$

where,

$$[K_E] = \int_0^L [B_0]^T [D] [B_0] dx + (N_{j1}^T C_{j1} N_{j1} + N_{j2}^T C_{j2} N_{j2})$$

$$[K_G] = \int_0^L \frac{d[B_L^T]}{d\delta^e} \sigma dx$$

$$[K_L] = \int_0^L [[B_0]^T [D] [B_L] + [B_L]^T [D] [B_0] + [B_L]^T [D] [B_L]] dx$$

$[K_E]$ represents the usual, small displacement stiffness matrix.

$[K_G]$ is dependent upon current stress level, and in fact accounts for the effect of axial force on the change of bending stiffness of the element, and is known as the initial stress matrix or the geometric matrix [65].

$[K_L]$ is due to large displacements and is variously known as the initial displacement matrix or the large displacement matrix [64] etc.

3.3 Evaluation of Sectional Properties

Computation of the element stiffness matrix requires sectional properties to be evaluated at element level. The important sectional properties that are to be evaluated include axial and flexural rigidities EA and EI respectively. These properties are in general evaluated at the nodes. Depending on the fact that whether a particular node has yielded or not, the appropriate value of the modulus of elasticity is taken for consideration. Thus the two case of an 'elastic section' and a 'yielded section' arise and are dealt with accordingly.

3.3.1 Elastic Section

At relatively low levels of load, when the section remains elastic, calculation of the axial and flexural rigidities are carried out in a straightforward manner:

$$EA = E \int_A dA$$

and

$$EI = E \int_A y^2 dA; \quad \text{if bending is about the x-axis}$$

or

$$EI = E \int_A x^2 dA; \quad \text{if bending is about the y-axis.}$$

3.3.2 Inelastic Section: Spread of Yield

As loading continues in an incremental analysis, some locations will be yielded according to the assumed stress-strain relationship. As the yielding starts, it will spread gradually over the cross section until the whole section is yielded. In order to include this effect in the analysis an approximate procedure suggested by Nethercot [66] was utilized. This procedure involves dividing the whole cross section into a large number of sub-elements as shown in figure 3.2. Within the limitation of simple beam theory, the total strain (including the residual strain) in each of these sub-elements is computed as loads are incremented. This strain is then used to check if that particular sub-element has yielded or not, and an appropriate value of effective modulus of elasticity E_{eff} is assigned to that sub-element. The axial and bending rigidities are then calculated by summing over all the sub-elements. It should be noted that yielding over part of the cross section will vitiate the assumption of a prismatic section and the flexural rigidity EI should refer to an axis passing through the centroid of the effective section.

Thus

$$EA = \sum_{i=1}^N E_{eff}^i \Delta A_i \tag{3.27}$$

and

$$EI = \sum_{i=1}^N E_{eff}^i y_i^2 \Delta A_i - \bar{y}^2 A_{eff} \quad (3.28)$$

Equation 3.28 is for bending about x-axis and, in both equations, N is the number of sub-divisions in the section.

$$\bar{y} = \frac{\sum E_{eff}^i y_i \Delta A_i}{\sum E_{eff}^i \Delta A_i} \quad \text{and}$$

A_{eff} is the area of the part of the section which remains elastic.

Taking advantage of symmetry, in the case of two dimensional analysis, it is possible to carry out the above calculations for only one half of the section (assuming that the residual stress pattern is also symmetrical) because in such a case the section will retain symmetry about at least one of its initial geometric axes of symmetry. Sectional properties for the total section are obtained by simply multiplying this quantity by a factor of 2. This gives a very useful saving in computer time.

3.4 Stress-Strain Relationship

As has been observed in the preceding section, the effective value of the modulus of elasticity, E_{eff} , has to be evaluated, depending on whether the particular section has yielded or not. It is now necessary to define a stress-strain relationship of the material.

The stress-strain relationship of structural carbon steel and high strength low-alloy steel are commonly approximated by an elastic-perfectly-plastic stress-strain curve. A further simplification is sometimes introduced by the rigid plastic representation, which assumes that there is no strain at a section, until the moment equals the plastic moment capacity of the section, after which unrestricted

plastic flow is allowed to occur in the section. The rigid-plastic representation can be used when members are primarily subjected to flexural action. However, if the members carry large compressive forces, the inclusion of elastic deformations and instability considerations become important. This is especially true when high-strength steel is used in the frame. In a general analysis scheme the need for including elastic-plastic behaviour is therefore quite clearly evident. The results in the elastic stage can be used to check the serviceability limit-states. On the other hand, the plastic stage is used to estimate the overload strength and to find whether or not the ultimate limit state concerned with structural safety is satisfied.

Strain-hardening has considerable influence on the load capacity, especially on small structures. In the case of tall structures, however, the effect of instability on the frame behaviour is far greater than that of strain hardening[67].

In the light of what has been mentioned above a general elastic-perfectly-plastic stress-strain relationship with the option of strain hardening characteristics is considered for the present case. Figure 3.3 shows typical stress-strain relationship which can be adopted in the analysis.

The total normal strain at any point is calculated by adding the direct axial strain and bending strain. In addition, if any residual strain is present in the section, that is also added. Thus if ϵ^a , ϕ^b and ϵ^r represent the average axial strain, the curvature at the section and the residual strain at the point under consideration respectively, then the normal strain at any point in the section is given by

$$\epsilon = \epsilon^a - y\phi^b + \epsilon^r \quad (3.29)$$

where y is the distance of the point from the neutral axis.

It then becomes a simple task to check whether the particular location in the section has yielded or not and an appropriate value of the effective modulus, E_{eff} is chosen accordingly.

3.5 Inclusion of Initial Imperfection

In the case of a perfect frame with ideal loading conditions, there will be no lateral deflection in the members of the frame until the bifurcation load is reached and such a process will essentially lead to an eigen value analysis [68]. On the other hand, in the presence of initial imperfections, such as geometric deviations, residual stresses etc. and / or non-idealised loading conditions being incorporated then, deflection will occur as soon as the load is applied. From a practical point of view, all real structural members have some form of imperfection. Residual stresses and initial out-of-straightness are the most common form of imperfection which any general frame analysis program must include. In the following sections inclusion of these two types of imperfection will be discussed explicitly.

3.5.1 Inclusion of Residual Stress

Structural steel shapes and plates contain residual stresses that result primarily from uneven cooling after rolling. The magnitude and distribution of residual stresses in hot-rolled shapes depends on the type of cross-section, rolling temperature, cooling conditions, straightening procedures and metal properties [69]. Cooling effects tend to produce patterned residual stress in the section, and the

straightening process destroys the well-defined pattern, making the distribution highly irregular in many practical sections. However, simple idealised patterns are normally adopted for the inclusion of the effect of residual stress in the analysis as they generally represent the worst case which can exist. Such patterns are based on experimental measurements. The various patterns of residual stress distribution considered in the present program for I-shaped sections are:

- Parabolic distribution
- Linear distribution
- Rectangular distribution

The parabolic distributions of residual stresses across the flanges and the web of I-sections are shown in figure 3.4 and these are generally accepted in the UK for rolled sections. Young [70] suggested following empirical formulae to define the controlling values of such a residual stress patterns:-

$$\sigma_f = 165 \left(1 - \frac{A_w}{1.2(2A_f)} \right) N/mm^2 \quad (3.30)$$

$$\sigma_{fw} = -100 \left(0.7 + \frac{A_w}{2A_f} \right) N/mm^2 \quad (3.31)$$

$$\sigma_w = 100 \left(1.5 + \frac{A_w}{1.2(2A_f)} \right) N/mm^2 \quad (3.32)$$

where A_w is the area of the web and A_f is the area of one flange. Compressive residual stress are considered as positive.

The linear pattern which is normally adopted in the USA for rolled sections is shown in figure 3.5 with the following controlling values as suggested

by Lehigh research [70,71]:

$$\sigma_f = 0.3\sigma_y \quad (3.33)$$

$$\sigma_{fw} = -0.3 \frac{A_f}{A_f + A_w} \quad (3.34)$$

A simple rectangular pattern (see figure 3.6) is usually assumed for welded sections. The areas in the immediate vicinity of the welds exhibit high tensile residual strains due to the cooling of the weld metal and is given by:

$$\sigma_T = -0.9\sigma_y \quad (3.35)$$

The residual stress elsewhere is assumed to be compressive and is given by

$$\sigma_C = 0.1\sigma_y \quad (3.36)$$

All these pattern mentioned above are accepted by the present program. If necessary by using a suitable multiplying factor the controlling values specified above may be varied. In addition to the above mentioned well-known patterns two more distributions may also be specified. The first one is a parabolic distribution with the values of σ_f , σ_{fw} and σ_w being selected by the user. The other one accounts for a more erratic distribution of residual stress in which the residual stress at a number of specified points along the flanges and the web are given as input data. Straight lines are then assumed by the program to obtain the residual stress at other points in the section.

The distribution of residual stress in any section should be such that static equilibrium of residual forces(F_r) and moment(M_r) about any axis is maintained (ie $\sum F_r = 0$ and $\sum M_r = 0$). In the first two pattern described above

the equilibrium check is automatically made by the program. Because of the symmetry of distribution about either axis, the moment equilibrium is automatically satisfied. It is only necessary to check the residual force. In the rectangular pattern, the area around the weld should be pre-chosen in such a way that the residual force becomes zero. In the last two patterns, since the values at the key points in the pattern are chosen by the user, a complete check of the static equilibrium must be ensured while selecting the values.

Once a residual stress pattern is chosen, the residual strain values at different locations across the section are easily obtained by dividing the residual stress by the modulus of elasticity. Use of equation 3.29 would then allow the calculation of the total strain, ϵ .

3.5.2 Inclusion of Geometric Imperfection

Practical columns possess some degree of initial imperfection, so its inclusion in analysis is important. The inclusion of geometric imperfection makes the column buckling problem one of a load-deflection type, as opposed to a bifurcation type of stability problem for a perfect column.

Initial shapes in columns are commonly taken as half sine waves with the specified central deflection as $L/1000$, where L is the length of the column. In general, if δ_0 is the initial central deflection, the deflection at any point along the column (see figure 3.7) is given by:

$$\delta^* = \delta_0 \sin\left(\frac{\pi x}{L}\right) \quad (3.37)$$

Imperfections of type-I and type-II as shown in figure 3.7 are the local geometrical imperfections, which arise from the initial out-of-straightness of the column.

However, for frames, global geometrical imperfection resulting from out-of-plumb of the frame which arise due to the erection tolerances, need to be considered as well. This global geometrical imperfection is a rather new concept and has been introduced in some recent code provisions [72],[73]. As shown in figure 3.8, this is specified by means of an initial sway to be incorporated in the analysis or by means of allowable tolerances. Although available experimental data on the measured out-of-plumb of entire structures is inadequate, statistical evaluation on actual structures by Beaulieu [74] and Lindner [75] form the basis of the Eurocode recommendations (CEC,1984) which are as follows:

The initial lean angle, ψ of the frame is given by

$$\psi = \frac{v_0}{H} = \frac{1}{250} r_1 r_2 \quad (3.38)$$

where $r_1 = \sqrt{\frac{5}{H}}$ and $r_2 = \frac{1}{2} \left(1 + \frac{1}{n}\right)$;

H is the overall frame height(m) and n is the number of stressed columns in a row.

Figure 3.9 shows one possible combination of the local and global imperfection [76].

In analysis, a set of imaginary lateral forces $\{P_0\}$ may be applied to simulate the effect of initial geometric imperfection. This imaginary lateral force vector $\{P_0\}$ is obtained as:

$$\{P_0\} = [K_G]\{\delta^*\} \quad (3.39)$$

where $[K_G]$ is the geometric stiffness matrix and $\{\delta^*\}$ is the initial nodal deflections.

The present program would accept local geometrical imperfections such

as single curvature or double curvature shapes in columns and also the global imperfection defined by equation 3.38 above.

3.6 Modelling of the Connection Behaviour

It has been shown in section 3.2 that the formulation of the semi-rigid element stiffness matrix requires an account of the connection stiffness, which makes it necessary to properly model and represent connection behaviour in the analysis. The nonlinear connection $M-\phi$ relationship has been approximated by the use of either linear, bi-linear, multilinear, polynomial, exponential or cubic B-spline models, the first being the most crude approximation and the last being the most sophisticated representation. The important features of these models have already been discussed in the previous chapter.

The present program utilizes a cubic B-spline [11] fitting through the experimental data points of the connection $M-\phi$ relationship and instantaneous stiffness of the connection in any loading step is evaluated from the slope of the fitted B-spline curve at the appropriate level of rotation or moment. Alternatively a multilinear representation of the $M-\phi$ relationship may also be accepted by the program.

3.6.1 Unloading and Reloading of Connection Under Monotonic Loading

One of the important characteristics of the semi-rigid connection is that the connection may show alternate loading and unloading response even under a set

of monotonic load increments. Thus the loading and unloading characteristic of a connection must be incorporated in any proper analysis routine.

Available moment-rotation curves of connection tests under cyclic and alternating loads [77], [78], [79], show a distinct linear range during unloading, with the stiffness being equal to the initial loading modulus k_0 (see figure 3.10). nonlinear behaviour sets in again after moment reversal leading to a strength under reversed loading equal to that under monotonic loading.

Because of the absence of sufficient $M-\phi$ data for unloading and reloading conditions, one possible simplification for frames under monotonic loads could be to use a linear unloading part as shown in figure 3.11. The start of unloading may be identified by a decrease in connection rotation. After unloading linearly, if the joint is reloaded, it can be assumed that it would follow the same linear path (CB) up to the point of the first unloading (ie point B) and then follow the nonlinear loading path BD as shown in figure 3.11. If unloading occurs again the same procedure is followed.

3.6.2 Connection Behaviour Under Cyclic Loading

Systematic study on connection tests under load cycles are not very common and only a limited information is available [78], [79], [80] on the basis of which the behaviour of the connection have been modelled [80]. This model has been implemented in the present program to enable the analysis of flexible frames in cyclic sway modes. Details of this model are presented in chapter 5.

3.6.3 Connection Offset Effect

The location of the connection in a frame in which the column bends about its major axis is not at the intersection of the centre-lines of the corresponding beam and column. Therefore an analysis, where members are represented by their centre-lines, could produce erroneous results if connections are assumed to act at the intersection of the centre lines of the beam and the column (see figure 3.12). In such cases the connection properties are assumed to be concentrated at some offset from the column centre-line. Rifai [12] studied the effect of connection offset on subassemblage behaviour and concluded that, for major axis column framing, the behaviour of a subassemblage is significantly affected if connection offset is not considered in analysis and this is particularly true if the connection is of flexible nature, as indicated in figure 3.13.

Rifai's model for connection offset is shown in figure 3.14. This model comprises of a normal beam-column element with a semi-rigid end, together with a stiff portion with a length of $D/2$, where D is the depth of the column section. The connection offset, i.e. the column segment between the column's centre line and the column's flange, is assumed to have infinite flexural and axial rigidities since the depth of the segment is very large. The internal node B can be condensed out [81] and consequently the analysis will not automatically yield the deformations at node B which are important in calculating the internal forces in beam BC. However since the portion AB is of large stiffness, it will only undergo rigid body motion and hence the deformations at node B can be easily obtained by a simple transformation.

3.7 Computer Program

For the purpose of the present study, a computer program has been developed by modifying the subassemblage program of [12] for the analysis of planar frames. This program has been run on the university's IBM-3083 computer using FORTRAN-77 language. It uses an incremental-iterative algorithm for handling the second-order elastic-plastic analysis of planar semi-rigid frames. Based on the formulation detailed in the preceding sections, the program traces the full load-deflection response and determines the ultimate load for the structure. The following sections describe the important features of the present program.

3.7.1 General Layout of the Program

The computer program for the analysis of semi-rigid plane frames is based on an incremental-iterative technique. The main steps followed by the program for the analysis of a structure are shown in the flow chart of figure 3.15. The steps involved are briefly discussed below:

Step-1: Read and Interpret Input Data

The input data which describes the problem is read and then interpreted in clear terms so that any reader looking at the output can have an insight of the problem being analysed. The input data necessary to define the problem can be classified into three main groups, such as:

- General data

- Section data

- Connection data

General data includes:

1. Geometry of the frame
2. Discretization of the frame
3. Boundary conditions
4. Analysis type and level of accuracy
5. Description of the applied loads
6. Specification of the imperfections

Section data furnishes following information:

1. Cross-sectional dimension of all members
2. Axis of bending
3. Material properties (stress-strain diagram)

Connection data supplies the B-spline co-efficients for the $M-\phi$ data of all the connections used. B-spline co-efficients may be obtained using a NAG [82] library routine available in the University's computer network. Alternatively a multilinear connection $M-\phi$ relationship may be used.

A detailed description of the input data for this program is available in reference [83].

Step-2: Process Initial Imperfection

Geometric as well as material imperfections are processed in this step according to the specified type of imperfection. The initial nodal coordinates along the member and residual strains across the section are calculated.

Step-3: Load Vectors

The applied load is converted into a set of nodal generalized forces and assembled to form the global load vectors.

Step-4: Stiffness Matrix and Boundary Conditions

The stiffness matrix is computed for each element using equation 3.24. The stiffness of the semi-rigid end is evaluated following the connection $M-\phi$ rule and this stiffness is taken into account when the element stiffnesses are computed. Following the standard transformation procedure, the element stiffness matrices are transformed from local to global coordinates and assembled into the global stiffness matrix. Boundary conditions are then imposed.

Step-5: Check for Stability

During each iteration before the solution of the stiffness equation is carried out, the stability of the structure is checked by evaluating the determinant of the structure stiffness matrix. A positive non-zero value of the determinant ensures that the stiffness matrix is non-singular and the structure is stable.

Step-6: Solution of the Stiffness Equations

In this step the stiffness equations are solved to obtain the unknown nodal displacements. The displacement values obtained from each iteration are added to obtain the total displacement at any load stage.

Step-7: Member Forces

Once the displacements are known, the strains are evaluated using the strain displacement matrix. Member forces are then obtained.

Step-8: Convergence Check

During each iteration in any load step, it is necessary to check the equilibrium of the applied and resisting forces. If the difference is sufficiently small, then it is assumed that convergence has been achieved for that load step and next load increment is applied.

3.7.2 Computing Technique

The various steps in the computer program have been identified and described in general terms in the preceding section. In this section computational techniques involved in implementing some important steps will be addressed.

3.7.2.1 Computation of Element Stiffness Matrix

The element stiffness matrix is computed by adding the three components as follows:-

$$[K_T^e] = [K_E^e] + [K_G^e] + [K_L^e] \tag{3.40}$$

$[K_E]$ is the elastic stiffness matrix based on small deflection theory. $[K_G]$ is the geometric stiffness matrix which depends on the axial force in the element and $[K_L]$ is the large displacement stiffness matrix which depends on the deflected shape at the start of the load increment. The mathematical expressions for each of these components have been shown in equations 3.24 to 3.26 in integral form. A numerical integration scheme was employed to evaluate these matrices. Four gauss points along the element length were assumed in the scheme, so that the cubic shape functions may be evaluated exactly. Elements which have semi-rigid nodes require the connection stiffness to be evaluated. This is done by determining the tangential stiffness, at the appropriate level, of the $M-\phi$ curve of the corresponding connection.

The element stiffness matrix evaluated in local coordinates needs to be transformed into global coordinates before being assembled into the global stiffness matrix. The transformation is carried out in the standard way [81], i.e.

$$[K_T^g] = [T]^T [K_T^e] [T] \tag{3.41}$$

where T is the transformation matrix defined by:

$$[T] = \begin{bmatrix} \cos(\alpha) & \sin(\alpha) & 0 & 0 & 0 & 0 \\ -\sin(\alpha) & \cos(\alpha) & 0 & 0 & 0 & 0 \\ 0 & 0 & 1 & 0 & 0 & 0 \\ 0 & 0 & 0 & \cos(\alpha) & \sin(\alpha) & 0 \\ 0 & 0 & 0 & -\sin(\alpha) & \cos(\alpha) & 0 \\ 0 & 0 & 0 & 0 & 0 & 1 \end{bmatrix} \tag{3.42}$$

where α is the angle between the local and the global axes. Figure 3.16 shows the local and the global axes for a general element and the local and global nodal displacements.

3.7.2.2 Nodal Load Vectors

In the finite element analysis of structures using the displacement method, the only permissible form of loading, other than initial stressing, is the application of concentrated loads at the nodal points. Consequently it becomes necessary for other forms of loading to be reduced to equivalent nodal forces, before the solution can proceed.

The equivalent nodal forces for any element subjected to uniformly distributed load of intensity, q can be formed as:

$$F^e = \int_{L_e} [N]^T q dx \quad (3.43)$$

where $F^e = [F_1, F_2, \dots, F_n]^T$; and $F_i = \int N_i q dx$ for $i = 1$ to n ; n is the number of degrees of freedom per element.

For a concentrated load, P

$$F^e = [N]^T P \quad (3.44)$$

where $F_i = N_i P$ for $i = 1$ to n .

N_i is evaluated for the value of x at which P is acting.

Using this standard procedure the equivalent nodal forces for any applied load can be worked out. The equivalent nodal load for each of the applied loads is calculated and assembled into the global load vector after the necessary transformation of the axes is performed.

3.7.2.3 Solution of the Stiffness Equation

Once the stiffness matrix and the load vectors are assembled, the next step is the solution of the stiffness equation for the unknown nodal displacements. The nodal displacements cannot be determined uniquely without the substitution of a minimum number of prescribed displacements to prevent rigid body movement of the structure. Unless this is done mathematically, the $[K_T]$ matrix would be singular, i.e. not possessing an inverse. The prescription of appropriate displacements after the assembly stage will permit a unique solution to be obtained, which means the equations are solvable if the boundary conditions are imposed. In structural problems, the most common boundary conditions are those in which some displacement components are restrained, i.e. $\delta_i = 0$; where δ indicates the displacement and i corresponds to the particular degree of freedom. This condition can be achieved by assuming zero values in all but the diagonal element in the row and column corresponding to the i th degree of freedom. The diagonal element of the stiffness matrix is set to unity.

The system of equations is then solved by Cholesky decomposition [81]. As long as the structure is stable (i.e. positive non-zero diagonal elements in the stiffness matrix) this method should yield the solution of the unknown variables.

3.7.2.4 Load Incrementation and Iteration Procedure

The way that nonlinear problems are tackled efficiently when using the finite element method of analysis is by the use of an incremental iterative technique, in which the external loads are applied in a number of increments. Within each incremental step, load iteration techniques are employed so that the predicted

response follows the actual response of the structure.

Incrementation of the load can be done to obtain any form of proportional or patterned loading as will be discussed later in this chapter. The iterative technique adopted here is a Newton-Raphson procedure. Because of the way the section properties and internal forces are computed, it is necessary to keep the number of iterations per load increment to a minimum and consequently the choice of a modified Newton-Raphson procedure was not a favourable one, since savings in computer time by a modified approach would have been wasted in computing the section properties and internal forces for an increased number of iterations.

At the beginning of each load increment the connection stiffnesses are updated and the same values of the connection stiffnesses are used for the successive iterations used in that particular load step.

Initially, a small displacement solution of the stiffness equation is obtained for the first load increment with $[K_G]$ and $[K_L]$ set to zero. The element stress resultants are computed from the known displacements. The geometric stiffness and large displacement stiffness matrices for the structure are evaluated. The total resisting force is then obtained using the total stiffness, $K_T (= K_E + K_G + K_L)$ and the known displacements. The difference between the resisting forces and applied forces represents a set of unbalanced forces for the given configuration of the model. Knowing the set of unbalanced forces on the model, the increment in nodal displacements can be obtained. The process is repeated until the configuration of the model maintains equilibrium with the applied loads to a sufficient degree of accuracy. The process is shown in figure 3.17.

3.7.2.5 Convergence Criteria

Convergence of the numerical process to the nonlinear solution must be checked after each iteration in order to ensure that the true solution is achieved. A global convergence criterion is employed for unknown variables (displacements) as well as the residual forces in each iteration. The numerical process is said to have converged if the following condition is satisfied:

$$\sqrt{\frac{\sum_{i=1}^n (X_i)^2}{\sum_{i=1}^n (Y_i)^2}} \times 100 \leq \textit{Tolerance} \quad (3.45)$$

In the above equation, n is the total number of degrees of freedom in the problem. A tolerance of 1.0 (ie 1%) is considered to be adequate for most cases [84].

For checking unknown displacements X in equation 3.45 would mean the incremental nodal displacements and Y denotes the total nodal displacements for any load step.

For checking the unbalanced force vector, X and Y in equation 3.45 refer to the unbalanced force and total applied force respectively [84].

3.7.2.6 Criteria for Critical Load

The load incrementation process described earlier is continued until the critical load level is reached; i.e. when the system becomes unstable. The critical condition is identified in one of the following three ways:-

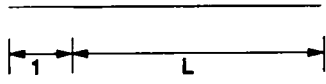
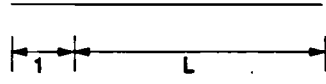
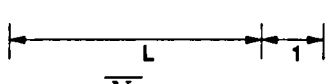
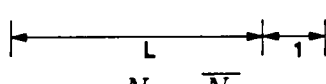
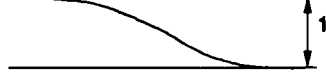
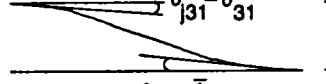


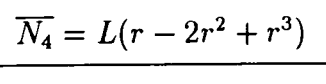
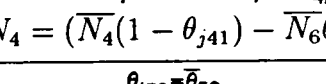
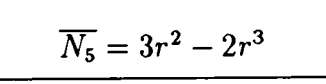
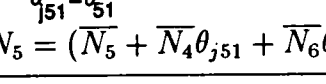
1. If the determinant of the global stiffness matrix is zero, the structure is said to have reached a critical condition. If however, at any stage the determinant is found to be negative, the program automatically steps back two load steps and reduces the increment size and in this way an adequately

accurate set of critical load values are obtained.

2. The second criterion uses the required number of iterations as an indicator of an unstable state and is based upon the consideration that, as the load level approaches the critical value, one or more out of balance member forces may increase rapidly and fail to converge at all. Hence, if the number of iteration cycles exceeds a specified value, the program will step back and reduce the increment size.
3. In this third criterion, the value of the maximum relative drift, i.e. the storey drift is used as an indicator of the critical state. Whenever the relative drift is found to be larger than a specified limit, the program stops further load incrementation and steps back to reduce the increment size and proceeds as usual until failure.

3.7.2.7 Incrementing the Applied Load

The loading process is divided into a number of stages and within each load stage a number of load increments of equal magnitude may be specified, or in any stage some loads may be considered to be constant (i.e. maintaining the same value as in the previous load step). This facilitates the application of proportional, patterned or even cyclic loads.

Mode	Element with Rigid Ends	Element with Semi-Rigid Ends
1	 $\bar{N}_1 = 1 - r$	 $N_1 = \bar{N}_1$
2	 $\bar{N}_2 = r$	 $N_2 = \bar{N}_2$
3	 $\bar{N}_3 = 1 - 3r^2 + 2r^3$	 $N_3 = \bar{N}_3 - \theta_{j31}\bar{N}_4 - \theta_{j32}\bar{N}_6$
4	 $\bar{N}_4 = L(r - 2r^2 + r^3)$	 $N_4 = (\bar{N}_4(1 - \theta_{j41}) - \bar{N}_6\theta_{j42})$
5	 $\bar{N}_5 = 3r^2 - 2r^3$	 $N_5 = (\bar{N}_5 + \bar{N}_4\theta_{j51} + \bar{N}_6\theta_{j52})$
6	 $\bar{N}_6 = L(-r^2 + r^3)$	 $N_6 = (\bar{N}_6(1 - \theta_{j62}) - \bar{N}_4\theta_{j61})$

$r = \frac{x}{L}$; θ_{jab} is the joint rotation at end b due to mode shape 'a'
and $\bar{\theta}_{ab}$ is the member end rotation at end b due to mode shape 'a'.

Table 3.1 Mode shapes for elements with rigid and semi-rigid joints at the ends.



Figure 3.1 (a) Element degrees of freedom.

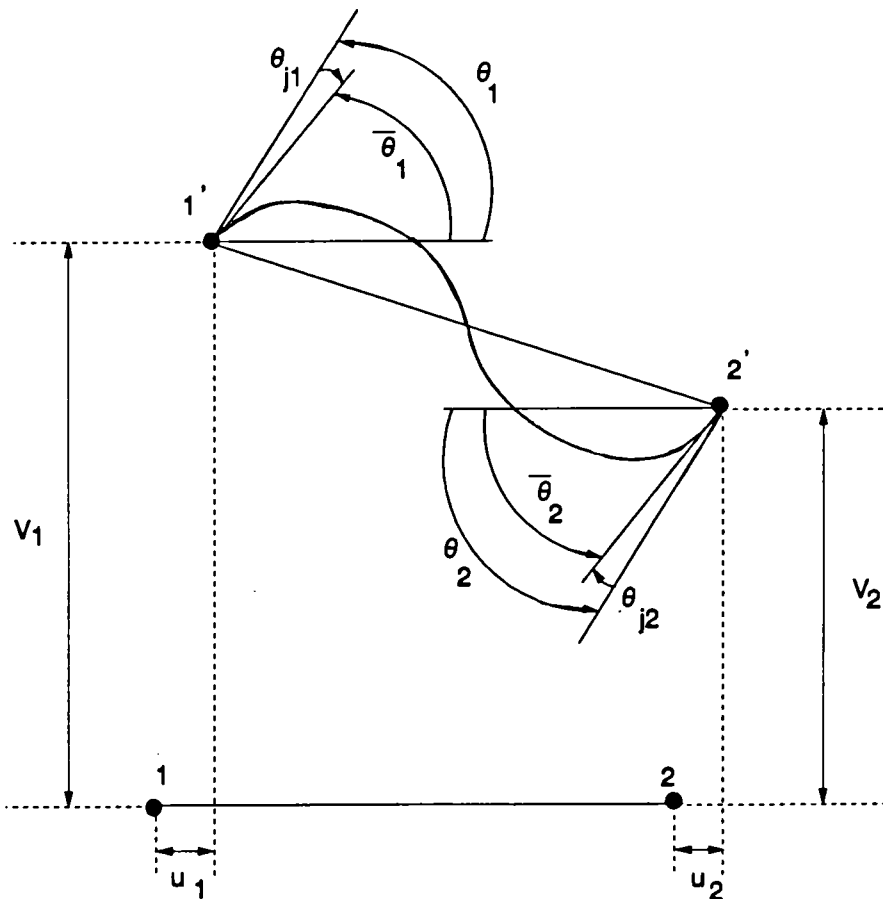


Figure 3.1 (b) Deformed shape of a semi-rigidly connected beam-column element.

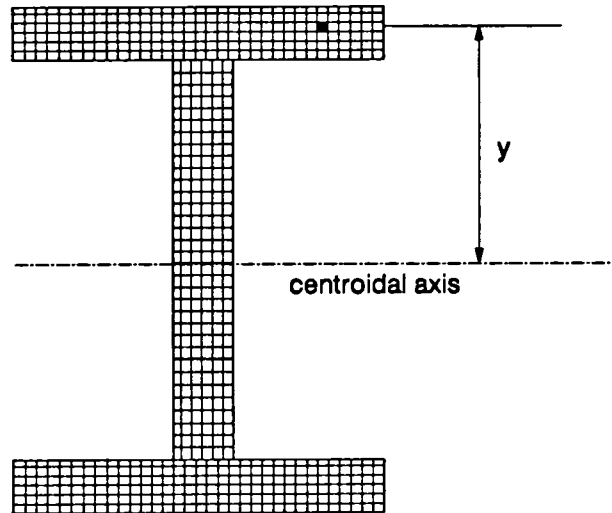


Figure 3.2 Dividing the cross-section for calculating the properties of the section.

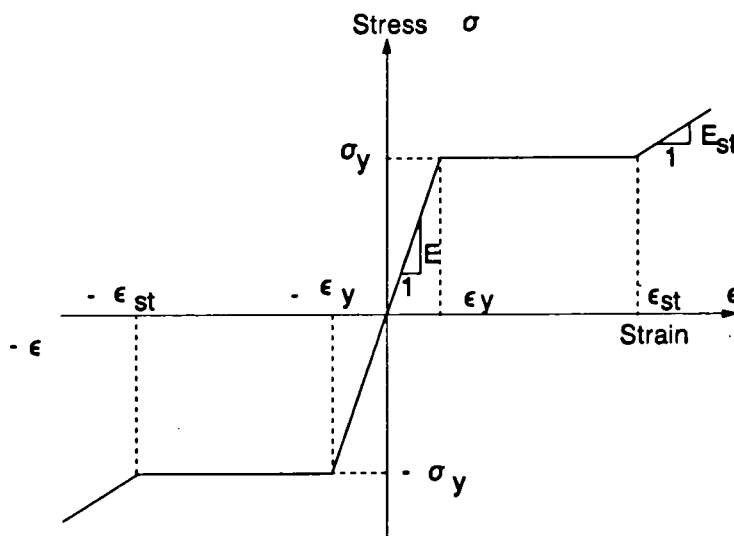


Figure 3.3 Idealised stress-strain relationship of the material.

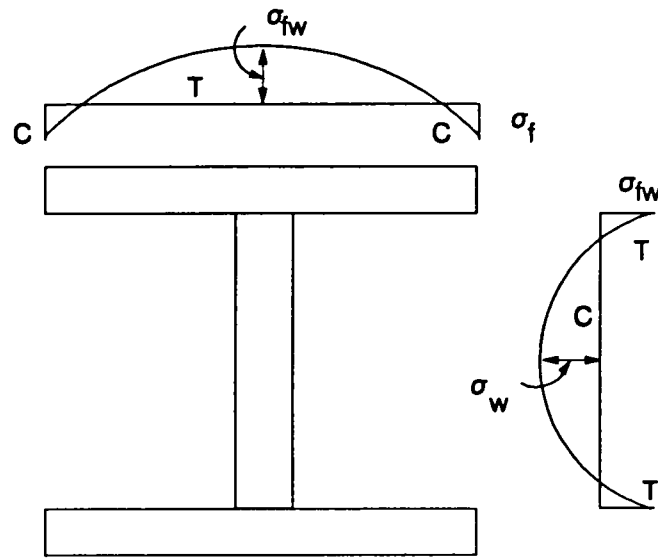


Figure 3.4 Parabolic distribution of residual stress.

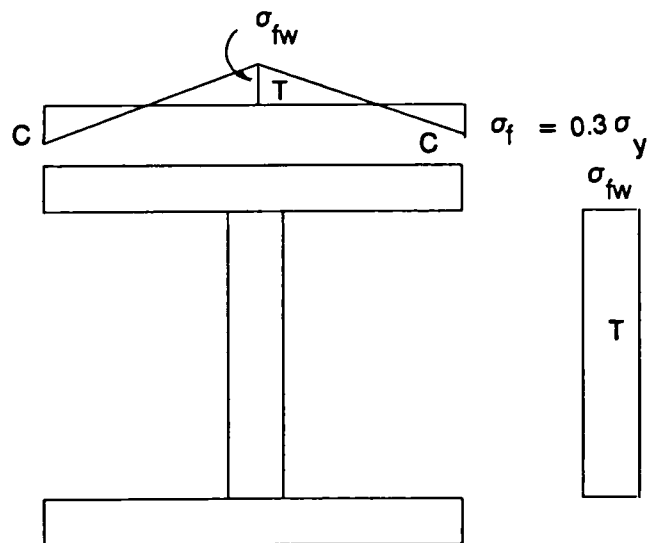


Figure 3.5 Linear pattern of residual stress.

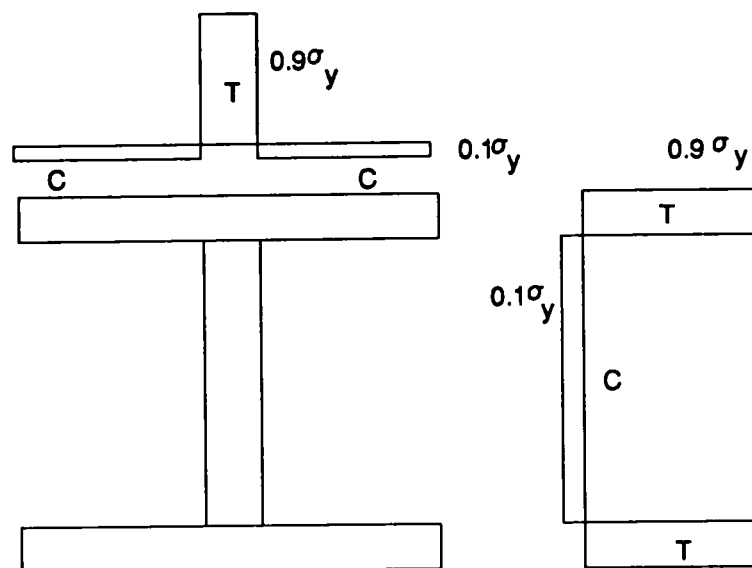


Figure 3.6 Rectangular pattern of residual stress.

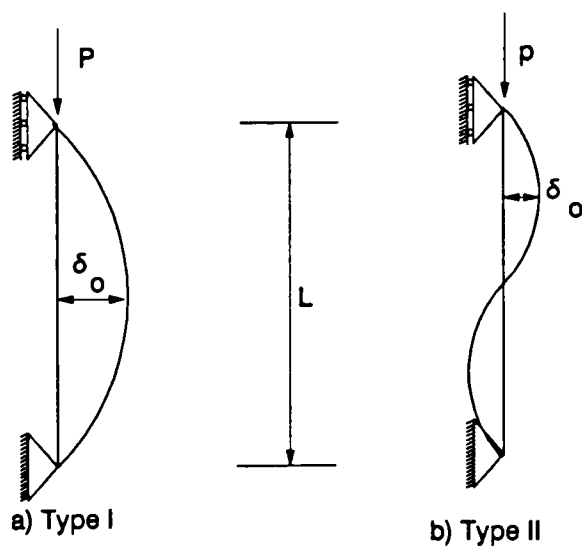


Figure 3.7 Possible local imperfection types.

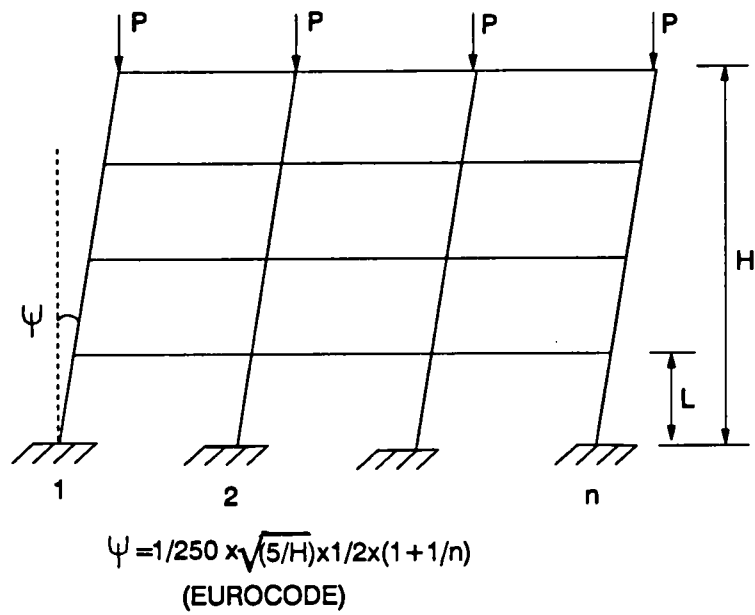


Figure 3.8 Global geometrical imperfection for frame.

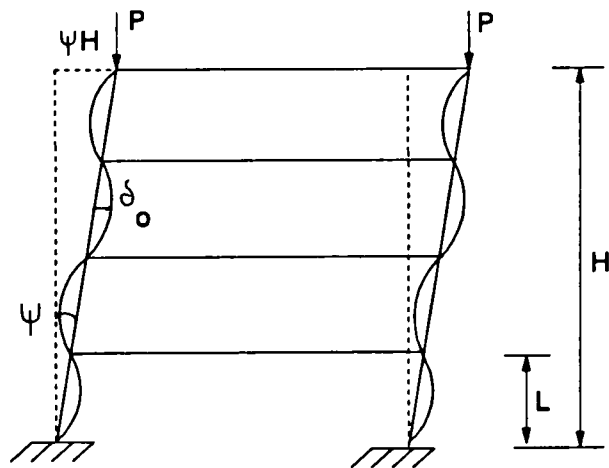


Figure 3.9 Combination of local and global geometrical imperfections.

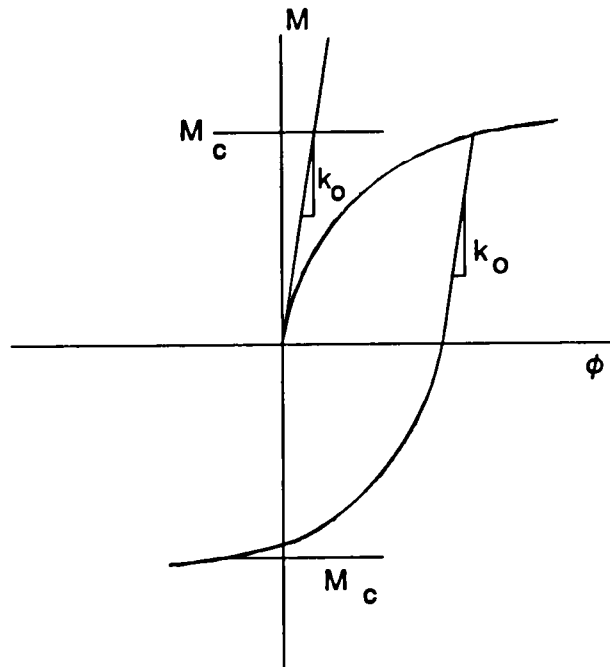


Figure 3.10 Loading-unloading characteristics of flexible connections.

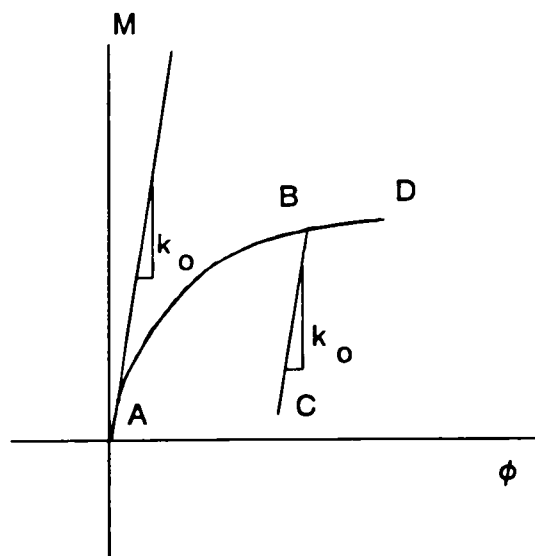
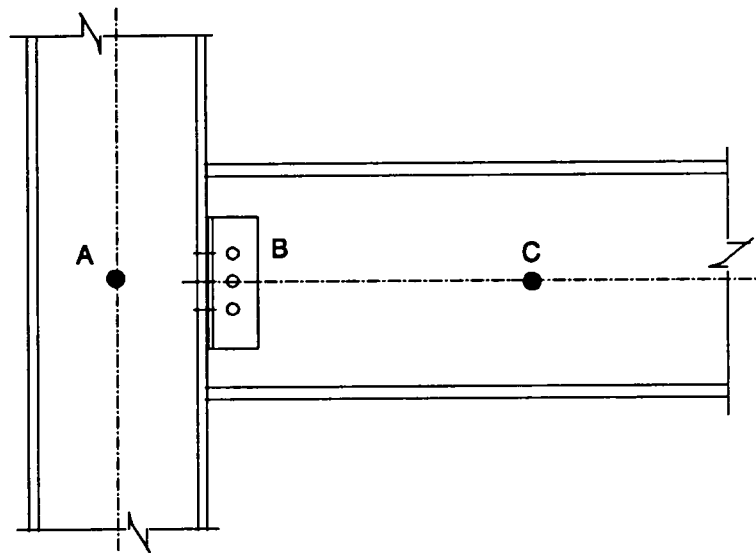
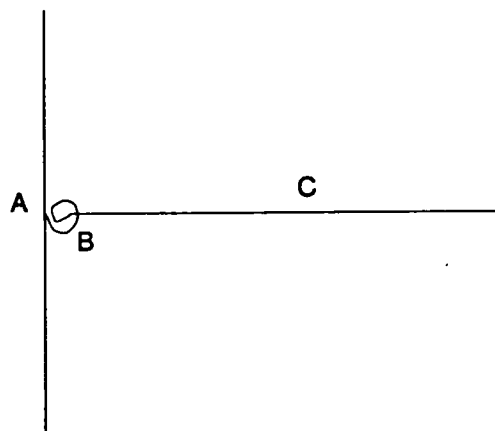


Figure 3.11 Simplified unloading model for connection.

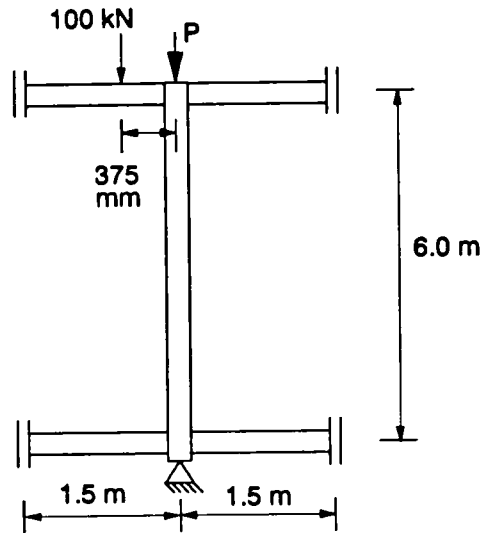


a) Actual beam-column joint.

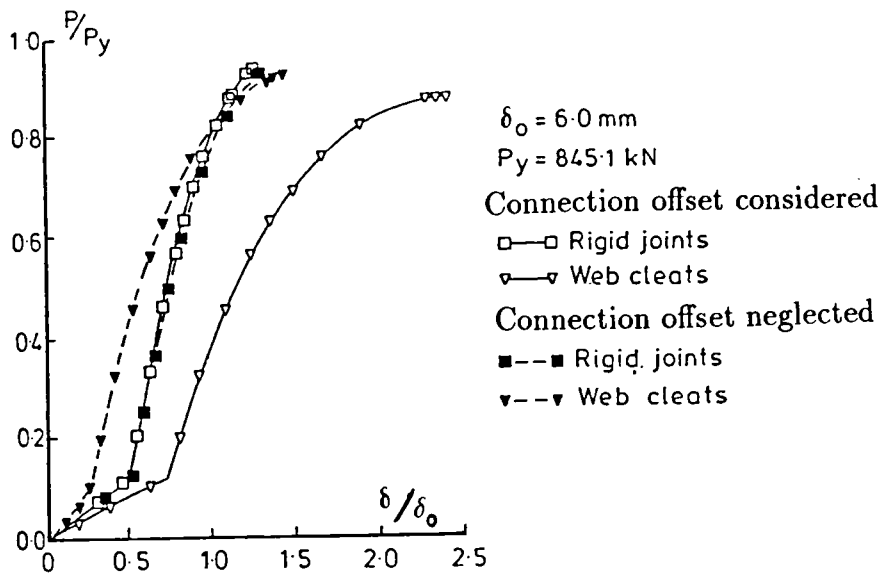


b) Centre line model neglecting joint offset.

Figure 3.12 Actual joint versus analytical model.

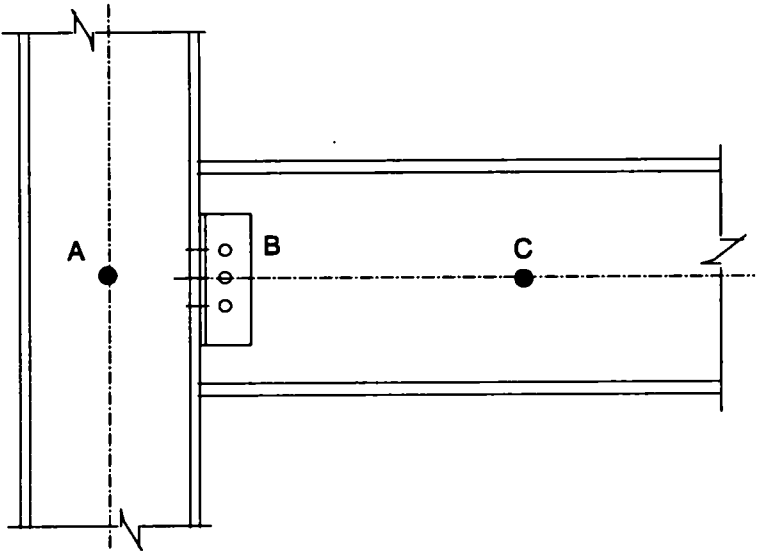


(a) Subassembly considered by Rifai [12] to study joint offset effect.

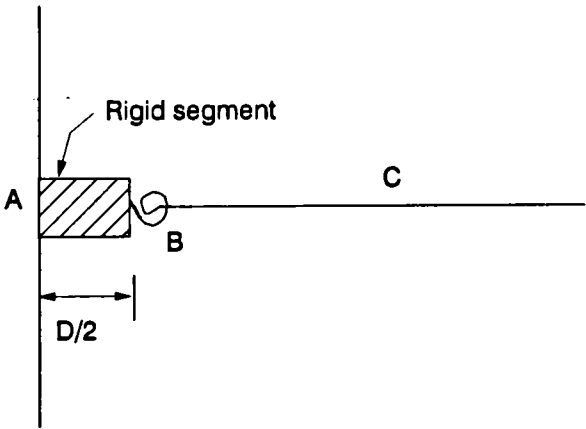


(b) Load-deflection curves for the subassembly of (a) above.

Figure 3.13 Effect of connection offset [12].



a) Actual beam-column joint.



b) Centre line model with joint offset.

Figure 3.14 Joint offset model [12].

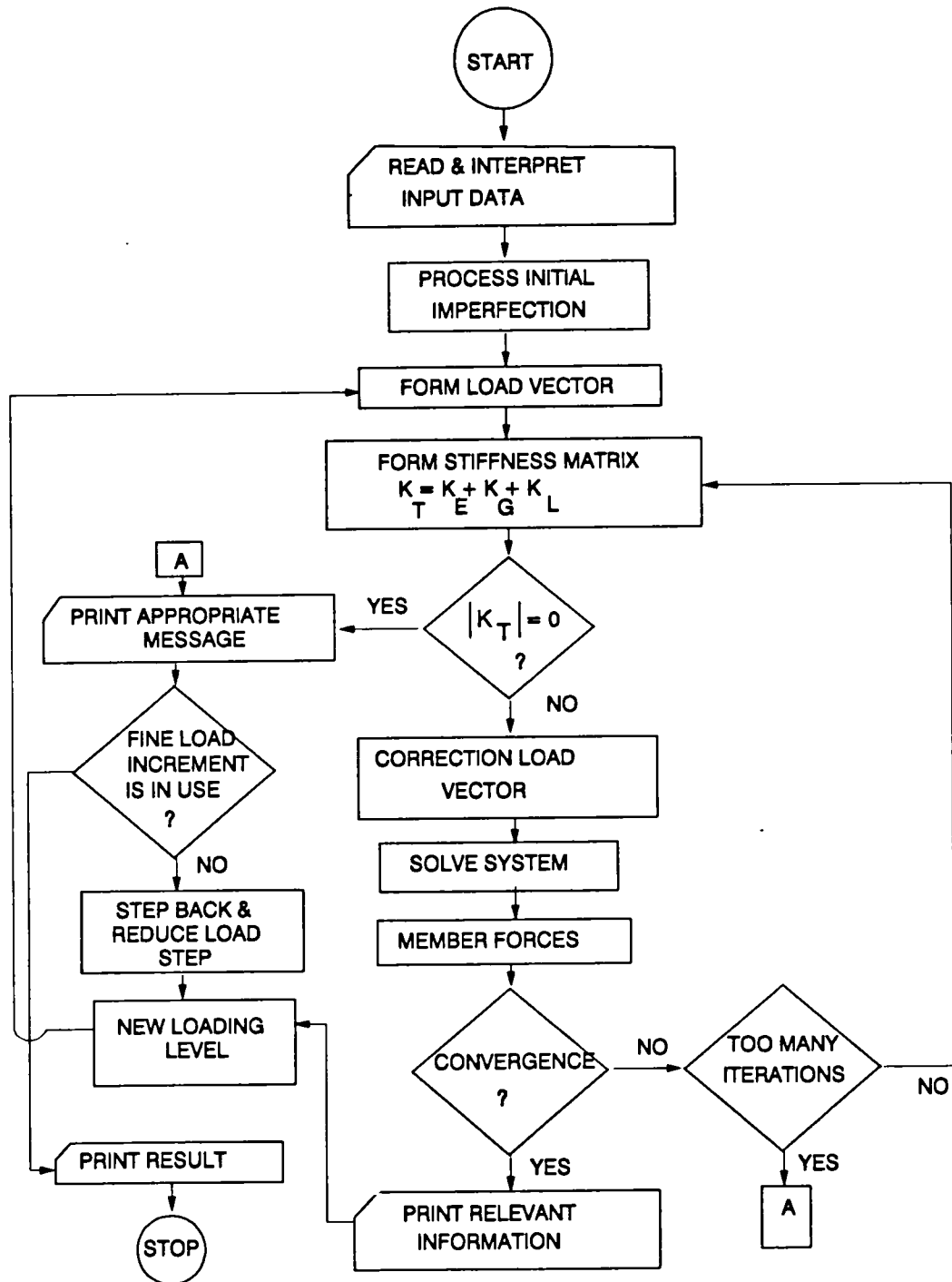


Figure 3.15 Flow chart for the computer program.

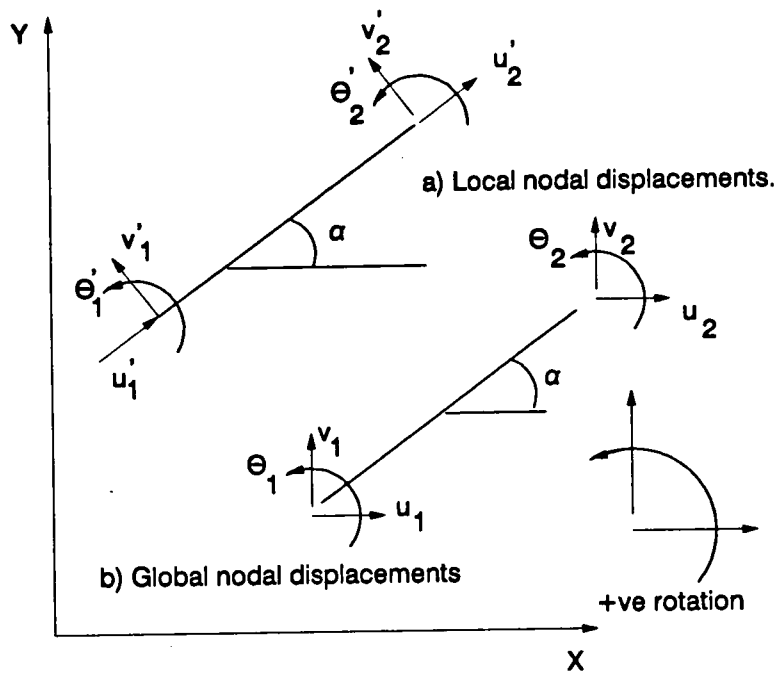


Figure 3.16 Local and global nodal displacements.

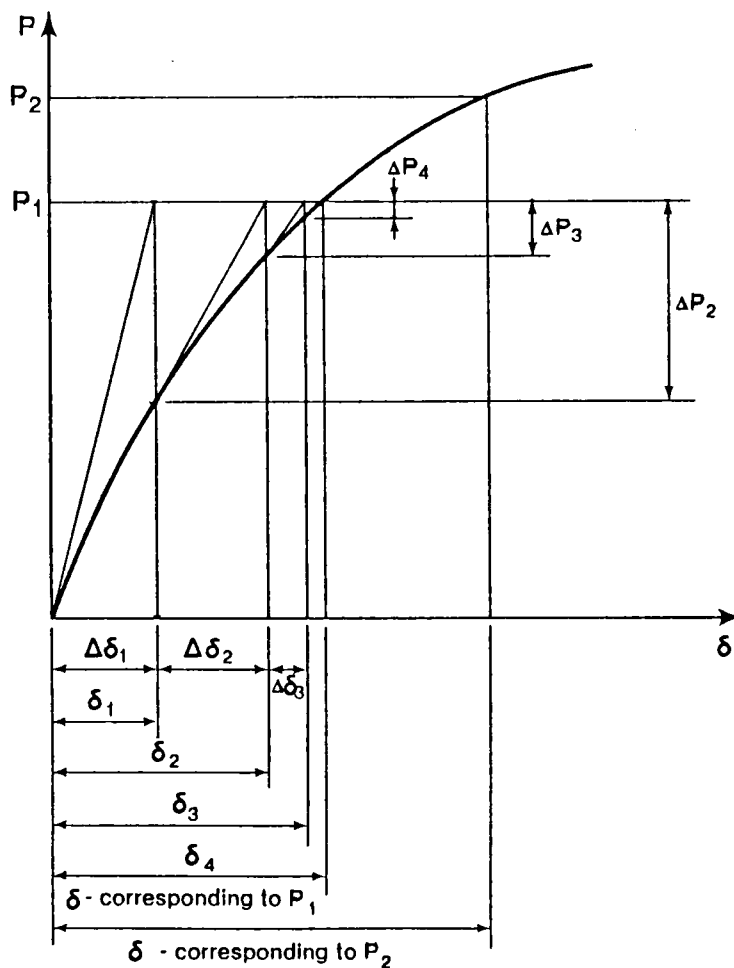


Figure 3.17 Newton - Raphson procedure.

Chapter 4

Verification of the Computer Program in Non-Sway Mode

4.1 Introduction

In order to demonstrate the validity of the predictions of the present program, it is necessary to make some comparisons of the predicted response with the other established results. In this chapter, an account of such comparisons will be made with reference to the non-sway case, whilst validation with the sway case is dealt with in the next chapter. Comparison with some available analytical work will be made first, followed by a further check against full scale frame test results. Once necessary verification of the computer program has been carried out, the program can be used for an extended investigation to study the influence of various parameters, which would eventually obviate conducting extensive and expensive experimental programs.

4.2 Load Deflection Analysis

The computer program as described in the preceding chapter, can be used to generate the complete load-deflection path for framed structures. The general procedure for obtaining the load-deflection response in a second order analysis is to apply load in an incremental fashion – allowing it to incorporate the changing geometry as well as the presence of axial force.

4.2.1 Load-Deflection Response of a Perfect and Imperfect System

A complete load-deflection response of the non-sway portal frame shown in figure 4.1(a), is considered. Two concentrated loads of equal magnitude are applied incrementally up to the failure of the frame. If the frame is geometrically perfect, and if the loadings are such that no primary bending moments are present in the members before buckling, there will be no lateral deflections in the members until the load reaches the critical value, P_{cr} . At the critical load, P_{cr} , the original configuration of the frame ceases to be stable and with a slight disturbance, the deflections of the members begin to increase indefinitely. However, if the system is not perfect, lateral deflections will occur as soon as the load is applied. The latter system is suitable to trace a complete load-deflection curve. For the framed columns of figure 4.1(a) three different cases have been considered:

1. Perfect system
2. Imperfect system – a sinusoidal initial shape of the column with an initial deflection at column mid height equal to $L/1000$.

3. As in (2) with an initial deflection at column mid-height equal to $L/10000$.

A parabolic distribution of residual stress was assumed in all the members of the frame of figure 4.1(a). The results of the three cases (1), (2) and (3) have been presented in figure 4.1(b). For perfectly straight columns the behaviour represents a case of bifurcation, where the columns remain perfectly straight throughout the loading history and start to deflect without bound when the critical state has been reached.

With a specified imperfection, the columns start to deflect with the application of load and traces a definite load-deflection path – depending on the magnitude of the imperfection as shown in figure 4.1(b). It can be noted that whatever be the load-deflection path, the ultimate load carried by the column is virtually the same, in all three cases.

The columns of the portal frame shown in figure 4.1(a) can be idealized as a single isolated column as shown in figure 4.1(c). With an initial out-of-straightness of the form of a half sine-wave defined by

$$y_0 = \delta_0 \sin\left(\frac{\pi x}{L}\right)$$

where δ_0 is the amplitude of the crookedness at the mid-height of the column and L is the length of the column.

Writing the differential equation of equilibrium and solving with appropriate boundary conditions it can be shown that the lateral deflection of any general point at a distance x from the origin is given by [68],

$$y = \left(\frac{\frac{P}{P_e}}{1 - \frac{P}{P_e}}\right) \delta_0 \sin\left(\frac{\pi x}{L}\right)$$

where P is the applied load and P_e is the Euler buckling load.

At a load level of $P=100$ kN and an initial central deflection of $L/1000$, the lateral displacement (relative) at the column mid-height is computed as 0.230 mm against the program predicted displacement of 0.235 mm, differing only by slightly over 2 per cent.

4.2.2 Effect of Increment Size in a Load Deflection Analysis

As described earlier, the incremental iterative approach used here allows the load increment size to be large enough not to become an economic hazard, in terms of CPU time.

Figure 4.2(a) shows the result of the study by Tebedge and Tall [85] emphasizing the effect of load increment size in a simple incremental technique. A cantilever column with an initial out-of-straightness assumed as $v_0 = (1 - \cos(\frac{\pi z}{L}))$ was analysed up to failure for a free end initial deflection value, v_0 , of $L/500$. Clearly the results of Tebedge and Tall are improved as the load increments become smaller. On the contrary, figure 4.2(b) shows the result of an incremental iterative approach using the present program. The problem in this case involves the analysis of the pinned portal shown in figure 4.1(a). Each column with a specified initial out-of-straightness of $L/1000$ was loaded by a concentrated load at the upper end. Use of three different increment sizes namely 10kN, 20kN, and 30kN produced essentially the same load deflection response. The displacement plotted here is the lateral deflection at the middle height of the column. A comparative estimate of the CPU time is also included in figure 4.2(b) for the

three cases considered. The marked reduction in CPU time, to less than 49 per cent of the reference level for a change in increment size from 10kN to 30kN was observed without noticeably losing any accuracy.

4.3 Behaviour Under Uniformly Distributed Load

As no test result can be found for a frame with semi-rigid connection under uniformly distributed loads attempts have been made only to demonstrate the response of a simple portal frame subjected to uniformly distributed beam load. Two idealized cases of joint behaviour are considered i.e. the rigid joint and the pinned joint.

The non-sway portal frame of figure 4.3(a) was subjected to uniformly distributed load up to failure. Two extreme joint conditions, namely the rigid and the pinned have been considered for the beam-to-column connections. Complete load-deflection responses for both of these cases were obtained. The load-deflection response for the rigid case is shown in figure 4.3(b) and for the pinned case is in figure 4.3(c). Both figures also include the responses obtained from another program [86] available in the department, which is regarded to be a reliable code for the analysis of rigid frames. Excellent correspondence in the elastic range can be observed between the results obtained from the two sources indicating that the general procedures for uniformly distributed load representations are reliable. However, in the inelastic region, the present program underestimates the ultimate load when compared to the prediction of ref [86]. Since the modelling of the inelastic action is approximate in the both cases some differences in behaviour can be expected. This matter will be addressed later in this chapter

in the context of comparison with the experimental results.

4.4 Comparison With Full Scale Frame Tests

In this section, comparison between the experimental and the analytical results will be reported. Tests on full scale frames are expensive and are therefore limited in number. There had not been any test results available for full scale semi-rigid frames until 1986, when Building Research Establishment (BRE) in a joint project with Hatfield Polytechnic and the University of Sheffield conducted a series of five full scale frame tests to study the influence of flexible connections on the overall frame behaviour. The two of these tests were conducted by Davison [32] as the Sheffield University part of the study and are referred to as Sheffield University Frame-1 (SUF1) and Sheffield University Frame-2 (SUF2). In the following sections comparison of results of SUF1 and SUF2 with the predictions of the present program are made.

4.4.1 Description of the Test Frames

SUF1 and SUF2 are two dimensional frames fabricated with the same sections and connection components as previously used in the connection tests by Davison [32]. This was done in order to ensure that an appropriate measure of connection stiffness could be accounted in the frame behaviour, from the replicated connection tests. The main structural members were of the same size, 254x102 UB22 beams and 152x152 UC23 columns. In SUF1, the beams were connected to the column flanges, while in SUF2 the beams were connected to the column

webs. In both cases top and bottom flange cleat connections were used. Figure 4.4(a) and 4.4(b) show the layout of the frame as tested and as viewed from the laboratory balcony. The frames were two bays in width, each 4.95 m wide and three stories in height – each 3.6 m high. These dimensions were chosen in the reference [32] as being representative of office construction and suitable for the beam size selected as well as conforming the available space in the laboratory.

Both frames were tested in the non-sway mode. Out-of-plane buckling and lateral displacements were prevented by bracing. Figure 4.5(a) shows the beam, the column and the frame bracing positions. Each column had a fixed base detail with a heavy base plate securely bolted to the strong laboratory floor.

Figure 4.5(b) shows the nomenclature used for the frames in general, and will be referred accordingly in the remaining part of this chapter. Each column and beam section was measured at regular intervals along its length. Cross sectional dimensions and properties of the beams and columns as measured before the actual test was conducted, appear in Appendix A.

Material properties like yield strength and modulus of elasticity varied widely from section to section as listed in [32]. An average yield stress of 285 N/mm^2 and modulus of elasticity of 210 kN/mm^2 can be regarded as reasonable for any interpretation of the test results.

Davison carried out residual stress measurements for a number of lengths taken from the columns used for the frame tests. The results of these tests indicated that residual stress distributions were rather erratic along the column length and, as such, no set pattern could be selected as being representative of residual stress in columns. The cause for this was attributed to the roller

straightening process.

The test frame had initial deflected shapes as described in figure 4.6(a) and (b) for frame 1 and frame 2 respectively.

The loading system was arranged in such a way that each beam was loaded independently at the quarter points by a spreader beam. Axial loads in the columns were also applied independently to the heads of the column. The frames were adequately instrumented in order to measure the applied loads, the distribution of forces round the frame, the deflections and the moment-rotation responses of the connections. A total of five main tests were performed on these Sheffield University Frames SUF1 and SUF2. These tests have been referred to elsewhere [87] in the generic name SUF_{xy}. For example, SUF12 would mean frame 1 test no. 2 and so on. A brief account of the procedures of two of these tests, the results of which have been considered here for comparison follows.

4.4.1.1 Test Procedure for SUF12

In this major axis frame test (where the columns were bent about their major axes) the columns were loaded to failure under a combination of beam loading and column loading applied to the two three storey high columns as in figure 4.4(a). The five beams of SUF1 were loaded incrementally to a level corresponding to the unfactored dead loads. Beams 2, 3, 4 and 6 were again incrementally loaded to levels corresponding to factored dead and imposed loads, while beam 5 was kept at unfactored dead load. At the end of beam loading, direct axial loadings were applied at the top of the column in positions 2 and 3 to 250 kN in five increments. The column in position 2 was then loaded to failure while the load on column 3

remained constant, after which column 3 was also incrementally loaded to failure.

The axial deformations on both columns were then released, the beam loads reduced to 53 kN per beam and eventually all loads removed from the structure.

4.4.1.2 Test Procedure for SUF22

This was a test where columns were bent about their minor axes. As in the case of SUF12, the beam loadings were carried out in the same fashion. After the beam loading phase, the three columns were loaded under axial deformation control in three increments of 1.0 mm and the resulting applied loads were recorded. Column 1 was then axially deformed to failure in successive increments of 1.0 mm initially and 0.5 mm near failure. Column 2 was then similarly loaded to failure, after which the applied column loads and beam loads were removed, in that order.

4.4.2 Comparison of the Test Result with the Prediction of the Present Program

The tests described in the preceding section have been modelled by the present program. For the analytical model the modulus of elasticity of the material was taken as 210 kN/mm^2 and a yield strength of 285 N/mm^2 was assumed. The cross-sectional dimensions for the members were taken as the average value of the dimensions measured before the test.

The connections in the analysis were modelled as semi-rigid joints rep-

resented by the B-spline fitting of the experimentally obtained moment-rotation curves shown in figure 4.7. It should be mentioned here that the $M-\phi$ relationships shown here are the outcome of replicate connection test carried out by Davison [32], before the frame tests have been conducted. Davison [32] and later Mugisa [87], both analysed the results of the frame tests and concluded that the connections in the frame behaved more or less in a similar fashion as they did in the connection tests, a fact also corroborated in the 3-D test scheme by Gibbons [88], especially in the case of a loading connection.

The loading pattern was chosen to be close enough to that adopted in the test schemes. Tables A.1 and A.2 of Appendix A, show the beam loading history of the major and minor axis frames respectively and table A.3 presents the loading history for the analytical model. Comparison of the analytical and experimental results on SUF1 and SUF2 are presented below:

4.4.2.1 Sheffield University Frame 1

The response of the beams of frame-1 under the beam loading phase appears in figure 4.8(a) to 4.8(e). The load deflection curves obtained from the test and analysis are plotted with the quarter point load value against the central deflection of each beam. Deflection of the beams are reported relative to their ends.

After the beam loading phase, columns in position 2 and position 3 were loaded up to an additional value of 250 kN each. Load on the external column was then held at 250 kN while the central column was progressively loaded to cause failure. The central column was failed at an additional load of 550 kN –

against a test failure load of 483 kN.

In a separate run, both of the above columns were loaded up to an additional 250 kN each in the same way, after which the external column was loaded up to failure, keeping the load on the central column at 250 kN. This resulted in a failure load of 610 kN (additional) for the external column. The corresponding failure load obtained from the test was 623 kN.

The latter scheme is slightly different from the test loading, in the sense that during the test the central column was loaded up to 483 kN (which is the test failure load) and then released to a value of 415 kN, while loading on the external column was started to cause its failure. In order to check whether this difference really matters or not, another run was made where the central column was loaded up to 490 kN (loading up to a level of 250 kN column load on either column was done as in the previous cases) and then the external column loaded up to failure. This also produced the same failure load of 610 kN as in the previous case.

Table 4.1 compares the additional column load required to fail the external and the central column of frame-1 with the corresponding test values. Prediction of the computer program SERVAR, as reported in reference [32] is also included in the table. The superiority of the present program is clearly demonstrated. However, the factors which might have caused these differences in failure load will be discussed later in section 4.4.3.

Figure 4.9 shows the comparison of the load-deflection response of column 7. The load transmitted to the column was plotted against its central deflection. The difference in column response to the beam loading phase and column loading phase is clearly apparent. The predicted response is fairly close to

the experimental results. During the column loading phase the prediction of the displacements is slightly higher than that of the test. Similar behaviour were also reported by Davison when he analysed the frame with the program SERVAR.

The bending moment distribution around the frame at a beam load level of 54 kN per beam is compared in figure 4.10 with the bending moments obtained from the test at or near the same applied load. A good correspondence between the test and the predicted values can be seen.

4.4.2.2 Sheffield University Frame 2

A comparison of the predicted response of the minor axis frame with the test result is reported here. The beam loading was applied in a similar way as in the test SUF12, but the exact values of the applied loads in different stages appear in table A.3. A comparison of these values with the applied test load (table A.2) would show some difference, although this should not have any bearing on the predicted response.

The responses for beams nos. 1 to 6 are reported in figure 4.11 (a) to 4.11 (f). As in the case of SUF1, the load-deflection response reported here shows the beam quarter point load as the ordinate and the central deflection on the abscissa. Beam deflections are measured relative to their ends. The predicted responses compare favourably with the measured responses, given the limitation of the comparison made herein and which is discussed later in this chapter.

Upon completion of the beam loading, the external columns were loaded up to a load of 150 kN each and the central column was loaded with 120 kN, after which column in position 1 was loaded up to failure. A failure load of 540

kN was observed. During the test the column in position 1 sustained a load of 451 kN.

When column in position 2 was loaded to failure (with loads on the other two columns kept constant at 150 kN), a failure load of 470 kN was predicted against an observed test failure load of 412 kN.

Table 4.2 tabulates the failure loads for both test and analysis for column in position 1 and 2. The predicted failure loads for both external and internal columns were higher than the actual load sustained by these columns in the test. For the external column the actual failure load was 84% of that predicted and for the central column this figure was 88%. Considering the limitation of the present comparison (see sec 4.4.3) this difference is not very significant.

The load-deflection behaviour of the column in position 1 is represented by plotting the load in the top lift (column 1) against the central deflection of the same column as shown in figure 4.12 (a). A close prediction of the column's central deflection is noticed during the beam loading phase and in the early part of the column loading phase up to a load of 300 kN in the column, after which the test column begins to soften rapidly leading to failure. However, the analytical results show a rather stiffer response in this top lift column. The initial shape of this column (see figure 4.6) coupled with the presence of any residual stresses in the section might have contributed to its soft response in the test.

The load deflection behaviour of the central column is presented by plotting the load against the central deflection of its middle lift (ie column 5) in figure 4.12 (b), which shows good correlation between the predicted result and the test performance. In the analysis this central column shows virtually

no lateral displacement up to the application of unfactored dead load in all the beams. After that, when the unsymmetrical loading has started, the column started to deflect rapidly and continued to do so until the end of beam loading. In the third phase of figure 4.12(b) the response of the column can be observed under column loading which shows a fairly stiff load-displacement behaviour. On the other hand, although the test response follows the same behaviour initially, it tends to deflect more than its analytical counterpart. One of the reasons for this can be appreciated by noting the actual initial shape of the test column as shown in figure 4.6. For this particular column the initial shape was favourable to the applied beam loading pattern.

4.4.3 Limitation of the Comparison

The comparison presented in the preceding section will now be examined in order to establish the extent to which the finite element model developed here represent the physical tests. It must be emphasized that an exact reproduction (or duplication) of physical tests by any analytical approach is never possible due to the complexity of the problem, the variability of the physical parameters, and the inevitable variation in material, fabrication process as well as measurement during the test. However, sound judgement to interpret the acceptability of any such result should be based on adequate consideration of the extent to which the above mentioned factors have been nullified. In the context of the present problem, an account of the factors that might have influenced the result is made here:

1. The physical properties of the cross-section as well as the material properties varied over a considerable range in the tests (see Appendix A). The wide variability in material and member properties normally encountered in practice are reflected. Although analytical modelling covering this variability is beyond the scope of this study, a knowledge about extent of this variability would be helpful for the understanding of the results presented.
2. The moment-rotation behaviour of the connections are reported [32], [87] to be similar in the frame and in isolated beam-column assembly. Based on this premise, the analysis program utilizes the $M-\phi$ characteristics of the connections as obtained from the connection test [32], which was a cruciform arrangement test and are therefore representative of the interior column connections. However, as no relevant $M-\phi$ relationship appropriate to the external column connections (cantilever arrangement) were available, the same behaviour has been assumed for all the connections irrespective of whether it was an internal or an external connection.
3. Residual stresses present in the off-cuts of the column were heavily influenced by cold straightening of the section [32]. As no well defined pattern could be assumed, these residual stress were in fact not included in analysis. However, this should not be an important short-coming during the beam loading and early part of the column loading, when all of the sections remain essentially elastic. The early softening of the central column during the test could be attributed to the presence of residual stress, which might have caused an earlier onset of material nonlinearity and a corresponding reduction in column strength.

4. The initial shape of the columns were not straight, neither they were initially deflected in a fashion that could be included in the present analysis. So in analysis, the columns were assumed to be initially straight.
5. The loads applied at the column head during the test were in fact acting eccentrically due to the rotation of the column stub above top beam level [32]. This will have induced some additional moment at the column head, resulting in a lower test load than the analytical prediction.

4.5 Concluding Remarks

In this chapter the predictions of the computer program, described in chapter 3, were compared with the available results. Comparison was made against analytical, numerical as well as full-scale test results in non-sway situation. Results of the comparisons have been critically examined and discussed. It is found that the prediction of the present program is reasonably accurate in representing the behaviour of flexibly connected frames. The program was, therefore, judged suitable for conducting extensive parametric studies.

Column designation	Test	Present program	SERVAR [32]
Ext. Col	623 kN	610 kN	735 kN
Central Col	483 kN	550 kN	609 kN

Table 4.1 Comparison of the additional column failure loads for SUF1.

Column designation	Test	Present program	SERVAR [32]
Ext. Col	451 kN	540 kN	N/A ^a
Central Col	412 kN	470 kN	N/A ^a

^aDoes not allow a minor axis bending to be examined

Table 4.2 Comparison of the additional column failure loads for SUF2.

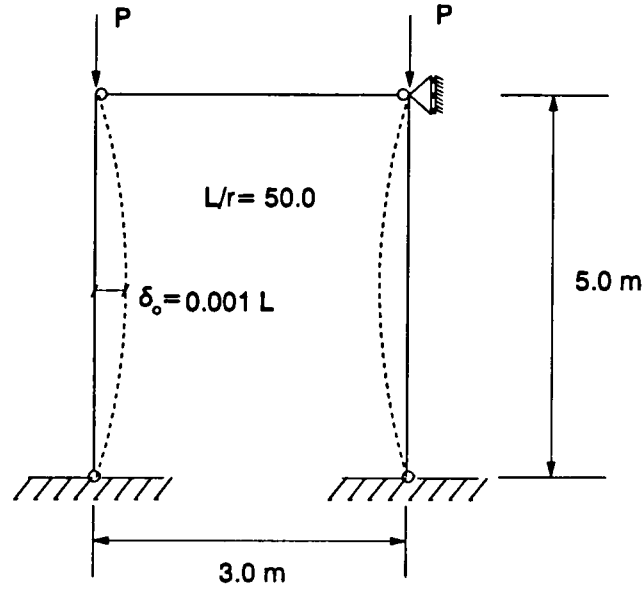


Figure 4.1 (a) Pinned portal used to generate load-deflection response for the column.

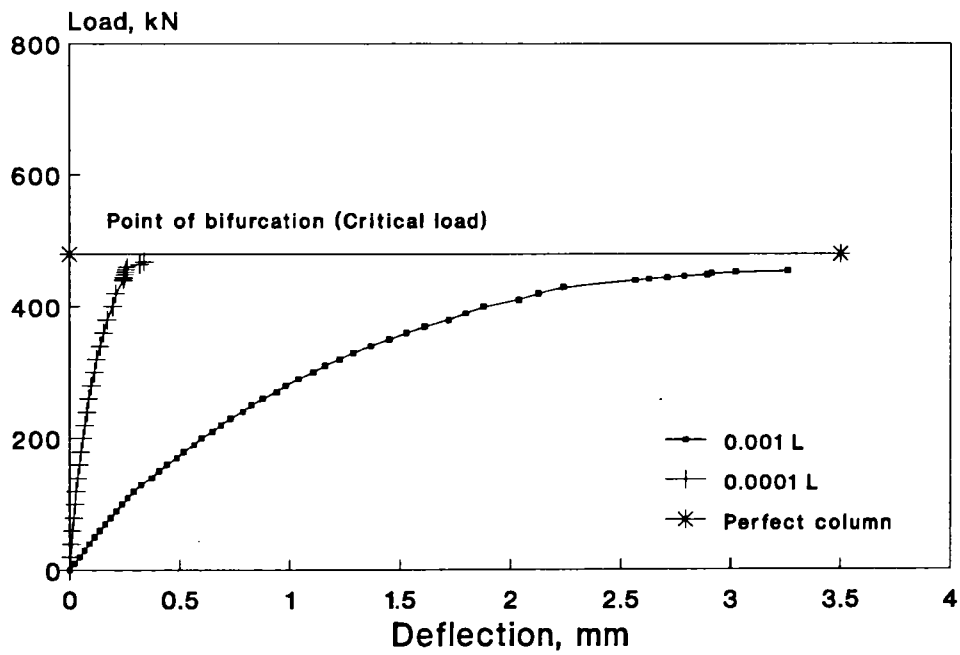


Figure 4.1 (b) Load-deflection behaviour of geometrically perfect and imperfect concentrically loaded column of figure 4.1(a).

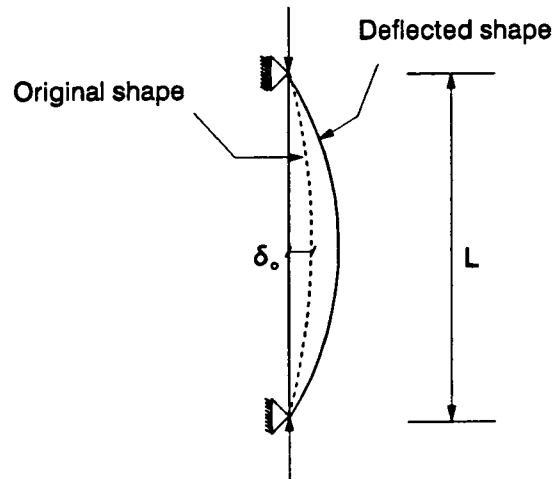


Figure 4.1 (c) Pin-ended idealized column with geometric imperfection.

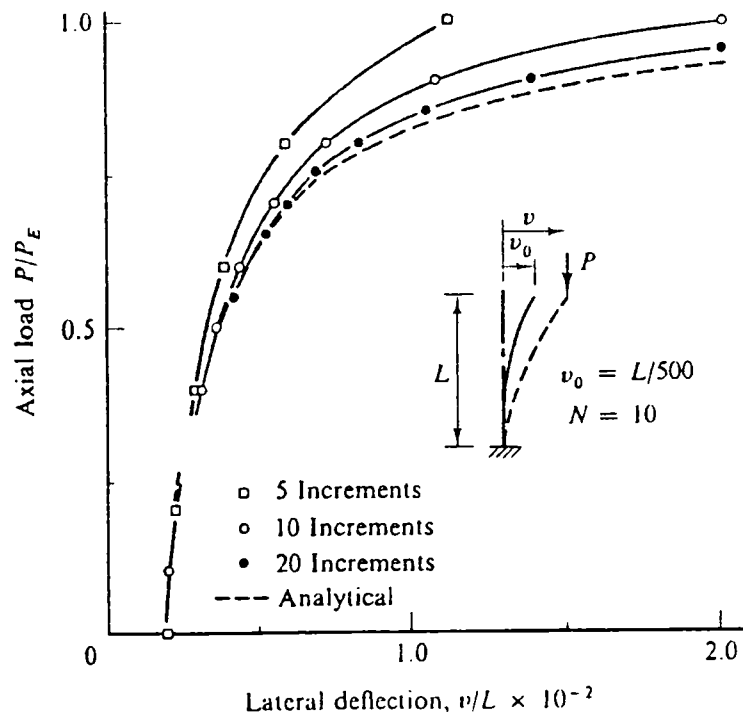


Figure 4.2 (a) Effect of number of load increments in simple incremental technique [85].

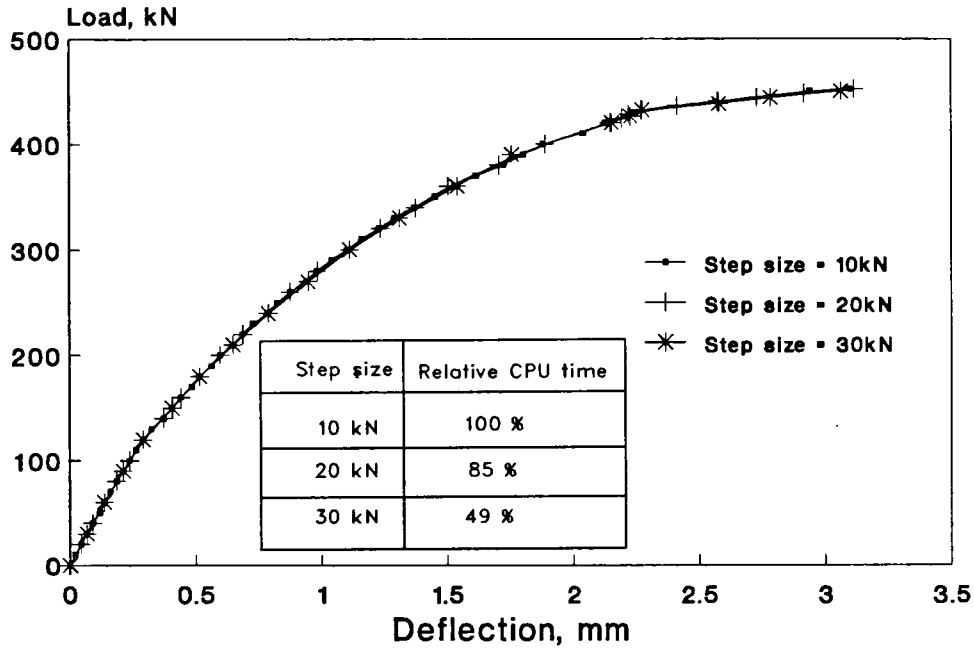


Figure 4.2 (b) Effect of increment size in the iterative incremental analyses.

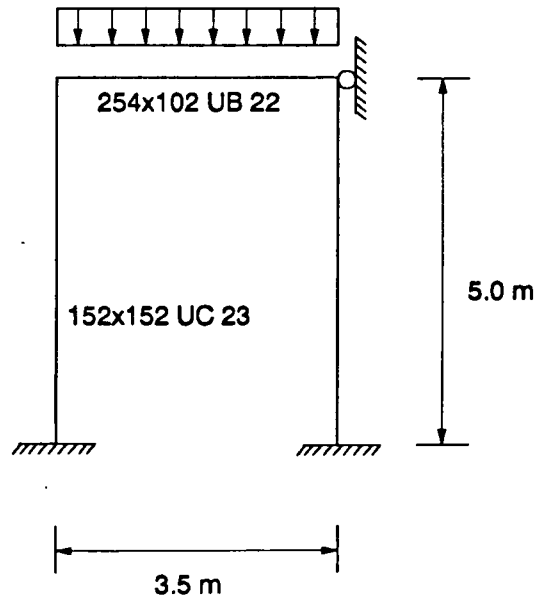


Figure 4.3 (a) Portal frame considered for comparison of the response of the present program with that of the computer program INSTAF [86].

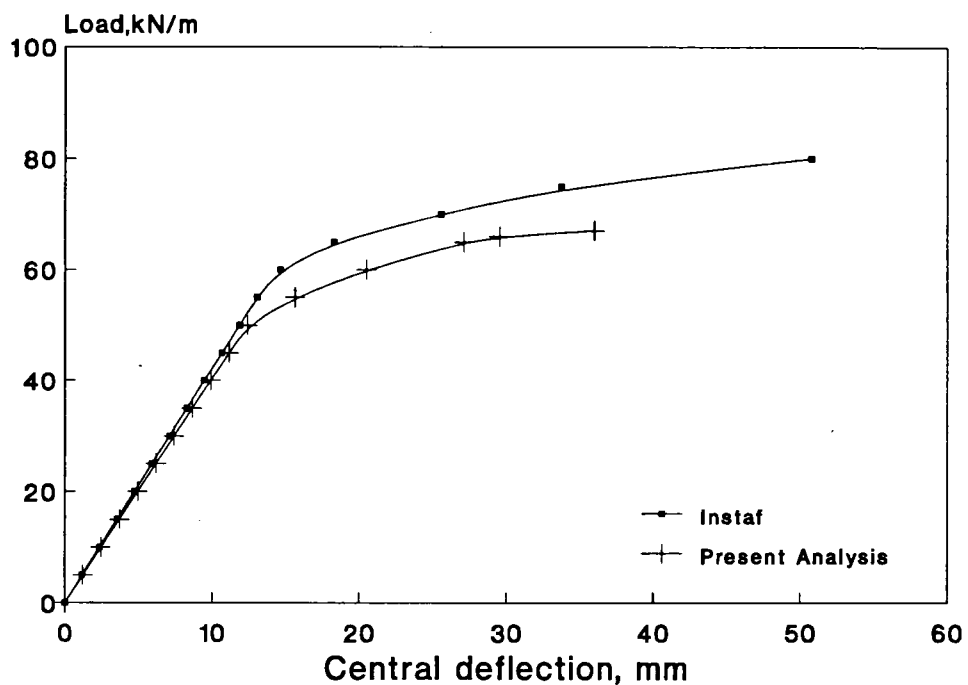


Figure 4.3 (b) Comparison of the load-deflection response for rigid portal of figure 4.3(a).

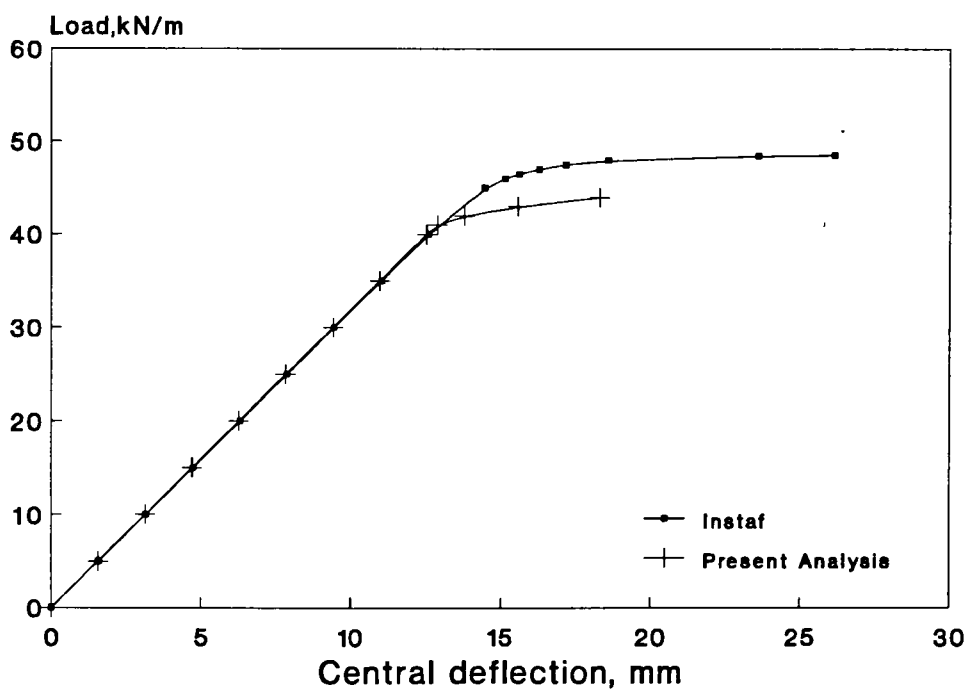


Figure 4.3 (c) Comparison of the load-deflection response for pinned portal of figure 4.3(a).

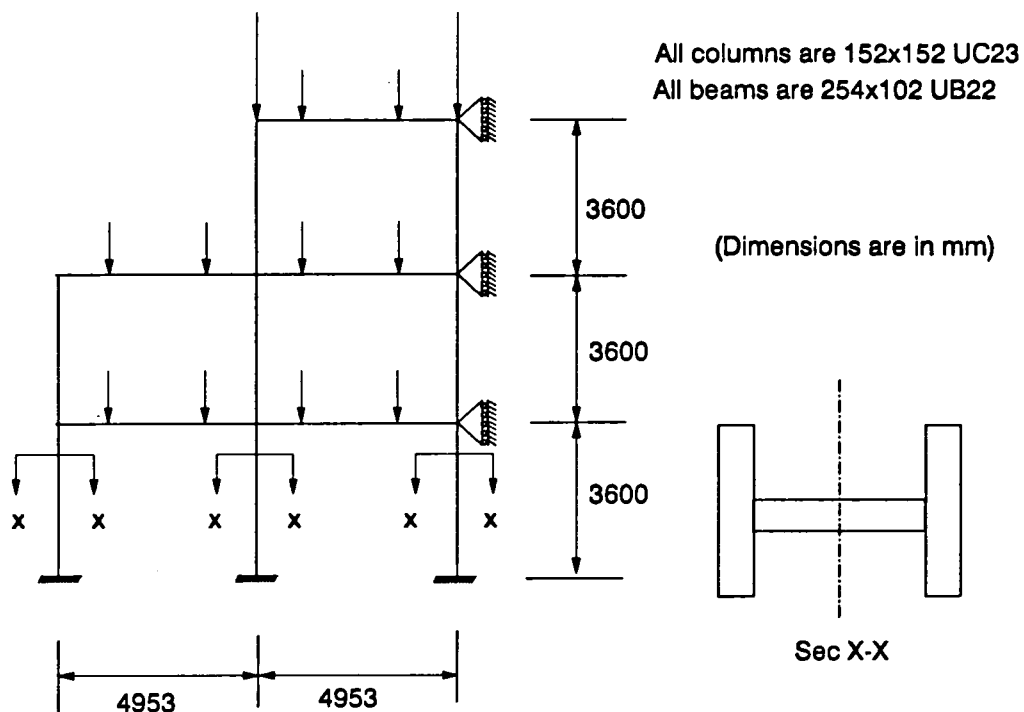


Figure 4.4 (a) Description of test frame SUF1.

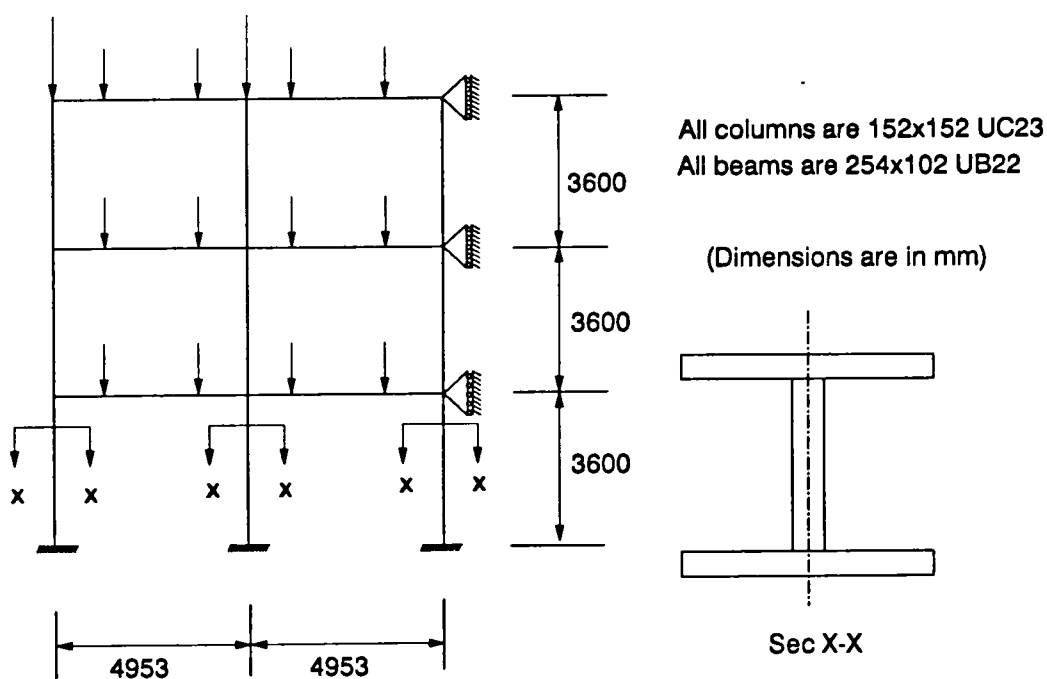


Figure 4.4 (b) Description of test frame SUF2.

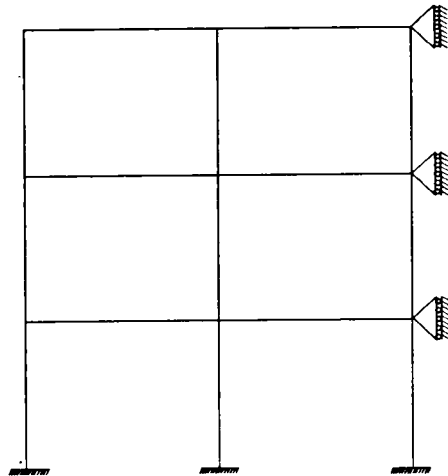


Figure 4.5 (a) Frame bracing locations (in-plane).

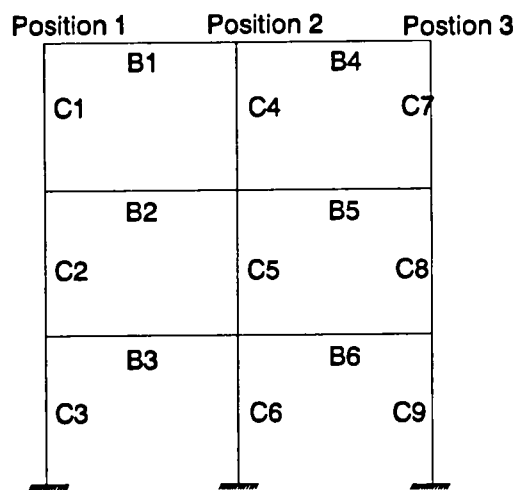


Figure 4.5 (b) Frame nomenclatures.

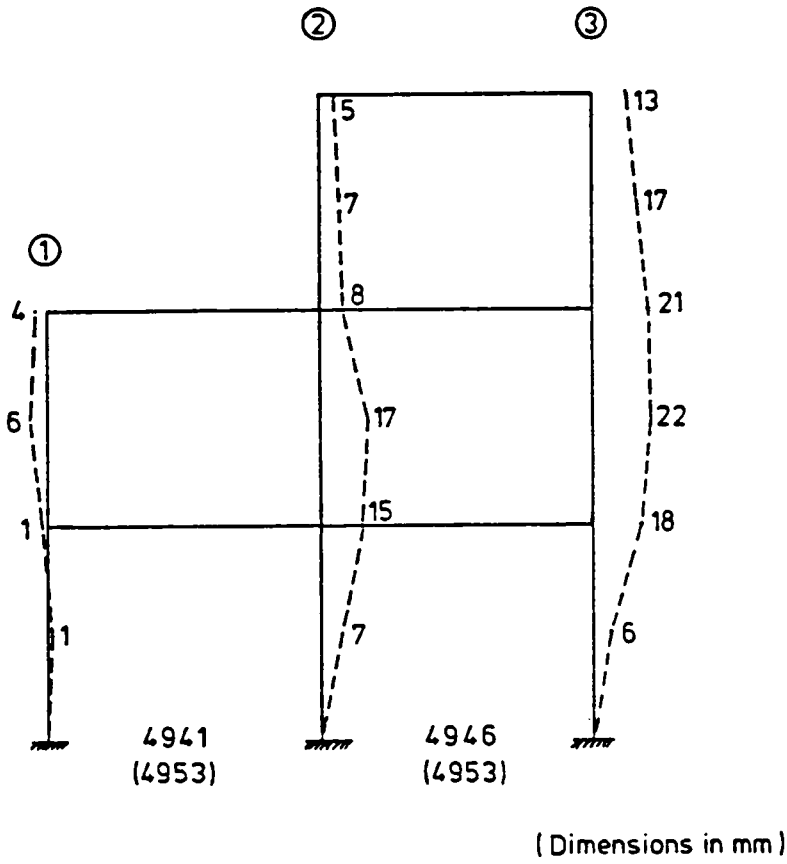


Figure 4.6 (a) Initial shape of SUF1.

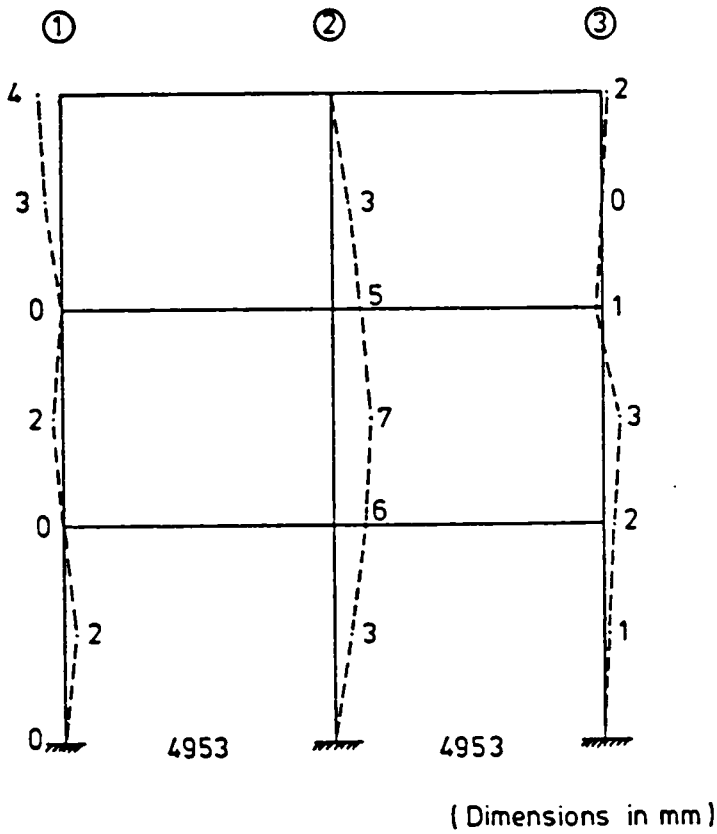


Figure 4.6 (b) Initial shape of SUF2.

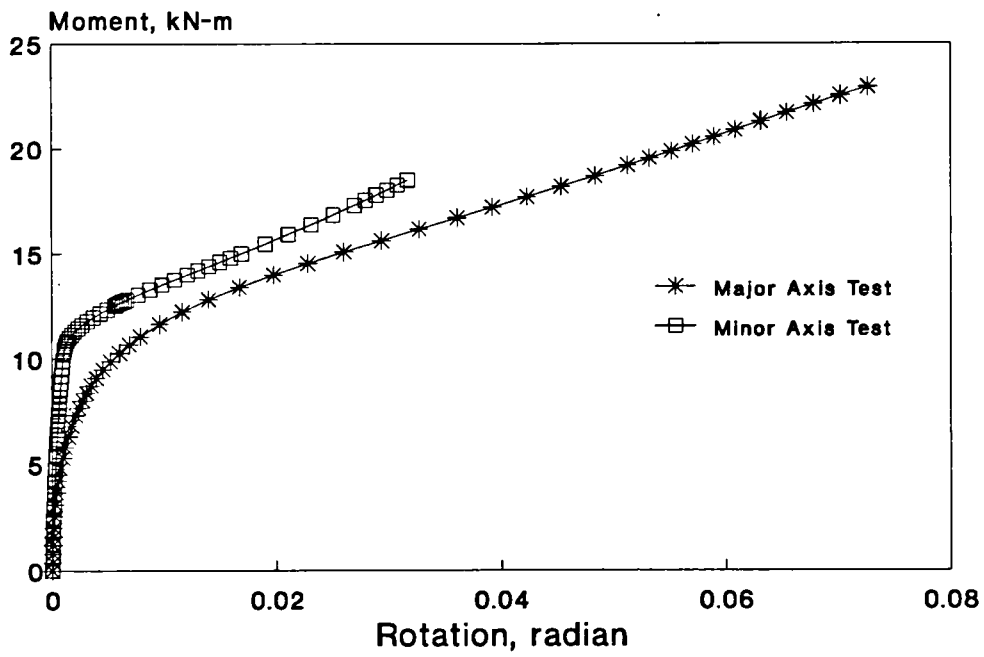
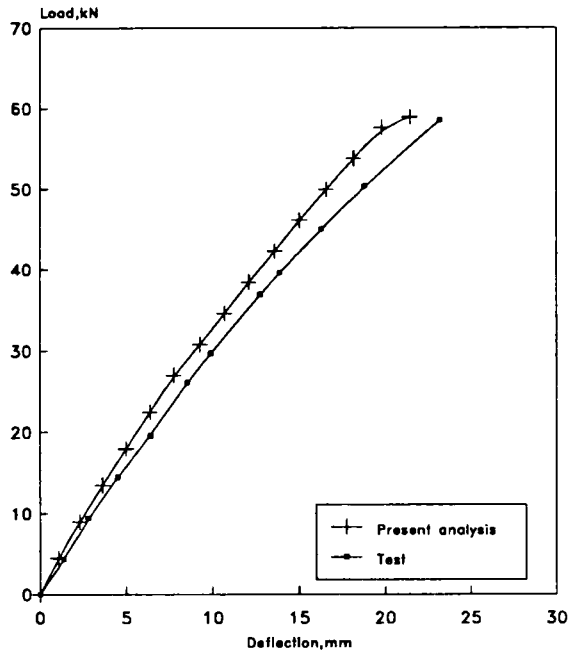
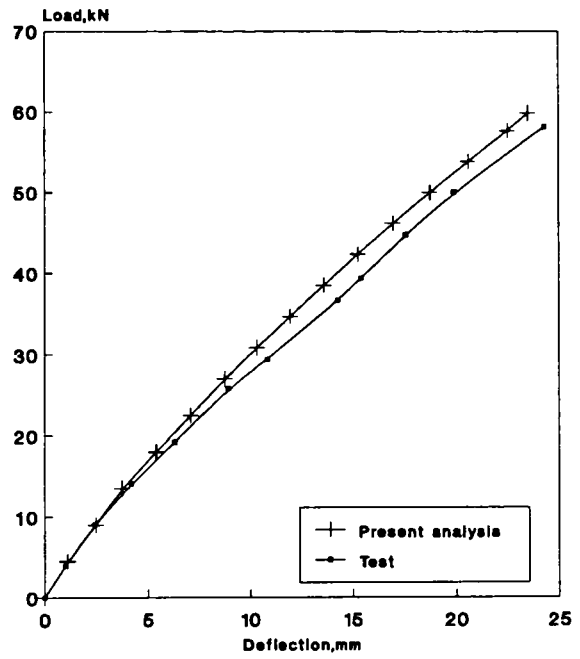


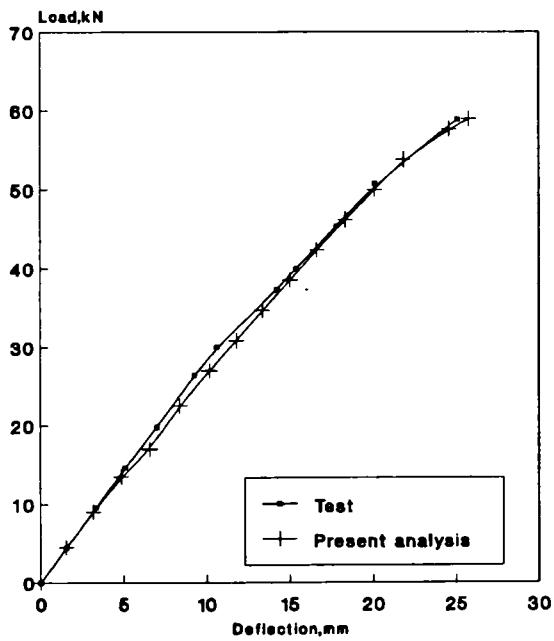
Figure 4.7 M- ϕ behaviour of the connections used in the frame tests.



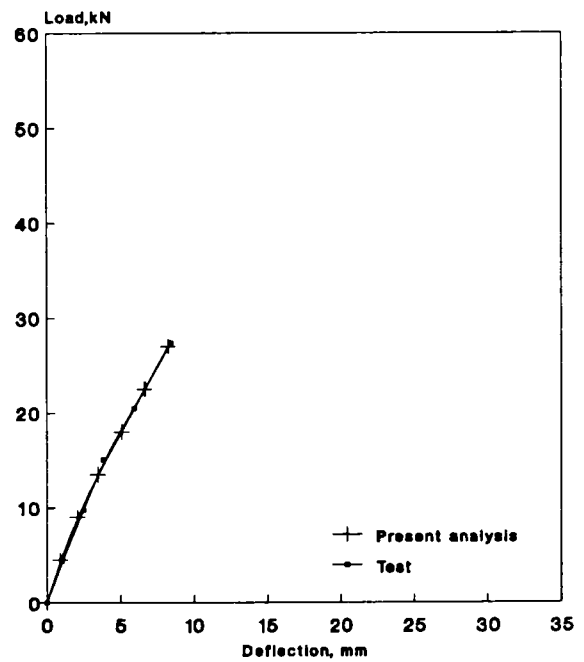
a) Beam 2



(b) Beam 3



(c) Beam 4



(d) Beam 5

Figure 4.8 Comparison of the beam load-deflection response for SUF1.

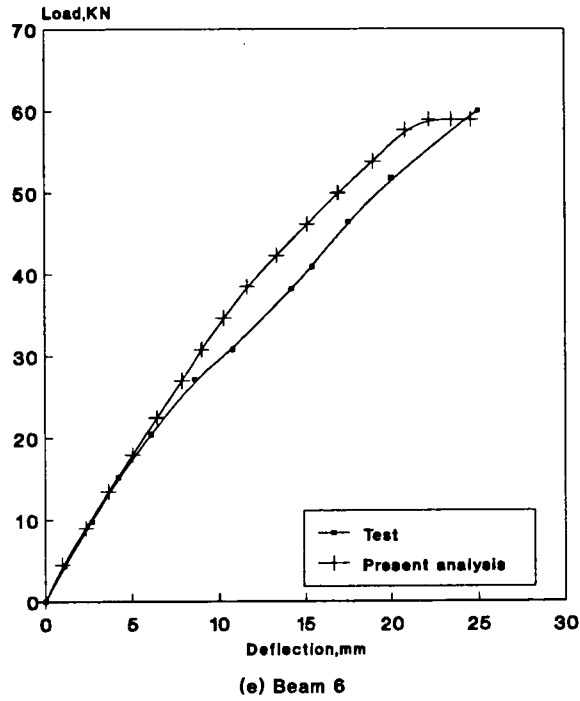


Figure 4.8 Comparison of the beam load-deflection response for SUF1.

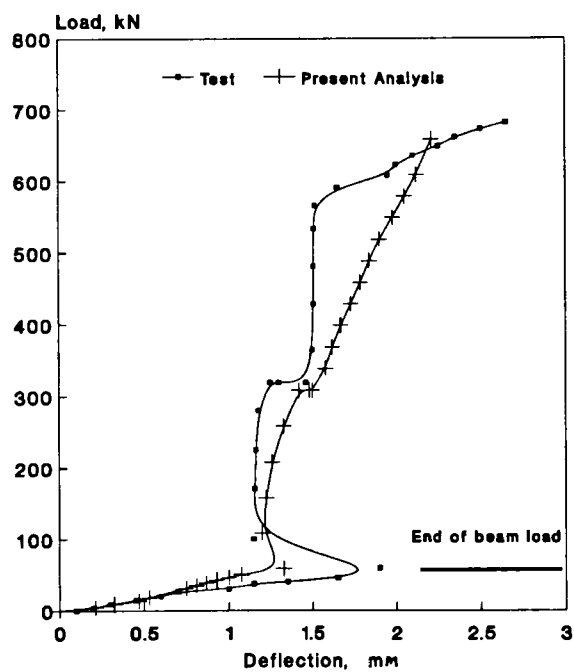


Figure 4.9 Comparison of the column (C-7) load-deflection response for SUF1.

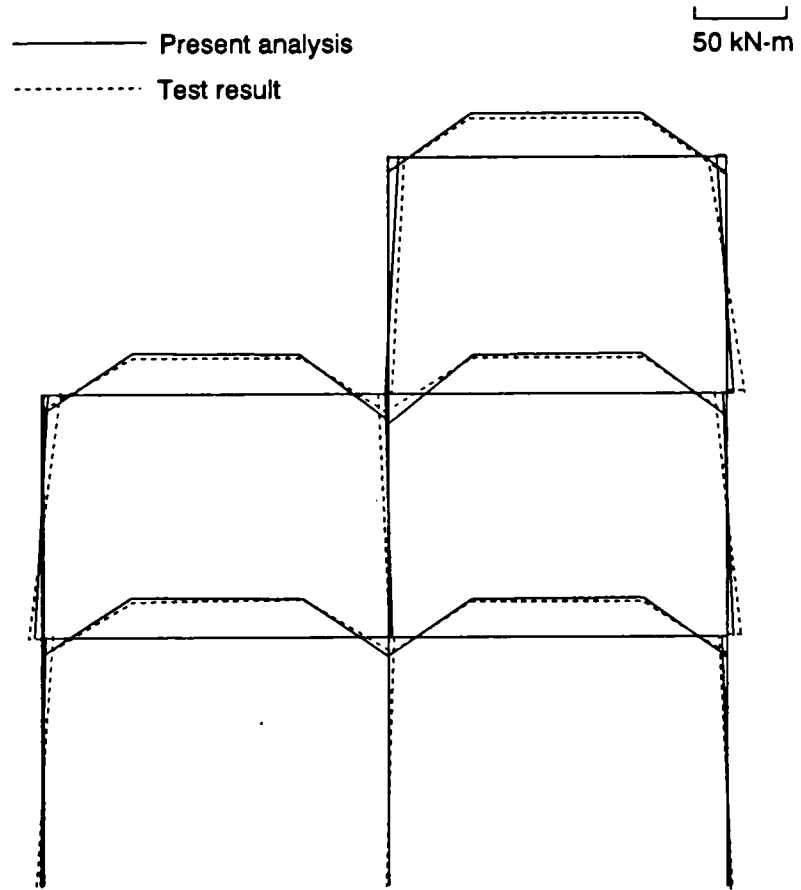
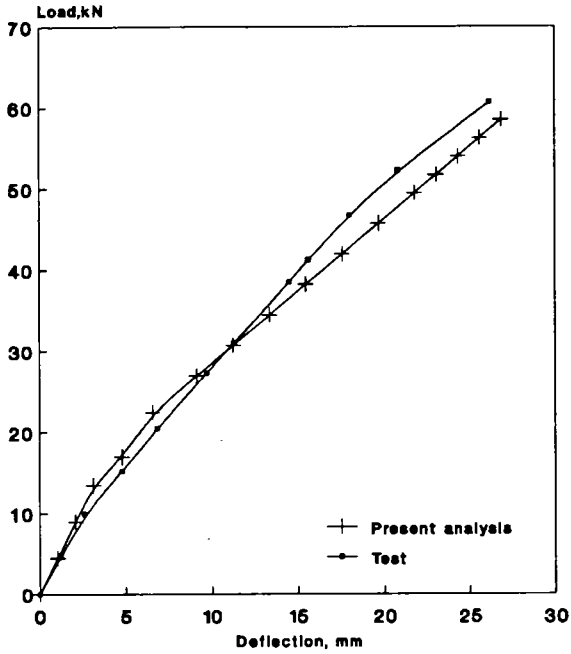
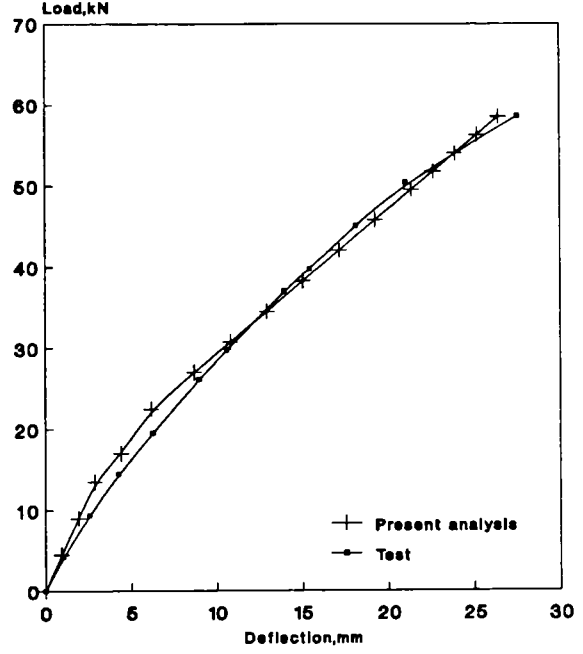


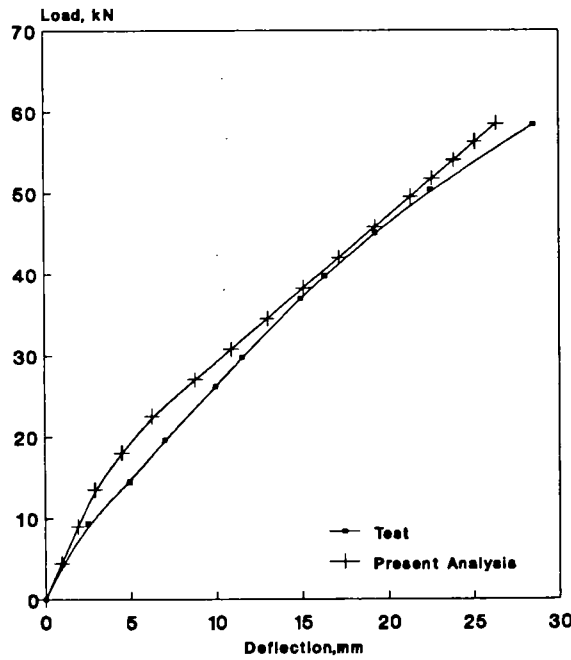
Figure 4.10 Comparison of the bending moments around the frame for SUF1.



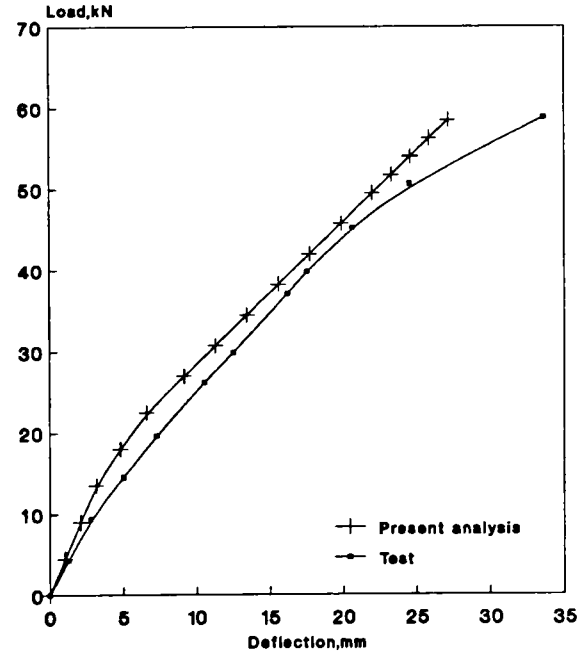
(a) Beam 1



(b) Beam 2



(c) Beam 3



(d) Beam 4

Figure 4.11 Comparison of the beam load-deflection response for SUF2.

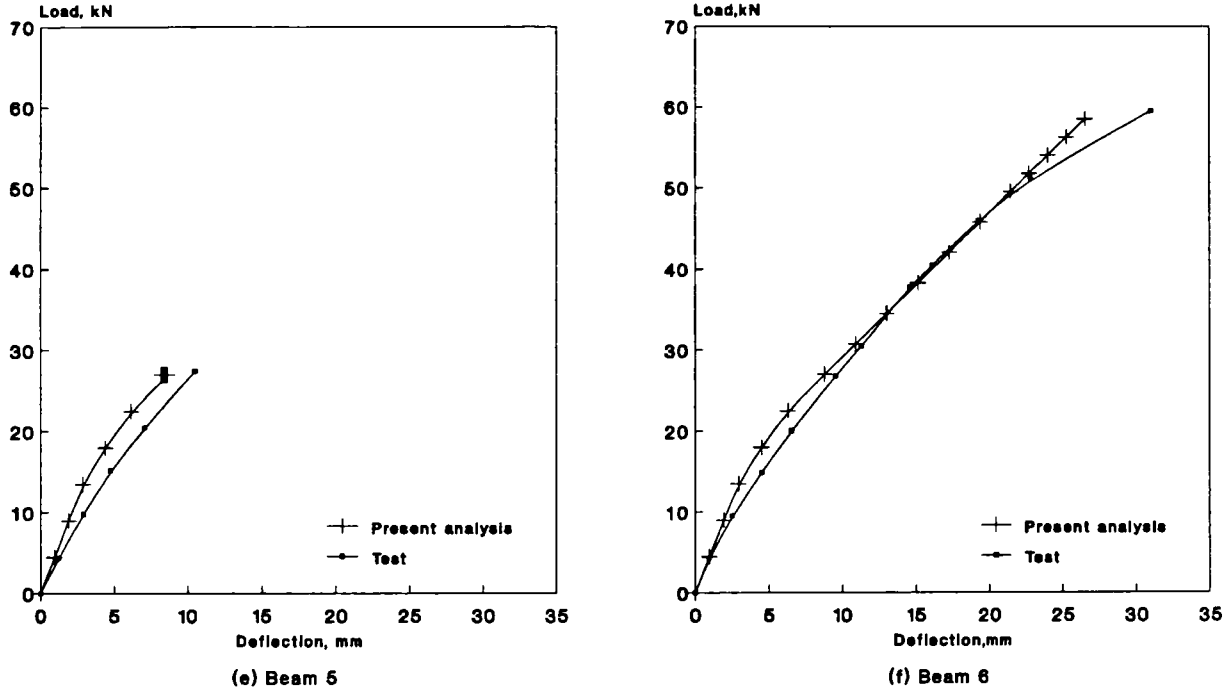


Figure 4.11 Comparison of the beam load-deflection response for SUF2.

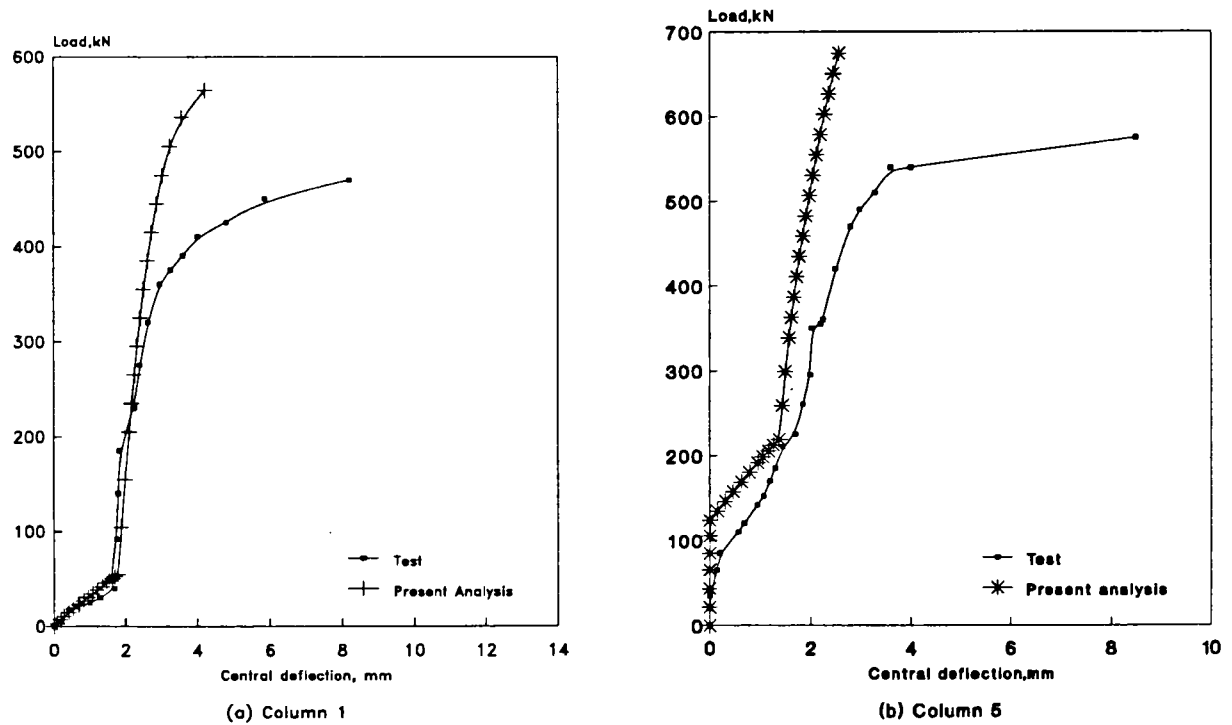


Figure 4.12 Comparison of the column (C-1 and C-5) load-deflection response for SUF2.

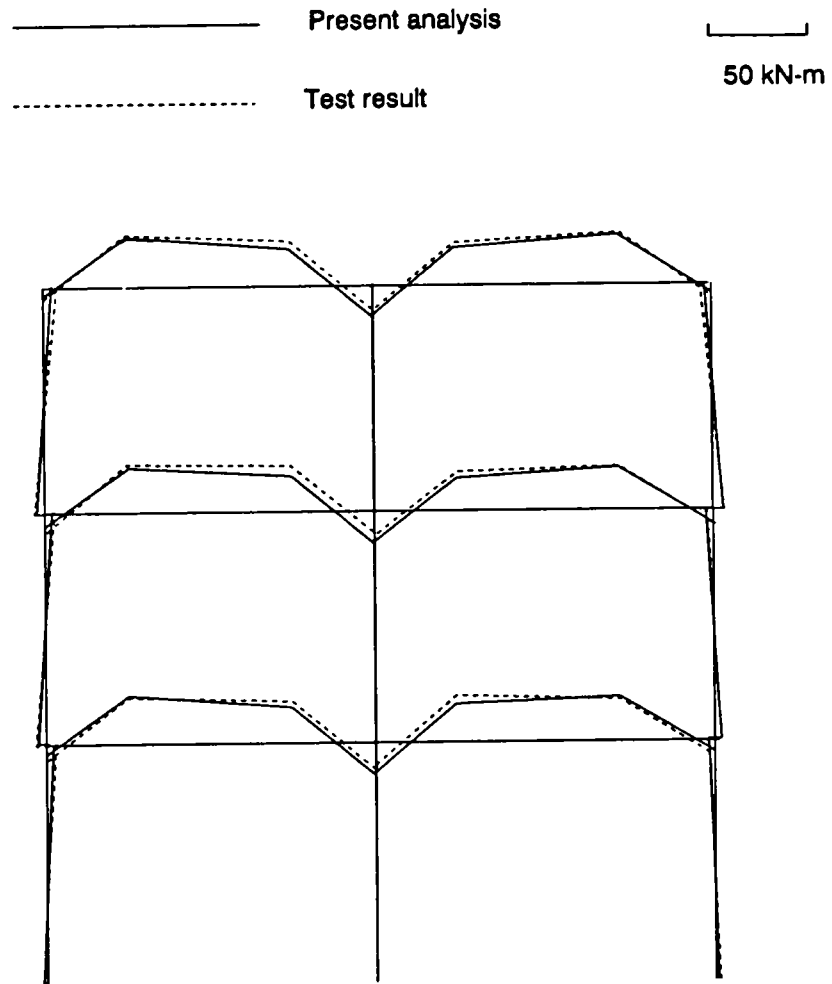


Figure 4.13 Comparison of the bending moments around the frame for SUF2.

Chapter 5

Verification of the Computer Program in Sway Mode

5.1 Introduction

In the preceding chapter the computer program described in chapter 3 was verified by comparing the predicted response with the observed response for frames in the non-sway mode. In a sway restrained case deformations are produced by the gravity loading only. Such deformations are mostly independent of the secondary effects (only $P-\delta$ effect is present but not $P-\Delta$) and are associated with connection behaviour which can be adequately represented by the simplified unloading model adopted in chapter 3. But, in an unbraced frame, secondary effects are more pronounced and connection loading-unloading characteristics need to be modelled in a more sophisticated way especially to handle cyclic loadings. Thus it is necessary to adopt a proper connection model and to show the validity of the

program in the following cases as well:

- Frames loaded by lateral loads
- Frames loaded with both vertical (gravity) load and lateral (wind) load.
- Frames loaded cyclically in the lateral direction to show reliability of the program when connections operate by successive opening and closing.

Unlike for braced frames, the testing of full scale unbraced frames is particularly rare because of inherent difficulties associated with the testing of such frames, in particular testing up to failure could give a potentially dangerous condition. The only known test scheme on flexible sway frames on half scale experiments are due to Stelmack [89]. Results of the various tests carried out by Stelmack at the University of Colorado have been made available to the author by the courtesy of Prof. K. H. Gerstle.

A brief description of the tests appears in the next section. A description of the analytical model and comparison of the predicted and observed responses are made subsequently. The findings of this chapter will also highlight the semi-rigid frame behaviour in cyclic loading cases.

5.2 Description of Frame Tests

5.2.1 General

Stelmack [89] conducted a total of ten tests on two different frame configurations, a one-storey, two-bay frame and a two-storey, one-bay frame. Using these two

geometrical shapes with various combinations of connection size and loading conditions different tests were conducted. Table 5.1 summarizes the various tests, and figure 5.1 and 5.2 show the geometric dimensions of the two configurations considered.

The test frames were fabricated from beam and column members of A36 steel W5 x16 wide flange (US nomenclature) sections. The column bases were pinned. The particular arrangement made at the column base is shown in figure 5.3(a).

The connections used in the frame tests were bolted flange cleat (top and seat cleat as in US) connections. Some of the frames were tested with 1/2 inch thick angles while others had 1/4 inch angles (see table 5.1) made from A36 steel. Details of the beam-column connection are shown in figure 5.3(b). Tests on the connections were performed by Stelmack in identical conditions to those of the frame tests. The moment-rotation characteristics of these two connections appear in figure 5.4 and figure 5.5. The tri-linearization parameters as proposed by Stelmack on the basis of four preliminary frame tests are also shown in the corresponding figures.

The cyclic lateral load was applied statically to the frames, i.e.the rate of application was slow enough so that dynamic effects need not be considered. Some of the tests were performed with lateral loads only, while some included both lateral and gravity loads (see table 5.1). The gravity load of 2.4 kip (10.68 kN) each were applied at locations shown in figures 5.1 and 5.2.

5.2.2 Choice of Tests for Comparison/Validation Purpose

As already mentioned that a total of 10 tests were conducted for various combinations of frame configuration, connection size and loading history. Attempts to model all of these tests analytically is neither possible nor warranted under the purview of this study. The author therefore made a choice of four tests from the reference, namely test-1, test-6, test-9 and test-10 and these will be referred by the aforesaid names for the remainder of this chapter. These tests were chosen because an in-depth description of these four tests was readily available in the reference [89] and they covered the whole spectrum of essential variables. Two of these tests are on one-storey, two-bay and the other two tests on two-storey, one-bay frames having combination of 1/2 inch and 1/4 inch connections and with and without gravity load.

5.3 Analytical Modelling of the Test Frames

A description of the analytical modelling of the test frame is given in this section. The frame dimensions and the finite element idealizations for the one-storey, two-bay frame and the two-storey, one-bay frame are shown in figures 5.6 and 5.7. The column feet were assumed to be frictionless pins. The value of the elastic modulus was assumed to be 20000 kN/cm^2 (29000 ksi) as supplied by Stelmack. The member flexural rigidity was computed as $EI=17550000 \text{ kN-cm}^2$ and an area of $A=30.19 \text{ cm}^2$ was taken from the tabulated standard cross-sectional dimensions for W5x16 sections. Since no measurements of the actual cross sectional dimensions

of the test members were reported in the reference the standard dimensions have been assumed for the members from the AISC manual [2]. No mention of the initial frame member shape was made in the reference, so members were assumed to be initially perfect. As mentioned in chapter 3, in the present program connection stiffnesses are evaluated only at the beginning of any load step, while this should be satisfactory for monotonic loading scheme, special attention is needed if cyclic loading is used. However, this problem can be avoided if at the point of each load reversal, the load steps are kept fairly small. This technique is illustrated in figure 5.8.

5.4 Modelling of the Connection Behaviour

As stated in chapter 3, the present program utilizes a B-spline curve fitting through the experimental $M-\phi$ data points and calculates the stiffness of the connection at any load level tracing the full nonlinear path of the connection behaviour. Unloading of the connection takes place depending on the loading pattern or as failure is approached and consequently an unloading stiffness is required which is evaluated as being equal to the initial stiffness of the connection. While this approach will handle most monotonic loading schemes (whether gravity or lateral wind load), special routines are necessary to deal with the cyclic loading pattern as adopted in Stelmack's test program.

Moncarz [90] used a tri-linearized model for the connection $M-\phi$ response in his linear elastic frame analysis program. The analytical prediction of the Moncarz's program was verified by the test results of Stelmack. For this reason the author decided to implement Moncarz's connection model in the present

program to enable the analysis of frames subjected to cyclic loading patterns. Moncarz's model was based on the assumption that the basic connection parameters required for analysis can be obtained from monotonic connection behaviour. The three stiffnesses k_1 , k_2 , k_3 and two limiting moment values M_{pl} and M_Y that are necessary to define these stiffnesses are shown in figure 5.9. The model makes the following assumptions:

1. Equal positive and negative branches of the initial response curve
2. Unloading will take place elastically with modulus k_1 .
3. Equal positive and negative strength envelopes.
4. Constant elastic range, equal to twice the initial elastic length $[M_{pl}]$ in one direction.

The moment-rotation hysteresis showing these characteristic assumptions appear in figure 5.10. In order to simplify the analysis piece-wise linear segments are used to represent the connection $M-\phi$ behaviour. This connection behaviour is shown in figure 5.11. Figure 5.12 shows the connection model response to an arbitrary load history.

Under a general cyclic loading, the moment-rotation path traversed by a typical connection under the assumption above and shown in figure 5.12 is explained below. The connection starts from a zero moment at the elastic stiffness k_1 and continues to load at that stiffness up to a moment of M_{pl} . If it starts unloading at any point 1 (below M_{pl}), it would unload, elastically through the origin, back to a point say 2. If the load is reversed now the connection will move towards the first quadrant maintaining the stiffness of k_1 up to M_{pl} . If the

loading continues in the same direction past M_{pl} , a stiffness of k_2 is assumed, until the moment reaches a value of M_Y . Now, say the load is reversed from point 3, elastic unloading (with a modulus = k_1) will take place until the moment drops by twice the value of M_{pl} . If it goes further the stiffness of k_2 is assigned. At point 4 (say) if the load is reversed unloading will take place in a similar fashion to that of unloading from point 3. If the loading is in the same direction and continues past M_Y , a stiffness of k_3 is assumed until the load is again reversed at point 5 (say). The unloading response from point 5 is similar to that from 4, i.e. unloading at k_1 for a distance of twice the elastic limit M_{pl} and then by stiffness k_2 until the lower bound stiffness of k_3 is reached. The elastic unloading to point 7 and back to point 8, through point 6 is simple to follow.

The connection model proposed by Moncarz was confirmed by the work of Marley [80]. Figure 5.13 shows the measured and the analytical moment-rotation curves for a pair of 4 in x 4 in x 1/2 in angles, 5 in long, connected by 3/4 in dia A-325 bolts to W5x16 members.

5.4.1 Connection Data

Marley [80] carried out a study on 1/2 inch and 1/4 inch top and seat angle connections with W5x16 members (connection and members similar to those used in Stelmack's test frame). His study showed that:

1. There is no apparent difference between the response of an interior and an exterior connection.
2. There is no apparent difference in the response of a connection whether it is loaded symmetrically or anti-symmetrically.

Therefore, he postulated that a single set of connection parameters (M_{pl} , M_Y , k_1 , k_2 , k_3) may be used for a connection in any analysis regardless of its loading or location within the frame.

Stelmack [89] carried out 4 preliminary frame tests (two with 1/4 inch connections and two with 1/2 inch connections). The average values of the connection parameters (M_{pl} , M_Y , k_1 , k_2 , k_3) are thus obtained by Stelmack and are shown in figure 5.4 and figure 5.5 for 1/4 inch and 1/2 inch connections respectively. Stelmack's chosen connection parameters are shown with the bounds provided by Marley [80] in figures 5.14 and 5.15 in order to demonstrate possible scatter in connection response that might occur in the actual tests. Marley observed that initial stiffnesses of the connection vary within a factor of two among the replicates.

5.5 Comparison of the Test Results and the Analytical Predictions

A comparison of the analytical prediction and the test results for tests 1, 6, 9, and 10 will be reported in this section. In each case, a brief description of the test will be given first, followed by presentation of test and analytical results. Since only the hard copies (Graphical) of the test results were available to the author, and not the explicit test results, it was deemed appropriate to present the results of the test and the analysis on separate sheets in general. This certainly would avoid the clumsiness considering the complicated nature of the loading, but still providing the necessary information to the reader. However, some segments of

test and analysis results will be shown on overlay plots at an enlarged scale.

5.5.1 Comparison with the Result of Test 1

The frame geometry of test 1, as appears in figure 5.1, is a two-bay, one-storey configuration. The connection was of 1/4 inch size (see figure 5.1). There were no gravity loads applied during the test and the lateral loads were applied cyclically. The load history consisted of cycles of equal positive and negative magnitudes of Q beginning at 0.25 kip (1.11 kN) and increasing to 0.5 kip (2.22 kN) increments to 3.0 kip (13.34 kN). The ± 2.0 kip (8.90 kN) and ± 3.0 kip (13.34 kN) cycles were repeated twice in the test to examine the stability of the cycles. The load values specified were only nominal, since during the test if it so happened (observed) that the required load value was likely to cause a displacement much larger than the anticipated value, then further increase in load was stopped and load was reversed to continue the cycle. For this reason the applied load cycles in the test were symmetrical only in a nominal sense. The ± 3.00 kip (13.34 kN) was actually +3.0 kip and -2.51 kip.

The analytical simulation of the load cycles were, however, perfectly symmetrical, i.e. they matched the nominal load values designated in the test and not the actual test values.

The test results in the form of lateral load vs. lateral displacement at the 1st floor level appears in figure 5.16. The predicted load-displacement behaviour for the same frame is shown in figure 5.17. Comparison between these two figures reveals that the predicted response matches the actual response very closely. As no gravity loads were applied in this test and the members were meant to

remain elastic, the only source of nonlinearity is due to the connection $M-\phi$ behaviour. Since the connections in the analytical model were represented by a series of straight lines to simulate the true nonlinear $M-\phi$ behaviour, the predicted response tends to follow distinct linear ranges of stiffness – as opposed to the smoother behaviour observed in the test. However, despite this difference, the deformations are predicted quite accurately, as can be seen by comparing the deflection values in almost all the controlling points. Reference [89] notes that beyond a displacement of 1 inch, the test response was somewhat softer because of the ‘kinking’ action of the connection.

The repeated cycles of ± 2.0 kip and ± 3.0 kip were found not surprisingly to be 100% stable in analysis and they were also reasonably stable during the test.

One other feature of the test needs to be mentioned here, that is the test was conducted to a deformation many times the allowable value of the serviceability limit specified by the most codes. The allowable lateral deflection of $h/300$ corresponds to a deflection value of 0.22 inch or 0.56 cm for this frame. This bound is achieved within the first 3 cycles. Because of the clumsiness of the load-deflection loops in the initial cycles of the test and analysis it was felt necessary to show a comparison of the test and analytical prediction at or near the $L/300$ limit in a magnified scale. This is done by an over-lay comparison of the first 4 cycles of the test and analytical load-deflection loops as shown in figure 5.18 (a) to (d). In cycles 1 and 2, elastic unloading takes place both in analysis and in the test, within the initial stiffness (k_1) range of the connection. The analytical model simulates a true replica of the actual frame behaviour as can be seen from the indistinguishable test and analytical response in these two

initial cycles.

Cycle 3 marks the onset of nonlinearity in the analytical as well as in the test load-deflection response. Because of this nonlinearity, inelastic unloading took place. The predicted loop matches closely the observed test response.

Load cycle 4 produces a deflection more than twice the allowable limit ($L/300$). Given the various approximations involved in the analytical model and also considering the non-ideal response that might have been observed in the test, the correspondence between the test results and the predicted results are very satisfactory.

5.5.2 Comparison with the Result of Test 6

The frame configuration for test-6 was a two-bay, single-storey frame as shown in figure 5.1. The angle connections were 1/2 inch thick and gravity loads were applied on both bays. The lateral load cycles were started with ± 0.5 kip, and then cycled at the following values: ± 1.0 kip, ± 2.0 kip, ± 4.0 kip, ± 6.0 kip, ± 8.0 kip, ± 10.0 kip and ± 4.0 kip. The lateral load was then increased to $+8.0$ kip and back to -2.5 kip, where gravity loads were removed, and two final cycles were applied between $+6.0$ kip and -4.0 kip. As mentioned before, these values are only nominal values. In the analytical modelling, however, these nominal values have been simulated.

The load displacement response for this test is shown in figure 5.19 and the corresponding prediction appears in figure 5.20. The load history in this case is quite complicated so is the load deflection response. There have been quite a number of sharp discontinuities in the test response beyond a load of 6 kip (26.69

kN) which was reported to be due to bolt slip in the connections. It was observed that the bolt slip occurred resulting in the sudden drop in load and the bolts then became bearing connectors as a result of which the load picked up again.

In the initial cycles, the correspondence between the test and the predicted response is very good. The enlarged plot of the predicted load deflection relationship is in figure 5.21 for the initial 5 cycles i.e. up to a load of ± 6.0 kip (26.69 kN). Table 5.2 compares the controlling deflection values between the test result and the predicted results for these 5 cycles. Within the range of ± 6.0 kip, the deflection reaches some 4 times the allowable value of $L/300$. It can be seen from figure 5.21 and table 5.2 that predicted response matches the test response quite accurately.

Beyond the range of 6 kip, the test response is softer than the analytical model. Larger deformations resulted from bolt slip which occurred during the test and some discrepancy in the predicted and observed response are noticed in the later cycles. It can be seen that unloading stiffness, in the test, is not elastic for as long as is predicted. This makes the predicted response stiffer in the negative side resulting in a predicted negative displacement much less than the test value. This error is carried forward as load is applied again in the positive direction.

The connection model adopted here assumes a fairly long (constant) elastic unloading irrespective of the location of the point of unloading. Although this assumption gives satisfactory results up to a deflection many times the $L/300$ limit (in this particular case 4 times), unloading from a point after a certain plastic deformation, as appears from the test result, seems to have a smaller elastic segment. No specific pattern can be identified here and further studies are

needed to confirm this behaviour.

5.5.3 Comparison with the Result of Test 9

This test involved the two-storey frame with 1/2 inch thick connections. No gravity load was applied. Lateral loads were applied at both floor levels, (see figure 5.2). At the 1st storey level, the lateral load cycle began at ± 1.0 kip and increasing by 1.0 kip up to ± 5.0 kip. The load at the 2nd storey level was one half the load at the 1st storey level, i.e. ± 0.5 kip and increasing by 0.5 kip up to 2.5 kip.

The test load-deflection responses for 1st and 2nd storey levels are shown in figures 5.22 and 5.23. Corresponding responses as predicted from the present program appear in figures 5.24 and 5.25. In these figures the load corresponds to that applied at the particular storey level, not the total load. Both test and analytical models show a linear response up to a load of 2.0 kip at the first storey and 1.0 kip at the second storey. The measure of frame stiffness is correctly represented in the analytical results.

Comparison of figures 5.22 and 5.24 for 1st storey and figures 5.23 and 5.25 for 2nd storey would show that the test response and the predicted response are quite close. The unloading points in both positive and negative ranges for both the stories matched well.

To present the comparisons in a more specific way, the 2nd storey load-deflection plots for cycles 2 and 3 and 1st storey load-deflections for cycles 4 and 5 are presented in an enlarged scale in figure 5.26(a) to (d). It may be of interest to note that the $h/300$ limit is 0.56 cm for the 1st floor and 1.12 cm

for the 2nd floor – as shown in figure 5.26. Since the load applied at the first storey was always twice that applied at the top storey, the responses at these two levels were comparable in both test and analysis. This leads to the fact that if cycle 2 predicts a response close enough to the test response for the 1st floor then it follows that correspondence between the test and analytical response at the second floor level will also be close. Figure 5.26 reveals how the predicted response compares with the test response for cycles 2, 3, 4 and 5. It can be seen that there is a satisfactory match up to a deflection well beyond the allowable deflection limit of $h/300$.

Two important features can be observed. The first is that up to a working range the connections exhibit a linear response. The second is that the tri-linearized connection model captures the actual response quite satisfactorily, even in the case of cyclic loading.

5.5.4 Comparison with the Result of Test 10

This test was again on a two-storey frame with 1/2 inch connection as in test 9 but this time gravity loads were applied to the first level. As shown in figure 5.2, two gravity loads of 2.4 kip (10.68 kN) each were applied at the 1st storey beam, prior to the application of any lateral loads. Unlike the previous tests, a large lateral load of 5.0 kip (22.24 kN) was applied to the first level (2.5 kip at the top level), unloaded back to zero, and then cycles of load were applied to ± 2.0 kip, ± 3.0 kip and ± 4.0 kip. After reaching -4.0 kip two cycles were applied from -4.0 kip to zero and then loaded to -5.0 kip, and finally back to zero.

In modelling this test, gravity loads were applied to the third points of

the 1st storey beams. Lateral loads were then applied at both storey levels in the same way as in the test program. The cyclic loading could not be achieved as in this case instability occurred at a load of 2.1 kip (9.319 kN) at the top storey, 0.4 kip (1.8 kN) short of the maximum 2.5 kip (11.12 kN) applied during the test to the top storey level. The comparison of the load-deflection responses between the test and the prediction from the present program for 2nd and 1st storey levels appear in figures 5.27 and 5.28. These figures show that initially the predicted response matches the actual response by a one to one relationship up to a displacement of approximately $L/300$, the allowable deflection limit. Correspondence between the test response and the predicted response is still very good up to deflection 7 to 8 times the allowable value. Beyond this displacement the analytical model failed due to elastic instability. The complete load deflection responses for 1st and 2nd storey levels of this frame test are shown in figure 5.29 and 5.30.

Unlike test 9, this test had gravity loads applied on the 1st storey beam. These gravity loads caused axial loads in the columns and also would tend to cause overturning (the $P-\Delta$ effect). The test result reported in the reference has been compared with the prediction of the Moncarz [90] program, which is a 1st order analysis formulation and assumes linear behaviour only. The test results have been reported to have compared accurately with the prediction of this program right up to the end of the 2.5 kip load applied at the 2nd storey level (5.0 kip at the 1st storey level). This suggests that, for some reason, the test frame was getting some resistance to counterbalance the second order effects. The present analytical model assumes the bottom supports of the frame to be frictionless pins – an ideal situation never met practice. However, to gain an insight into what extent the test condition might have differed from the assumed analytical model

– a few trial models were analysed by the author. The parameters for these trial models are described in table 5.3. Figure 5.14 shows how the $M-\phi$ response of one of the extreme trial models compare with the bounds suggested by Marley [80]. It appears from table 5.3 that with a column bottom stiffness of 125 kN-m/rad, the trial model 4 can sustain the test load without an instability mode of failure as reported in the preceding paragraph. The comparison of the predicted response for the trial model no 4 and test response for the 1st and the 2nd storey levels are shown in figures 5.31 and 5.32.

The present analysis considers second order effects that are produced by the presence of axial force and also by the vertical loads acting at the displaced joints. The structure in this case, under both gravity and lateral load, undergoes a displacement which is more than 7 times the working sway limit (see figures 5.27 and 5.28), are bound to have the destabilizing effect of $P-\Delta$. For a frame, the ultimate capacity is reached when the combination of axial force and joint displacement reduce the stiffness of the structure so that the frame becomes unstable.

Although the full simulation of the load history for this test could not be made, it can be seen from figures 5.27 and 5.28 that the present program can predict the sway deformation up to a deflections many times the normal allowable limit. Therefore, in the light of what has been argued in the preceding paragraph, the prediction of the present program may be regarded as satisfactory.

5.6 General Discussion on the Comparison

The analytical prediction of the load-deflection response for the frames of tests 1, 6, 9 and 10 have been presented and compared with the test response. While the analytical models have been constructed from the information available to the author – there are some points which need to be mentioned for a proper understanding of the extent to which the comparisons made in the preceding section can be regarded as satisfactory. Following are the areas in which the test condition may be different from the analytical model:

1. All connections, irrespective of their locations, are assumed to behave in a similar way – which may not be the case in test situation. The possible scatter in the connection behaviour as shown in figures 5.14 and 5.15, suggests that the connection parameters can be quite different in any particular test, than those assumed in the analytical model. It is important to note that the scatter shown in figures 5.14 and 5.15 is a measure of possible variation in replica connection tests.
2. Actual measurements of the member sizes were not available and standard section sizes have been used, with uniform member properties.
3. No member or frame imperfections were reported – consequently perfect members and frames have been used.
4. The bases of the columns were devised to act as frictionless pins (see figure 5.3(a)). It is not unlikely that some restraint may be present there. However, the initial analytical model assumes the column base as perfectly pinned.

5. The connection model itself is based on certain simplified assumptions. Although based on experimental evidence, these assumptions need further examination. One possible difference that appears from the comparison presented in the previous section is that the stiffness of the connection response after a load reversal depends upon the location in the load history of the reversal. For example, the stiffness of a connection after load reversal seems to depend upon the amount of plastic strain that it has undergone. After a high displacement the length of elastic unloading decreases, and thus the test response is significantly softer (see test 6; unloading after a load of +8.0 kip). However, no specific pattern for a general behaviour can be identified and the adopted model may be considered satisfactory.
6. The amount of experimental error – some 10% has been estimated in the strain gauge reading had been mentioned in the reference.

Having mentioned these shortcomings, it can be concluded from the results presented in the previous section, that the analytical capability developed here predicts satisfactorily accurate behaviour for flexibly connected sway frames under either monotonic or cyclic lateral load.

5.7 General Observations for Frames Under Cyclic Loading

The results of Stelmack's test scheme together with the analytical prediction presented in this chapter gives an insight into the behaviour of flexible frames under cyclic lateral loading in particular and lateral loading in general. A number

of distinctive features can be identified which are discussed here.

For the structure considered here the response of the connections, at an allowable deflection limit of $L/300$, remains fairly linear. This fact is important in making any simplification to the nonlinear connection behaviour, at least for the working range.

Even though the connections were flexible, the repeated load-deflection loops are found to be very stable. This means that there are no incremental deflection effects as load cycles are repeated, a behaviour which is very important considering the flexible nature of the connection.

The assumption made by Marley regarding the connection model produces reasonably good results, with the only discrepancy arising from the fact that the length of elastic unloading was smaller than that assumed in the connection model – especially when load reversal took place after a fairly high load level.

The lateral drift of a frame under a set of loads is highly dependent on the stiffness of the connection.

5.8 Concluding Remarks

In this chapter an algorithm for the modelling of the connection behaviour under cyclic loading has been implemented. This addition enabled the computer program described in chapter 3 to be used for analysing the flexibly connected frames under cyclic loading arising either due to the wind or pseudostatic seismic action.

Four half-scale tests conducted in the University of Colorado under a cyclic loading history have been analytically modelled and the responses compared. A satisfactory correlation between the test results and the analytical predictions have been observed. General comments on the behaviour of the flexible frames under cyclic loading have also been made.

TEST No.	1-Storey 2-Bay	2-Storey 1-Bay	Conn. Angle Thickness	Gravity Loads
1	Yes	-	1/4 "	No
2	Yes	-	1/4 "	Yes
3	Yes	-	1/4 "	Yes
4	Yes	-	1/4 "	Yes, 1 bay only
5	Yes	-	1/4 "	No
6	Yes	-	1/2 "	Yes
7	-	Yes	1/4 "	No
8	-	Yes	1/4 "	Yes, 1st level
9	-	Yes	1/2 "	No
10	-	Yes	1/2 "	Yes, 1st level

Table 5.1 Summary of the tests conducted by Stelmack [89].

Cycle No.	Load Value kN	Deflection in cm	
		Test	Present
1	0.5	0.165	0.166
	-0.5	-0.165	-0.141
2	1.0	0.305	0.285
	-1.0	-0.305	-0.281
3	2.0	0.619	0.598
	-2.0	-0.619	-0.619
4	4.0	1.27	1.373
	-4.0	-1.40	-1.41
5	6.0	1.95	1.918
	-6.0	-2.38	-2.326

Table 5.2 Comparison of the controlling deflection between the test-6 result and the prediction of the present program for the first 5 cycles.

Trial No.	Col. Base Stiffness kN-m/rad	Mutiplying factors for			Comments
		k_1	k_2	k_3	
1	50	0.85	0.75	2.5	Failed at 2.25 kip at the 2nd storey
2	100	0.8	0.70	3.0	Failed at 2.5 kip at the 2nd storey
3	125	0.77	0.70	3.5	Not failed but stiffer response compared to the test
4	125	0.75	0.70	3.4	Not failed; response matches the test result

Table 5.3 Parameters for the trail model for test 10.

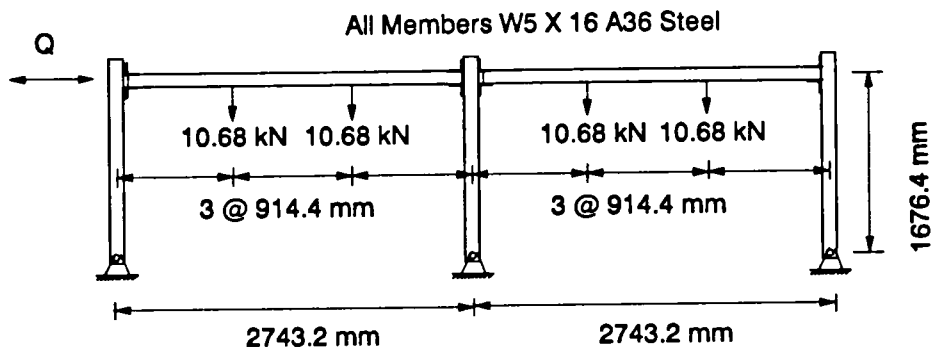


Figure 5.1 One-storey frame details.

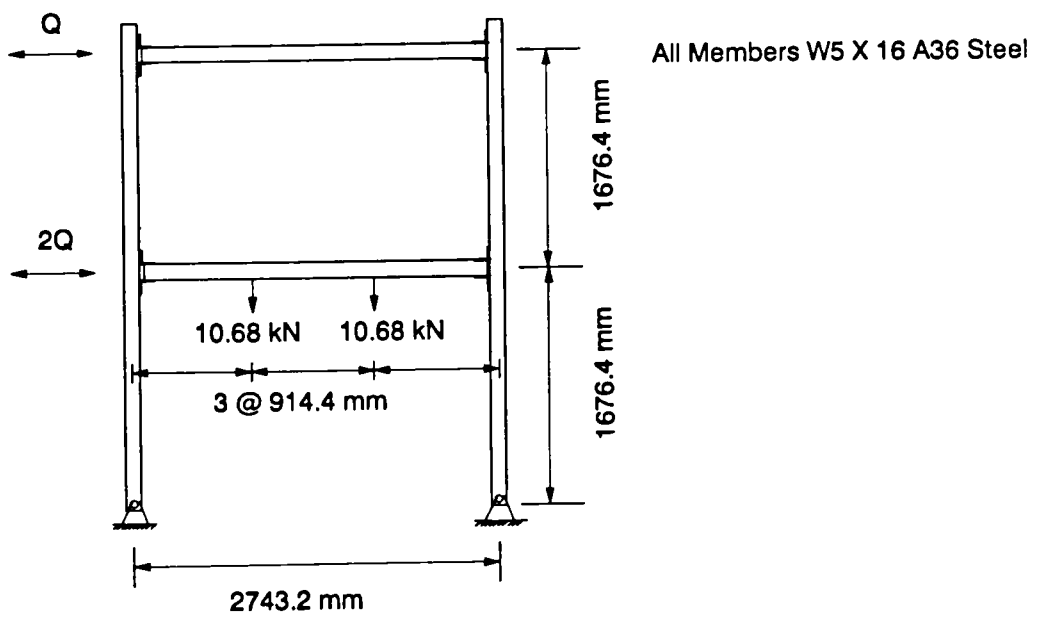


Figure 5.2 Two-storey frame details.

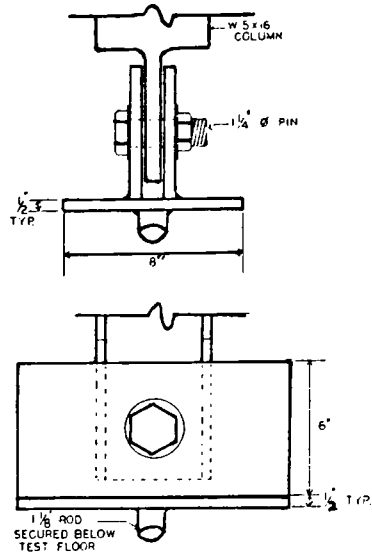


Figure 5.3 (a) Support arrangement at the column foot.

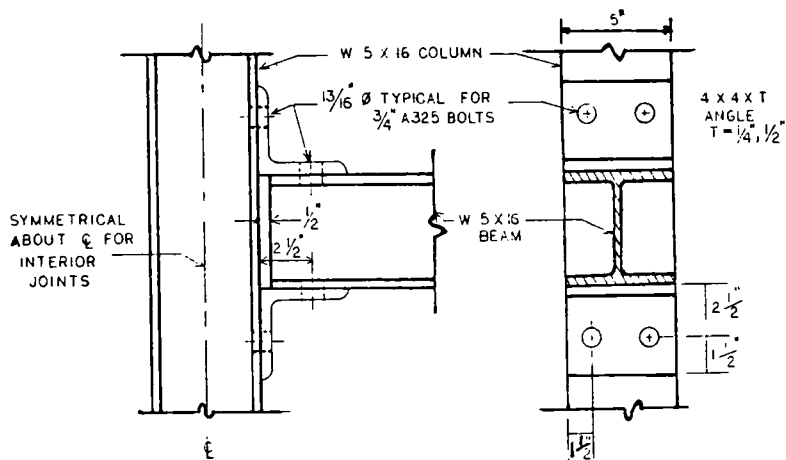


Figure 5.3 (b) Beam-to-column connections.

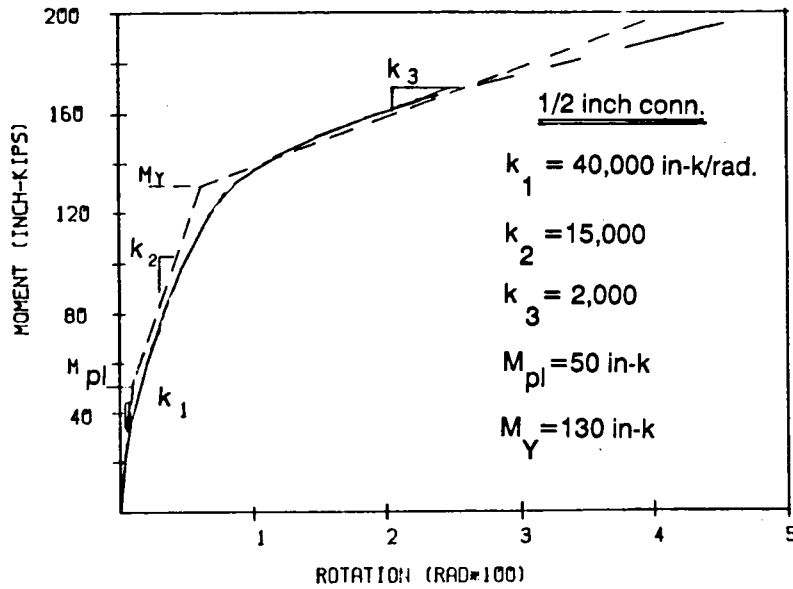


Figure 5.4 Trilinear parameters for 1/2 inch connections [89].

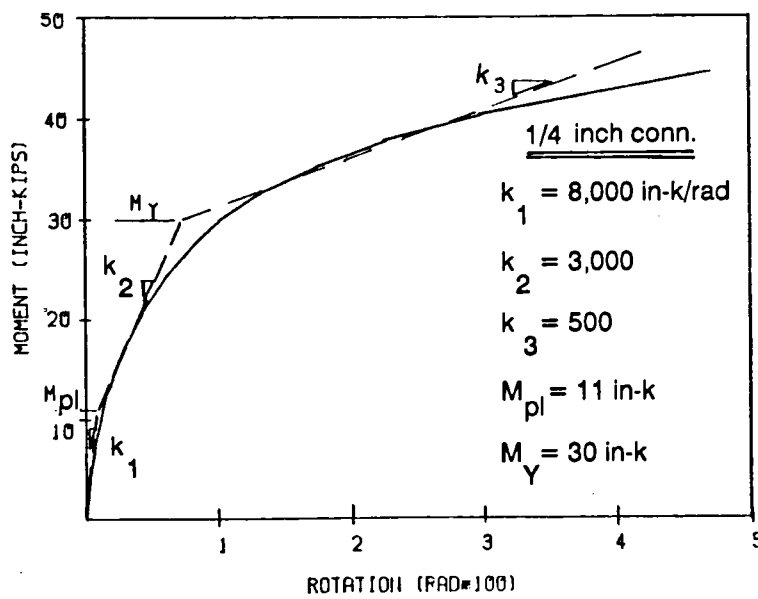


Figure 5.5 Trilinear parameters for 1/4 inch connections [89].

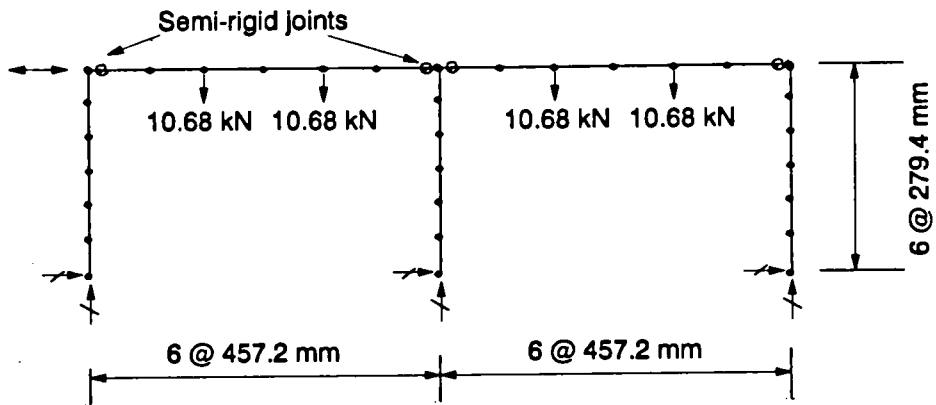


Figure 5.6 Finite element idealization for one-storey frame.

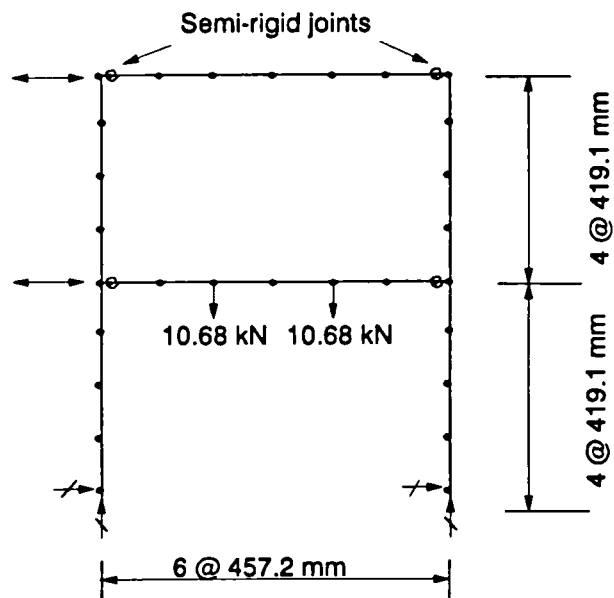


Figure 5.7 Finite element idealization for two-storey frame.

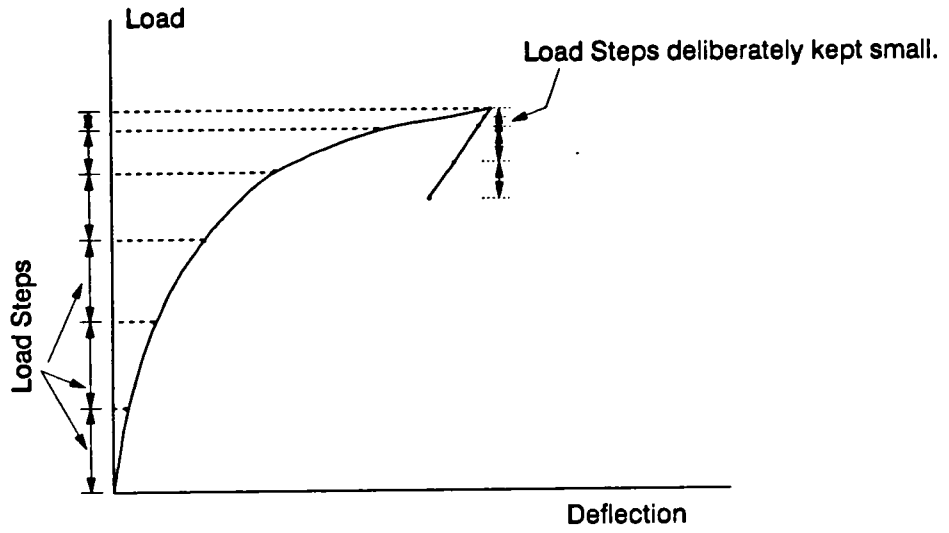


Figure 5.8 Load reversal technique.

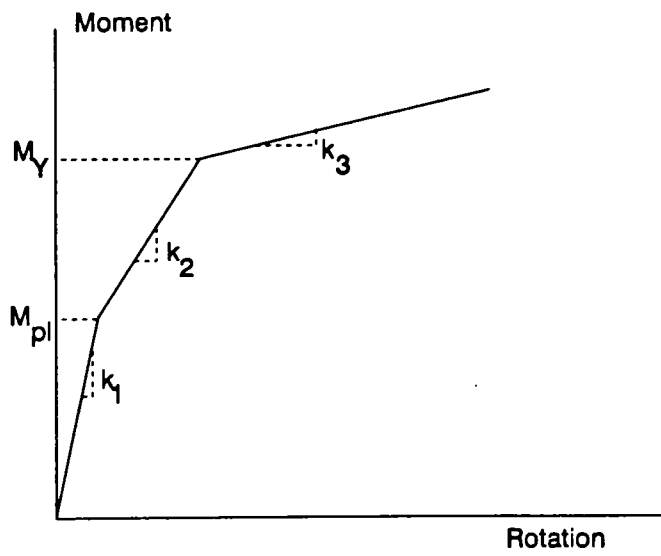


Figure 5.9 Moncarz's connection trilinearization model [90].

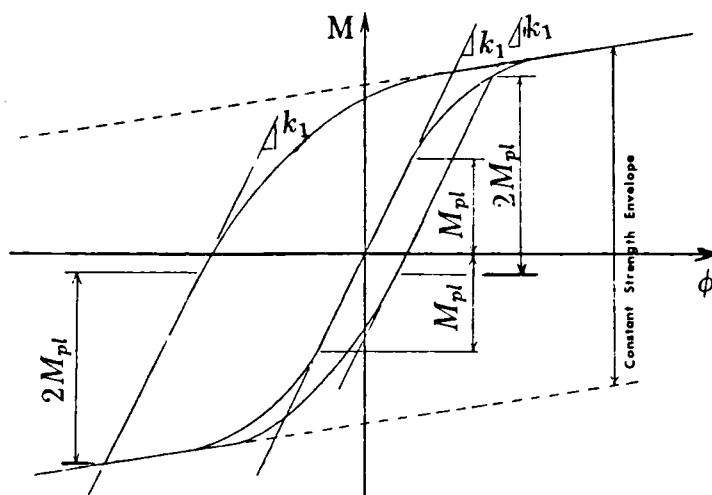


Figure 5.10 $M-\phi$ hysteresis exhibiting connection model assumptions [80].

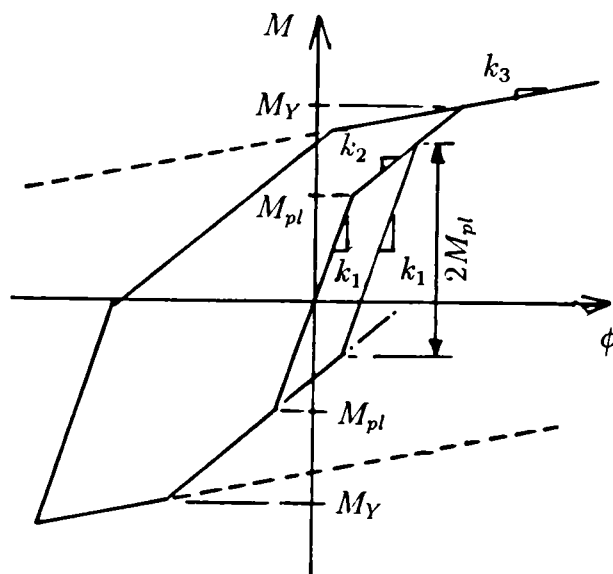


Figure 5.11 Analytical connection representation.

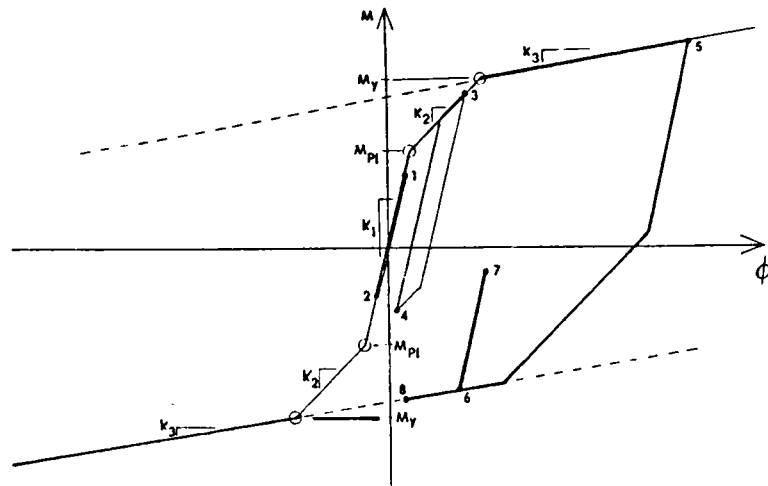


Figure 5.12 Connection model response to a general loading history [80].

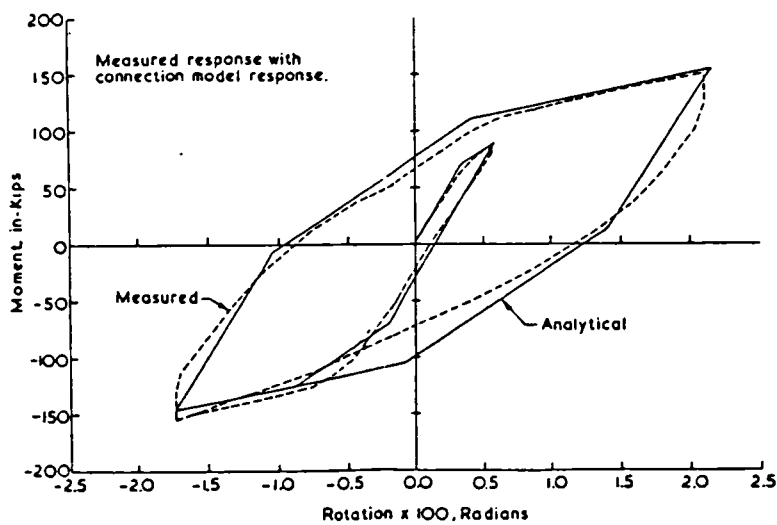


Figure 5.13 Comparison of the predicted and measured response [80].

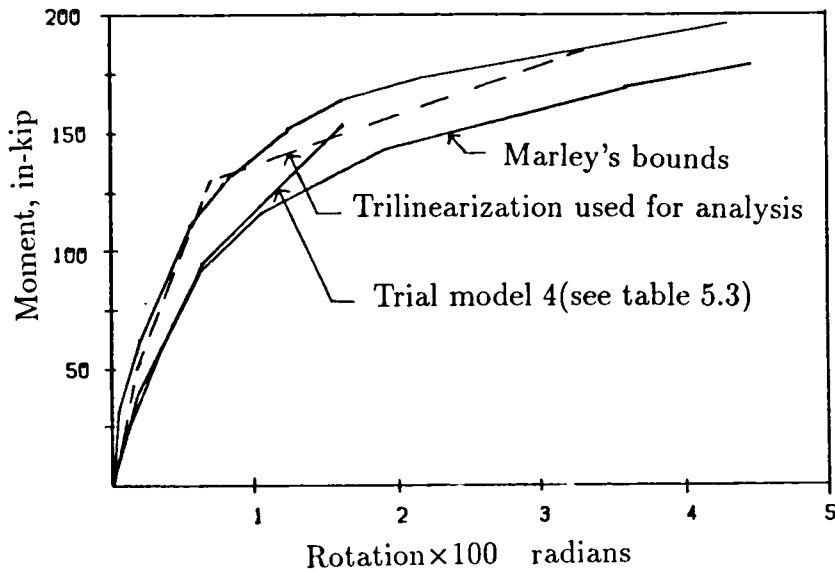


Figure 5.14 Comparison of Marley's 1/2 inch connection results with the trilinearized representation of $M-\phi$ characteristics.

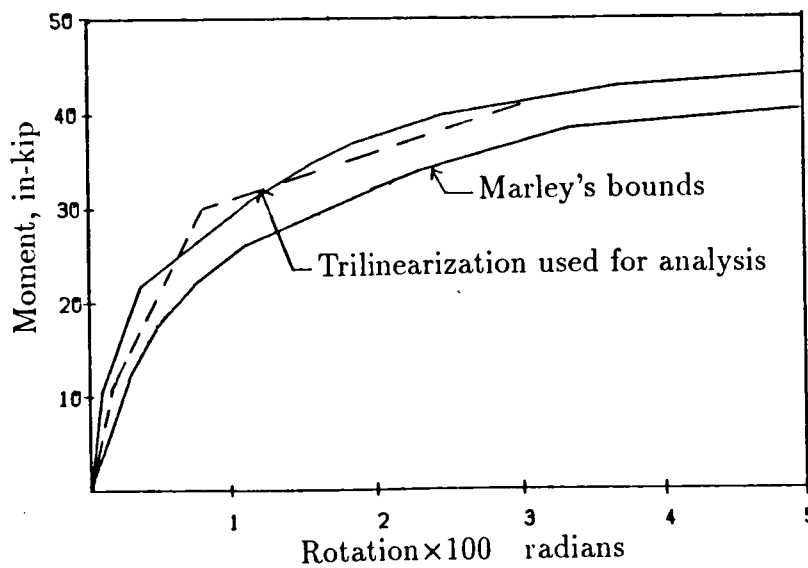


Figure 5.15 Comparison of Marley's 1/4 inch connection results with the trilinearized representation of $M-\phi$ characteristics.

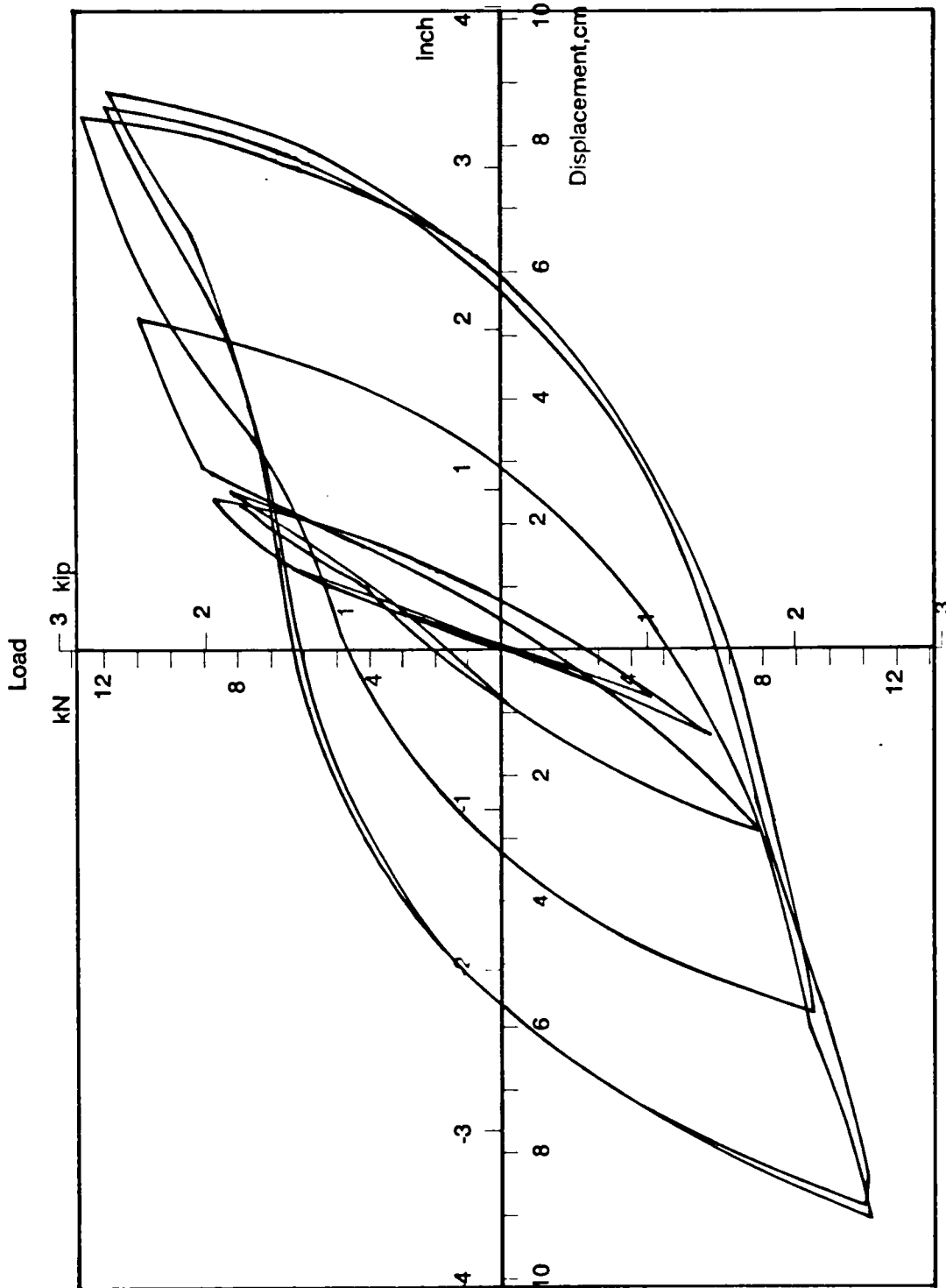


Figure 5.16 Test load-displacement curve for test-1 [89].

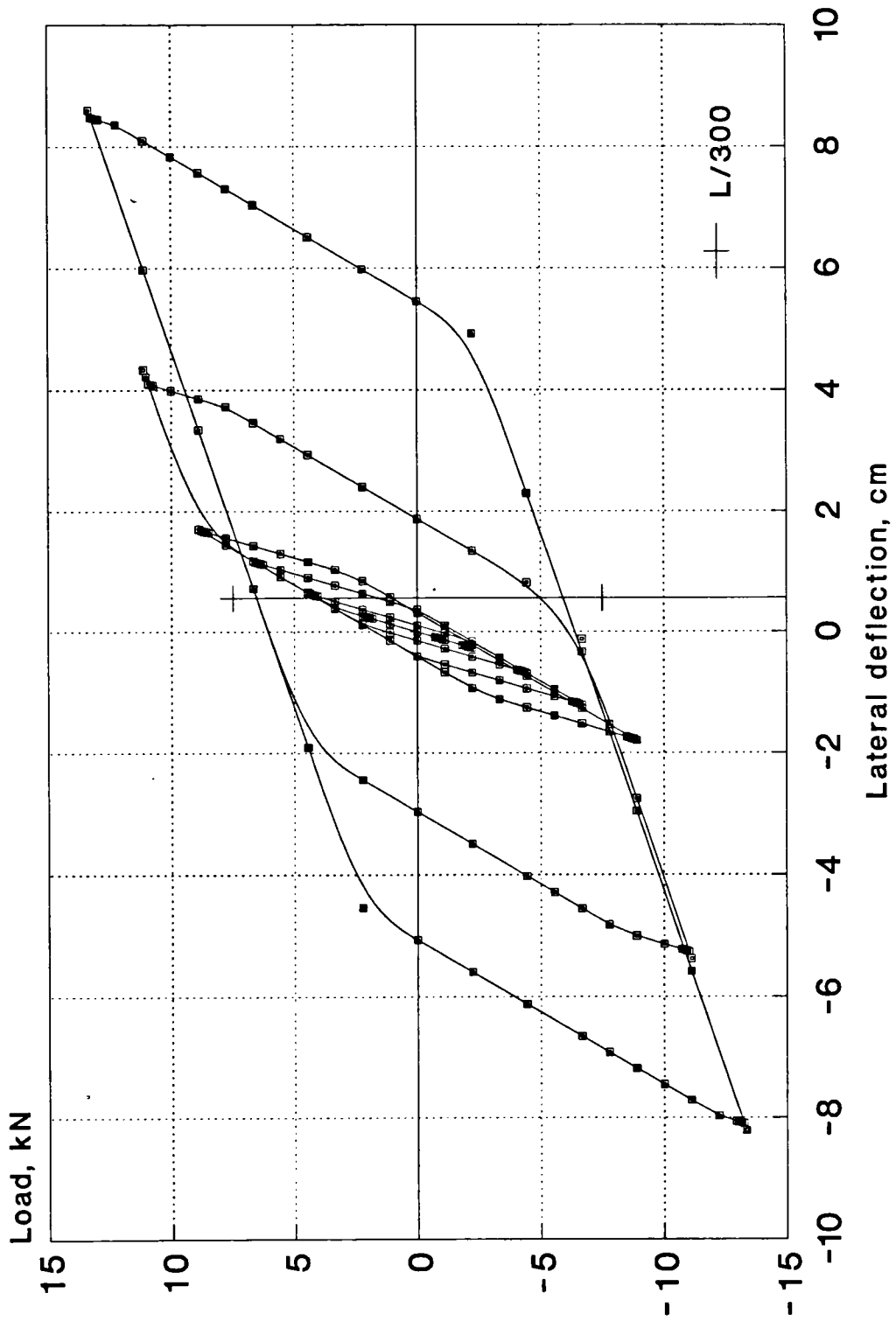


Figure 5.17 Load-deflection response as predicted from the present program for test-1.

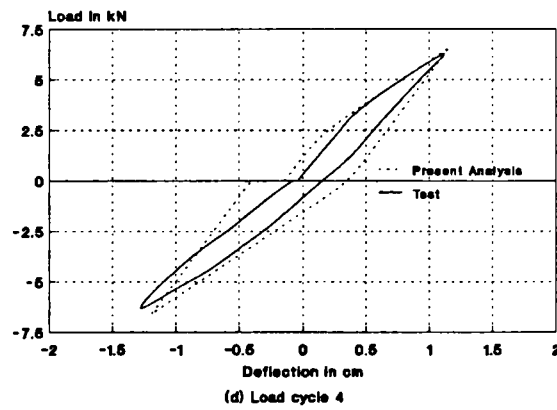
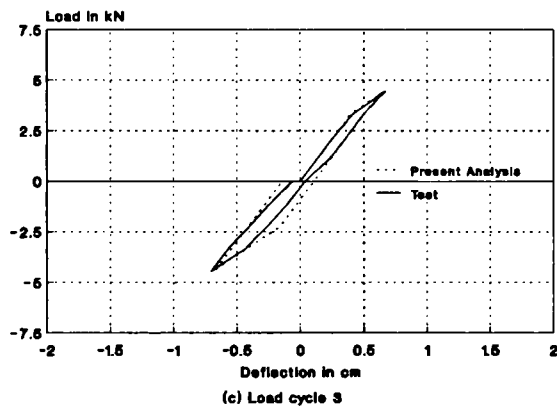
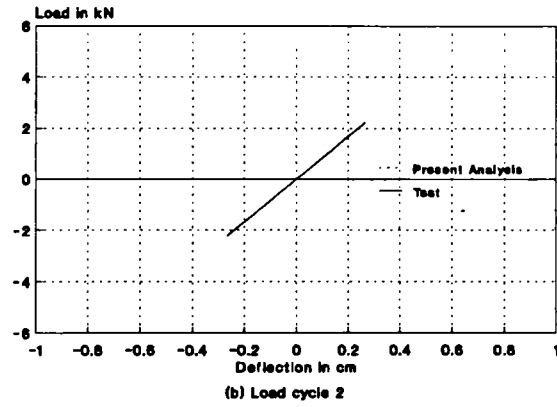
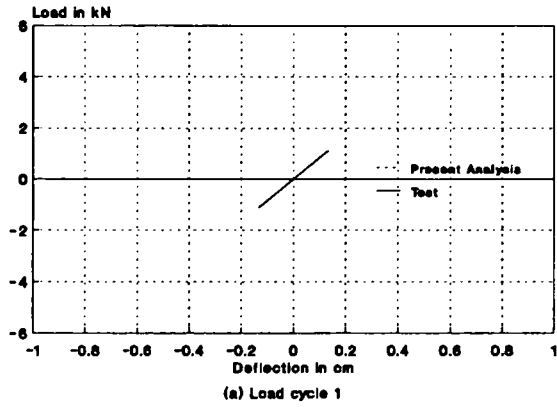


Figure 5.18 Comparison of the measured and predicted load-deflection response for the initial four cycles of test-1.

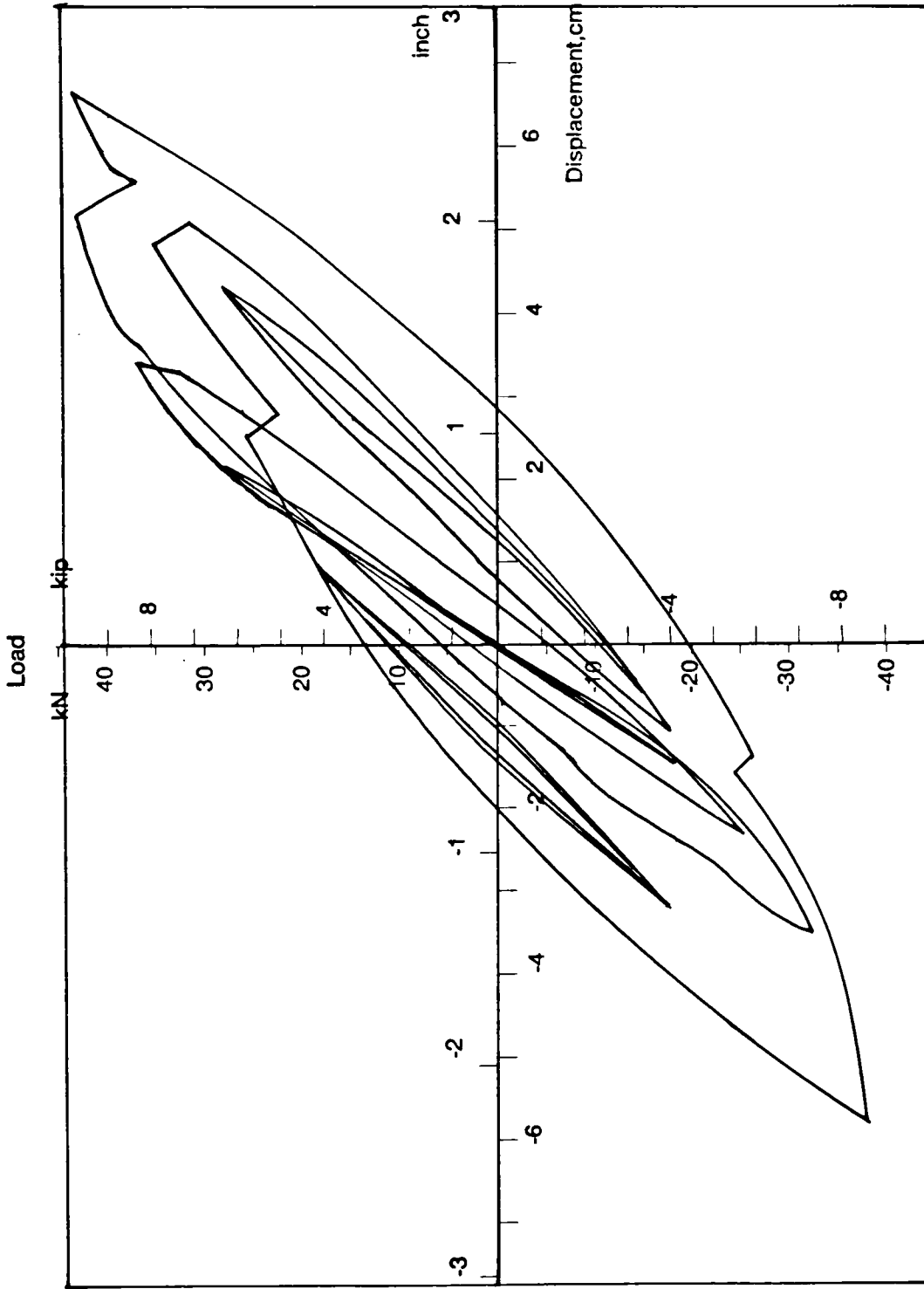


Figure 5.19 Test load-displacement curve for test-6 [89].

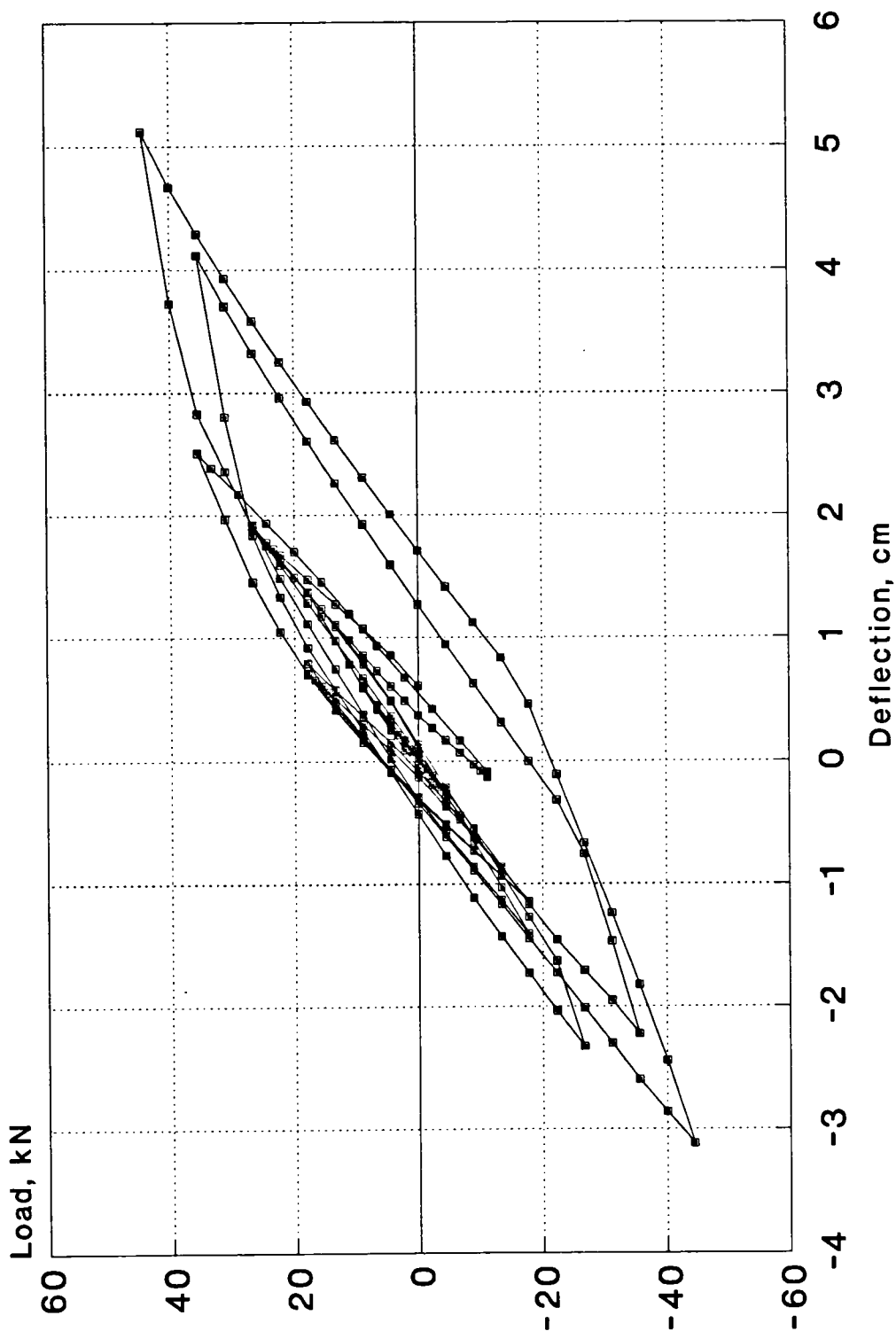


Figure 5.20 Load-deflection response as predicted from the present program for test-6.

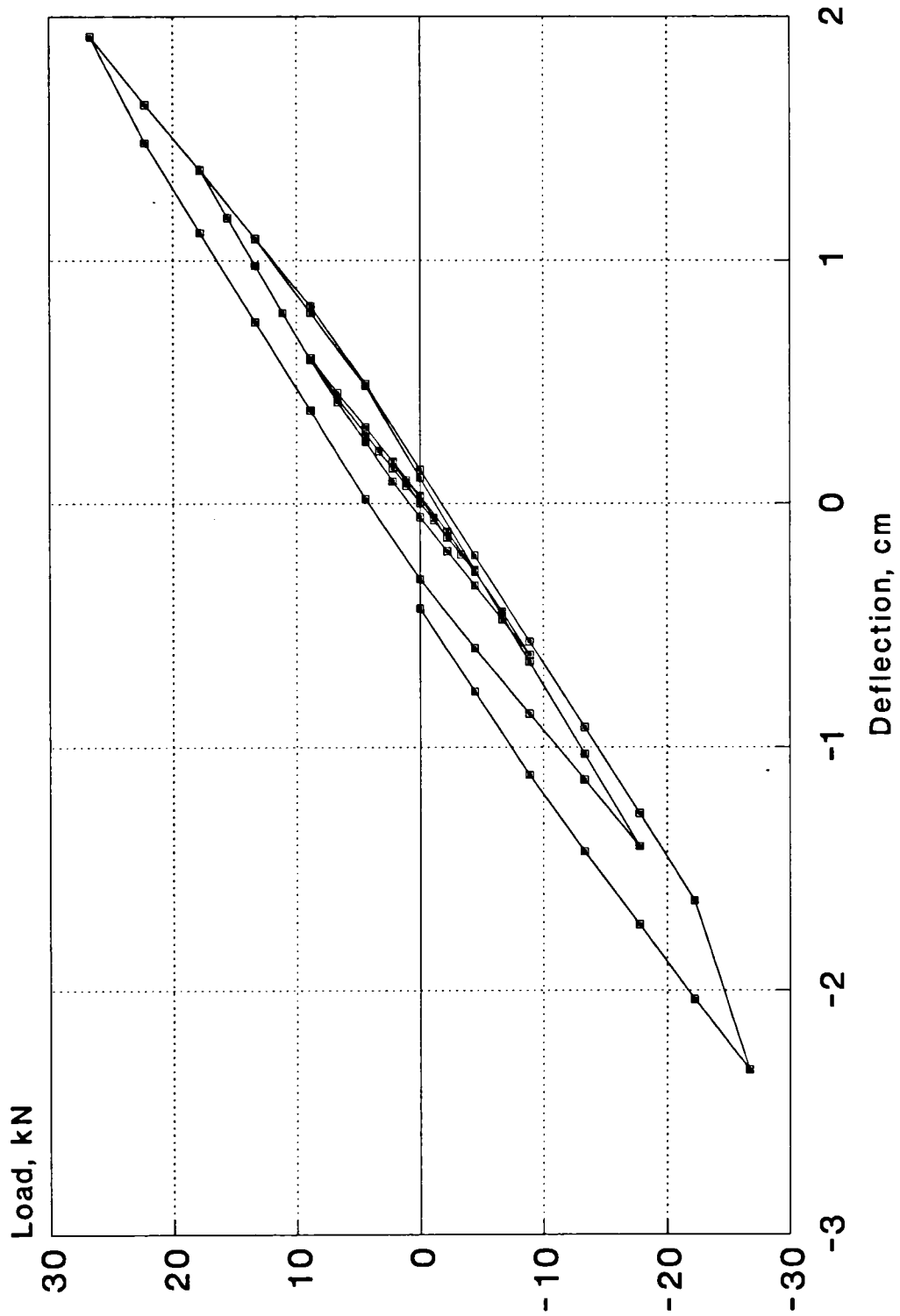


Figure 5.21 Enlarged plot for the predicted load-deflection response of 5 initial cycles in test-6.

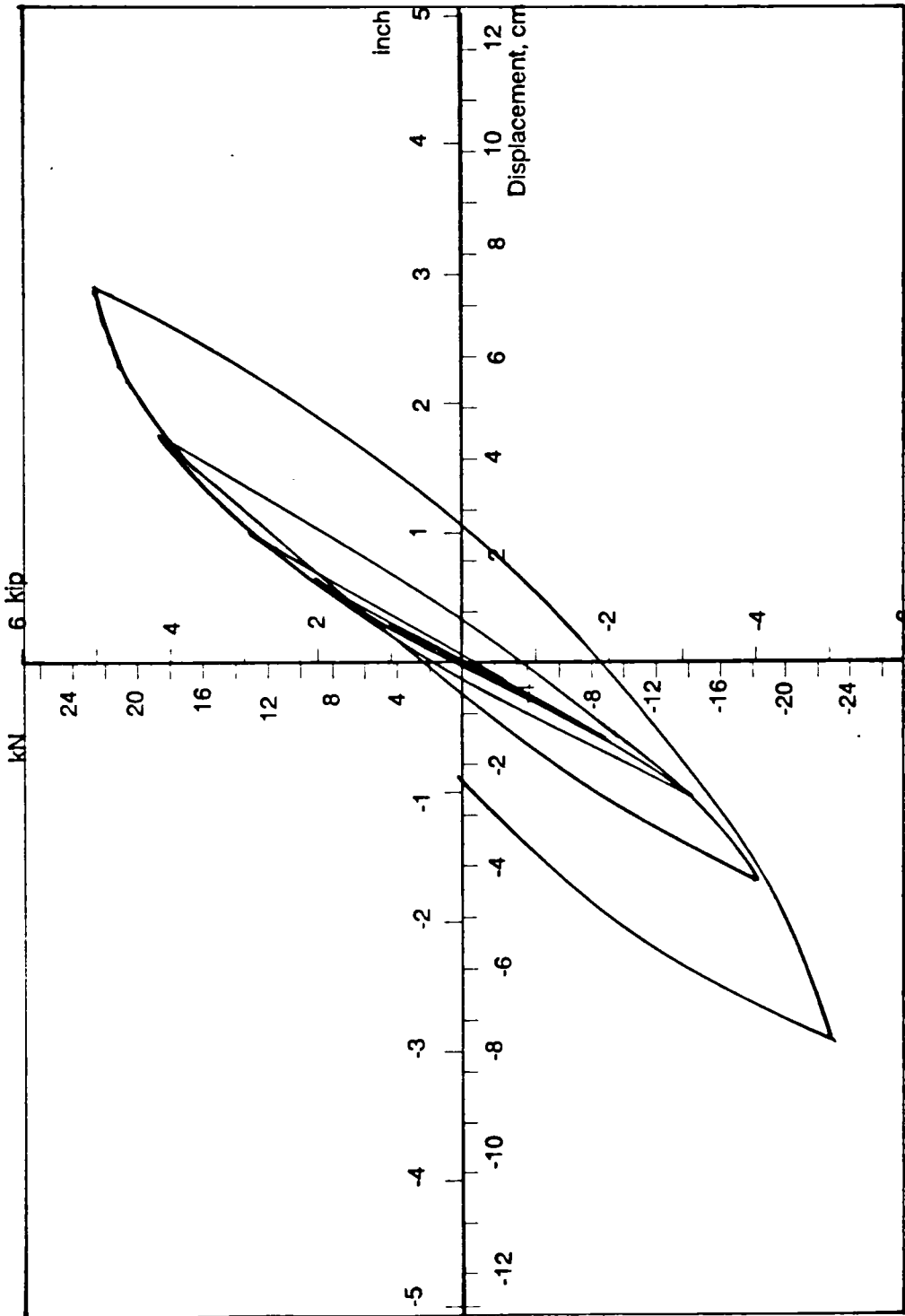


Figure 5.22 Test load-displacement curve for first storey of test-9 [89].

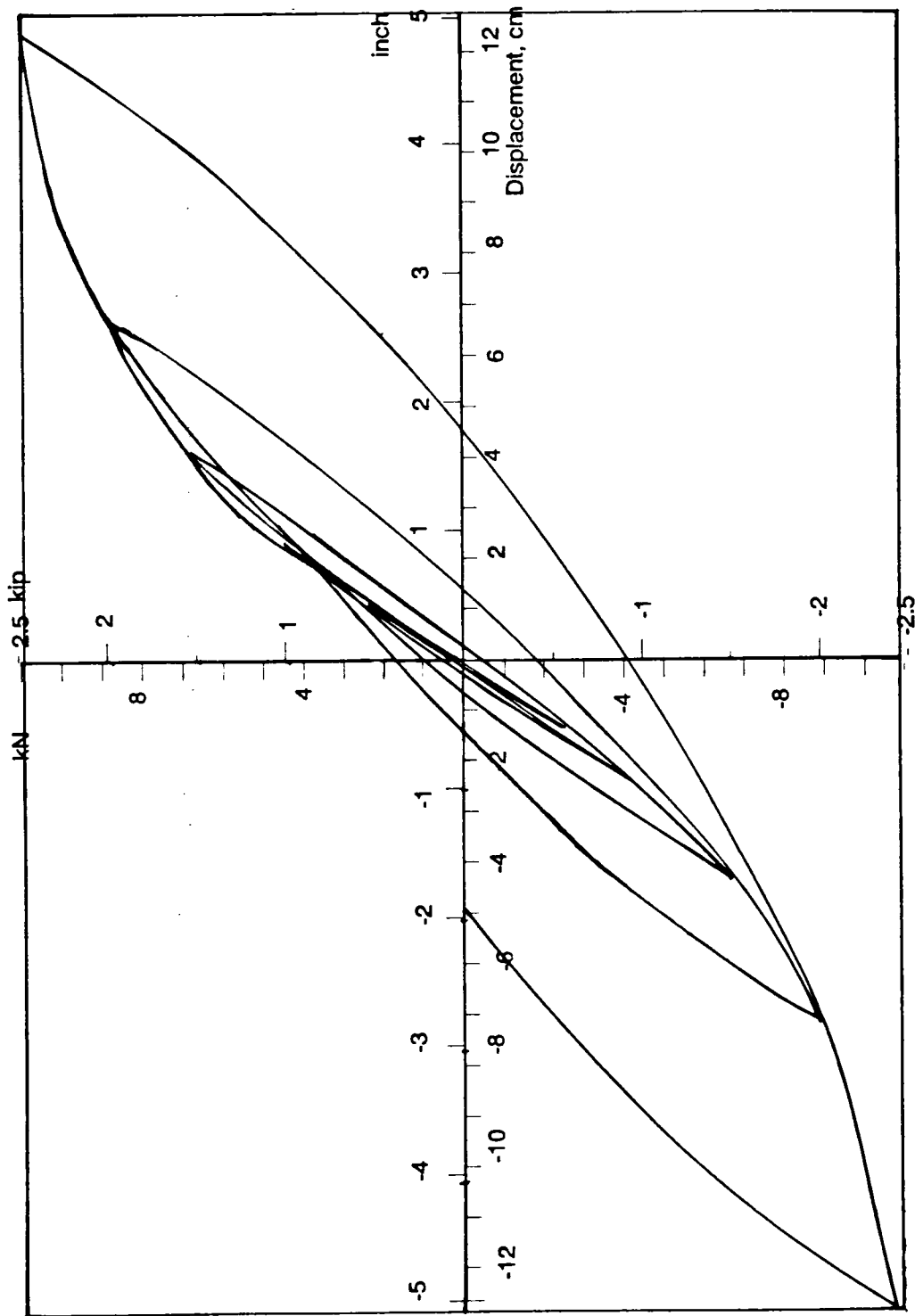


Figure 5.23 Test load-displacement curve for second storey of test-9 [89].

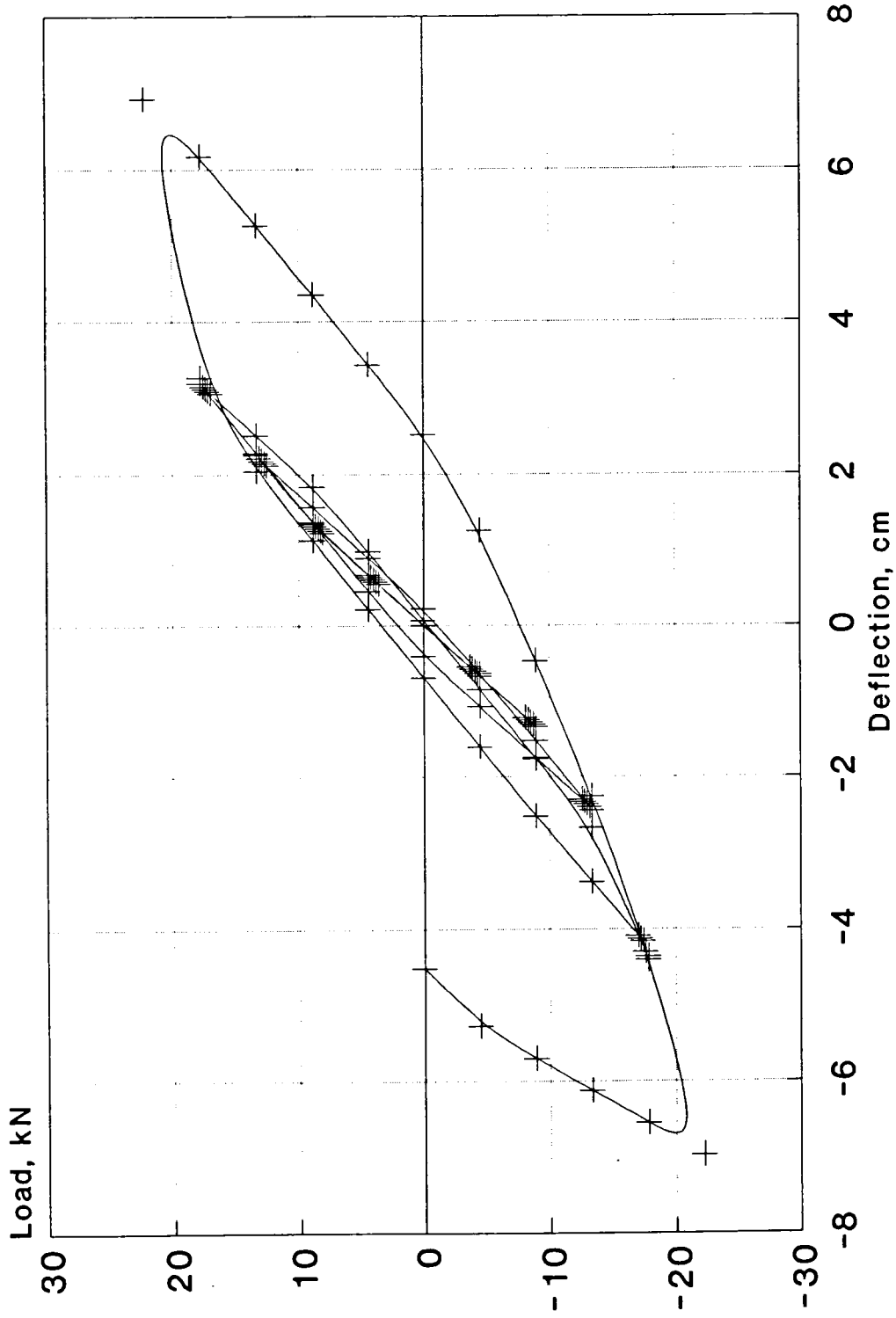


Figure 5.24 Predicted load-deflection response for the first storey of test-9 frame.

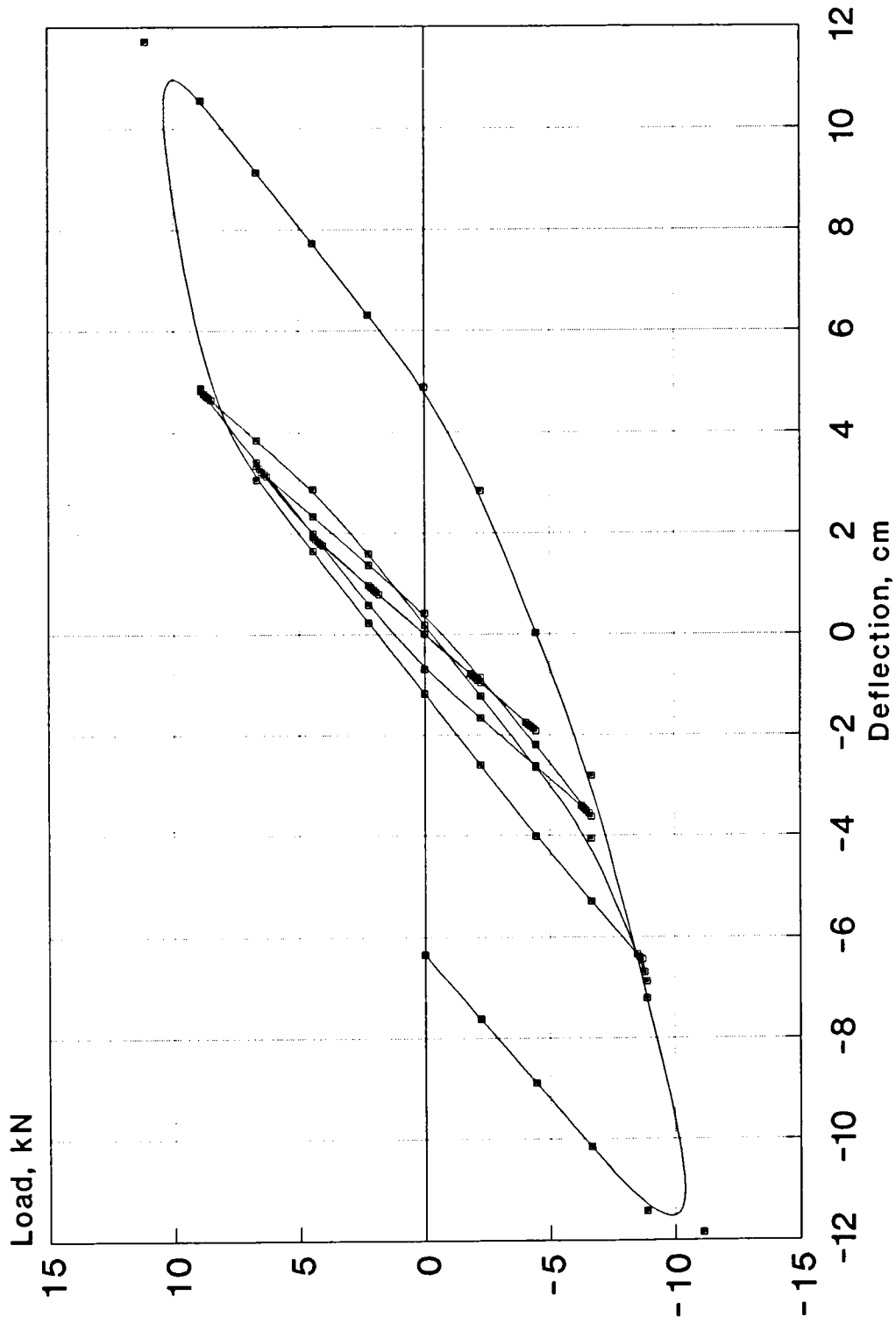


Figure 5.25 Predicted load-deflection response for the second storey of test-9 frame.

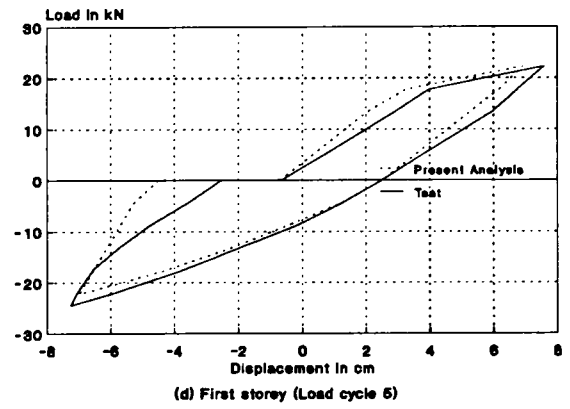
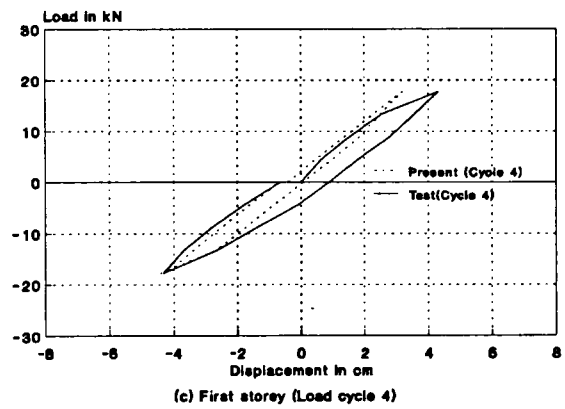
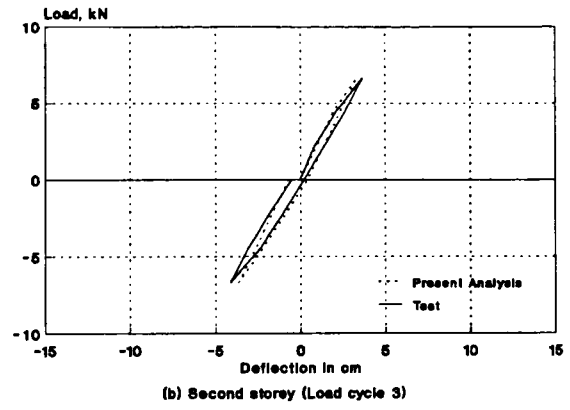
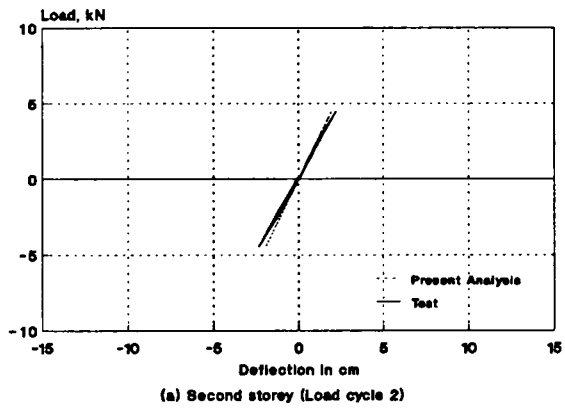


Figure 5.26 Comparison of the predicted and measured load-deflection response for different cycles of test-9.

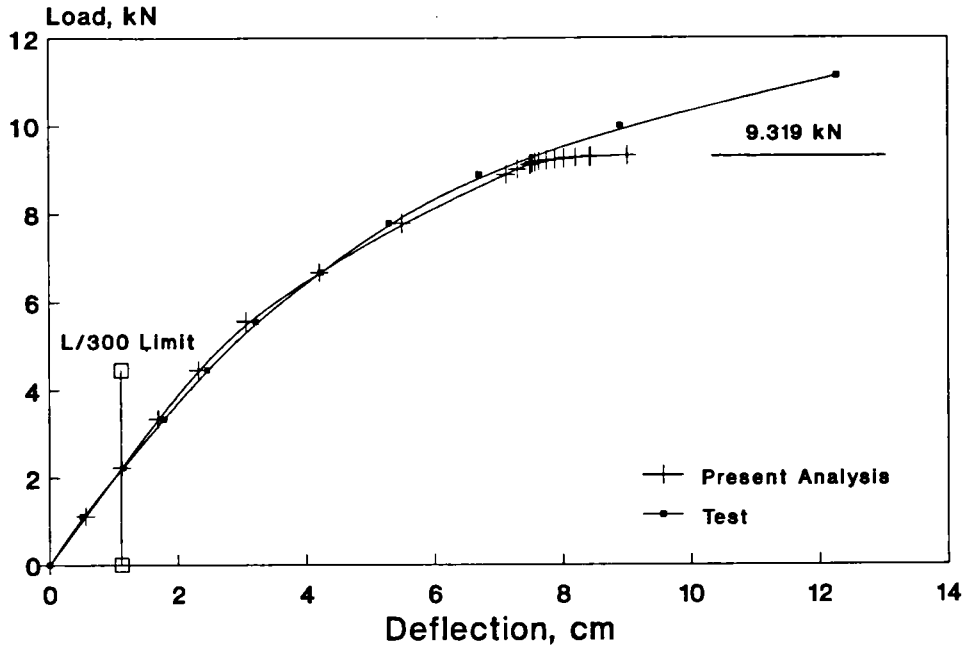


Figure 5.27 Comparison of the predicted and measured load-deflection response for the second storey of test-10.

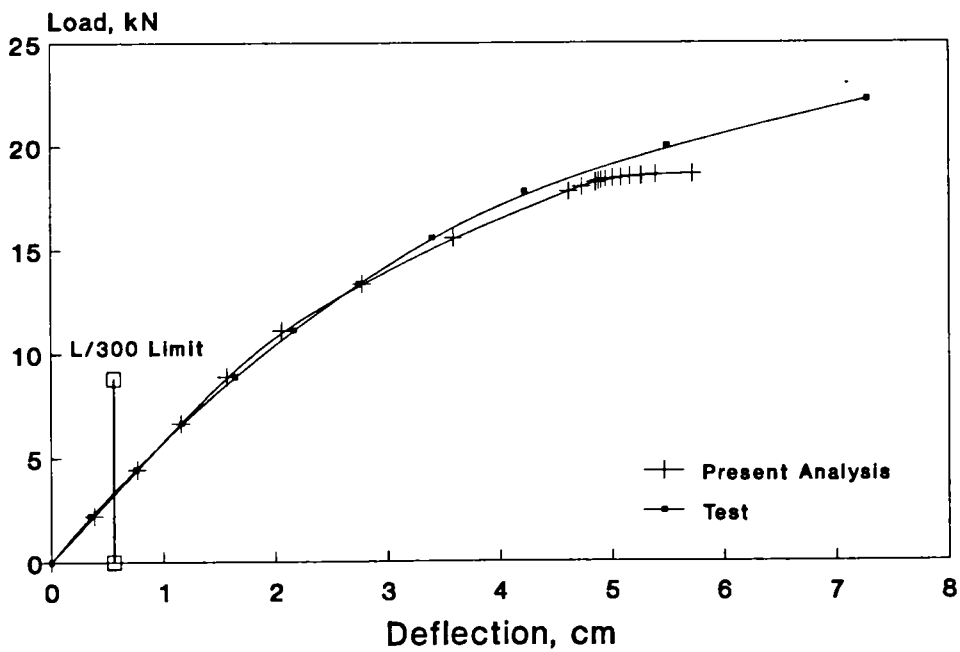


Figure 5.28 Comparison of the predicted and measured load-deflection response for the first storey of test-10.

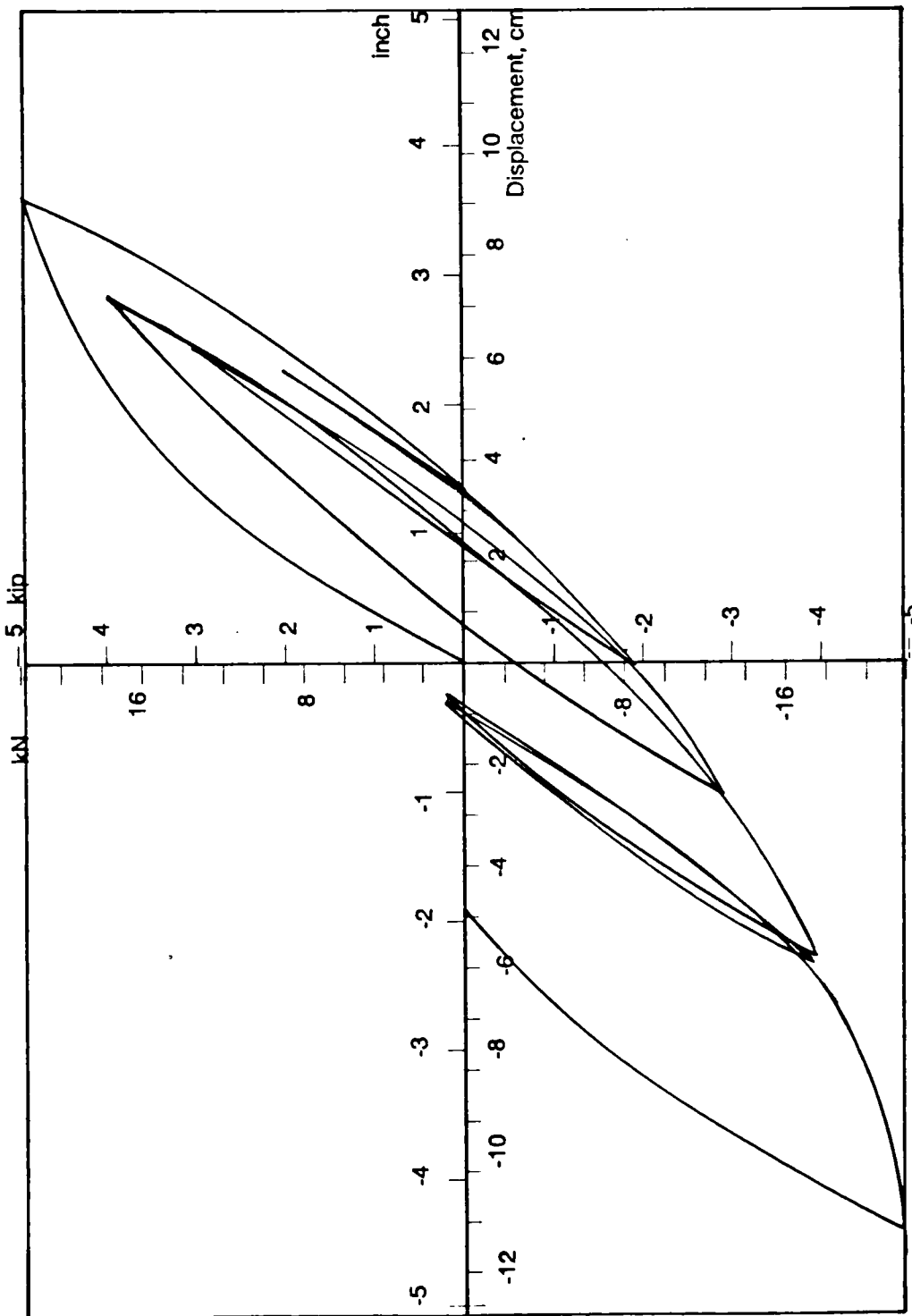


Figure 5.29 Test load-displacement curve for the first storey of test-10 [89].

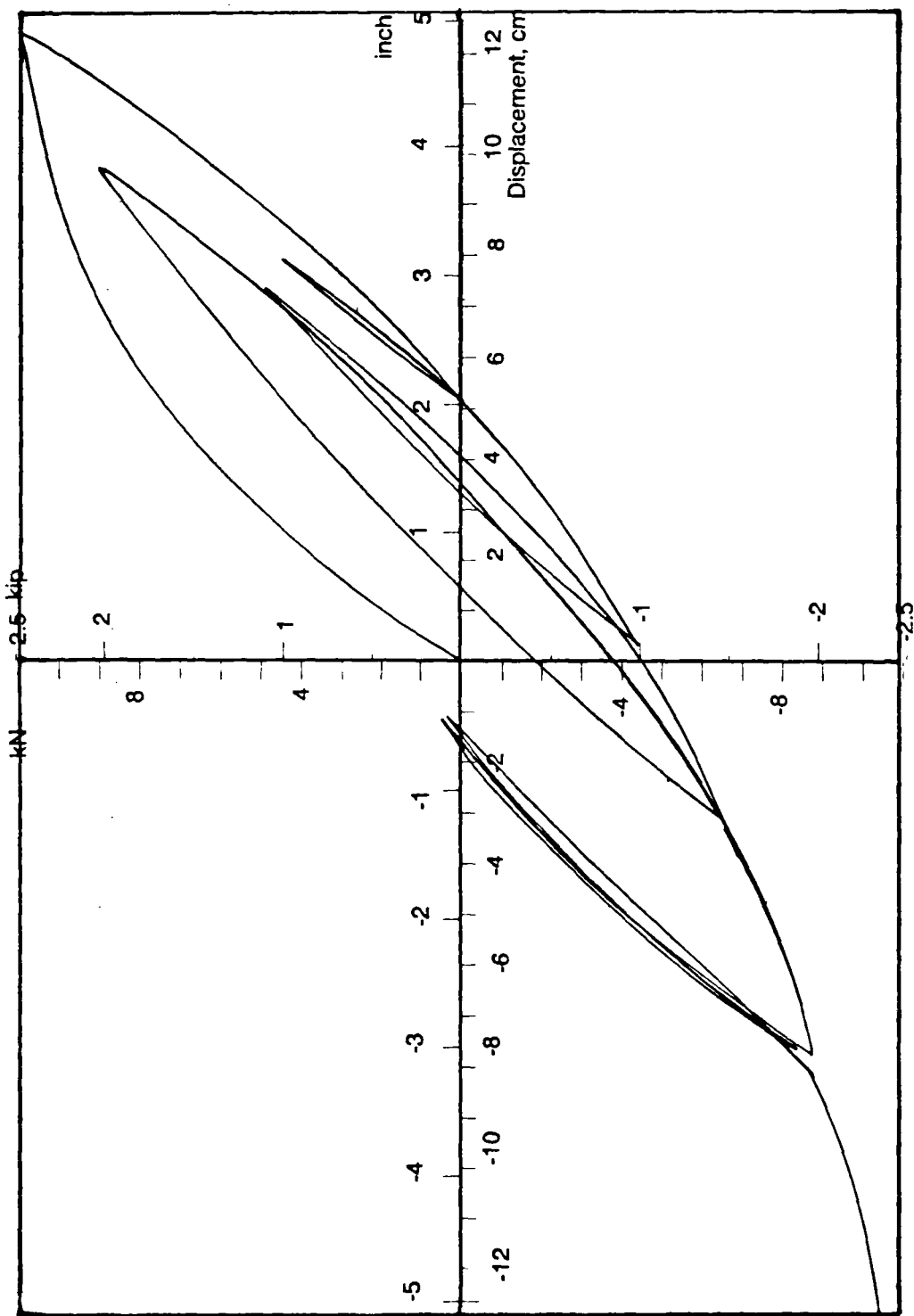


Figure 5.30 Test load-displacement curve for the second storey of test-10 [89].

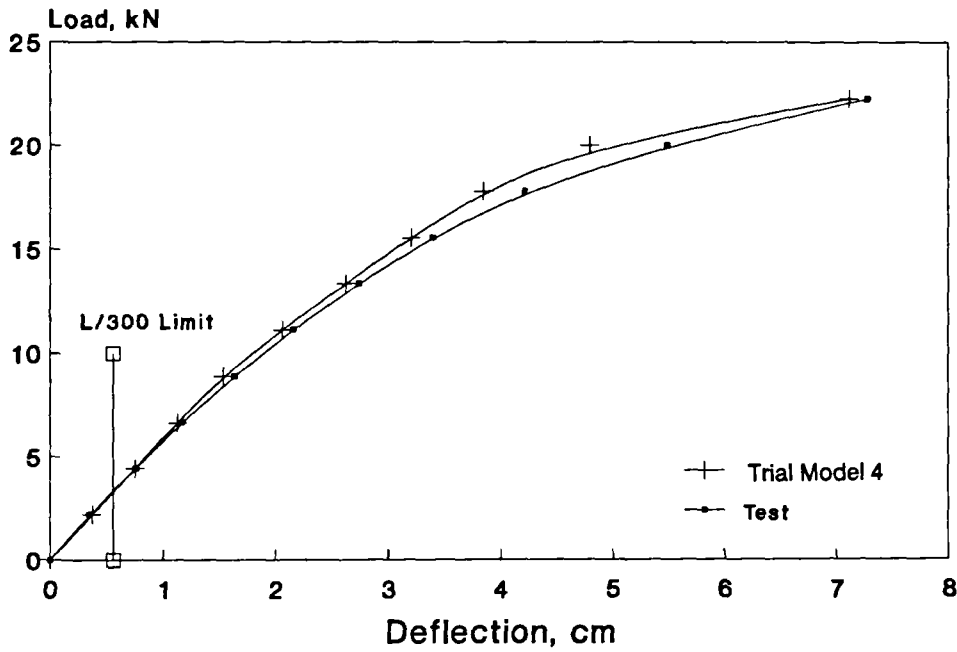


Figure 5.31 Comparison of the first storey load-deflection response between the test result and the analytical prediction assuming the parameters of table 5.3.

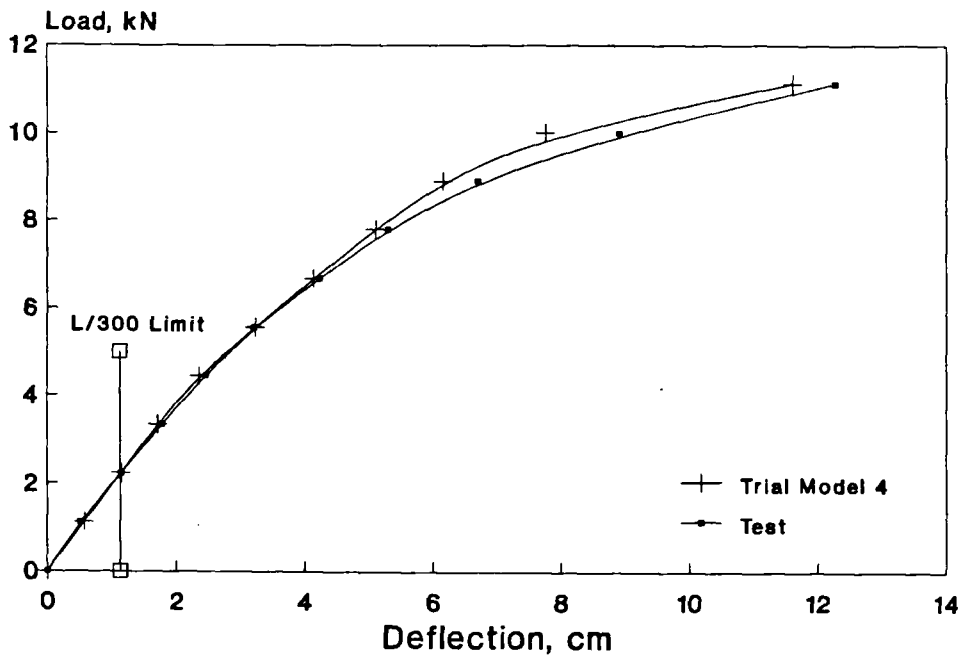


Figure 5.32 Comparison of the second storey load-deflection response between the test result and the analytical prediction assuming the parameters of table 5.3.

Chapter 6

Behaviour of Semi-Rigid Steel Frames

6.1 Introduction

The computer program, described earlier in chapter 3 and subsequently validated against full scale test results in chapters 4 and 5 for non-sway and sway cases respectively, has been used for conducting a parametric study. The main aim of this parametric study is the identification of the most influential design parameters. Once this has been done qualitatively, the basis for design guide lines for semi-rigid frames can then be developed.

The study described in this chapter is based on realistic connection data. Three types of flexible connections are used, namely flange cleat (FC), flush end plate (FEP) and extended end plate (EEP) connections. The connection responses used were those obtained by Davison [32] who made observations

on the behaviour of the connections in isolated tests and also as components in subassemblages and full frames. He found that connections in the frame or subassemblage behave more or less in the similar fashion as they do in the isolated connection test. In this study attempts have been made to consider the parameters in the typical range that are normally found in the building frames.

The next section describes the parameters varied in the study. Important results are then presented followed by detailed discussion and finally the design implications of the findings are set out.

6.2 Scope of the Parametric Study

The parametric study was limited to a 3-storey, 2-bay non-sway frame as shown in figure 6.2. The beams were all 254x102 UB 22 and the columns were 152x152 UC 23. The reason why these particular dimensions were selected is that for this combination of beam and column a consistent set of data exists [32]. From a survey [91] of over 550 tests world-wide, no other combination of beam and column were found for which $M-\phi$ data for different types of connection are available. It was initially envisaged that connection stiffness would be a primary influence on the frame behaviour and therefore an important requirement for any design method.

6.2.1 Connection Details

The moment rotation relationships of the connections used are shown in figure 6.1. The program utilizes a cubic B-spline curve fitted through the experimental

data points, from which the connection stiffness may be evaluated at any load stage. In addition to the three connections, idealized rigid and pinned connection were also included in the analytical programme.

6.2.2 Geometric Dimensions

The geometric dimensions of the frame in figure 6.2 were varied over the range shown in table 6.1. The study consisted of the following 3-stage variation of the parameters.

Stage-1: For a beam span of 5.0m and the storey height $h_1 = h_2 = h_3 = x$, where x was taken as 3.6m, 5.6m and 7.5m. The effect of the three connection types described earlier, and the perfect rigid and pinned connections have been studied for each of these cases giving a total of 15 cases. Each of these cases were studied with following combination of imperfections:

1. Perfect column
2. Lehigh type residual stress in column
3. Initial geometric imperfection (L/1000)
4. Combination of both (2) and (3) above.

Stage-2: This is the same as stage 1 with the only difference being that $h_1 = h_3 = 3.6\text{m}$ was kept constant, while h_2 was varied. Three values of h_2 were considered and they were 3.6m, 5.6m and 7.5m.

Stage-3: Unlike the two previous stages, in this stage beam spans were varied.

Beam spans of 6.0 and 7.0m were associated with three different storey heights ($h_1 = h_2 = h_3 = x$), while x was taken as 3.6m, 5.6m and 7.5m.

6.2.3 Load Combinations

Four different loading conditions, types A, B, C and D have been considered which are shown in figure 6.3. A description of the various loading types follows:

In loading type A, concentrated beam loads were applied at the quarter points of each beam up to a value of 27kN (F_1) each, in sequence-1. In sequence-2, the loading in beams no. 1,3,4 and 5 were increased by a further 22kN (F_2) each, while no additional load was applied in the remaining beams. The loading pattern was chosen to produce the most onerous effect of beam loading on the middle lift of the central column. Load sequence 3 starts with an axial load of 50kN in the top of the central column. This load was continued to be incremented until failure.

Type B loading corresponds to beam load only case, where the beams are loaded in the same way as described in loading type A, with the difference that the loads in the second sequence were continued until failure occurred. No column loads were applied in this case.

In loading type C, purely in academic interest, only column load was applied on the top of the central column, and increased to failure.

In contrast to the sequence of type A loading, in type D the axial column load on the central column was applied first up to a value of 450kN. Then, in sequences 2 and 3, beams were loaded in the same fashion as in sequence 1 and

2 of loading type B until failure.

6.2.4 Imperfections

Two types of imperfection have been used in order to study the influences of the imperfection on the strength of the semi-rigidly connected frames. The first is the geometric one using a sinusoidal shape for the column and the second is material with Lehigh type [71] residual stress pattern being adopted. Two shapes of geometric imperfection, shape-1 and shape-2 are shown in figure 6.4. Unless mentioned specifically, the term geometric imperfection, in this chapter, would refer to shape-1. A value of central deflection of $L/1000$ has been used as this is commonly specified by the codes of practice [1], [2]. The residual stresses found in the rolled sections are often quite random in both magnitude and distribution. The actual distribution of residual stress in the flange of a wide-flange section falls between the parabolic and the linear stress distribution [92]. Figure 6.5 shows if the controlling residual stress values at the flange tips are both taken as $0.3\sigma_y$, then the linear pattern would produce the most onerous effect [93]. For this reason the linear pattern of residual stress with the controlling values shown in figure 6.6 has been used in this study.

6.2.5 Material Properties

An elastic-perfectly-plastic material behaviour was assumed in the analysis. Strain hardening was neglected as it has virtually insignificant influence on the load capacity of the tall structures such as those considered under the purview of this parametric analysis. The yield stress was taken as 285 N/sq. mm and the mod-

ulus of elasticity was assumed to be 210 kN/ sq.mm.

6.3 Influence of Connection Stiffness on the Behaviour of Frames

6.3.1 General

The important results of the parametric study are presented here to demonstrate how connection stiffness influences the overall behaviour of the frame. In presenting the results, the principal aim will be to identify the influential parameters which may have implications in the development of any design method for semi-rigid frames. Unless otherwise specified, the discussion in the remainder of this chapter will be on the stage-1 frames subjected to type-A loading.

6.3.2 Ultimate Capacity of Semi-Rigid Frame

The strength capacity of the frames of stage-1, subjected to loading type-A are shown in figure 6.7, against the corresponding connection type. In representing the connections along abscissa, non-numeric connection nomenclatures have been used. This has been done deliberately to avoid any misrepresentation of the connection by a numeric index (initial connection stiffness, for example), until a convincing conclusion is reached regarding the suitability of such a numeric index which could represent the connection performance. The effect of various parameters on the connection performance in the frame can be seen clearly in figure 6.7, in which the additional column loads carried by the frame are shown

against the connection types. Results of the frames with three different storey heights are included in these figures. Figure 6.7(a) shows the frame strength for a perfect system, i.e. members are free from geometric as well as material imperfections. It can be observed that the strength increasing effect of the stiffer connections is more significant for slender frames. For the shorter storey heights considered (those typically found in building frames) connection stiffness seems to have virtually no influence on the strength. Although surprising, this is quite conceivable, because the particular loading adopted here causes a column failure and the column in these cases being fairly stocky sustained a load which is very nearly close to its squash load. On the other hand, it can be seen from the figure that with higher storey height, the frame strength was low with pin connections and shows an increase in strength when stiffer connections are used. Another important observation from figure 6.7(a) is that with stiffer connections the shorter frames sustained lower load than the corresponding value with pin connection. This can be explained by noticing the distribution of internal forces in the members. For example, the axial force and the bending moment values in the lower lift of the central column for the different cases discussed in figure 6.7 (a) are shown in figure 6.8 (a) and (b). The values shown in figure 6.8 correspond to the end of sequence 2 for type-A loading. It can be seen from figure 6.8 (a) and (b) that the stiffer connections have attracted higher forces in the central column and the adopted loading type in this case was such that failure was in that particular column, as a result of which the beneficial effect of the connection stiffness has been suppressed, at least in terms of strength capacity. For an external column, however, the share of beam load will be correspondingly less. The loss of strength for an increased connection stiffness has also been reported in the work of Davison et al [42] and Ackroyd et al [35].

Figure 6.7(b) records the frame responses where Lehigh type residual stress has been assumed in the column. The pin connected frame suffered some loss of strength due to the presence of residual stress, but when any form of connection stiffness was present, the frame has sustained practically the same load as that of the corresponding perfect frame. With the presence of residual stress the onset of inelastic action in the column occurred much earlier in the loading sequence as can be seen from figures 6.9(a) and (b) which shows the variation of the column top end moment (left hand ordinate) and the column EI ratio (right hand ordinate) with the axial stress carried by the column, C6, of 3.6m storey height frame and with flange cleat connection. The EI ratio, in the figure presents the column's instantaneous flexural stiffness as a fraction of its elastic flexural rigidity. It can be seen that when the column is free from residual stress it remained elastic until it had sustained an axial load as high as $0.93 \sigma_y$ and with a co-existing moment of considerable magnitude. On the other hand when residual stress is present inelastic action in the column started at a level of $0.61 \sigma_y$, whence column stiffness starts to degrade. Consequently the column end moment also started to be shed and the columns in this case were called upon to resist a lower moment associated with a given value of axial load (albeit with a corresponding lower EI ratio). As a result of this action, at failure, the frame with residual stress in the column carried virtually the same load as the one without any residual stress.

In figure 6.7(c) the corresponding features associated with geometric imperfection in the column are shown. In this case, for the two shorter frames considered, the ultimate loads are slightly lower (especially when some form of connection is present) than those shown in figure 6.7 (a) for a perfect frame. However, it can be observed that the slender the frame is the more vulnerable to

geometric imperfection.

Figure 6.7(d) presents a more practical case, when the columns are subjected to both geometric and material imperfections. It can be seen that the presence of both imperfections is not synergistic and loss of strength is not too alarming as long as some form of connection is present. Research on isolated columns, of course, reported the diminishing effect of the connection stiffness when associated with imperfections [4]. The present findings with framed column of practical slenderness range, however, does not show any serious detrimental effect on the strength due to the presence of imperfections, particularly when connection stiffness of some form is present.

Summary of Observations on Figure 6.7:

For frames loaded in a manner that failure is due to column instability following observations can be made:

1. Within the practical range of frame slenderness, connection stiffness does not improve the frame strength, provided the loading is such that a column failure occurs. This finding is in agreement with the observation of Jones et al [4] on isolated columns, that most significant improvement in column strength for an increased connection stiffness occurs for column of slenderness beyond practical range.
2. The deleterious effect the imperfection produces on frame strength is greater for a pinned frame. Connection stiffness, of whatever magnitude, reduces this effect.
3. The combined effect of both imperfection types are not additive in the frame of shorter storey height (that normally found in building frames) when some form of connection is present.

Figure 6.10 shows the same results (of figure 6.7), but in a different form, in order to delineate the imperfection sensitiveness of the frame for different types of connection. Figures 6.10 (a) to 6.10 (d) show the cases of Pin, FC, FEP and EEP connections respectively. In these figures the additional column load (that applied in load sequence 3 of type A loading) required to cause failure is plotted against the column slenderness ratio L/r , where L is the length of each column (storey height). The four cases shown in figure 6.10 are:

1. Perfect Column
2. Column with Lehigh type residual stress
3. Column with initial central deflection of $L/1000$ and
4. Columns having both (2) and (3) above.

It can be seen quite clearly from these figures that with the use of stiffer connections, the scatter between the failure loads of the perfect and the imperfect frames becomes less pronounced. In a simple frame (pin connected) the geometric imperfection has more effect on more slender frames. The presence of residual stresses has only a moderate effect on the frame strength. Figure 6.10 (b) shows that within the typical slenderness range that are found in building frames, the mere presence of a connection is sufficient to narrow down the detrimental effects of the imperfections on the frame strength, as demonstrated here with a flange cleat connection.

With a flush end plate connection, figure 6.10 (c) shows more or less similar behaviour as for the flange cleat connection. Figure 6.10 (d) shows a more

uniform behaviour for the entire range of slenderness considered which means that the connection stiffness, in this case, is sufficient to offset the effect of the imperfections.

For all the four cases presented in figure 6.10 it can be observed that, for the shortest frame ($h=3.6\text{m}$), the presence of both types of imperfection is not additive as is the case with taller frames.

Figure 6.11 presents the frame response for type B loading. As defined earlier in section 6.2, type B loading refers to the patterned beam loading continued until the failure. No direct load on the column was applied. The ordinate in figure 6.11 represents the magnitude of each of the two concentrated loads at failure in any of the heavily loaded beams. The abscissa represents the particular connection type. Results of all the three storey heights considered in this study are shown in figure 6.11. No imperfection was considered in the members. Unlike the results of type A loading (shown in figure 6.7 (a)), the increasing stiffness of the connection in this case has led to higher failure load with the exception of the rigid connection case. As failures in this case are located in the beams, the frames sustained higher load as long as the connection moment relieved the span moment. However, with rigid connections, large moments are built up at the beam ends and the frame failed at a lower load. This behaviour may be due to the fact that since an elastic-perfectly-plastic material behaviour has been assumed in the analysis, when the moment in a section reaches its full plastic capacity the structure is said to have failed.

In the next case the hybrid loading type-D was considered in which a column load of 450kN was applied incrementally on the central column and patterned beam loads were then applied as in sequence 1 and sequence 2 of type

B loading. The values of the individual loads on the beams at failure, are shown against the corresponding connection types in figure 6.12. Results of all three different storey heights are included. As in figure 6.11 the values in the ordinate refers to the value of a single load, on any of the heavily loaded beams at failure. The application of column load (of the order of $0.5 P_Y$) has again resulted in failure in the column. The consequence is that higher connection stiffness has caused higher forces in the column, which eventually suppressed any strength increasing effect due to an increased connection stiffness.

Figure 6.13 presents a case where a concentrated load is applied on the top of the central column. This is a case of pure academic interest, rather than a practical one. For the frame with a storey height of 3.6m the column carried the full squash load for all the five connections considered. The frames with 5.6m storey height and with pin and FC connections also sustained the full squash load. However, the same frame with the even stiffer FEP, EEP and rigid connections carried a little higher load than the column squash load P_Y . This is because of the fact that as the connection-to-beam stiffness increases relative to the column, part of the load is carried through the beam to the two external columns, allowing the central column to take some more load. The tallest frame with storey height 7.5m has columns which are rather slender ($L/r= 115.3$) and with pin connections it carried a load of 520kN increasing to the full squash load when FC connections were used. Further increases in connection stiffness (with FEP, EEP and rigid connections) led to a load higher than the squash load in the same way as explained in the preceding case.

6.3.3 Flexible End Moment and Its Distribution to Column Ends

The nomenclature 'Flexible End Moment' (FLEM) for flexible or partially restrained (PR) frame derives from its similarity with Fixed End Moment (FEM) for fixed or rigidly supported member, and has been used in the literature [94]. In other words FLEM refers to the moment that develops at the end of the beam, which is connected to a column by means of a flexible connection. In this section the results of the parametric study relating to the development of FLEM will be presented. Consideration will also be given to the distribution of this FLEM to the column ends. For the sake of brevity the results of stage-1 subjected to the type-A loading scheme on perfect frames will be presented in detail and reference will be made to other cases as appropriate.

6.3.3.1 Beam End Moment

The variation of the beam end and span moment with the applied beam load is presented first. Figures 6.14(a), (b) and (c) show the beam moment for beams number 1, 2 and 3 respectively for frames with the flange cleat connection and subjected to type-A loading scheme. The effect of the nonlinearity of the connection response is clearly evident when examining the end moments and significant differences in the performance of internal (right hand end) and external (left hand end) ends of the beam are noticeable. As will be seen later in section 6.4, that internal connection undergoes a smaller rotation than its external counterpart for a given load level and thus operates at higher connection stiffness. Beams no. 1 and 3 were loaded up to the full designated value i.e. two loads of 49.5 kN each

(99 kN on each beam), whereas beam no.2 was loaded up to 27kN (54 kN on the beam). As the beams were loaded, the connection attracted moment initially at a high rate and then at a gradually diminishing rate, reaching a limiting value of end moment. Consequently the development of span moments were initially modest but after a certain stage, when the end moments had reached their limiting value, virtually all the moments due to the applied load were developing in the span (centre). Figures 6.15 and 6.16 represent the cases of frames with flush end plate and extended end plate connections respectively. The general behaviour is more or less as that described in figure 6.14 for the flange cleat connection. The limiting moment that developed at the beam end appears to be the full capacity of the connection for the interior end, and approximately half of that value for the exterior end. Also it can be observed that connections in the lower floor beams provide more restraint than those of the top most floor. However, some interior connection might have behaved differently just because of the particular loading adopted, i.e. after the commencement of differential loading in the adjacent beams.

6.3.3.2 Column End Moment

The column in a frame carries moment as well as axial load induced by the beam loading. An assessment of the column end moment is, therefore, an important step in any refined column design procedure. The parameters which control the transfer of moment from the beam end to the column end will be identified here.

Figure 6.17 presents the moment at the top of column C6, plotted against the effective connection stiffness, C^* for frames with 3 different storey heights, each having 3 different beam-to-column connections. The parameter C^*

as defined by Bjorhovde [3] is as follows:

$$C^* = \frac{\frac{2EI_b}{L_b}}{\left(1 + \frac{2EI_b}{L_b}\right)} \quad (6.1)$$

The moment shown in the figure corresponds to the end of beam loading phase. In the computation of C^* used in figure 6.17 a secant stiffness (based on 10 millirad rotation) has been used to represent the connection stiffness. The basis of this secant stiffness will be discussed later in this chapter. For a given beam span, beam depth and connection, increasing the column length has the implication of reducing the column stiffness. Viewed from that perspective, figure 6.17 would indicate that for a given beam-to-connection stiffness, the more slender the column, the smaller will be the moment transferred or the smaller will be the moment developed at the beam end, since it will be shown later that column moment is a direct consequence of the beam end moment. Also it is noticeable from the figure that the effect is progressively greater for stiffer connections. This, however, leads to the fact that restraint provided by a connection, depends not only on the stiffnesses of the beam and the connection, but also on the stiffness of the column to which the beam is connected. Consequently it becomes important that any basis for the design of semi-rigid frame or the classification of connections should take this into consideration. In the next chapter a proposal for the development of such a basis will be presented.

6.3.3.3 Column Moment: A Fallacy of So Called Simple Design

Figures 6.18 to 6.20 present the moment attracted at the top end of column C6 against the applied loads. The abscissa of these figures set an arbitrary scale, in which stages 1, 2 and 3 refer to the last three load steps during the beam loading phase (i.e. sequence 2) of type A loading. Results from frames with

the 3 different flexible connection types (described earlier in section 6.2) appear in figures 6.18, 6.19 and 6.20 in succession. Also included in these figures are the approximate moments (dashed line), based on fixed eccentricity of beam reactions – as suggested by the UK code of practice [1] for simple design. The solid lines represent the results of rigorous analysis by the present program for the different column lengths considered. For all the three types of connection considered the column moments developed were proportional to the applied beam loads. However, it must be borne in mind that this proportionality is not valid for the entire loading history, as has been seen in figures 6.14 to 6.16, for the beam end moments. Nevertheless, the essential message of is that, at relatively high levels of loading, the column moment is directly proportional to the magnitude of beam loading and the stiffer the column the higher will be the moment attracted into the column. Another important fact that is revealed here is that even a flexible connection like the flange cleat produces higher column moments than those estimated by a nominal 100 mm eccentricity (from the face of the column in major axis bending). Similar quantities for an external column (lower end of column C2, in this case) are presented in figure 6.21. Only the results relating to the frame with storey height equal to 3.6 m are shown. The behaviour of other frames having different storey heights retained more or less the same pattern as shown for the interior column (see figure 6.18 - 6.20). Although the load stages designated 1, 2 and 3 of figure 6.21 and those of figures 6.18, 6.19 and 6.20 represent the same loading stage, the internal columns were subjected to balanced loading up to a level of 54 kN per beam and consequently are subjected to a smaller moment.

6.3.3.4 Distribution of Beam End Moments in the Column

The beam end moment plus the moment produced by the eccentricity of the beam end shear constitute the total moment to be considered in the column. It is conventional to apportion this moment to the upper and lower column in proportion to their respective stiffnesses. Figures 6.22 (a), (b), (c) and (d) show the distributions of moment in the columns at joints J2, J3, J5 and J6 as beam loads are applied for a frame with 3.6 m storey height and flange cleat connections. The disparity in the distribution of moments in the adjoining columns (of a junction) of apparently equal stiffness is due to the particular deformed shape of the columns as produced by the adopted loading type (type-A). Figure 6.23 shows the exaggerated deformed shape of the columns at two different stages. Initially at a beam load value of 27 kN each, the external column tends to form a double curvature shape in the upper lifts (figure 6.23(a)). Accordingly the stiffnesses of the columns in the adjoining storeys vary depending on the conditions at the far end.

The central column does not show any bending up to 27 kN load (i.e. up to the end of symmetric beam loading). As the load sequence 2 proceeds, all three lifts of the central column tend to bend in single curvature. The end of column C4 at junction J4 simulates a virtually no rotation situation, because of symmetric loading on the adjoining beams. So at junction J5, column C4 is stiffer than column C5. Similarly the lower fixed end of column C6 makes it stiffer than its immediately upper counterpart column C5 at J6. This explains, therefore, the distribution of the column end moments at junction J5 and J6.

The distribution of the moments at the end of column at junction J2,

J3, J5 and J6 for frames with FEP and EEP connections are shown in figures 6.24 and 6.25 respectively. The general behaviour in these two cases is similar to that shown in figure 6.22 with respect to the FC connection.

6.4 Connection Rotation at Failure

For non-sway frames failure is dependent on many factors including loading type, frame geometry, member sizes etc. In this section the development of connection rotation with the applied loading is discussed with particular emphasis on the level of connection rotation at failure. Figures 6.26 to 6.28 record the variation of the column load against rotation of the connection for all the three connection types considered. All three figures refer to the frame with 3.6m storey height. The column load shown, refers to the column immediately below the corresponding connection. The rotation of connections no. 1, 2, 5, and 7^{††} are shown, from which it can be seen that 1 and 5 are external connections whereas 2 and 7 are internal connections.

The overall behavioural pattern for flange cleat, flush end plate and extended end plate connections are similar, although the stiffer connections have suffered relatively smaller rotations. At the top level, connection no. 1 has undergone slightly more rotation than connection 2 because of the flexibility of the external column, at the end of beam loading. At the 2nd floor level again the external column suffered slightly more rotation than the internal one, at a load level prior to the commencement of differential loading in the adjacent beams. Connection 5, being associated with beam 2, started to unload when the loading on B2 was ceased.

^{††} Connections 1 and 2 are at the left and right ends of beam B1, connections 3 and 4 are at the left and right ends of beam B4 and so on.

Both the internal connections shown in these figures, started to unload with the commencement of the load on the internal column. This phenomenon is well explained elsewhere [12,20]. However, the phenomenon of moment shedding is discussed in the next section.

Having seen the progression of the connection rotation with increasing load, it is now proposed to examine the level of connection rotation at the failure condition for the various cases studied under this parametric study. Tables 6.2 to 6.5 present the percentage of cases, corresponding to a certain range of rotation at failure for the three different types of connection considered. For this purpose rotation of connection no. 7, which is liable to be highest rotation among the internal connections considered here. Table 6.2 summarises the results of stage-1 parameters with type-A loading scheme. The statistics shown in this table also include the cases with imperfections as described in section 6.2. It can be seen that the maximum rotation at failure was below 10 milli- radian even with the rather flexible flange cleat connection. This rotation was much less with flush end plate and extended end plate connections. For given connection types, the presence of imperfections (material or geometric) does not significantly influence the level of rotation at failure.

Table 6.3 shows the corresponding statistics for stage 2 frames, which shows the effect of variation in slenderness of the upper and lower column with respect to the connection under consideration. These figures, when compared with the figures of table 6.2 (perfect conditions only), show a slightly higher level of rotation. However, in most cases failure occurred at the vicinity of a connection rotation of 10 milli- radian.

Tables 6.4 and 6.5 present the level of connection rotation for the stage-

3 cases where beam spans of 6.0 m (span/depth = 23.6) and 7.0 m (span/ depth = 27.6) were used. The figures in these tables indicate that increased beam flexibility would result in a higher connection rotation at failure. With the 6.0 m beam span most of the values of connection rotation at failure were around 10 to 12 milli-radian. However, with the 7.0 m beam span, connection rotation much higher than 10-12 milli-radian range was observed, especially with the flange cleat connection. It must be emphasized that this particular beam was too slender to be used with such a flexible connection in any practical structure.

The findings presented in tables 6.2 to 6.5 clearly demonstrate that the connection rotation level at failure in a practical non-sway structure is unlikely to be greater than 12 milli-radian and depending on the connection stiffness this rotation could be even less than 5 milli-radian. So a general recommendation of connection rotation level may not be appropriate for all connections, although a maximum limit of 12 milli-radian seems justifiable, for non-sway cases.

6.5 Moment Shedding and the Effect of Initial Geometric Imperfection

The phenomenon of moment shedding has been well described by different researchers [95,96,97]. In the context of semi-rigid frame response a clear understanding of this phenomenon is essential, since the selection of a suitable value of moment is a prerequisite for any column design procedure. Also, the presence of initial geometric imperfection may play an important part towards controlling the magnitude of this moment. In this section a number of case studies

will be presented to delineate the effect of geometrical imperfection on the value of column moments in general, and on the phenomenon of moment shedding, in particular. Before these results are presented a brief account of the previous work on moment shedding reported by other researchers is made first.

During the verification of their analytical model Poggi and Zandonini [95] used Davison's subassemblage tests [32]. The dimensions and loading pattern for one of the tests (ST8) are shown in figure 6.29(a). The symmetric beam loads were applied first, after which axial loading on the column was applied and continued until failure. The non-dimensionalized load vs. moment plot in figure 6.29(b) shows the development of moment in the beam ends and the column end at the top joint. It can be seen that failure occurred when the column axial load was in the vicinity of $0.62 \sigma_y$, suggesting an elastic instability mode of failure. Analytical prediction closely matched the test results and no sign of moment shedding was observed.

Chen [96] analysed a portal frame in a non-sway condition and under proportional beam and column loading using two different proportions of beam-to-column load as shown in figure 6.30(a). In the first case beam loading was deliberately kept small in order to keep the beam section elastic, while in the second case a relatively higher beam loading was applied so that inelastic action could begin in both the beam and the column simultaneously. Using three different connections, flexible, stiff and rigid (figure 6.30(b)), an elasto-plastic analysis was carried out up to failure for each loading case mentioned above. The moment-load plots for these cases are shown in figure 6.31(a) and (b). It was concluded in the reference that moment shedding commences as soon as inelastic action begins in the column while the beam remains wholly elastic. Also it was

observed that, the more flexible the joint, the later will be the commencement of moment shedding. On the other hand, no moment shedding occurs if yielding in the column is accompanied by yielding in the beam, since their relative stiffness will remain more or less unchanged. The same reference also showed the effect of applying column load after the application of beam loading for the simple portal frame shown in figure 6.32(a). It has been reported that the magnitude of the column end moment (due to beam loading first) decreases as the column axial load increases, except for the very flexible connection, as shown in figure 6.32(b). It can be seen that even for the rigid connection, when the moment shedding effect is most pronounced, the rate of decrease (shedding) is very small. Rifai [97] reported a decrease in column end moment with the gradual plastification of the column as axial load was applied on the column subassembly of figure 6.33 (see figure 6.34(a)). This matches the observation of Chen as reported earlier. Rifai [97] also reported a dramatic decrease in column end moment as axial column load is applied after the application of beam load on the subassembly beam (see figure 6.34(b)).

Having set out this background attention is now focussed on some of the examples studied by the author using the present program. Various loading schemes have been considered in combination of two geometric imperfections (shape 1 and shape 2, see figure 6.4). The results indicate that the presence of an imperfection affects the moment values in the column. Loading types A and B are the same as described in section 6.2 earlier and having an imperfection pattern as shown in figure 6.4. Loading types A1 and B1 refer to the same sequence of loading as in A and B but a direct opposite pattern of beam loading was applied in these cases. Beams no 3 and 5 were subjected to a load value of 27 kN (54 kN on beam) after which loading on these two beams were discontinued. Loading of

the remaining beams were continued until the commencement of column loading (in type A1) or up to the failure (type B1). Loading A1 and B1 has the same implication of loading type A and B but opposing the direction of initial geometric imperfection shown in figure 6.4 (i.e. the dashed line). In the following section a clockwise moment in column end is regarded as negative. Figure 6.35 shows the column force against the column top end moment for column 6. The three distinct parts of the force-moment relationship shown correspond to the three phases of the loading adopted. The initial segment up to a force value of slightly below 200 kN presents the response to the symmetric beam loading phase where no moments were attracted in the column when no imperfection was specified. The column imperfection has drawn a slight moment (of the order of $0.014 M_{pc}$). In the second phase when beams were loaded unsymmetrically the column attracted moment at a dramatic rate. In the final phase when the column axial load was applied, only a moderate amount of further moment occurred at the column end and prior to failure, shedding of this moment took place as the plastification in the column began. This general pattern was observed in the all four cases reported in figure 6.35. Thus the effect which an initial imperfection produces on the magnitude of column end moment is not a significant one. The interesting point that can be observed from this figure is that, depending on the loading pattern and the direction of the initial shape, the presence of initial imperfection can in fact reduce the column end moment instead of increasing it. In figure 6.35 the column end moment for loading type A is less for the imperfect case than that in the case of the perfect one. However, loading type A1 produced more moment when associated with column imperfection compared with the case of a perfect column. Figure 6.36 records the force-moment relationship for the same column (column C6) but with loading type B and B1, each with and without column

imperfection. The initial response, in this case, is similar to that explained in connection with figure 6.35, the only difference being that the column moment continued to build up as beam loads are continued. The beam finally failed and as the column was elastic no sign of moment shedding was observed.

The two cases presented here refer to the response of column end moment. The corresponding central moments for the same column (C6) are shown in figures 6.37 and 6.38. Once again, depending on the loading pattern and direction of initial imperfection, the magnitude of the moment at column centre could be more or less than the corresponding values for a perfect column system. Figure 6.39 explains the way moments are induced in the column due to imperfections for type A and type A1 loading. As initial geometric imperfections are modelled by applying a set of nodal force as shown in figure 6.39(a) the direction of the column end moment will be as shown. Although the initial imperfections were chosen to give the most unfavourable condition for type A (or B) loading, it only produced an unfavourable moment at or near midspan and the column end (top) moment was relieved. On the contrary, for type A1 (or B1) loading (for which the imperfection was in opposite direction) the moment at or near the column centre was reduced due to the presence of imperfection while the end moment was aggravated.

The other important feature of figure 6.35 which needs to be discussed here is that the response of column as the transition from a beam loading to column loading occurs. References [96] and [97] reported moment shedding to occur as soon as the column load was applied after the application of beam load had stopped (see figures 6.32(b) and 6.34(b)). References [95] and [32] on contrary, did not observe the column end moment to reverse as the column axial

load was applied (see figure 6.29(b)). Figure 6.35, however, is in line with the observation of the latter references where moment shedding occurred only at the commencement of inelastic action in the column (see also figures 6.31(a), 6.34(a)). In order to clarify these rather paradoxical observations three different beam loading patterns (see figure 6.40) have been considered on the frame each of which was subjected to axial load on the either central column or the external column on the left. To economise on computer time beam loads were restricted to 18 kN (ie. 36 kN per beam), after which column load was applied. The resulting member end moments at joints J1, J2 and J3 on the external column and J4, J5 and J6 on the central column are shown in table 6.6 and table 6.7 respectively. Upon application of the column load, the end moments on the beams (connected to the column being loaded) are relieved (reduced) in all the cases, irrespective of the loading pattern adopted and also independent of the location of the column (external or internal) being loaded. As the external moments in all the joints remain the same as prior to the application of column load, the changes in the beam moments have to be balanced by a corresponding change in the column moment. In tables 6.6 and 6.7, ΔM refers to the change in moment due to the application of a 50 kN load on the column after beam loading has stopped. It can be seen that to maintain the joint equilibrium the column end moments are either increased or decreased. In the external column most of the cases show a decrease (underlined figures in the table 6.6), but in the case of the internal column only three cases (out of a total 9 cases shown) can be identified where column moments have been declining as the column load was applied.

Now it is clear that, in a frame when column loads are applied following beam loads, moment shedding is not a necessary phenomenon and even when it occurs the rate of decrease in moment may be very slow.

6.6 Conclusion

In this chapter a limited parametric study concerning the behaviour of a semi-rigid frame to various loading arrangements, frame geometry, connection stiffness and presence of imperfections has been presented. The sensitiveness of these parameters has been identified and the implications discussed. However, some most significant conclusions are summarized here.

1. The use of stiffer connections may increase or decrease the frame strength, depending on the frame geometry and the particular loading type adopted. However, stiffer connections would result in less deflections.
2. Practical connections tend to reduce the frame's susceptibility to strength loss due to the presence of imperfections when compared to ideal pin connections.
3. The strength increasing effect of the stiffer connections is more significant for slender frames and for shorter storey heights (those typically found in building frames) connection stiffness seems to have virtually no influence on frame strength.
4. The presence of both material and geometric imperfections together is not synergistic for semi-rigid frames.
5. The normal initial geometric imperfection ($L/1000$) affects the column moment only moderately.
6. The exact sequence of the application of the beam load and the column load, in general, does not appear to have any significant bearing on the load carrying capacity of a semi-rigid frame.

7. Interior connections, in general, tend to undergo less rotation than the exterior ones and under the symmetric condition draws higher moment than the exterior end.
8. For a given connection-to-beam stiffness, increasing the column slenderness will decrease the end moment developed.
9. The concept of a fixed eccentricity of the beam end shear to estimate the disturbing moment in the column could in some cases grossly underestimate the column moment and this end moment is in fact a function of the stiffnesses of the beam, the column and the connection.
10. For non-sway frames, the maximum connection rotation at or near the failure can be taken as 12 milli radian for most frames of reasonable dimensions – although a value of 10 milli radian can be considered adequate for most practical purposes. This rotation level is not very sensitive to the presence of imperfections. However, for stiffer connections a failure rotation less than 5 milli radian has also been observed.
11. The phenomenon of moment shedding in columns may occur either due to degradation of column stiffness due to the initiation of inelastic action or due to the application of column load after beam loading phase. However, it is not a necessary phenomenon.
12. From the view point of the designer, the moment shedding phenomenon need not be a consideration in design since the rate of decrease in moment in a framed column was found to be insignificant, even if it occurs.

Stage No.	Beam Span (m)	Storey Height (m)		
	L_b	h_1	h_2	h_3
1	5.0	3.6	3.6	3.6
		5.6	5.6	5.6
		7.5	7.5	7.5
2	5.0	3.6	3.6	3.6
		3.6	5.6	3.6
		3.6	7.5	3.6
3	6.0, 7.0	3.6	3.6	3.6
		5.6	5.6	5.6
		7.5	7.5	7.5

Table 6.1 Range of geometric parameters considered.

Imperfection	Conn. Type	Cases with Failure Rotation			
		0-5 m rad	5-10 m rad	10-12 m rad	12- m rad
Perfect	FC	0	100%	0	0
	FEP	33.33%	66.67%	0	0
	EEP	100%	0	0	0
Residual stress present	FC	0	100%	0	0
	FEP	33.33%	66.67%	0	0
	EEP	100%	0	0	0
Geomet. imperfect column	FC	0	100%	0	0
	FEP	33.33%	66.67%	0	0
	EEP	100%	0	0	0
Both Geomet. & material. imperfection	FC	0	100%	0	0
	FEP	66.67%	33.33%	0	0
	EEP	100%	0	0	0

Table 6.2 Percentage of cases (Stage-1) for different levels of failure rotation.

Imperfection	Conn. Type	Cases with Failure Rotation			
		0-5 m rad	5-10 m rad	10-12 m rad	12- m rad
Perfect	FC	0	66.67%	33.33%	0
	FEP	0	100%	0	0
	EEP	66.66%	33.33%	0	0

Table 6.3 Percentage of cases (Stage-2) for different levels of failure rotation.

Imperfection	Conn. Type	Cases with Failure Rotation			
		0-5 m rad	5-10 m rad	10-12 m rad	12- m rad
Perfect	FC	0	0	33.33%	66.67%
	FEP	0	33.33%	66.67%	0
	EEP	0	100%	0	0

Table 6.4 Percentage of cases (Stage-3: 6.0 m beam span) for different levels of failure rotation.

Imperfection	Conn. Type	Cases with Failure Rotation			
		0-5 m rad	5-10 m rad	10-12 m rad	12- m rad
Perfect	FC	0	0	0	100%
	FEP	0	0	33.33%	66.67%
	EEP	0	100%	0	0

Table 6.5 Percentage of cases (Stage-3: 7.0 m beam span) for different levels of failure rotation.

Load case	Joint no	Stage of Col. Load	M_b	ΔM	M_{cu}	M_{cl}	ΔM
1	1	Before	5.18			-6.42	
		After	5.05			<u>-6.29</u>	
				-0.13			+0.13
	2	Before	7.77		-4.97	-4.08	
		After	7.67		<u>-4.90</u>	<u>-4.05</u>	
				-0.10			(+0.07+.03)
	3	Before	6.85		-4.65	-3.47	
		After	6.80		<u>-4.62</u>	<u>-3.45</u>	
				-0.05			(0.03+0.02)
2	1	Before	4.95		-6.28		
		After	4.80		<u>-6.13</u>		
				-0.15			+0.15
	2	Before	1.084		-1.181	0.162	
		After	0.796		<u>-1.029</u>	-0.298	
				-0.288			(+0.152+.136)
	3	Before	7.18		-3.61	-4.93	
		After	7.11		<u>-3.53</u>	-4.94	
				-0.07			(0.08-0.01)
3	1	Before	5.76		-7.10		
		After	5.64		<u>-6.98</u>		
				-0.12			+0.12
	2	Before	8.33		-5.36	-4.33	
		After	8.24		<u>-5.30</u>	<u>-4.30</u>	
				-0.09			(+0.06+.03)
	3	Before	7.47		-5.02	-3.80	
		After	7.42		<u>-4.99</u>	<u>-3.78</u>	
				-0.05			(0.03+0.02)

Table 6.6 Change of beam and column end moment due to application of column axial load in external column.

Load case	Joint no	Stage of Col. Load	M_{br}	M_{bl}	ΔM	M_{cu}	M_{cl}	ΔM
1	4	Before	14.07	-13.95			-1.24	
		After	13.88	-13.76			-1.24	
					(-0.19+0.19)			0.0
	5	Before	13.09	-13.32		0.014	+2.13	
		After	12.95	-13.18		0.0138	0.215	
					(-0.14+0.14)			(-0.002+0.002)
	6	Before	13.80	-13.49		-0.12	-0.183	
		After	13.74	-13.43		-0.12	-0.183	
					(-0.06+0.06)			(0.00+0.00)
2	4	Before	3.84	-7.98			5.48	
		After	3.56	-7.80			5.50	
					(-0.28+0.18)			+0.10
	5	Before	2.06	-9.21		4.53	3.97	
		After	1.74	-9.11		4.63	4.09	
					(-0.32+0.1)			(+0.10+.12)
	6	Before	3.10	-8.89		4.17	2.97	
		After	3.04	-8.82		4.19	2.94	
					(-0.06+0.07)			(0.02-0.03)
3	4	Before	5.36	-7.51			3.49	
		After	5.10	-7.28			3.52	
					(-0.26+0.23)			+0.03
	5	Before	8.05	-4.58		-2.00	-2.798	
		After	7.87	-4.40		-2.00	-2.798	
					(-0.18+0.18)			(0.0+0.0)
	6	Before	4.485	-8.905		1.65	4.12	
		After	4.425	-8.79		1.58	4.135	
					(-0.06+0.115)			(-0.07+0.015)

Table 6.7 Change of beam and column moments due to the application of the axial column load in the central column.

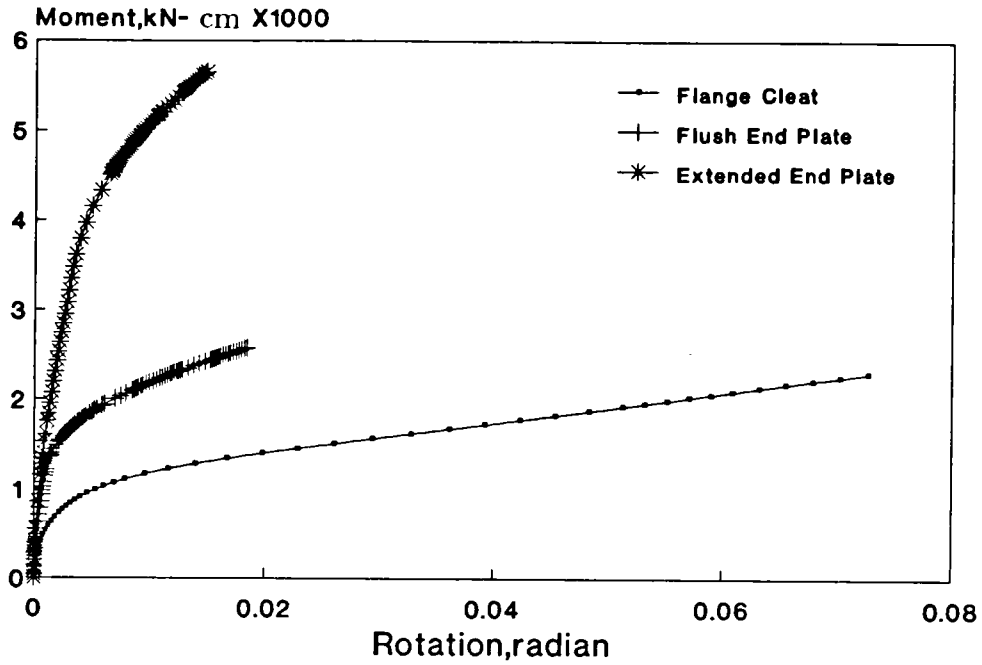


Figure 6.1 Moment-rotation relationship of the three connections considered.

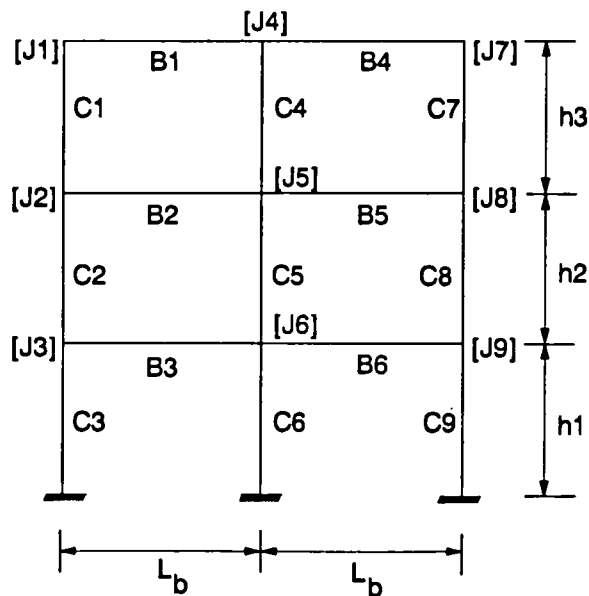


Figure 6.2 Frame geometry and designation of the members.

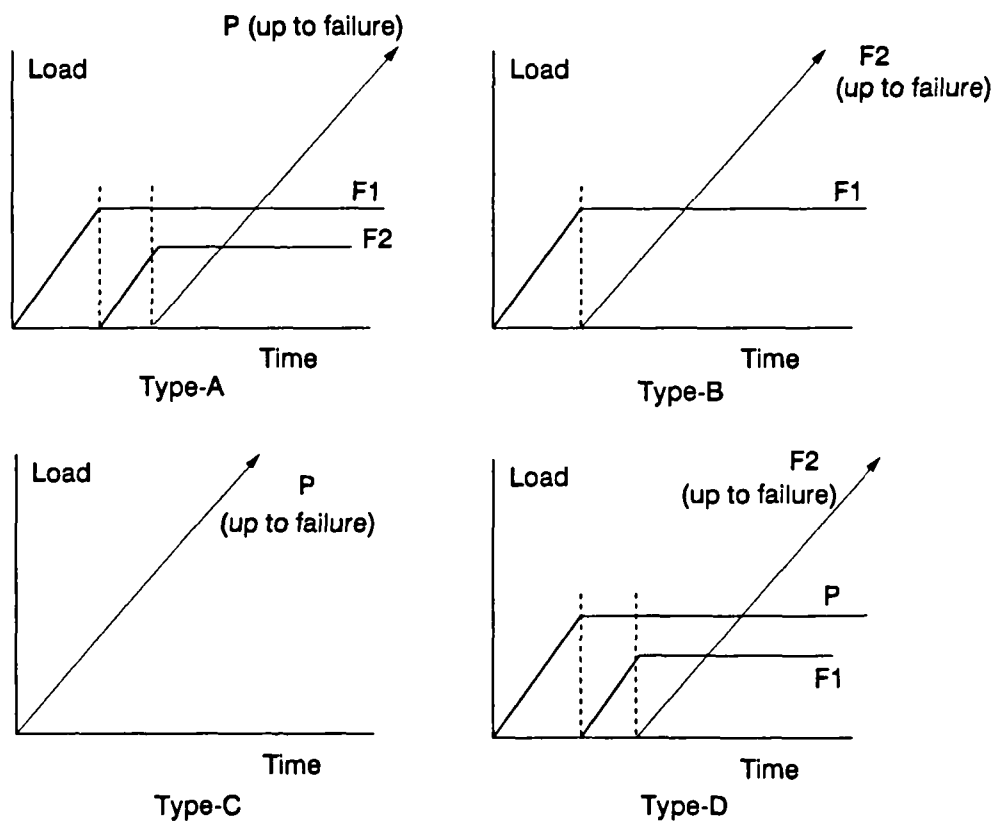
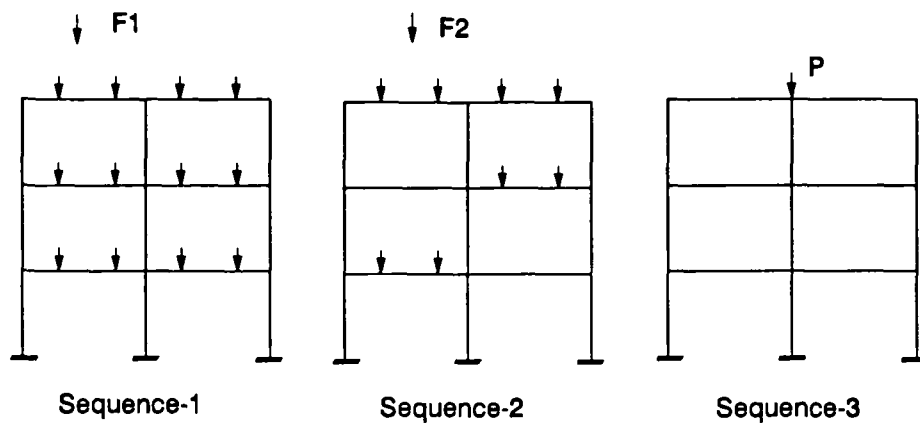


Figure 6.3 Loading types used in the parametric study.

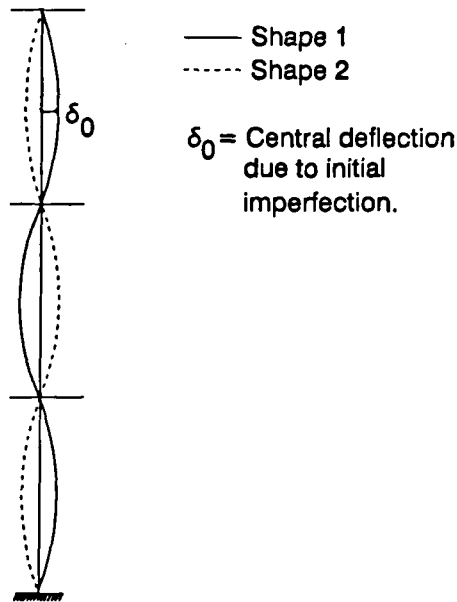


Figure 6.4 Initial geometric imperfections in the column.

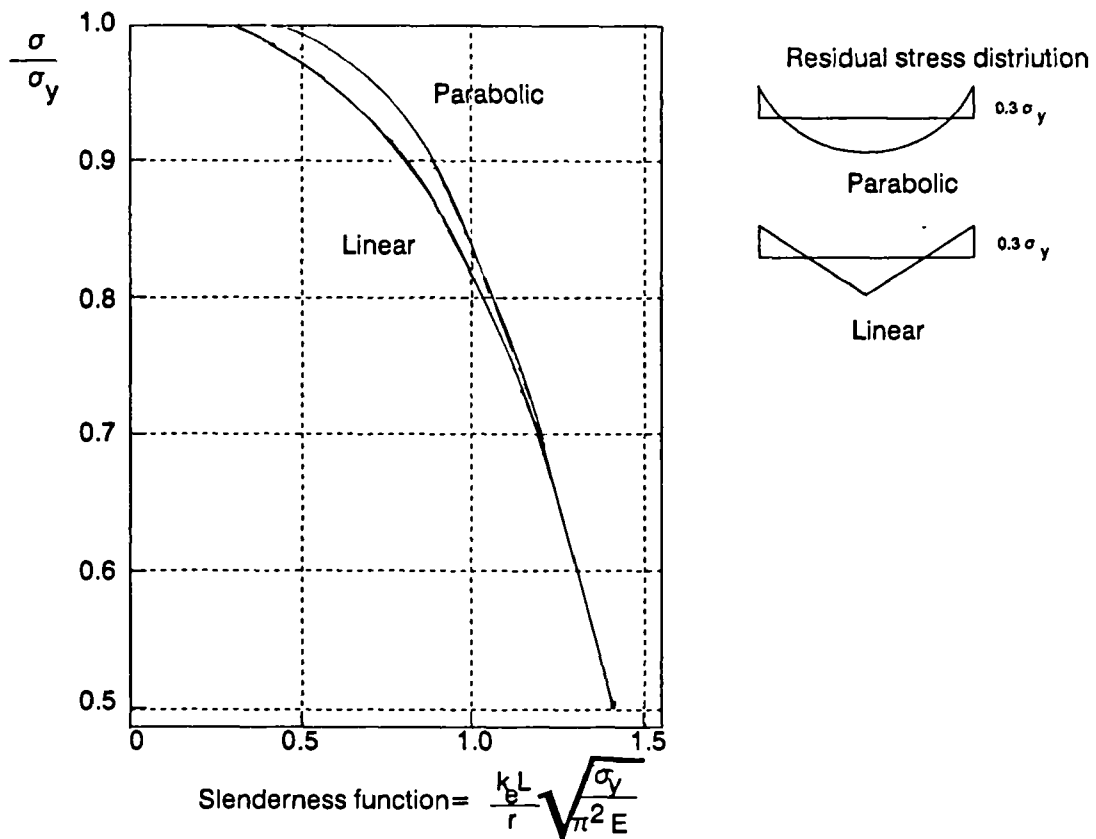


Figure 6.5 Column strength curves for two different patterns of residual stress [93].

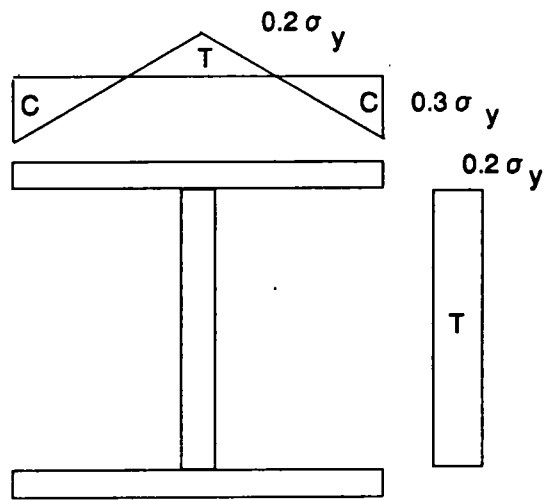
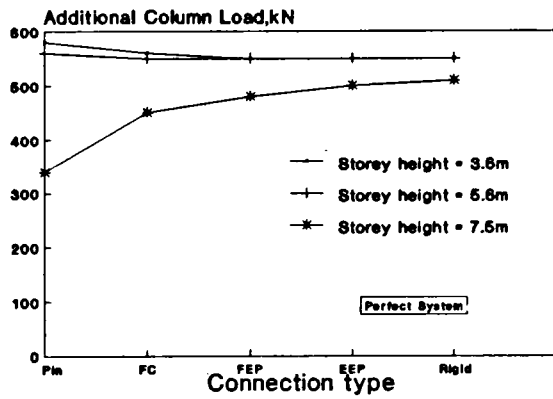
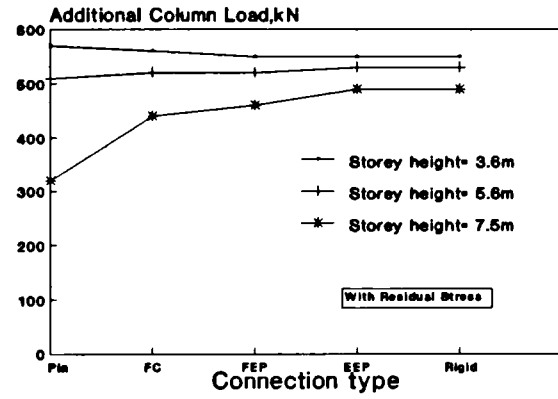


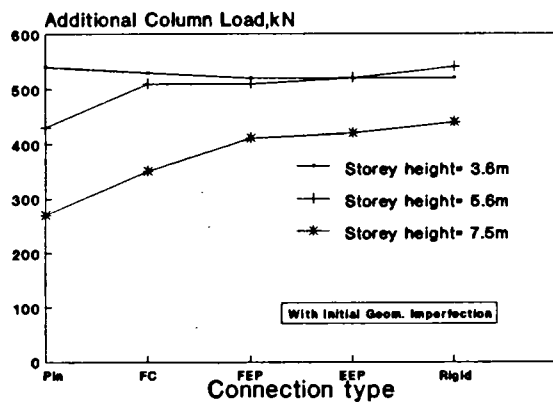
Figure 6.6 Residual stress pattern used in the study.



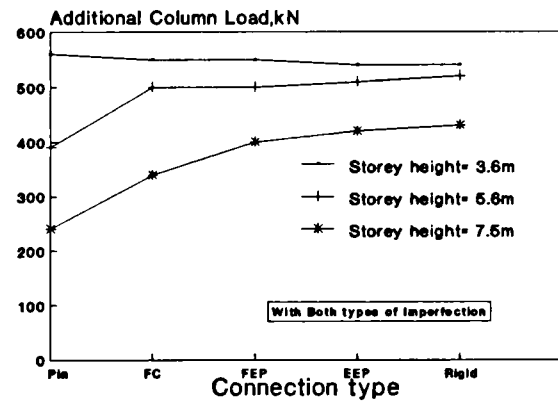
(a)



(b)

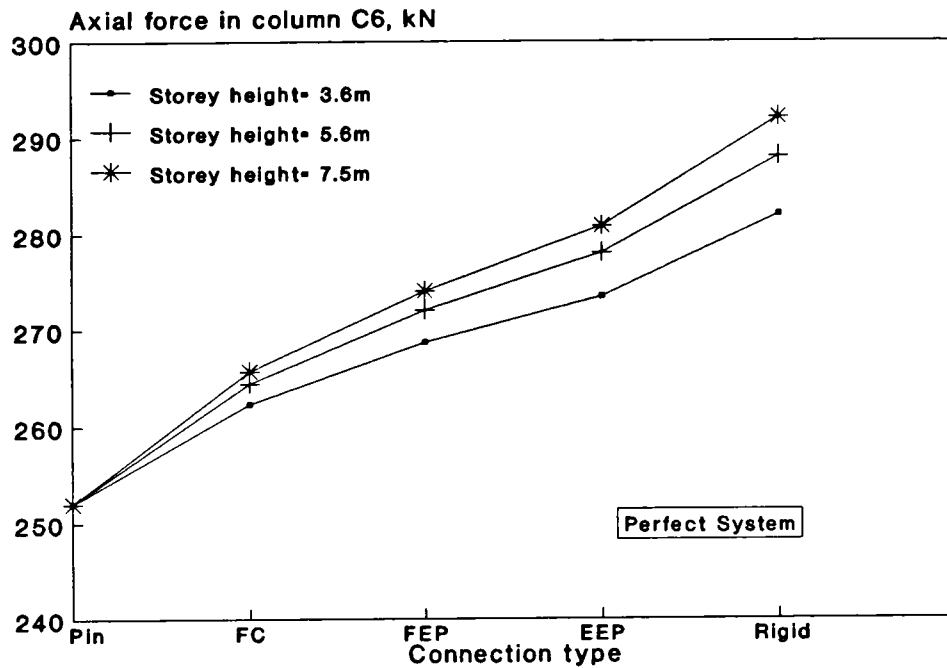


(c)

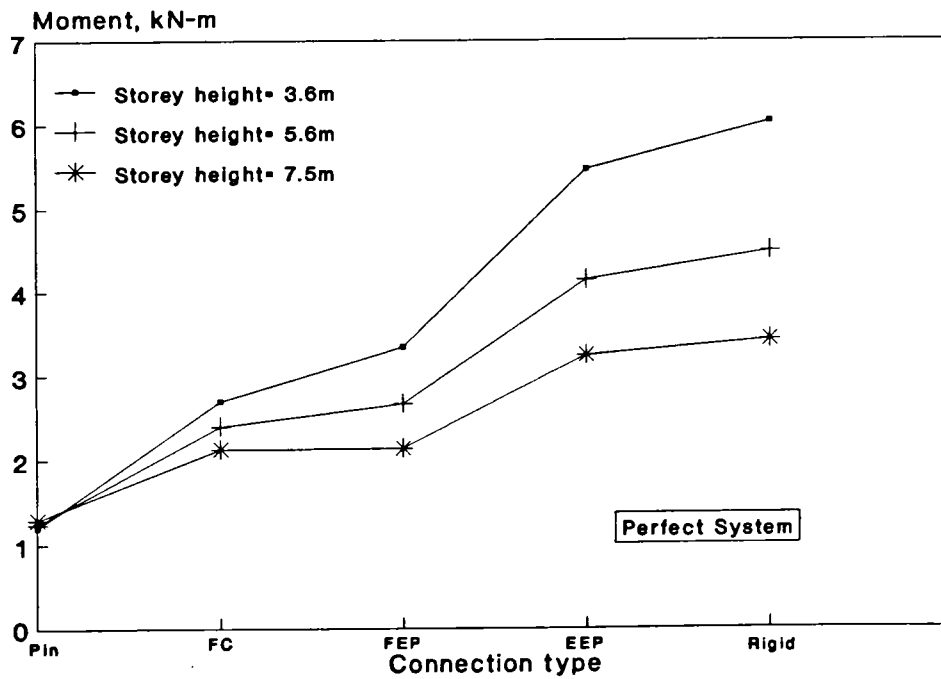


(d)

Figure 6.7 Frame strength for different conditions (type-A loading).

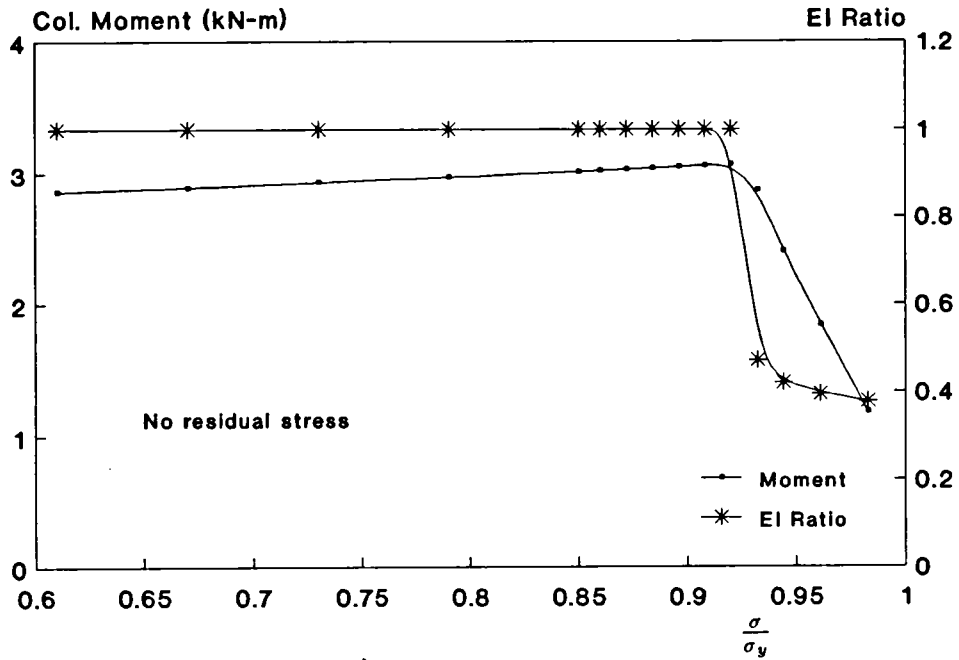


a) Axial force in column C6

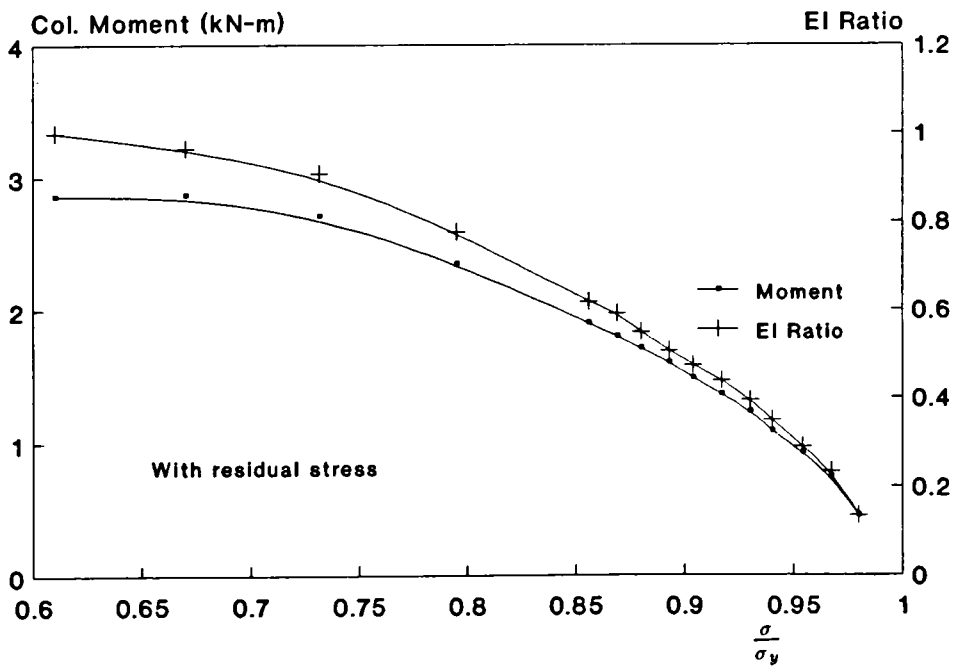


b) Moment at the top of column C6

Figure 6.8 Internal force distribution in column C6 at the end of beam loading phase (ie end of sequence 2).

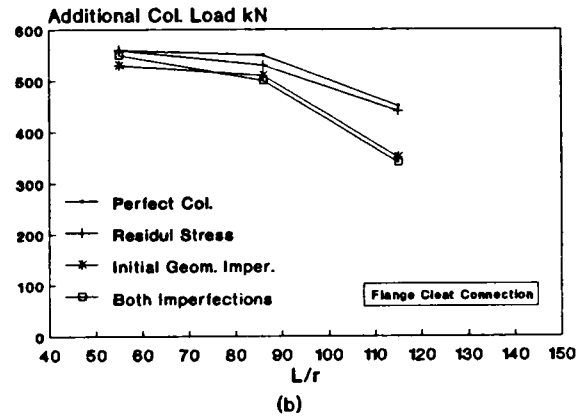
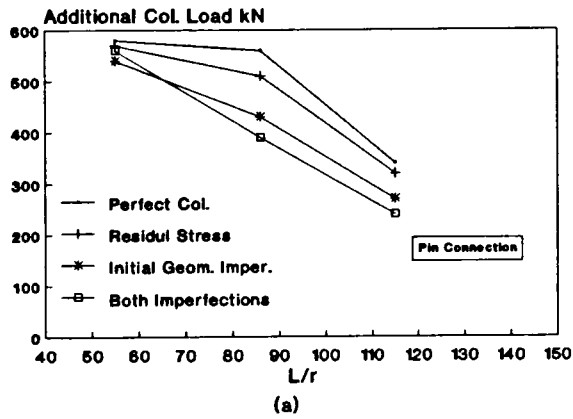


a) No residual stress.



b) Residual stress present.

Figure 6.9 Effect of the presence of residual stress on degradation of stiffness and moment.



Note: L= Height of a column lift
r= Radius of gyration

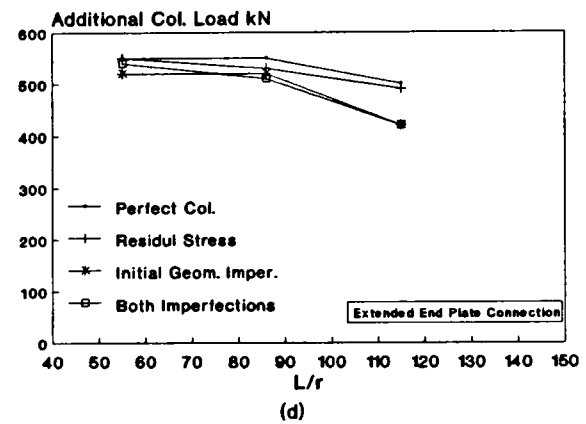
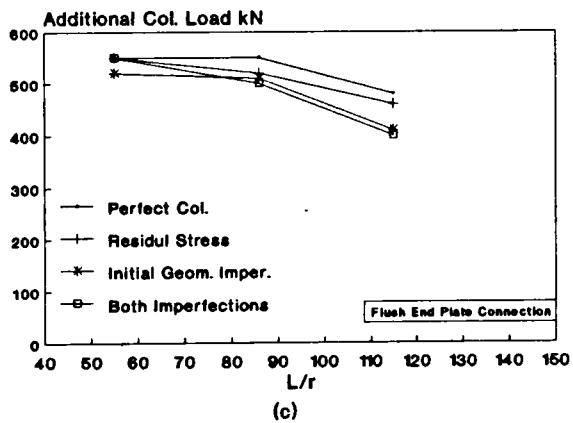


Figure 6.10 Effect of imperfection on frame strength for different connection types (type-A loading).

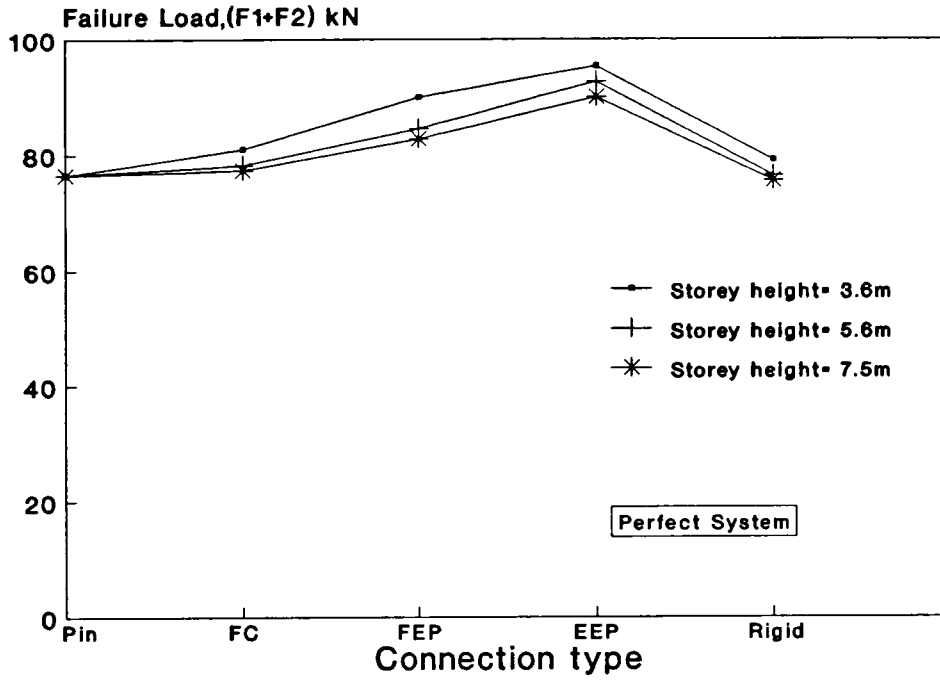


Figure 6.11 Variation of frame strength for different connection types (type-B loading).

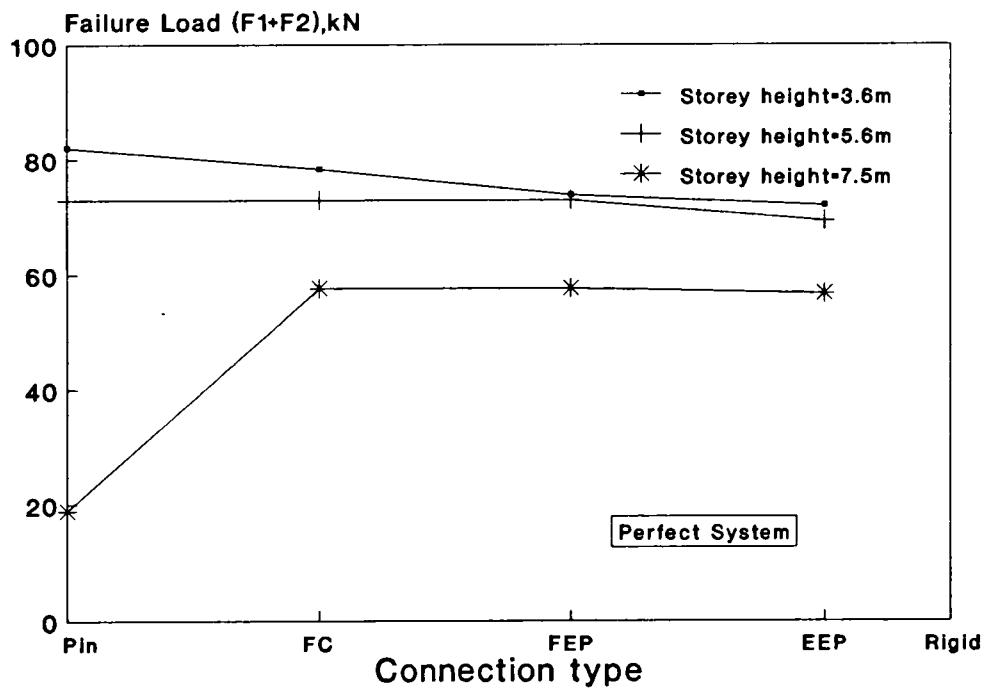


Figure 6.12 Variation of frame strength for different connection types (type-D loading).

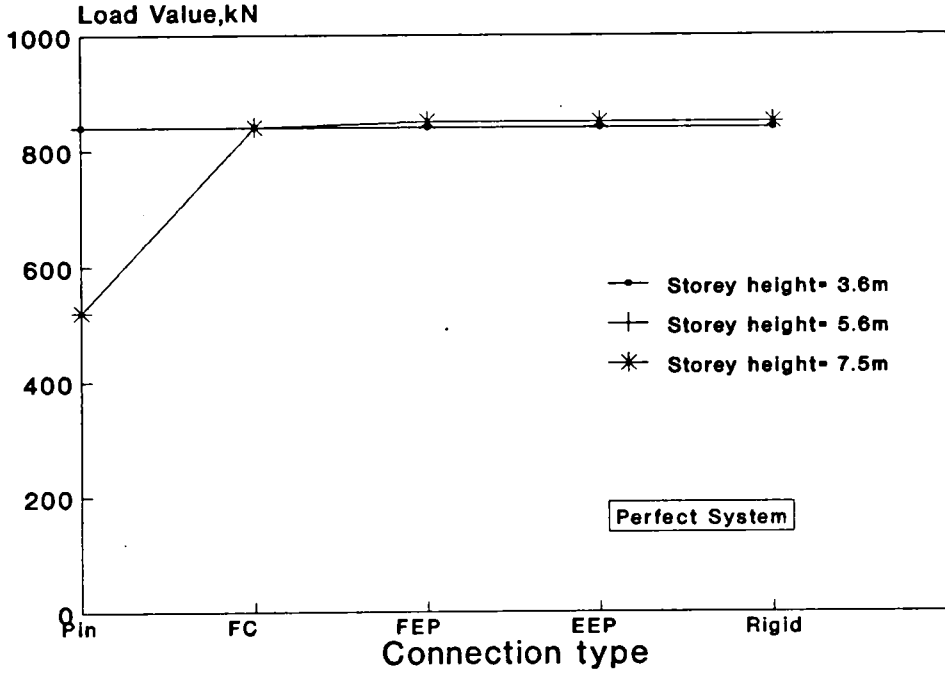
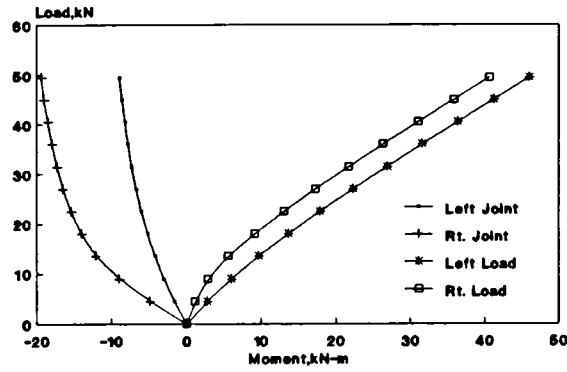
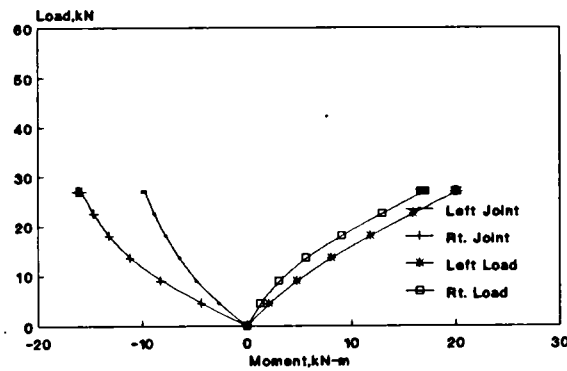


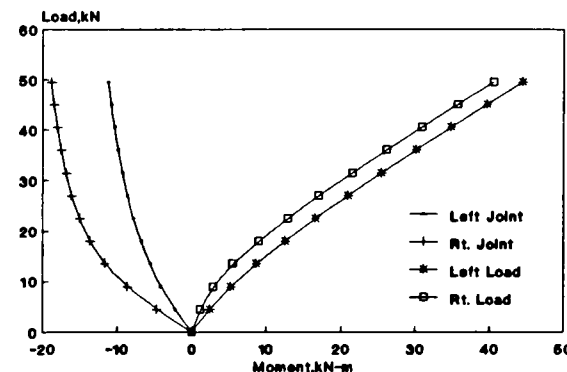
Figure 6.13 Variation of frame strength for different connection types (type-C loading).



(a) Beam 1



(b) Beam 2



(c) Beam 3

Figure 6.14 Variation of beam moments for frame with flange cleat connections (storey height = 3.6 m).

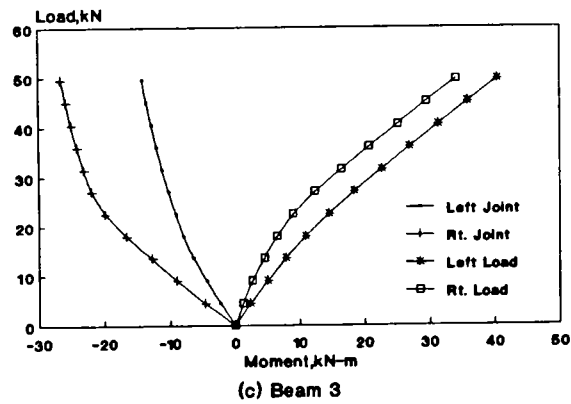
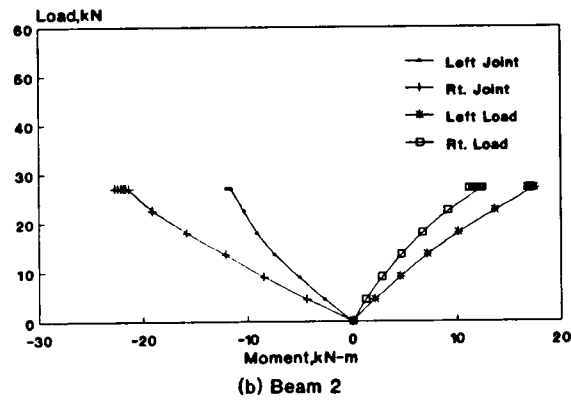
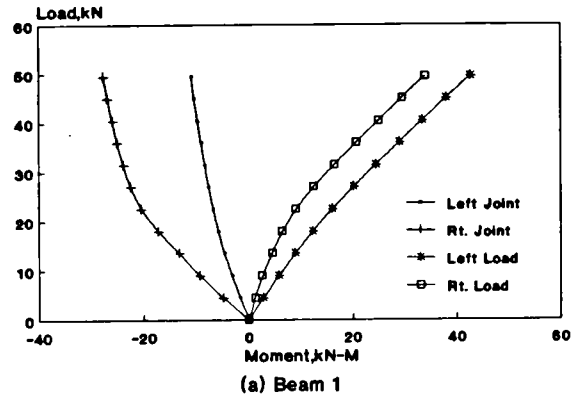


Figure 6.15 Variation of beam moments for frame with FEP connections (storey height = 3.6 m).

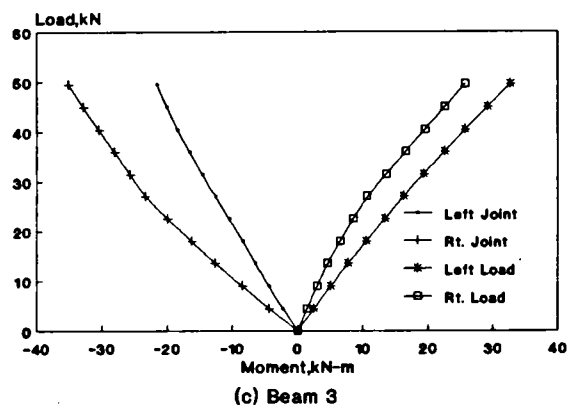
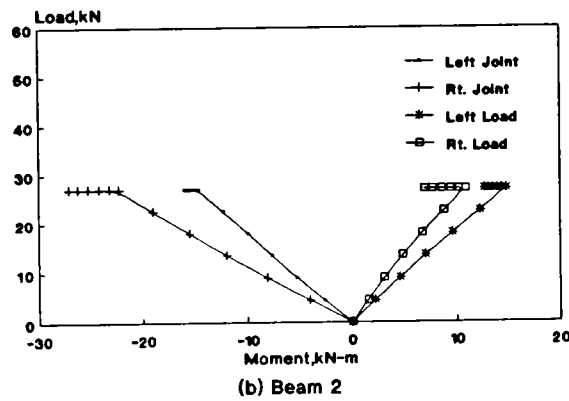
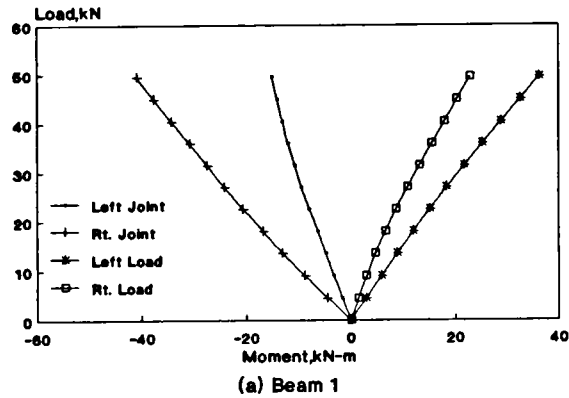


Figure 6.16 Variation of beam moments for frame with EEP connections (storey height = 3.6 m).

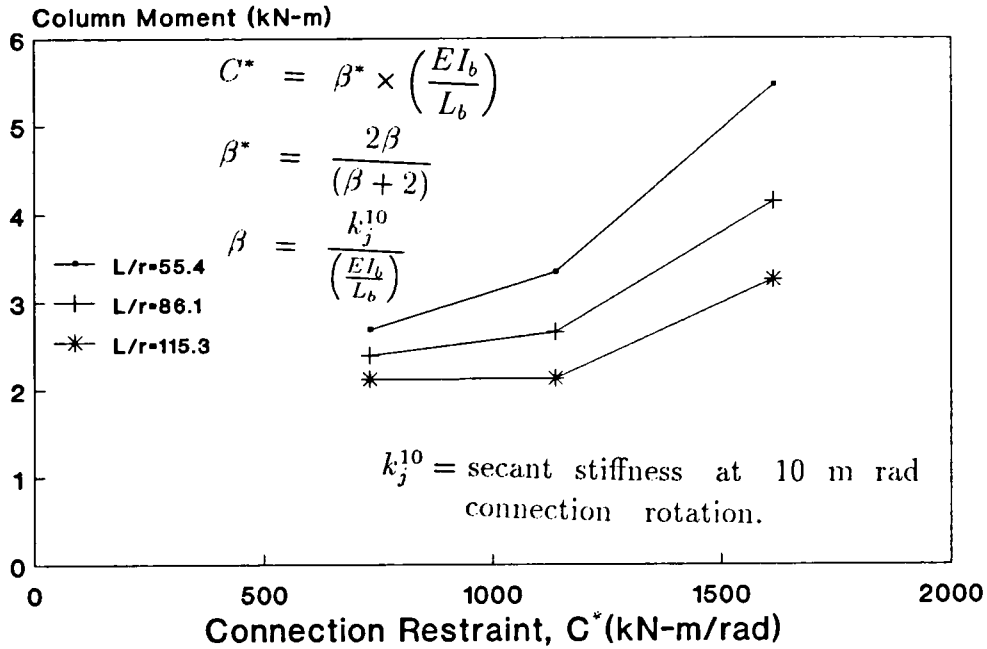


Figure 6.17 Influence of relative beam-column-connection stiffness on the development of column moment (moment at the end of col. C6 at the end of beam loading phase are shown).

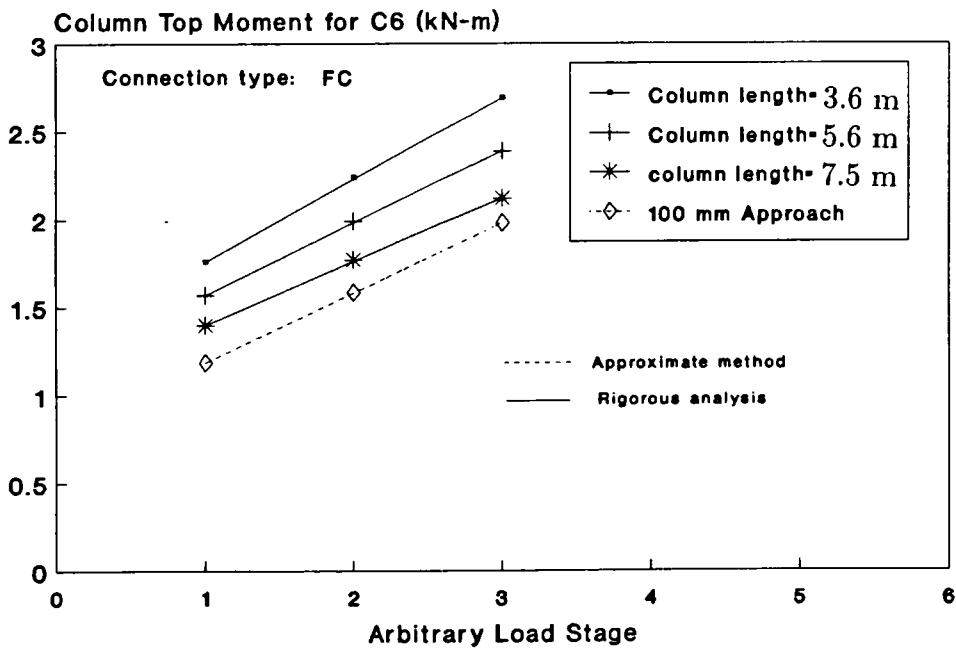


Figure 6.18 Column (C6) end moment for the last three load stages in the sequence-2 (connection type FC).

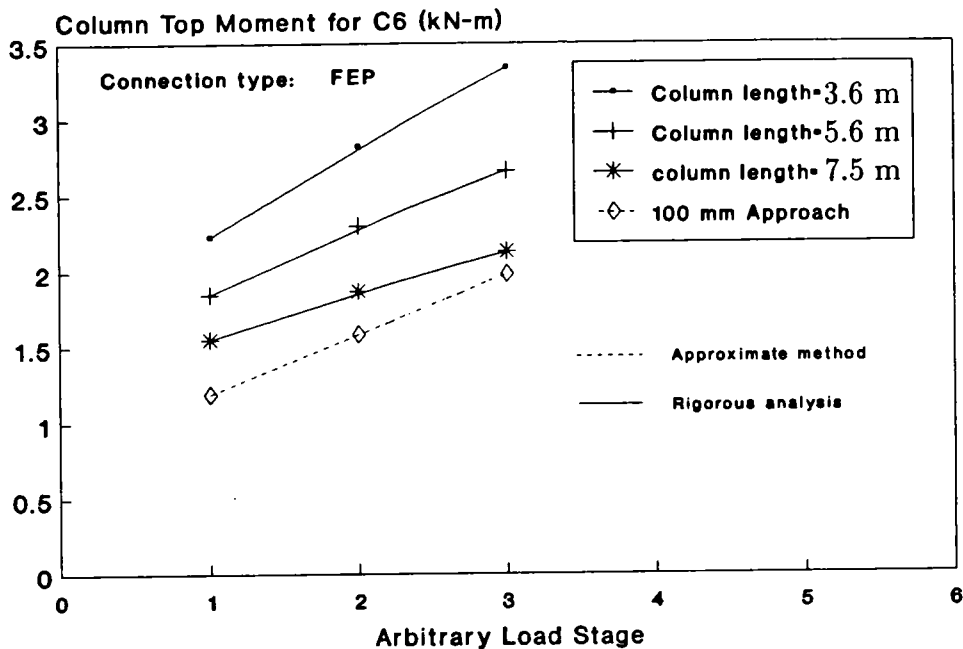


Figure 6.19 Column (C6) end moment for the last three load stages in the sequence-2 (connection type FEP).

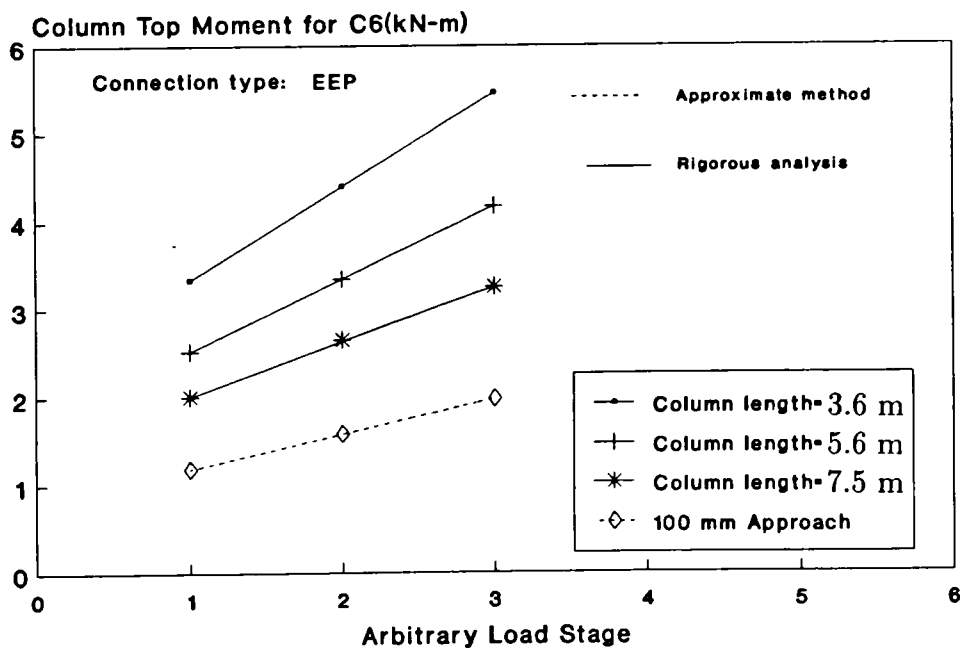


Figure 6.20 Column (C6) end moment for the last three load stages in the sequence-2 (connection type EEP).

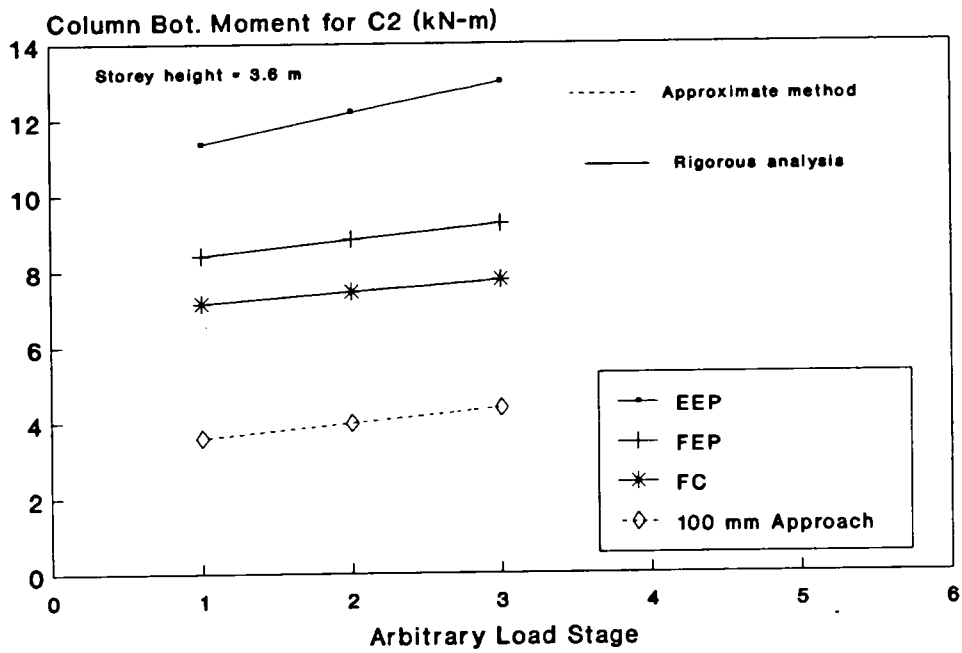
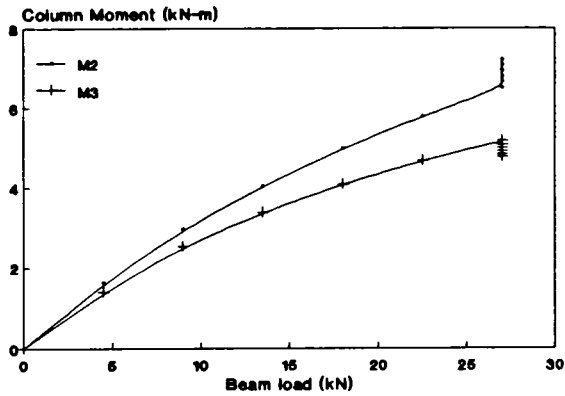
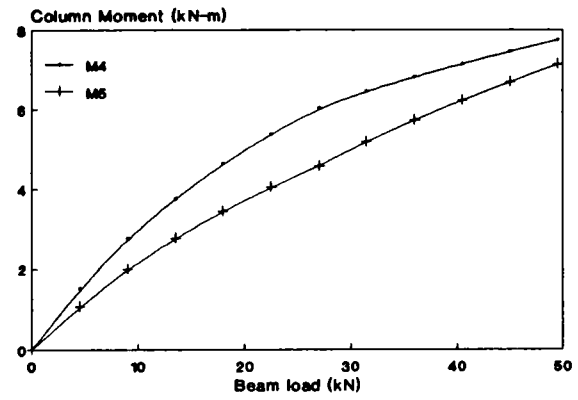


Figure 6.21 Effect of connection-stiffness on column moment.

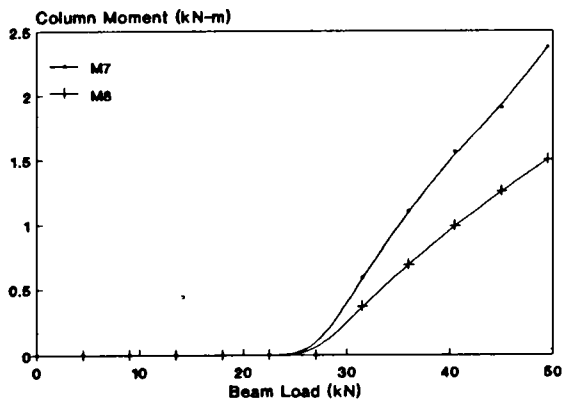


(a) At Joint J2

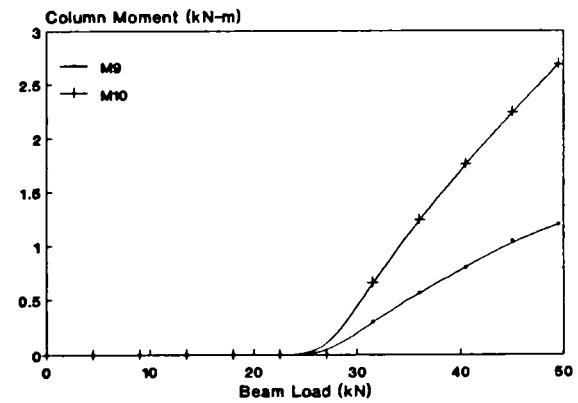


(b) At Joint J3

Note: At each joint, the moment M_n and $M_{(n+1)}$ refer to the moment at the ends of upper and lower columns (see figure 6.23).



(c) At Joint J5



(d) At Joint J6

Figure 6.22 Distribution of beam end moments to columns for flange cleat connection (3.6m storey height).

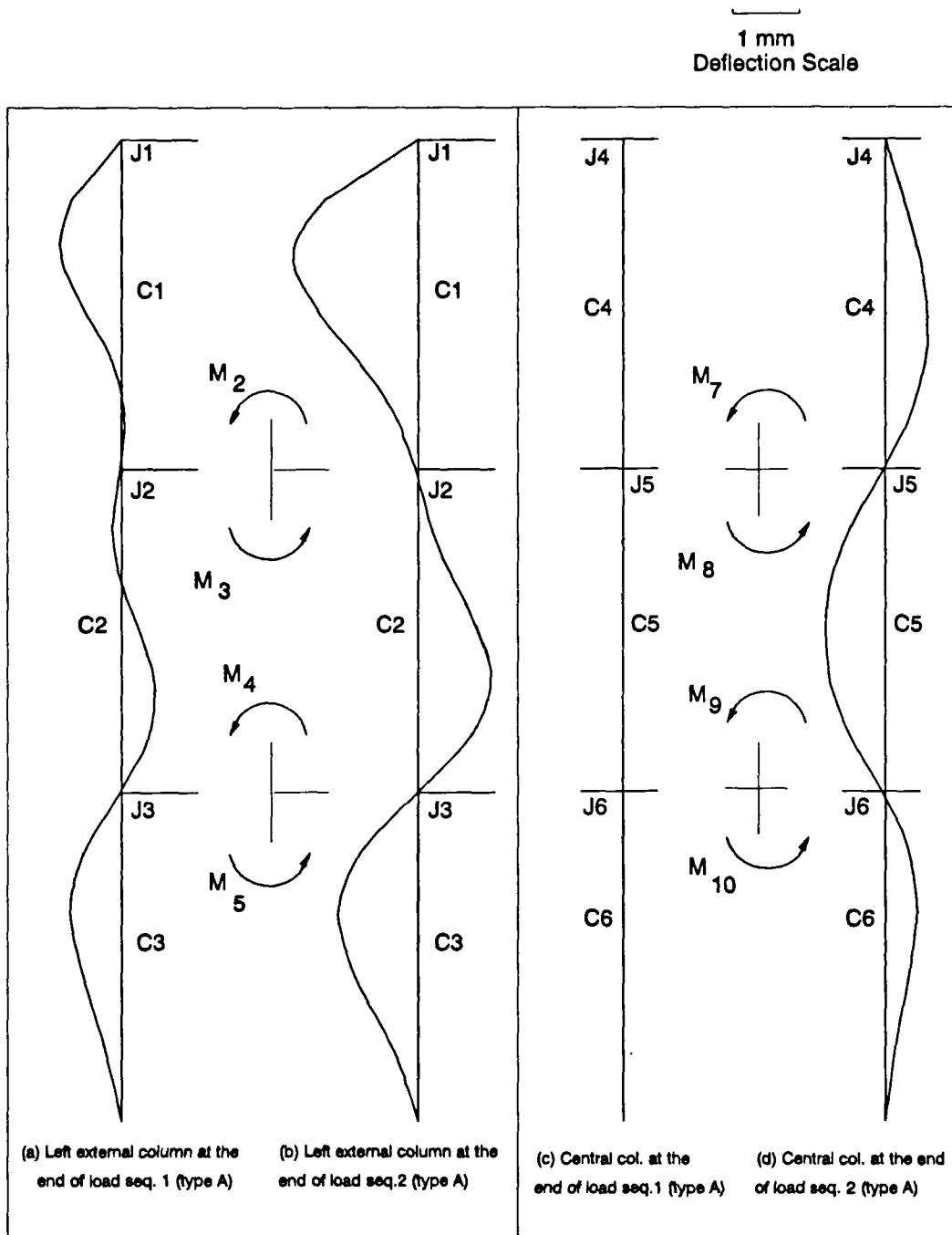
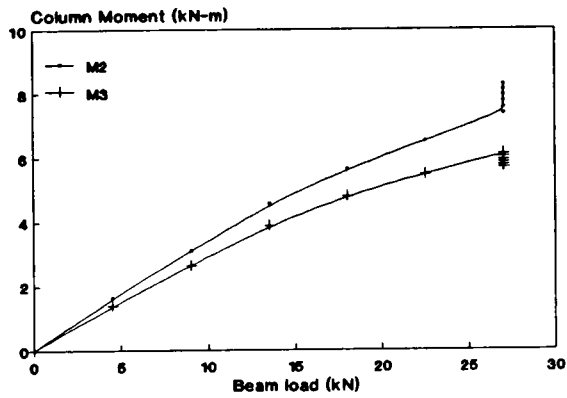
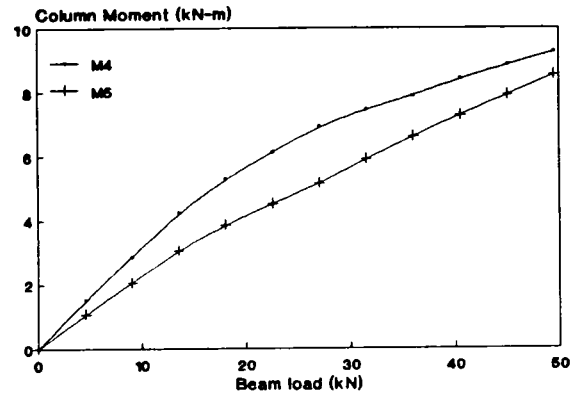


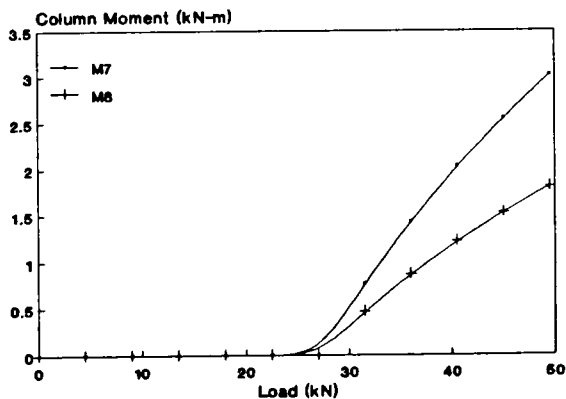
Figure 6.23 Deformed shape of the column.



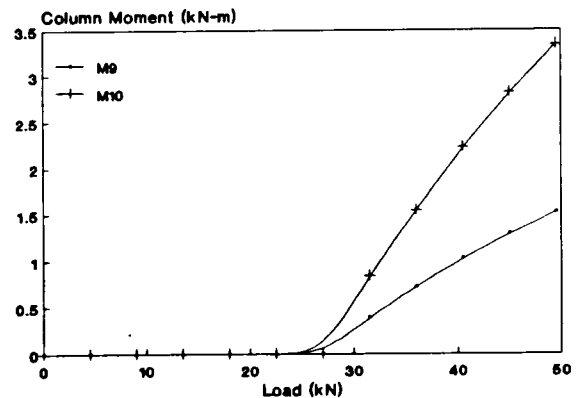
(a) At Joint J2



(b) At Joint J3

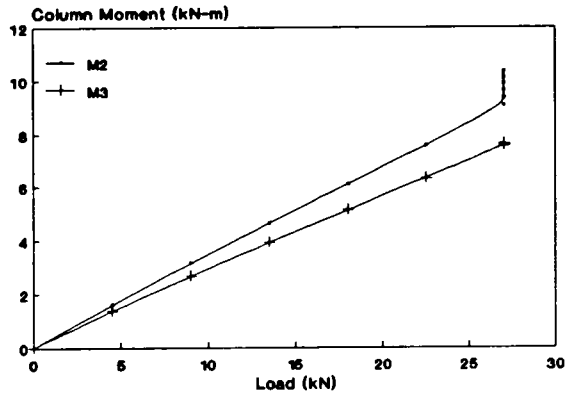


(c) At Joint J5

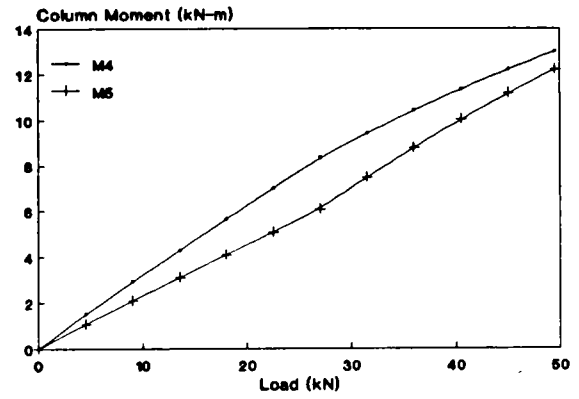


(d) At Joint J6

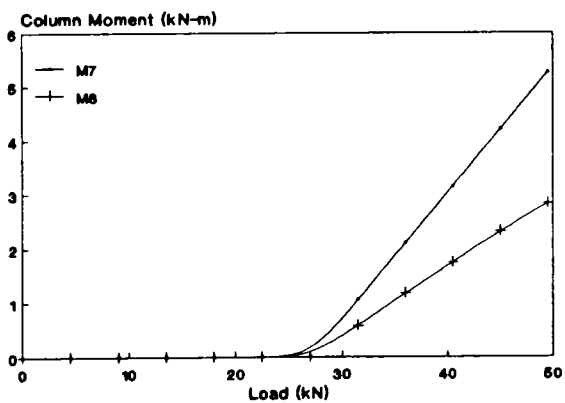
Figure 6.24 Distribution of beam end moments to the columns for flush end plate connection (3.6m storey height).



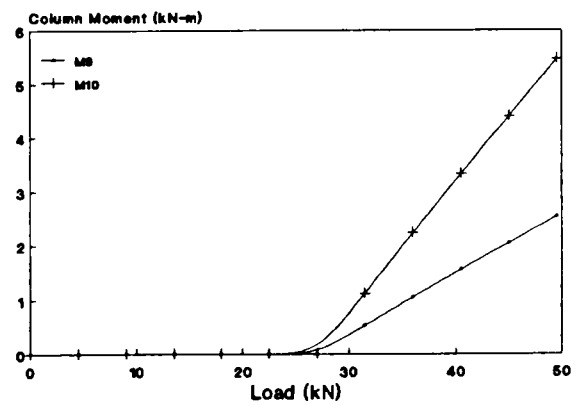
(a) At Joint J2



(b) At Joint J3



(c) At Joint J5



(d) At Joint J6

Figure 6.25 Distribution of beam end moments to columns for extended end plate connection (3.6m storey height).

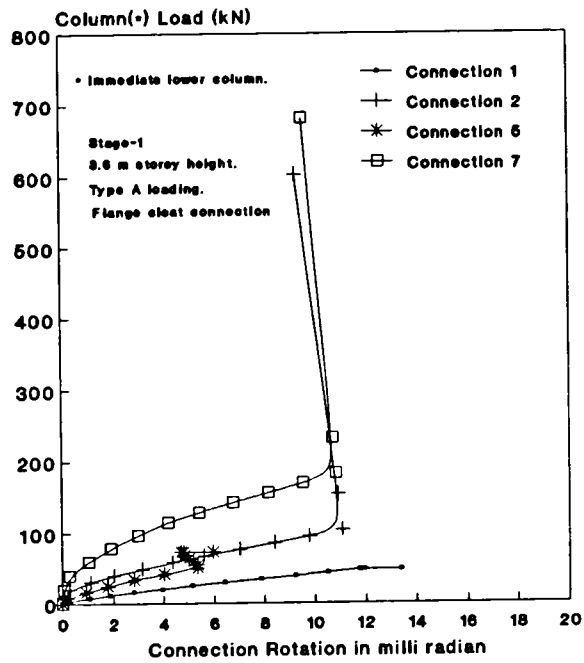


Figure 6.26 Development of connection rotation with applied load for flange cleat connection.

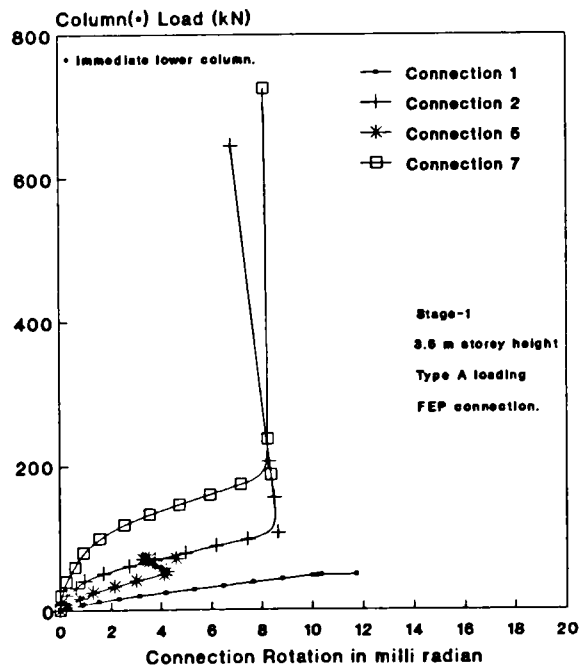


Figure 6.27 Development of connection rotation with applied load for flush end plate connection.

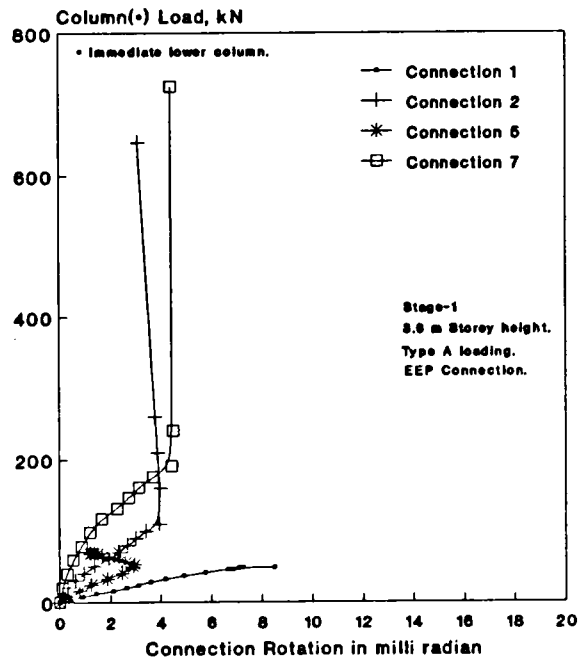


Figure 6.28 Development of connection rotation with applied load for extended end plate connection.

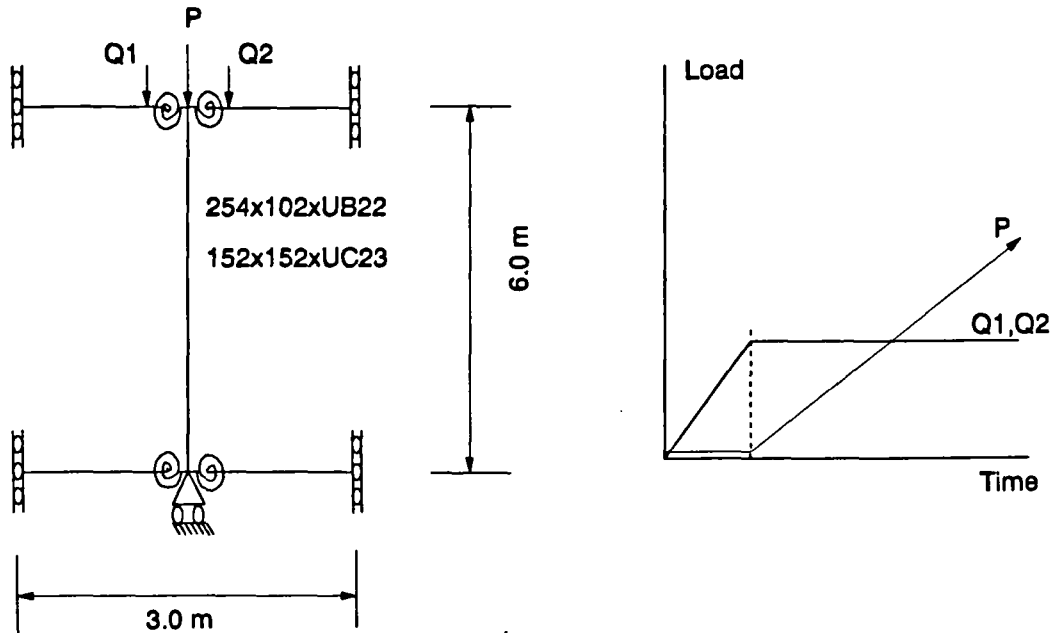


Figure 6.29 (a) Geometry and loading of Poggi et al's subassemblage [95].

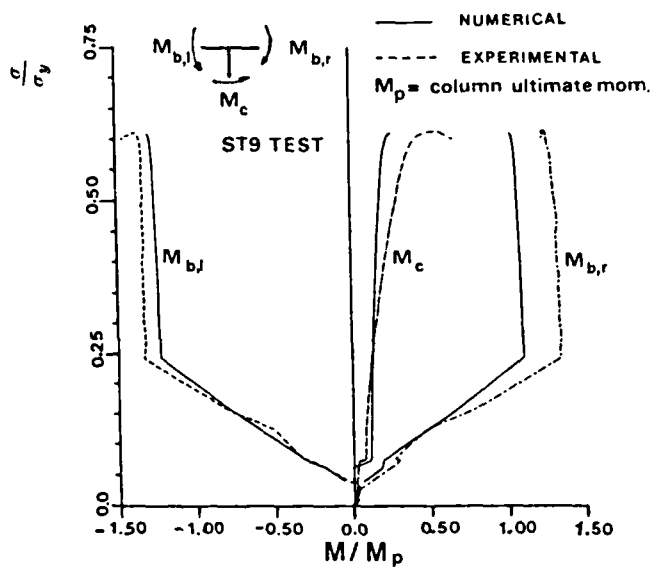


Figure 6.29 (b) Response of the subassemblage of figure 6.29(a) [95].

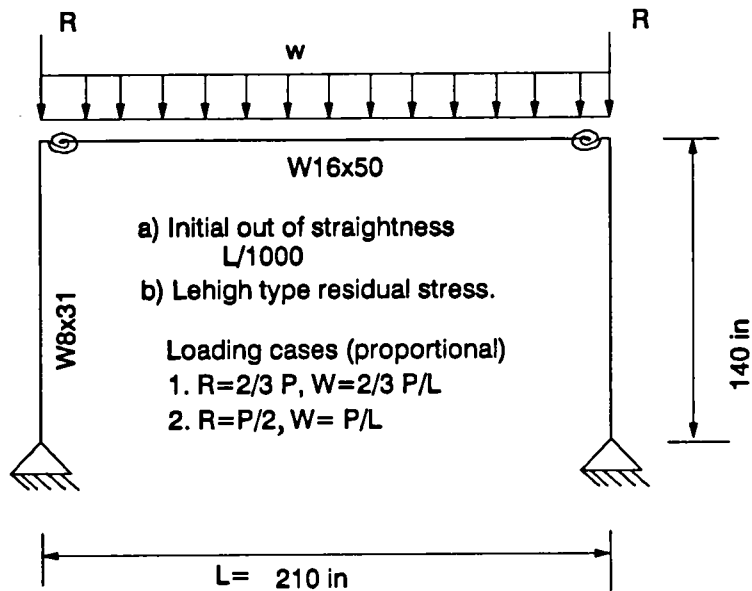


Figure 6.30 (a) Portal frame analysed by Chen [96].

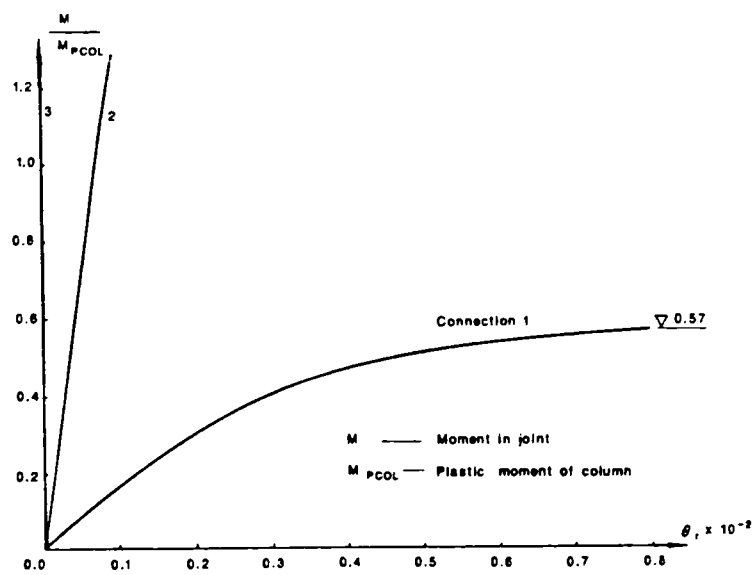


Figure 6.30 (b) Connection $M - \phi$ behaviour used by Chen [96].

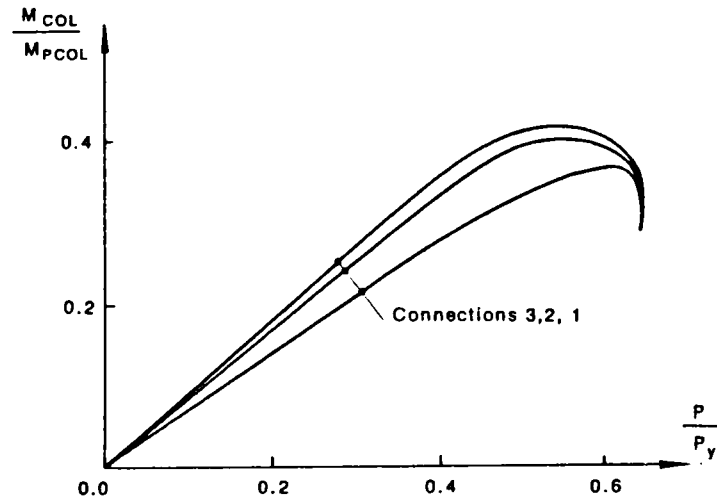


Figure 6.31 (a) Response of the non-sway frame of figure 6.30(a) for case-1 loading [96].

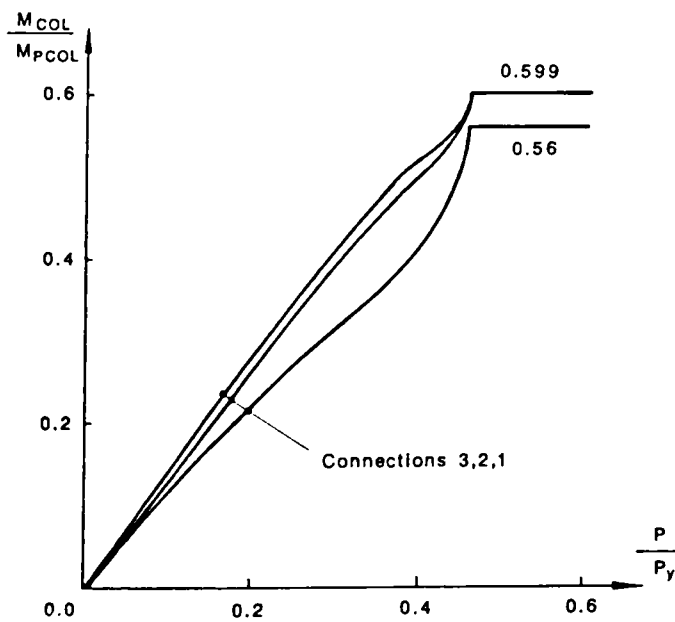


Figure 6.31 (b) Response of the non-sway frame of figure 6.30(a) for case-2 loading [96].

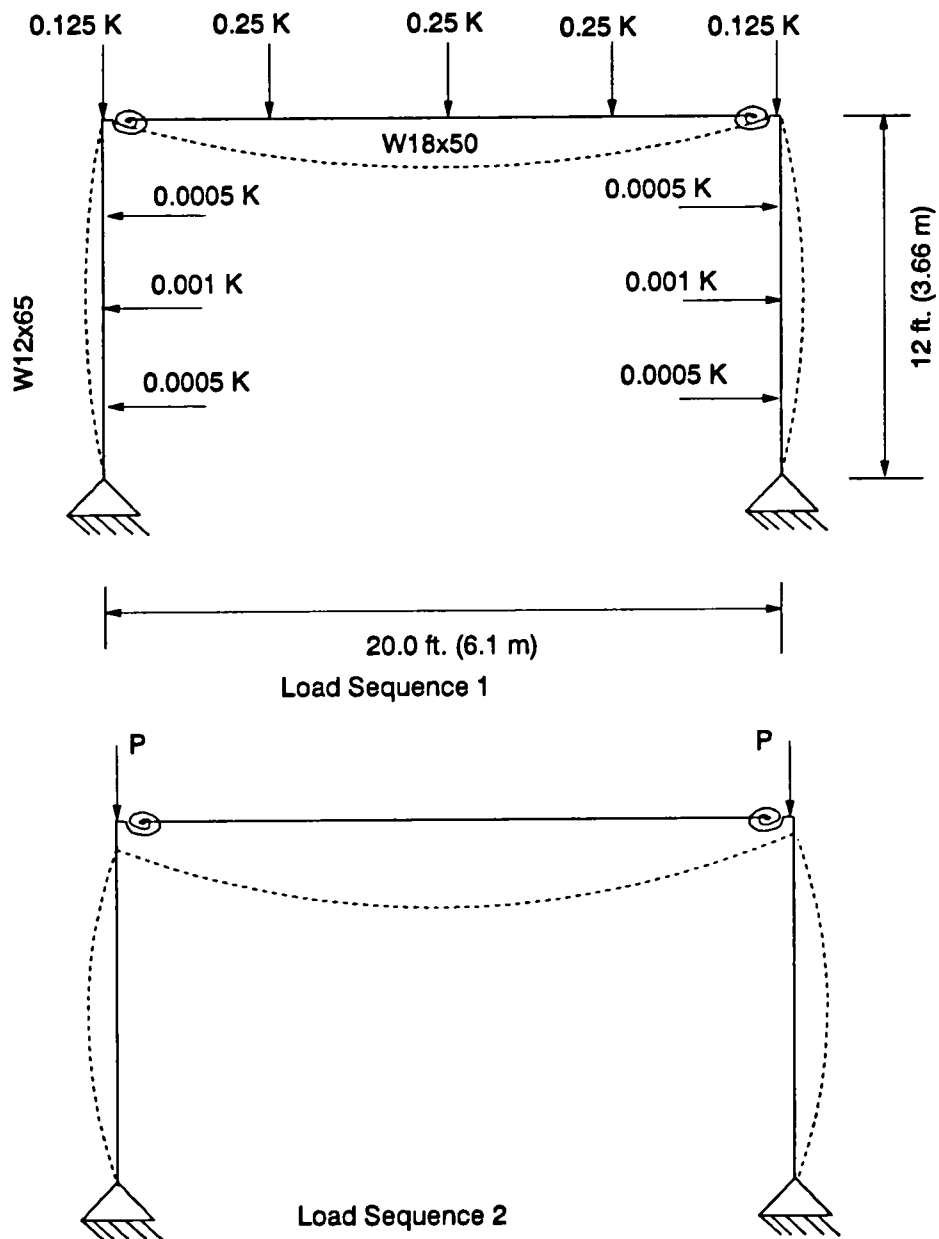
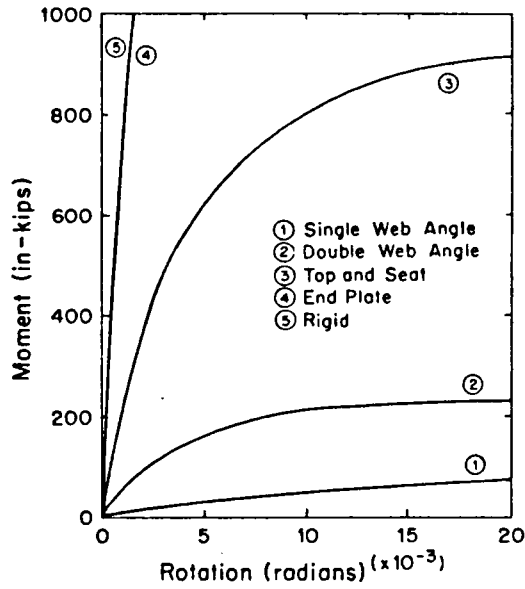
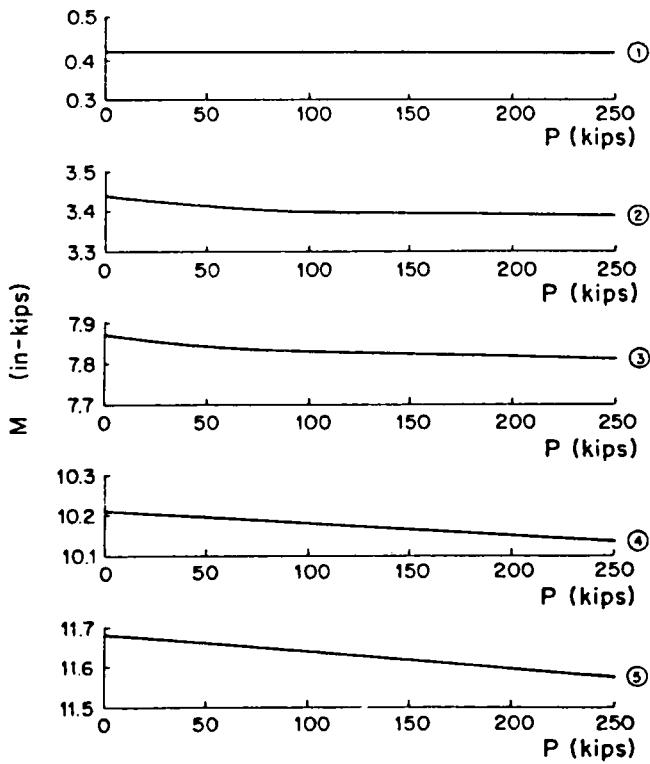


Figure 6.32 (a) Geometry and loading of Chen's frame [96].



Connections used for the study of the simple portal frame of figure 6.32(a).



Variation of column end moment for various connections in the load seq. 2

Figure 6.32 (b) Results of study by Chen [96].

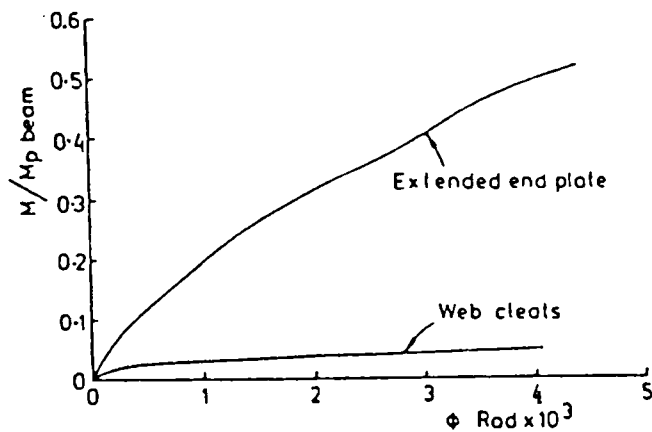
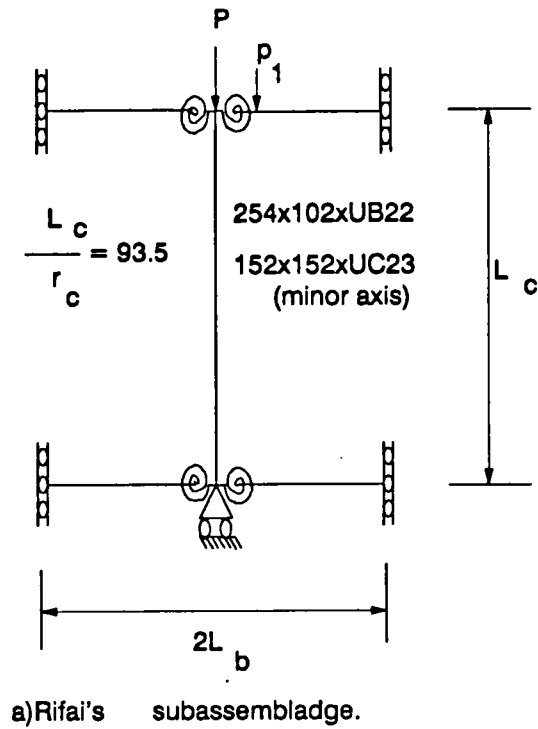


Figure 6.33 Column subassemblage and connection characteristics used by Rifai [97].

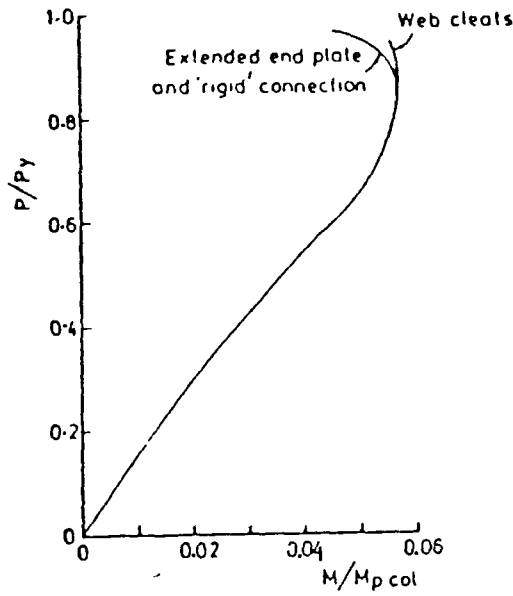


Figure 6.34 (a) Variation of column end moment with column axial load for subassemblage of figure 6.33 – axial column load only [97].

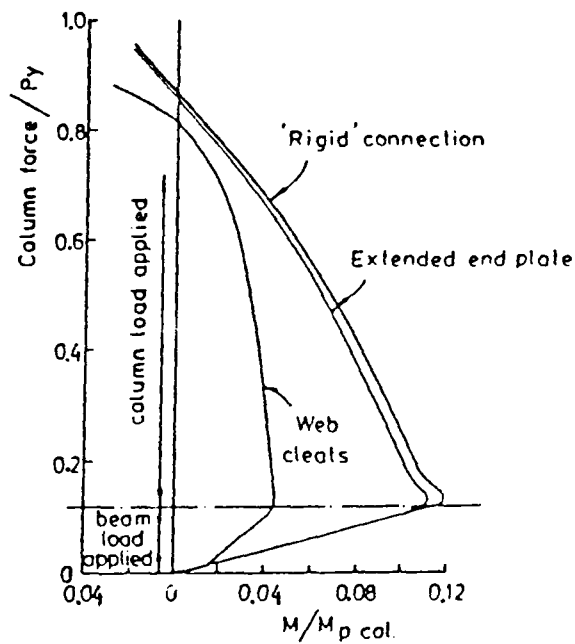


Figure 6.34 (b) Variation of column end moment with column axial load for subassemblage of figure 6.33 – beam loads present [97].

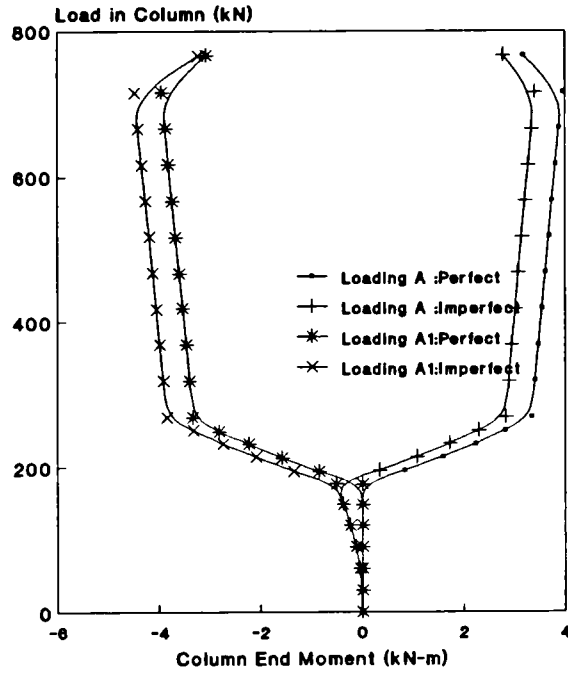


Figure 6.35 Column (C6) end moment for different load cases.

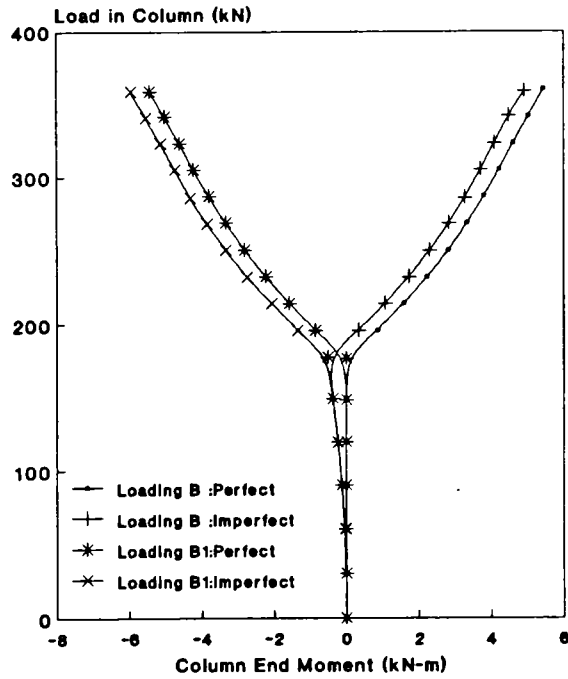


Figure 6.36 Column (C6) end moment for different load cases.

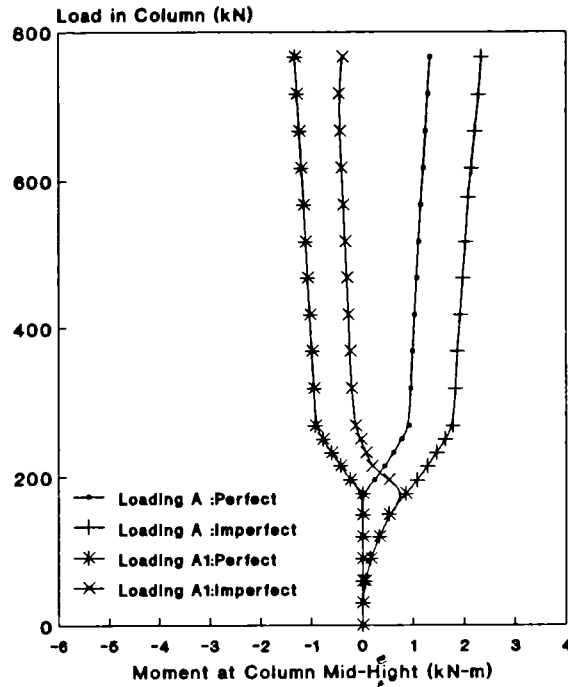


Figure 6.37 Moment at the centre of column C6.

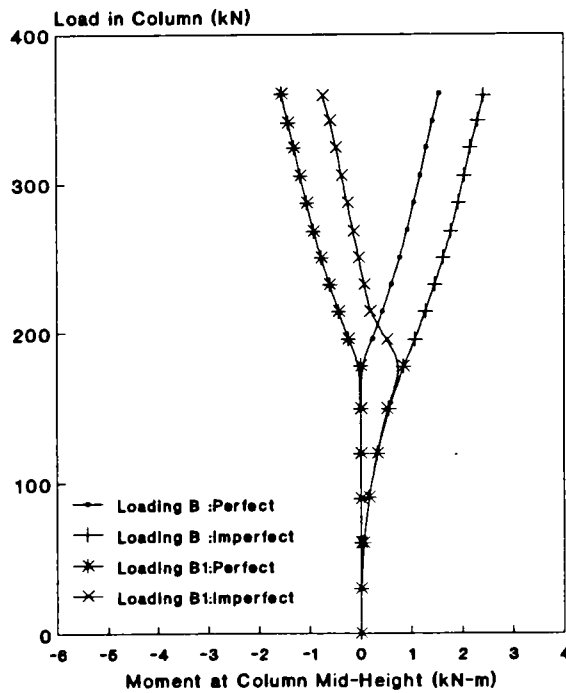


Figure 6.38 Moment at the centre of column C6.

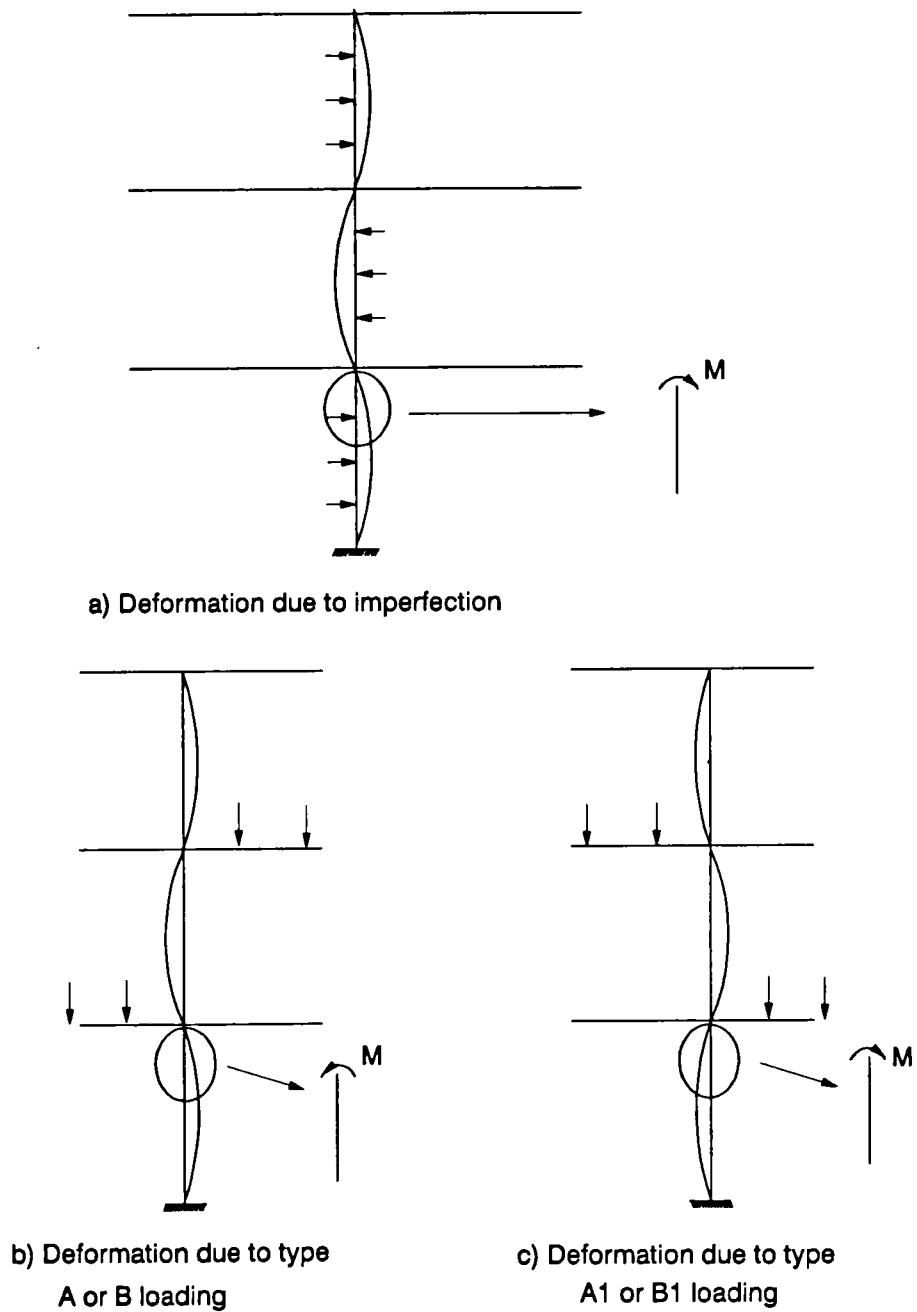


Figure 6.39 Column deformation pattern due to various loading condition.

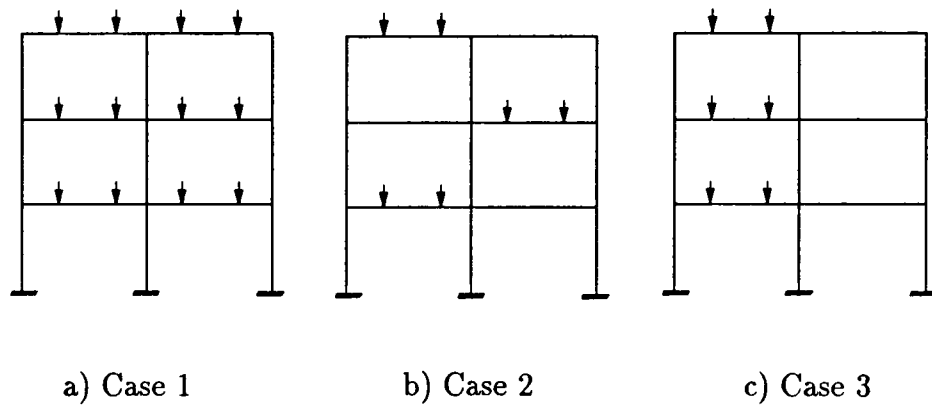


Figure 6.40 Loading patterns for tables 6.6 and 6.7.

Chapter 7

Simplified Design Approach for Non-Sway Semi-Rigid Frames

7.1 Introduction

The discussion in this thesis so far has been restricted to the prediction of frame response by using a computer program which includes various sources of nonlinear effects. Such results are useful to understand the importance of various secondary effects, and to determine the strength and failure modes of the structures. This approach, however, is well beyond routine design office practice. As a consequence it becomes imperative that results of such a rigorous method of analysis be cast in a form such that the general conclusions may be drawn for design purposes. Therefore, this chapter is devoted to the formation of simplified design guide-lines for semi-rigid frames, one of the principal objectives of this research work.

The reason for the general reluctance in using the semi-rigid concept

in design is because of the fact that the designer lacks two things:

1. Sufficient knowledge of the behaviour of the connection in terms of strength and stiffness.
2. A simple practical method of analysing semi-rigid frames.

The former is actually an impediment to the latter. In order to pave the way for the development of a simplified design method the main bottle-necks for such development will be identified first. The appropriate representation of the connection performance will be addressed and finally proposals for new simplified design techniques will be presented followed by worked examples to demonstrate the validity of the proposed method. However under the purview of the present research programme, only sway prevented cases have been considered and the discussions in this chapter relate only to non-sway frames.

7.2 Semi-Rigid Connection Behaviour: Implications for Design

7.2.1 General

It is now a well established fact that all types of practical steelwork connections possess some ability to transfer moment. The degree of this ability depends on the connection type, connection size and bolt size as well as bolt arrangements. Since the early attempts of studying connection behaviour, it is known that the relationship between connection moment and connection rotation is nonlinear.

Considerable research effort to quantify the effect of the physical connection parameters on this relationship have been made all over the world. This chapter focusses on the primary obstacles in the formulation of design guide-lines for semi-rigid frames and identifies the gap in the available information which in turn exposes the potential research need. From a world-wide survey [91] of connection moment-rotation relationships, the principal parameters which control the $M-\phi$ characteristics are identified here— which eventually points to the information necessary for a realistic design method to evolve. Almost all the publications on this topic are limited to studying the effect of various connection parameters on the moment-rotation characteristics with results obtained from a single source, where tests may suffer set-backs (either compensating or cumulative) due to identical arrangements of testing. Here attempts are made to focus the influence of various parameters – from a global view point. Representation of nonlinear connection behaviour by a simpler one is thought to be the first step for the development of any design method. It will be shown how this can be done. Attention is also drawn to the EC-3 [98] recommendation for the classification of joints on the basis of the connection $M-\phi$ relationship.

7.2.2 Connection $M-\phi$ Relationship

The single most important consideration of any semi-rigid design is the connection behaviour represented by its moment-rotation characteristic. This is the relationship between the moment transmitted by the joint and the rotation of the beam relative to the column (see figure 7.1). Although connection rotation has been variously defined [7], [99], [100]; the procedure for a correct measurement of the connection rotation is given in [100].

Attempts to study the connection behaviour dates back to early 1900's when Wilson and Moore [10] carried out tests on riveted joints. Since then a considerable number of tests on connection have been carried out – the primary objective of all of which were to identify parameters influencing the $M-\phi$ behaviour. These are discussed below.

One important feature of the connection $M-\phi$ characteristics that is required in any analysis is the connection stiffness which is the slope of the connection moment-rotation curve. The nonlinear nature of the connection relationship suggests a progressively lower value of connection stiffness as the rotation increases – a feature of great significance in any analysis. Thus care must be exercised in representing connection stiffness in the analysis. Some early models utilized a linear stiffness based on the initial tangent stiffness. Although instantaneous stiffness in an incremental analysis would be the ideal solution, a multilinear representation of the $M-\phi$ relationship may also be satisfactorily used [4]. Nevertheless, the important parameters affecting the connection rigidity are identified [4,99] as:

1. Depth and length of the connected beams
2. Type and size of the fastener
3. Thickness of the connection components
4. Physical properties of angles, members and fastener material
5. Whether connected to column web or column flange or girder web
6. Local beam flange buckling
7. Column web yield

8. Column stiffener yield
9. Beam and column contact during deformation
10. Connection gauge

Although attempts to numerically simulate connection $M-\phi$ behaviour have been made [5] [101] [102], their use is still limited, particularly for the lack of authoritativeness in predicting the true behaviour under a set of general conditions. Jones [11] had shown the inadequacy of some of the empirically predicted $M-\phi$ relationships. To date the only dependable (though expensive) way of obtaining connection $M-\phi$ relationship for subsequent use in analytical procedure is the full scale physical testing.

Despite the availability of a large body of $M-\phi$ data obtained from the tests on connections all over the world, their appraisal on a common yardstick is difficult by the fact that non-standard connections as well as non-standard testing procedures have been adopted. This makes the prediction of member behaviour with similar other connections a difficult task.

7.2.3 Present State of Information

In this section an account of the inconsistencies of the available information pertaining to the $M-\phi$ relationship of a connection is given. Nethercot [103], Kishi et. al. [104], and Structural Stability Research Council [105] provide information on the moment-rotation data of typical connections. Results of the connection tests so far carried out in different part of the world are now embodied into a computer data-bank [91] at Sheffield. This holds a collection of some 550 datasets,

involving commonly used connection types. It was originally thought that it could be used to provide an on line information to be utilized in research institutes and design offices. That expectation however, could not be achieved for two reasons. Most of the tests so far conducted furnish information that for some reasons or other are inconsistent for design practice, as will be shown later. The second reason is related to the non-standard practice of connection detailing. For example, to carry the same load, different designers may come up with different dimensions even if both choose the same type of connection. These similar but not identical connections, might have different moment-rotation responses, depending on different bolt size and spacing, plate sizes, and angle sizes. The sensitivity of the moment rotation relationship with the various connection parameters will be shown later.

Figure 7.2 in effect compares the moment rotation relationship for four flange cleat connections [108] with one flush end plate [106] and one extended end plate connection [107]. Important parameters for these connections are given in tables 7.1 and 7.2. It can be seen that the flush end plate connection may have a smaller stiffness than the flange cleat connection, depending on dimensions of the connected member as well as connection elements. So it is important that, while considering connection stiffness, all the variables that effectively control connection behaviour must be borne in mind. It is totally wrong to judge a connection stiffness purely the basis of a given connection type, rather it is the $M - \phi$ curve of the connection that provides the information relating to its performance in the structure.

Figure 7.3 shows clearly the discrepancy between the available test data and the realistic information needed in design [109]. The beam and column sizes

used in the tests conducted so far are not representative of those used in practice in multistory construction. This omission needs to be rectified since even identical connections would produce different moment rotation relationship if connected to different beam and column sizes and any design taking connection restraint into consideration must be based on appropriate representative behaviour of the connection moment-rotation relationship.

Figure 7.4 presents the results of the same four flange cleat connections [108] (see table 7.2). From a survey of 63 different available test results on flange cleat connections these four results are selected here to show how beam and column sizes influence the moment-rotation relationship for a connection which have nearly the same connection elements. It is surprising to note that, from the survey of the available tests it appears that not a single test scheme was planned in order to quantify the effect of beam and column sizes on the moment-rotation behaviour of a connection in which connection parameters were kept constant while beam and column sizes were varied. Details of the various parameters used for these tests are in table 7.2. Curves 1 to 4 in figure 7.4 are the $M-\phi$ relationship for tests for which relevant test parameters are shown against serial number 1 to 4 in table 7.2. In this table, the equivalent British sizes of universal beams and columns are also indicated where a close enough section is available in both US and British practice. This is repeated in subsequent tables. Tests no.1 and 2 (as designated in table 7.2) have all identical parameters except two, the beam size and the angle length. It has been established elsewhere [7] that angle length is not an important parameter in controlling the $M-\phi$ behaviour of a connection. Thus the only effective variation between tests 1 and 2 are the beam sizes. It is apparent from figure 7.4 that connection stiffness depends to a significant extent on the size of the beam and the column to which it is connected. Tests no. 3

and 4 of table 7.2 also signify this fact. Table 7.3 describes the features of two different tests by Hechtmann [108]. The moment rotation relationship for these two cases are presented in figure 7.5. This particularly shows the effect of beam size on the connection stiffness. From the limited information no trend could be established to extrapolate the $M-\phi$ relationship for the nominally same connection connected to different member sizes. To this end further study is needed in determining the quantitative effect of the member sizes.

The observations made in the preceding paragraphs quite appropriately suggests that the information available to hand from the test results does not place the designer in a position of practising semi-rigid design. Since for a sound, viable design, the designer must have all his choices or options open in choosing member sizes and connections. However, if the $M-\phi$ relationship for the chosen members and connections, remains inaccessible to the designer, he will not be encouraged to use any new approach and would rather continue to design structures by the conventional methods. Table 7.4 presents the summary of available test results [91] for the four commonly used type of connections showing number of tests carried out for both major and minor axis bending of the column. Clearly information about connection performance for column minor axis bending has not kept pace with that of major axis flexure. Information regarding the test arrangement, ie whether cruciform, cantilever or extended cantilever could not be obtained from reference [91]. It is appreciated that it is unlikely that balance will be kept among these three categories of test arrangements, whilst the importance of using relevant connection information in the practical situation of either external or internal column is a vital one. It appears that a concerted effort to obtain the $M-\phi$ relationships for the commonly used connection types is required and, to this end, standardization of connections would be advantageous.

Standard testing and reporting of the standardised connections on an international basis would allow the consistent exchange of information among different research groups which will bridge the gaps in the available information so as to provide a uniform basis for the evolution of semi-rigid design.

7.2.4 Reliability of Connection Response and Its Implication

The available moment-rotation information for a connection is often based on one single test. Fabrication differences and field conditions are likely to result in some degree of variation in connection performance. Figure 7.6 shows $M-\phi$ curves from replicated tests of top and seat angle connections performed under laboratory conditions [110]. Considerable random scatter can be observed and it was reported that the initial stiffness varied within a factor of two. Conditions in the field might cause a scatter greater than those shown in figure 7.6. It will be shown later in this chapter that overall structural response is not very sensitive to a certain degree of variation in the $M-\phi$ behaviour of the connection. This demands that extreme accuracy in representing connection behaviour in the analysis is not warranted. On the other hand, the designer must have confidence in the extent of variation the designed structure is likely to suffer due to an anticipated level of variation in the connection response. This aspect is discussed by considering the following 3 cases.

Nethercot et al [8] showed that for a 10 per cent shift in $M-\phi$ curve, the response of the beam was almost unchanged as shown in figure 7.7. It can be seen that the shift in load displacement response due to 10 per cent shift in

connection $M-\phi$ relationship is insignificant.

Using the present program the 3- storey, 1-bay frame of figure 7.8 was analysed with three different connection stiffnesses. The first connection (C) used was assumed to have a linear stiffness of 1803 kN-m/rad. The other two connections (designated as C_{10} and C_{20}) considered here were 10 times and 20 times stiffer than the first one. Table 7.5 presents the results of the analyses for the above mentioned frame with two different span lengths of 5.0 m and 6.5 m. The moment and deflection values shown in table 7.5 correspond to the top floor beam at a uniformly distributed load of 15.6 kN/m. All three beams were equally loaded and their behaviour were more or less similar to those shown in the table for the top floor beam.

The column subassemblage of figure 7.9(a) was analysed to develop the column strength curves for three different connections whose $M-\phi$ relationships are shown in figure 7.9(b). Figure 7.9(c) shows that the column strength curve with connection types 2 and 3 are virtually coincident and only a small difference in strength can be observed for the column with connection type 1, although the $M-\phi$ response of the connection 1 falls far short of that of connections 2 and 3.

The three cases mentioned above clearly demonstrate that the overall frame response is not very sensitive to the precise $M-\phi$ relationships of the connections. The second of the three cases presented above categorically shows that a variation in connection stiffness by a factor of 2, does not make any appreciable difference from a practical view point and the predicted response will be well within the range of tolerance that is accepted in engineering practice. It is found that, if a connection response in the actual structure is stiffer than that assumed in design calculation, the beam deflection is overestimated at the

expense of under-estimated moments at beam end. Nevertheless, as long as their variation in the assumed and actual $M-\phi$ response is not dramatic the designer need not worry about the safe performance of the structure. Thus the semi-rigid provision of BS 5950 stipulation that inclusion of connection flexibility in the frame design must be based on the experimental evidence of a $M-\phi$ relationship is satisfactory. In the next section it will be shown how the nonlinear $M-\phi$ response of the connection can be represented in a simpler form so as to enable its use in a design office context.

7.2.5 Simplified Representation of the Connection Response: Linearization of the $M-\phi$ Relationship

Perhaps the most seemingly intractable obstacle in the development of a semi-rigid frame design method is the nonlinear nature of the connection $M-\phi$ relationship. Although this nonlinearity is easily taken into account using an incremental technique in a computer program, this is not suitable for the routine practical design and therefore some simplified representation of this $M-\phi$ behaviour which would provide results of acceptable accuracy is very much warranted. Representation of the connection stiffness by the initial tangent of the $M-\phi$ relationship has been proposed by many researchers. Bjorhovde [3] showed that the support rotation of simply supported beams of practical dimensions (laterally supported W18X50 sections in A36 steel with a 25 ft span and subjected to a uniformly distributed load up to the allowable level) would typically be equal to 0.0092 radians. Use of a semi-rigid connection, he observed, would certainly cause a rotation less than this figure. At such a low level of rotation it was claimed that the over-estimation of the restraining moment by the use of initial tangent stiffness is

likely to be small (see figure 7.10). Figure 7.11 shows the actual frame response determined by constructing a beam-line. The estimated moment M'_{sr} based on the initial connection stiffness is higher than the actual moment M_{sr} . It can be seen that the discrepancy between M'_{sr} and M_{sr} is dependent on the beam line. For a rather flexible beam (a flatter beam line) M'_{sr} will move close to M_{sr} which implies that for some frames this approach will give better results than for the others. However, at factored loads or near failure, appreciable unconservative behaviour would be predicted if one uses this approach. A conservative approach would use more flexible connection response, which immediately suggests the choice of a secant stiffness. The use of a linear secant stiffness would require the definition of a level of rotation or moment to be used. As shown in chapter 6, in most non-sway frames of practical dimensions failure takes place with a connection rotations of around 10 milli radians. Thus the use of this rotation level, for determining a secant stiffness seems a reasonable lower bound approximation. A secant stiffness corresponding to a rotation of 10 milli radian k_j^{10} has also been suggested elsewhere [112]. Figure 7.12 illustrates this stiffness for a range of three different joints. Although for relatively stiff semi-rigid connections, the rotation at failure could be much less than 10 milli radian, k_j^{10} might cause an unduly conservative result. An alternative simplification of this situation could be the use of beam line as shown in figure 7.13. A beam line intersects the vertical axis at a moment value equal to the end moment of a fully rigid beam and the horizontal axis at a rotation value equal to the rotation at the end of a simply supported beam. For a simply supported beam subjected to uniformly distributed load and equal end moments at its end, the end rotation is given by,

$$\phi = \frac{wl^3}{24EI} - \frac{M_E l}{2EI} \quad (7.1)$$

This is a linear relationship between the moments and the rotations at the ends of the beam. A similar relationship for any loading type can be easily written. As shown in the figure 7.14, this approach to a secant stiffness will provide a much closer representation of the actual connection response than the k_j^{10} approach. Later in this chapter (see section 7.3.2) it will be shown that a secant representation of the connection stiffness by a beam-line approach produces results that are satisfactory for practical purposes.

7.2.6 Limitation of the Secant Stiffness Approach

It has been shown in the preceding section that the secant stiffness based on the beam line approach can be a suitable substitute to the actual nonlinear connection response for the routine design practices. The secant stiffness is a lower-bound approximation of the connection stiffness as opposed to the upper bound represented by the initial connection stiffness. For a frame, a lower stiffness causes a higher deflection than the actual value and the connection would have to transmit a higher moment due to gravity loads than that accounted for in design. Zootmeijer [113] has shown that in calculating the stability of the frame the use of secant connection stiffness provides a safe approximation, as long as the ultimate moment capacity of the connection is not assumed to be greater than the point of intersection of the secant stiffness with the actual moment rotation curve. He also showed that as long as the connection has sufficient rotation capacity for the assumed failure mechanism to be reached, using a lower stiffness than actual will not be unsafe. Therefore, the $M-\phi$ characteristics has to intersect the beam-line, otherwise it will imply that there is insufficient rotation capacity available.

7.2.7 Classifying the Joint as Semi-Rigid

In the conventional analysis of a structure, where perfect pins or perfect rigid connections are assumed, real connections seldom show such idealized behaviour. It is customary to regard connections such as an extended end plate as rigid and a web cleat connection as pinned, although it has been shown that actual performance of the connection should be judged by its $M-\phi$ relationship. This has been correctly appraised by the EC-3 [98] in its attempt to classify the beam-to-column joints as rigid, semi-rigid and pinned. However, the EC-3 classification takes only the influence of the beam and the connection into account and therefore disregards the role of the column stiffness. In the next section (see section 7.3.2) it will be shown that the overall extent of the semi-rigid effect is dependent on the stiffness of the beam, the connection and the column.

7.3 Semi-Rigid Action in Non-Sway Frames: Simplified Approach

7.3.1 General

Various codes of practice recognize the inherent advantage of semi-rigid design without actually specifying how this advantage can be practically incorporated in design practice. In the preceding section it has been shown that the main requirement for the development of semi-rigid design method is the formulation of design methods which will be simple to use but, at the same time, will give reliable results. The underlying assumption, however, is that the designer has the

connection $M-\phi$ relationship at his disposal. To this end the discussion here will be limited to predicting the first order elastic behaviour, although the general principles for a plastic design method will be identified.

7.3.2 Basis for Semi-Rigid Design

In design terms the semi-rigid action in frames implies an interaction between the beam, the column, and the connection. Incorporation of the joint characteristics in the analysis becomes important if the strength and/or stiffness of the connection is less than the strength and / or stiffness of the beam [113]. If a joint characteristic is taken into account it has to be considered in relation to the strength and the stiffness of the corresponding beam and column. The following section is intended to demonstrate how the relative stiffnesses of these interacting components influence the overall frame behaviour.

7.3.2.1 Interaction between the Beam, Column and Connection

The semi-rigid action in a frame is dependent on the interaction of the stiffness of the beam, the column, and the connection. Figure 7.15 is used to explain why the interaction of all three components is an important consideration.

A beam of stiffness k_b has connections of stiffness k_j at its ends. Figure 7.15(a) shows the hypothetical case where the connection is attached to frictionless pins. Figure 7.15(b), on the other hand, shows that the connections transmitting the forces to a fully fixed support. In the first instance the beam is effectively a simply supported one, while in the second case, the beam's behaviour will be completely dependent on the connection stiffness k_j . Figure 7.15(c) repre-

sents the real situation where the beam is connected to a column of finite stiffness via the connection. This situation is in between the two extreme cases of (a) and (b) mentioned above. Consideration of column stiffness (k_c) becomes vital in this case, as the behaviour will be dependent on k_j , k_b , and k_c . Thus in a practical frame design or analysis all three stiffnesses influence the response. The exact determination of the extent to which these factors govern the frame behaviour could lead to a daunting task for every day design office practice. However, a practical solution could be achieved if non-dimensional design aids are developed for a range of magnitudes of k_j , k_b and k_c . In order to make progress in this area a limited parametric study has been conducted, which is described in the following section.

7.3.2.2 Parametric Study

As already pointed out, the purpose of this parametric study is to find out how the relative stiffness of the beam, the column and the connection control the overall behaviour of the frame. In this instance, this study is limited to the three storey non-sway frame shown in figure 7.8. Three different beam spans were considered namely, 5.0m, 6.5m and 8.0m. All three stories were of equal height and kept constant at 3.5m for all cases. Three different universal beam sections and four different universal column sections were used. These covered a beam span to depth ratio from 14.0 to 31.5. The dimensions of the beams and columns used in this study are shown in table 7.6. Seven different connection stiffnesses were considered including ideal pin and ideal rigid connections. The combination of the above variables gave a total of 252 cases. All three beams at the different storey levels were incrementally loaded by uniformly distributed

loads up to a value of 24 kN/m. Since only the role of the relative stiffness of the beam, the column and the connection in the elastic range was considered in all cases, loading was continued up to this value, which was taken as the design ultimate load (based on the capacity of the beam, B1 for a 5.0 m span). Assuming a combined load factor of 1.5, the working load can be assessed as 16 kN/m. Based on the discussion of section 7.2.5, the connection stiffness in each case was represented by a constant stiffness as shown in table 7.7. These stiffness values are assumed to be representative of the secant stiffness at working load as determined by the beam line approach. The discrepancy that is apparent here (due to the different size of the beam and so the different location of the beam-line) has been ignored as was the difference in connection behaviour due to the variation in beam and column sizes. This will not affect the validity of the conclusions drawn regarding the effect of the relative stiffness of the beam, the column and the connection.

7.3.2.3 Limitation of Using Linear Connection Behaviour

In this section, the effect of using linear behaviour of the connection, instead of the actual nonlinear behaviour is examined. It is assumed that connections B and C have the $M-\phi$ relationship as shown in figure 7.16 when connected to beam B1 and column C1. The beam line at working load of 16.0 kN/m gives the secant stiffness (see figure 7.16) $k_B = 674$ kN-m/radian and $k_C = 1803$ kN-m/radian for connections B and C respectively.

The frame described above, with a span of 5.0 m and beams B1 and column C1 was analyzed for both connection type B and connection type C. The loading is uniformly distributed load acting on all three beams as described

above. The actual behaviour (full nonlinear) of the connections in both cases was incorporated in the analysis for comparison with the results of the linear representation of the connection stiffness.

In table 7.8, the average stiffness values for all the connections of the frame are shown as the load is incremented from zero to the designated value. Results of using both connections B and C are included in the table. The ratios k_{B_i}/k_B and k_{C_i}/k_C record how the instantaneous stiffnesses (k_{B_i} or k_{C_i}) at various load levels compare with the secant stiffnesses at working load level (k_B or k_C). In the case of connection B this ratio is 7.50 initially at zero load level and 0.24 at the ultimate design load level. This means that a linear secant stiffness underestimates the connection performance in the initial loading stage and overestimates it at or near the ultimate load. What follows is that, at the working load level, an average effect is produced which is fairly close to the actual behaviour. Figure 7.17(a) shows the development of the moments at the mid-span and at the ends of the top floor beam for connection type B. Results of using a secant stiffness determined by the above mentioned approach gives acceptable agreement with that obtained by considering the actual nonlinear connection behaviour. Similar favourable agreement can be observed in the load- central deflection response of the same beam as shown in figure 7.17(b)

Figures 7.18(a) and (b) present the similar responses with connection type C. Table 7.9 compares explicitly the corresponding values at working load (on which the secant stiffness is based) and at ultimate load. The difference in the deflection and moment values obtained by linear approach are within 2-3 per cent of that obtained considering the actual behaviour of the connection.

7.3.2.4 Presentation of Results

The results of the cases analysed will be presented and discussed here and, unless otherwise stated, the behaviour of the top floor beam will be discussed.

A set of typical results is assembled in table 7.10 for the 5m span frame. At working load level, the beam end moments are tabulated as a percentage of the free moment (simply supported span moment) for various combinations of beams, columns and connections. The figures in table 7.10, are indeed a measure of restraint to the beam. Connections designated as B, C, D have stiffness values listed in table 7.7. Connections B_{10} and C_{10} are ten times stiffer than connection B and C respectively whilst connection C_{20} is 20 times stiffer than connection C.

In table 7.10, connections are arranged from lower to higher stiffness from left to right as are the beams; ie. the smallest one, B1 is on the extreme left and the largest one, B3 is at the extreme right. Column sizes increases downwards from C1 to C4.

A close inspection into the table reveals that, for a given connection and column, increasing the beam size makes the connection less effective. Again, for a given connection and beam, increasing the column size will increase the overall restraint to the beam. This increase in restraint is more significant for a moderate to stiff connection than for a relatively flexible one. For example, for connection type B, connected to beam B1, changing the column from C1 to C4 would cause a mere 2.5 per cent shift in the end moment, whereas for connection B_{10} (which is 10 times stiffer than B) the same change would inflict an 17.2 per cent increase in end moment. This figure would be much higher for an even stiffer connection. This leads to the conclusion that any attempt to assess the restraint

provided by a connection must incorporate the relative stiffness of the beam and column and linked with the connection stiffness itself.

The values of table 7.10, together with the corresponding values for the frames with 6.5 m and 8.0 m spans can be best studied by plotting them in a non-dimensional form. Figures 7.19 and 7.20 are two such plots with connection to beam stiffness, $\frac{k_j}{(EI/L)_b}$ in the abscissa and non-dimensionalized end moment (M_E/M_{FREE}) as ordinate. The graphical software package [114] used here restricts a maximum of eight relationships to be compared in one plot, so a selection has to be made from the available beam to column stiffness ratios shown in table 7.10. Figure 7.21 presents a selection of $\frac{(I/L)_b}{(I/L)_c}$ ratios selected from the two preceding figures and shows the same relationship in terms of a more uniformly spaced beam to column stiffness ratio. Despite the fact that these data were generated from the analysis of cases with different values of span/depth ratio, they show very good correlation between the curves representing the various beam-to-column stiffnesses. This figure can actually be used as nomographs for determining the moments in a frame subjected to uniformly distributed load, taking into account the relative beam-to-column stiffness and also the stiffness of the connection. From the known values of stiffnesses of the connection (linear secant) and the beam, the abscissa of the nomograph is entered and then choosing the appropriate curve for k_b/k_c the end moment is obtained from the ordinate. The data of figure 7.21 corresponds to the top floor beam. The beams in the lower floors will receive higher restraint as depicted in table 7.11. The quantities compared in table 7.11 are the beam end moment (M_E), the span moment (M_{span}) and the central deflection (δ_c) of the beam. The three example cases shown in table 7.11 are randomly chosen. It will be shown later how the same nomograph (like that of figure 7.21) can be used for the beams and columns at

different locations by selecting the appropriate stiffness coefficient.

7.3.2.5 Estimation of Moment for a General Loading Type

The previous section has demonstrated that, for semi-rigid frames subjected to gravity uniformly distributed load, the estimates of bending moment can be made possible via the use of nomographs developed from a series of case studies. Although the same principle should be valid for any loading types, it is neither practical, nor possible to foresee the full range of circumstances that may arise in practice. Therefore, for a general purpose it is necessary to devise design method which is free from any set of conditions. McCormick [115] has shown that the end moment of a beam, for any loading condition, is given by

$$M_E = \frac{M_F}{\left(1 + \frac{k_b}{k_c} + \frac{k_b}{k_j}\right)} \quad (7.2)$$

where,

M_F is the fixed end moment, k_b is the beam stiffness,

k_c is the column stiffness, k_j is the joint stiffness;

If certain assumptions are made regarding the deformation of the frame members, explicit expressions for the terms in the right hand side of equation 7.2 can be derived. For this purpose following assumptions are made:

- i) For an exterior column the point of inflection is at the mid-height.
- ii) For an interior column, the deformation will be dependent on the frame geometry (symmetric or not) and the loading. For a perfect symmetric case zero flexure in the interior column can be assumed but the most onerous case will be a single curvature bending caused by a chequer board pattern of loading.
- iii) The fixed end moment at the interior end can be computed by assuming the

far end pinned and the fixed end moment at the exterior end can be computed by assuming the far end fixed.

In the line with these assumptions, explicit conditions that would arise at various locations are discussed below:

Beams with far end at external column

$$k_b = \frac{3EI_b}{L} \quad \text{and} \quad M_F^i = \text{Fixed End Moment} \times 1.5$$

Beams with far end at internal column

$$k_b = \frac{2EI_b}{L} \quad \text{and} \quad M_F^e = \text{Fixed End Moment}$$

Top storey columns

$$k_c = \frac{6EI_c}{h}$$

Middle storey columns

$$k_c = \left(\frac{6EI_c}{h} \right)_u + \left(\frac{6EI_c}{h} \right)_l$$

The connection stiffness, k_j can be taken as the secant stiffness based on an appropriate beam line as described in section 7.2.5. Appendix B contains worked examples on the basis of the above approach. Four examples on two different frame configurations have been considered. The results obtained by this approach have been compared with the results of rigorous analysis using the present program and were found to be satisfactory as can be seen in Appendix B.

7.3.2.6 Beam Deflection at Serviceability

One of the major obstacles for the use of semi-rigid design is that the sagging deflection may be excessive when compared to those resulting from rigid design to meet the requirement of the serviceability limit state. The simple beam deflection

is 5 times as great as the rigid beam deflection (see figure 7.22) which indicates the potential advantage of limiting the deflection if the inherent semi-rigid connection stiffness is taken into account. From strength considerations it is contemplated that the use of semi-rigid design will lead to lighter beams (than those used for simple design) but it must be ensured that the serviceability requirements are also met. In the foregoing sections methods to assess the bending moments in semi-rigid frames under gravity loads have been developed. To check the serviceability condition, it is important that the designer be able to assess the deflections without resort to the complexities of a rigorous method of analysis.

Figures 7.22 (a) and (b) show the well known central deflection equations for a beam subjected to uniformly distributed load with the extreme support conditions of simply supported and fixed ends. The elastic deflection for a simply supported beam is five times as great as that of one fixed at both ends. The fixed supported beam has at its end a moment M_F as against zero end moment for a simply supported beam. The partially restrained beam of figure 7.22(c) has an end moment M_{PR} which is less than the fixed end moment M_F . Clearly the deflection of a partially restraint beam δ_{PR} would be greater than δ_{fixed} but smaller than δ_{ss} . Therefore, from the known values of δ_{ss} , δ_{fixed} , M_F and M_{PR} it is possible to scale δ_{PR} by employing elastic principles as follows:

$$\delta_{PR} = \delta_{fixed} + \frac{M_F - M_{PR}}{M_F} (\delta_{ss} - \delta_{fixed}) \quad (7.3)$$

Now the above equation will give the deflection of a beam with partially restrained ends. The calculation of δ_{ss} , δ_{fixed} and M_F is fairly simple. Calculation of M_{PR} can be accomplished using the approach described earlier. For the computation of the deflection of semi-rigidly framed beams the above equation must

be modified because of the effect of column flexibility. For a framed beam, the deflection equation for serviceability conditions are:

$$\delta_{SR} = \delta_{rigid} + \frac{M_r - M_{sr}}{M_r} (\delta_{pin} - \delta_{rigid}) \quad (7.4)$$

where,

M_r = Beam end moment for rigid frame analysis

M_{sr} = Beam end moment for semi-rigid frame analysis

δ_{pin} = Beam deflection for pinned or simple frame

δ_{rigid} = Beam deflection for rigid frame

Computation of M_{sr} can be performed by the method described in the preceding section. M_r is the limiting case of M_{sr} and so can be computed by the same method by assuming a high value of connection stiffness. Neglecting the axial column deformation δ_{pin} can be approximated by the same formula (see figure 7.22) as δ_{ss} . The value of δ_{rigid} can be computed by using the slope deflection equation [116]:

$$\theta_A = \theta'_A + \frac{\Delta}{L} + \frac{l}{3EI} \left(M_{AB} - \frac{M_{BA}}{2} \right) \quad (7.5)$$

The relevant terms in equation 7.5 are described in figure 7.23. Equations can be written for the beam and the column end rotations θ_{21} and θ_{23} respectively (see figure 7.23(b)) and for a rigid frame,

$$\theta_{21} = \theta_{23}$$

The resulting value of Δ which is obtained from solving equation 7.5 is δ_{rigid} .

Should the above approach of computing δ_{rigid} prove to be tedious, the designer could easily use a linear elastic frame analysis program to obtain δ_{rigid} . It is hoped that every design office should have access to such program nowadays.

7.3.2.7 Example of the Calculation of Deflection

The nomograph of figure 7.21, together with the procedures described in the previous section, will now be used to obtain the central deflection of the top floor beam of the frame (span = 5.0m) shown in figure 7.8. The beam section is B1 and the column section is C1 as listed in table 7.6. The central displacement at a load intensity of 24.0 kN/m is computed as follows:

$$E=210 \text{ kN/mm}^2 \quad \delta_{pin} = \frac{5wl^4}{384EI} = 3.342 \text{ cm}$$

$$\delta_{rigid} = 1.91 \text{ cm (from rigorous analysis)}$$

$$M_r = 26.78 \text{ kN-m (using the nomograph)}$$

For Connection 'B'

$$k_j=674 \text{ kN-m/rad}, \quad k_b = \frac{EI_b}{L_b}=1168.65 \text{ kN-m/rad}, \quad k_c = \frac{EI_c}{L_c}=741.06 \text{ kN-m/rad}$$

$$\frac{k_j}{k_b}=0.576 \quad \frac{k_b}{k_c}=1.58$$

$$\text{using figure 7.21, } M_{sr}=0.11 M_{FREE} = 8.25 \text{ kN-m/rad.}$$

The computation of the deflection for connection types $B, B_1, C, C_{10}, C_{20}$ and D (using equation 7.4) are shown in table 7.12. Also included in that table are the deflections computed by using the present computer program. It can be seen that the predicted displacement by the above approach is very close to that obtained by the rigorous analysis. Thus it appears the method described can be justifiably used for the computation of elastic deformation of the beams of semi-rigid frames.

7.3.2.8 Moments in the Column

In chapter 6, it has been shown that for partially restrained (or semi-rigid) frames the column moments are much greater than those estimated by the codes of practice. Baker [117] observed that tests showed that real eccentricities could be as great as five times than those recommended by the structural code. However, the cases studied in chapter 6 show that in semi-rigid frames the column moments (M_{col}) can be approximated simply by

$$M_{col} = M_E + \text{beam reaction} \times \text{eccentricity of the reaction} \quad (7.6)$$

where M_E is the beam end moment. The eccentricity of the reaction is equal to half the column depth in the case of major axis bending and zero otherwise. This, however, assumes the beam reaction to act at the column face, which may not be true for connections like the flange cleat. In the author's view this can be neglected and the above equation can be used satisfactorily. The end moment of the beam can be obtained by using the method already described and, for columns other than the top storey one, the column moment should be apportioned in proportion of the respective column stiffness. Column stiffness however, should be based on the deformed shape due to any anticipated loading arrangement in the frame taking into account the support condition at the far end.

7.3.2.9 Design of Axially Loaded Columns

The strength of a column in a frame depends considerably on the restraint provided by the connection and the adjacent members. Consequently it necessitates the inclusion of this influence in the design of the column. One convenient way of

including this interaction effect is to use the concept of effective length, which is defined as the length of an equivalent pin ended column that will give the same critical load as for the actual column. For isolated columns, the effective length can be explicitly determined [68] if the end conditions are known. But, when a column is part of a frame, the ideal solution would be based on the interaction of the complete structure aiming at the search for the load at which the overall frame stiffness vanishes. However, for design purposes, this procedure is impractical and a more traditional method of isolating the individual member is much more desirable.

For a rigid jointed frame, the method of calculating the effective length of a column have been suggested by Julian and Lawrence [118] and Wood [53]. The effective length of a column in a semi-rigid frame is dependent on the stiffness of the joint which makes the inclusion of this effect complicated by the fact that this stiffness is not a constant value. The situation is further complicated because some of the connections associated with the column may be unloading while others are being loaded. While researchers have suggested different solutions to this problem, almost all are based on the representation of the connection stiffness by the initial tangent of the connection $M-\phi$ relationships. Reference [13] observed that this approach is correct for a bifurcation type of buckling problem, but, in reality column end deformations will occur prior to the attainment of the maximum (critical) load and consequently the effective stiffness of the connection will tend to decrease with increasing load.

The most promising way of incorporating the influence of connection stiffness in determining the effective length of the column is due to Bjorhovde [3]. The method actually uses the AISC G-factor alignment chart for arriving at

suitable values of the effective length factor. For use with the BS 5950 effective length charts Davison [32] modified the definition of some of the terms involved in the computation. The modified G-factor approach and the modified BS 5950 approach are well documented elsewhere [32],[57] and therefore will not be repeated here. Davison's computation, based on an initial connection stiffness, showed a predicted axial capacity of up to 10 per cent more (unsafe prediction) than the test results (see table 7.13). The cases shown in table 7.13 corresponds to the sub-assembly tests by Davison [57]. The subassemblages were subjected initially to equal beam load and then column load was applied until failure (see figure 7.24).

The use of a secant stiffness for the representation of the connection has been discussed earlier. Based on a k_j^{10} , the secant connection stiffness at 10 milli rad connection rotation, the computation of the effective length factor and the design load were recalculated by the author. Computations by both the AISC G-factor approach and by the BS 5950 approach are explicitly shown in table 7.14 and table 7.15 respectively. The calculation in these tables are based on the principles laid down in reference [3]. Since the beam loads were applied only on the top beams, one connection at the top joint was assumed effective, while both the connections at the bottom joint were considered to be effective. Once the effective length of the column is established the next stage is the determination of the column strength for a given column slenderness. In the inelastic range the column strength can be estimated by the following formula [119]

$$\sigma_c = \sigma_y - \frac{\sigma_p}{\pi^2 E} (\sigma_y - \sigma_p) \left(\frac{k_e l}{r} \right)^2 \quad (7.7)$$

where,

$\sigma_c = \text{critical stress}$

$\sigma_y = \text{yield stress}$

$\sigma_p = \text{proportional limit stress}$

Replacing σ_p by $(\sigma_y - \sigma_{RC})$, where σ_{RC} is the residual stress and assuming a residual stress equal to $0.5\sigma_y$, equation 7.7 finally reduces to

$$\sigma_c = \sigma_y - \frac{(\sigma_y)^2}{4\pi^2 E} \left(\frac{k_e l}{r} \right)^2 \quad (7.8)$$

This equation is plotted in figure 7.25. Tabulated values of the critical average stress predicted by the above equation for structural steels having various yield stresses are available [60].

Equation 7.8 facilitated the computation of the column design loads shown in tables 7.14 and 7.15. The use of secant stiffness has resulted in higher effective length factors (than those of table 7.13) for all four cases, although the predicted loads in table 7.14 are still on the unconservative side. This is because the approach used to calculate the strength of the column in the reference [57] is different from that of equation 7.8. The effective length factors as obtained in table 7.14 may be used with BS 5950 (section 4.7.5) and all four cases reported in table 7.14 would produce a 'Test Load/ Predicted Load' greater than one (1.25, 1.08, 1.11 and 1.15 respectively). The G-factor approach appears to be relatively insensitive to the connection stiffness. However, it can be seen that the prediction of design loads by the modified BS 5950 as shown in table 7.15 compare favourably with those obtained by the column-subassemblage tests [57].

A further documentation of the method is shown in tables 7.16 to 7.19, against the results of full scale frame tests [32]. The description of the frame tests-1 and test-2 can be seen in chapter 4. Unlike the computations of tables 7.14 and 7.15, the calculations for tables 7.16 to 7.19 had to be based on some

assumed data (see corresponding tables), since the properties of the relevant test column were not available. Correspondence between the test results and the predicted column capacity is quite satisfactory, despite the presence of moments in the external column due to beam loading (unlike those in subassembly tests). It must be emphasized however that these moments were of modest magnitude.

Thus for the cases considered the axial carrying capacity of the column can be estimated by the above procedure using a k_j^{10} connection stiffness.

7.3.2.10 Design of Columns Under Combined Axial Load and Bending

The design of beam-column is usually tackled by the interaction equation of the form:

$$\phi \left(\frac{P}{P_u}, \frac{M}{M_u} \right) \leq 1.0 \quad (7.9)$$

where,

P = Axial thrust at failure

P_u = Ultimate load for a centrally loaded column

M = Maximum bending moment at failure

M_u = Ultimate moment capacity in the absence of axial load

The explicit form of equation 7.9 varies from code to code. An overview of these forms allowing for semi-rigid effects is given elsewhere [112]. The calculation of the axial carrying capacity of a column was discussed in the preceding section. The assessment of the column moment in semi-rigid frame has also been

discussed above, which should make the use of the interaction formulae rather straightforward.

7.3.2.11 Plastic Design of Semi-Rigid Frame

To exploit the full advantage of semi-rigid design, a plastic design approach should be considered. For the non-sway case, the calculation of the first order force distribution should prove relatively straightforward with acceptable accuracy. However, following important points need to be considered.

1. For partial strength connections, if the moment at the mid-span reaches the plastic moment (M_p) of the beam and those at the ends reach the full connection capacity (M_c) then for the beam of figure 7.26

$$M_c + M_p = \text{Free Moment.}$$

2. If the calculation is based on the above mechanism, the designer has to be satisfied that the column's plastic moment (M_{pc}) is greater than (M_c). In this case any possible reduction in M_{pc} , due to the presence of axial load should be considered.
3. In the event that a plastic hinge is developed at the connection, the column should not be designed as end restrained, rather it should be designed with an effective length equal to unity.
4. If the connection is too stiff, the first plastic hinge will occur at the beam end. In that case the connection must have sufficient rotation capacity to

complete the full beam mechanism, from which a condition for minimum rotation capacity can be derived [120].

5. If the connection is rather flexible, the first plastic hinge will occur at the beam centre and no requirement of minimum rotation capacity is required. However the $M-\phi$ relationship must satisfy the requirement of minimum stiffness in order that serviceability deflection limit is not exceeded. Reference [120] shows explicitly how the condition for the minimum stiffness requirement can be formulated.

7.4 Conclusions

The main obstacles for the development of a design method for semi-rigid frames have been identified in this chapter. They are namely, the lack of dependable information on connection behaviour and the highly nonlinear nature of the connection $M-\phi$ response. A linear secant representation of the connection behaviour has been proposed by the author, which has subsequently been used to quantify the design forces and the serviceability deflections for a non-sway semi-rigid frame. These forces and deflections were found to correlate well with those obtained from rigorous analyses.

Using the secant representation of the connection behaviour, an existing method of determining the axial capacity of a (semi-rigid) framed column has been examined. It has been shown that the modified BS 5950 approach to effective length gives better results than those produced by the AISC G-factor approach (both methods being used in conjunction with the column strength curve of equation 7.8).

Conn. Designation (Ref)	Beam size	Column size	Pl. Len. mm	Pl. Thkn. mm	Bolt Arrangement	Bolt dia mm
FEP [106]	254x146 UB43	203x203 UC71	290	15	NTB 2x1 NTC 2x1	20
EEP [107]	305x165 UB46	254x254 UC89	N/A	16	NTB 2x2 NTC 2x2	16

NTB=No. of bolts of T. angle on beam, NTC=No. of bolts of T. angle on column.
 NCB=No. of bolts of C. angle on beam, NCC=No. of bolts of C. angle on column.

Table 7.1 Details of FEP and EEP connections shown in figure 7.2.

Conn. Designation (Ref)	Beam size	Column size	Tension Angle	Comp. Angle	Bolt Arrangement	Bolt dia mm
1 [108]	305x165 UB40	254x254 UC73	150x90x12x171	150x150x12x171	NTB 2x2 NCB 2x2 NTC 2x1 NCC 2x2	19
2 [108]	W12x50*	254x254 UC73	150x90x12x200	150x150x12x200	NTB 2x2 NCB 2x2 NTC 2x1 NCC 2x1	19
3 [108]	356x171 UB51	305x305 UC97	150x90x15x180	150x150x15x180	NTB 2x2 NCB 2x2 NTC 4x1 NCC 2x2	19
4 [108]	457x152 UB67	W14x58*	150x90x12x254	150x150x22x190	NTB 2x2 NCB 2x2 NTC 4x1 NCC 2x2	19

* No equivalent British Standard section.

Table 7.2 Details of flange cleat connections shown in figure 7.2.

Conn. Designation (Ref)	Beam size	Column size	Tension Angle	Comp. Angle	Bolt Arrangement	Bolt dia mm
1 [108]	406x178 UB60	305x305 UC97	150x90x15x300	150x150x20x184	NTB 2x2 NCB 2x2 NTC 4x1 NCC 2x2	19
2 [108]	457x152 UB67	305x305 UC97	150x90x15x300	150x150x20x184	NTB 2x2 NCB 2x2 NTC 4x1 NCC 2x2	19

Table 7.3 Details of the flange cleat connections from reference [108].

Connection Type	No of Tests	
	Major Axis Bending	Minor Axis Bending
Flange Cleat	57	6
Flush End Plate	54	21
Header Plate	39	0
Extended End Plate	69	0

Table 7.4 Available connection test results [91].

Span m	Connection Designation	Beam end moment as % of free moment	Central deflection cm
5.0	C	19.6	1.643
	C_{10}	33.0	1.326
	C_{20}	34.6	1.290
6.5	C	24.0	4.32
	C_{10}	37.98	3.225
	C_{20}	39.2	3.140

Table 7.5 Effect of the variation of connection stiffness.

Member Designation	British Standard Section Serial Size	Overall Depth, mm	I_{x-x} cm^4
B1	254x102 UB22	254	2863
B2	305x102 UB28	308.9	5415
B3	356x127 UB33	348.5	8167
C1	152x152 UC23	152.4	1263
C2	203x203 UC46	203.2	4564
C3	254x254 UC 73	254.0	11 360
C4	356x368 UC 202 (very stiff)	374.4	66 307

Table 7.6 Member serial sizes and properties used in the analysis.

Connection Designation	Stiffness Values kN- m/rad
A	0.00001
B	674.0
C	1803.0
B_{10}	6740.0
C_{10}	18030.0
C_{20}	36060.0
D	1695000.0

Table 7.7 Connection stiffness values for the different connections used in analysis.

Load step	Conn. Type B		Conn. Type C	
	k_{Bi} kN-m/rad	k_{Bi}/k_B	k_{Ci} kN-m/rad	k_{Ci}/k_C
1	5055.0	7.5	23080.0	12.8
2	1408.0	2.09	2885.0	1.6
3	1348.0	2.00	2614.0	1.45
4	1178.0	1.75	2308.0	1.28
5	1038.0	1.54	2272.0	1.26
6	1025.0	1.52	2236.0	1.24
7	1011.0	1.50	2200.0	1.22
8	829.0	1.23	1800.0	0.998
9	647.0	0.96	1551.0	0.86
10	465.0	0.69	1424.0	0.79
11	390.9	0.58	1352.0	0.75
12	330.3	0.49	1244.0	0.69
13	283.1	0.42	1172.0	0.65
14	249.4	0.37	1136.0	0.63
15	222.4	0.33	991.6	0.55
16	202.2	0.30	901.5	0.50
17	182.0	0.27	829.4	0.46
18	175.0	0.26	739.2	0.41
19	168.5	0.25	685.14	0.38
20	161.8	0.24	631.05	0.35

Table 7.8 Comparison of the secant stiffness values with the tangent stiffness of the nonlinear connection at different load levels.

Load magnitude kN/m	Conn. type B				Conn. type C			
	Actual nonlinear		Linear secant		Actual nonlinear		Linear secant	
	M_E/M_{Free} %	δ_c cm	M_E/M_{Free} %	δ_c cm	M_E/M_{Free} %	δ_c cm	M_E/M_{Free} %	δ_c cm
15.6	13.5	1.79	11.3	1.83	21	1.61	20	1.64
24.0	10.8*	3.64*	12.0*	3.19*	18	2.58	21	2.53

* Plasticity in beam.

Table 7.9 Effect of using a linear secant representation of the nonlinear connection M- ϕ behaviour.

Conn. Beam → Colm. ↓	Beam end moment as percentage of free moment																	
	B			C			B ₁₀			C ₁₀			C ₂₀			D		
	B1	B2	B3	B1	B2	B3	B1	B2	B3	B1	B2	B3	B1	B2	B3	B1	B2	B3
C1	11.0	6.0	3.9	19.6	11.51	7.75	29.0	19.2	13.7	33.0	22.8	16.8	34.6	24.14	18.4	35.7	25.20	19.13
C2	13.0	7.30	5.0	24.4	15.3	10.96	40.0	29.5	23.0	46.8	37.4	30.8	49.3	40.8	34.4	51.3	43.7	37.8
C3	13.3	7.6	5.3	25.9	16.6	12.0	43.7	33.7	27.1	51.9	44.0	38.0	55.0	48.6	43.3	57.4	50.7	48.3
C4	13.5	7.8	5.43	26.6	17.18	12.6	46.2	36.6	30.1	55.5	49.3	44.2	59.1	55.0	51.22	62.3	60.4	58.7

Table 7.10 Effect of the beam and column stiffness in influencing the effectiveness of the connection restraint at working load level (5.0 m span).

Span m	Beam	Column	Connection	Storey level	M_E kN-m	M_{span} kN-m	δ_c cm
6.5	B2	C1	B	1	7.55	75.43	2.75
				2	8.09	74.88	2.77
				3	6.75	76.3	2.88
6.5	B3	C3	C	1	37.2	43.89	0.848
				2	38.7	42.26	0.815
				3	34.2	46.69	0.967
5.0	B1	C1	B	1	6.09	42.5	1.729
				2	6.5	42.1	1.749
				3	5.5	43.14	1.84

Table 7.11 Variation of restraint at different storey levels.

Connection Designation	End Moment M_{sr} (kN-m)	$\frac{M_r - M_{sr}}{M_r}$	$\delta_{predict}$ (cm)	δ_{prog} (cm)	%Error
B	8.25	0.692	2.87	3.19	10.0*
B_{10}	21.75	0.188	2.167	2.18	0.9
C	14.70	0.451	2.53	2.53	0.0
C_{10}	24.75	0.076	2.01	2.04	1.4
C_{20}	25.95	0.031	1.95	1.99	2.0
D	26.78	0	1.91	1.95	2.0

* Plasticity in beam.

Table 7.12 Prediction of serviceability deflection.

Test No./ Col. Bending Axis	σ_y N/mm ²	Area of the Col. sq. mm	Eff. Length Factor, k_e	$\frac{\text{Test load}}{\text{Predicted Load}}$
ST3 (Minor)	265	2914	0.52	0.95
ST4 (Major)	273	2983	0.55	1.06
ST6 (Minor)	288	2874	0.51	0.90
ST8 (Minor)	279	2837	0.52	0.95

Table 7.13 Comparison of the test load with the predicted load (after Davison [57])

Note: See table 7.13 for additional information.

$$E=210 \text{ kN/sq. mm} \quad k_b = \frac{EL_b}{L_b} = 1959.12 \text{ kN-m/rad}$$

$$k_c = \frac{EL_c}{L_c} = 139.10 \text{ kN-m/rad (Minor axis)} \quad \text{Factor, } G = \frac{\sum (\frac{EL_c}{L_c})}{\sum C^*}$$

$$k_c = \frac{EL_c}{L_c} = 431.50 \text{ kN-m/rad (Major axis)} \quad \text{Distribution factor, } k = \frac{\sum (\frac{EL_c}{L_c})}{(\sum \frac{EL_c}{L_c} + 0.5 \sum C^*)}$$

Test Desig. and Bending Axis	k_j^{10} (kN-m/rad)	$\beta = \frac{k_j^{10}}{k_b}$	$\beta^* = \frac{2\beta}{\beta+2}$	$C^* = \beta^* \times k_b$	G_{top}	G_{bot}	k_e	Predicted Load(kN)	$\frac{\text{Test load}}{\text{Predicted Load}}$
ST 3 (Minor)	541.09	0.276	0.242	474.1	0.29	0.15	0.59	546.0	0.95
ST 4 (Major)	1056.08	0.539	0.424	830.67	0.52	0.26	0.66	714.0	1.06
ST 6 (Minor)	1382.13	0.705	0.521	1020.70	0.14	0.07	0.55	599.0	0.86
ST 8 (Minor)	1271.18	0.649	0.490	959.97	0.14	0.07	0.55	579.6	0.89

Table 7.14 Comparison of the subassemblage test load with the predicted load by G-factor approach using k_j^{10} connection stiffness.

Test Desig. and Bending Axis	k_j^{10} (kN-m/rad)	$\beta = \frac{k_j^{10}}{k_b}$	$\beta^* = \frac{\beta}{\beta+4}$	$C^* = \beta^* \times k_b$	k_{top}	k_{bot}	k_e	Predicted Load(kN)	$\frac{\text{Test load}}{\text{Predicted Load}}$
ST 3 (Minor)	541.09	0.276	0.06	118.0	0.70	0.54	0.75	407.4	1.28
ST 4 (Major)	1056.08	0.539	0.12	235.1	0.79	0.65	0.81	664.5	1.14
ST 6 (Minor)	1382.13	0.705	0.15	293.9	0.49	0.32	0.64	518.0	1.00
ST 8 (Minor)	1271.18	0.649	0.14	274.3	0.50	0.34	0.65	496.0	1.04

Table 7.15 Comparison of the subassemblage test load with the predicted load by BS 5950 effective length chart using k_j^{10} connection stiffness.

Note: See chapter 4 for details of the test.

Assumed data:

$$E=210 \text{ kN/sq. mm}, \quad \sigma_y = 275 \text{ N/mm}^2$$

$$\text{Col. Area}=2980 \text{ mm}^2 \quad k_b = 1175.38 \text{ kN-m/rad} \quad \text{and } k_c = 736.75 \text{ kN-m/rad}$$

Column No.	Secant Conn. Stiffness k_j^{10} (kN-m/rad)	$\beta = \frac{k_j^{10}}{k_b}$	$\beta^* = \frac{2\beta}{\beta+2}$	$C^* = \beta^* \times k_b$	G_{top}	G_{bot}	k_e	Predicted Load(kN)	$\frac{\text{Test load}}{\text{Predicted Load}}$
6	1056.08	0.90	0.62	728.7	2.0	1.0	0.82	763.6	0.98
9	1056.08	0.90	0.62	728.7	10.0	1.0	0.86	758.0	1.01

Table 7.16 Comparison of the frame test load (major axis) with the predicted load by G-factor approach using k_j^{10} connection stiffness.

Column No.	Secant Conn. Stiffness k_j^{10} (kN-m/rad)	$\beta = \frac{k_j^{10}}{k_b}$	$\beta^* = \frac{\beta}{\beta+4}$	$C^* = \beta^* \times k_b$	k_{top}	k_{bot}	k_e	Predicted Load(kN)	$\frac{\text{Test load}}{\text{Predicted Load}}$
6	1056.08	0.90	0.18	211.6	0.93	0.0	0.68	781.1	0.95
9	1056.08	0.90	0.18	211.6	1.0	0.0	0.70	778.8	0.98

Table 7.17 Comparison of the frame test load (major axis) with the predicted load by BS 5950 effective length chart using k_j^{10} connection stiffness.

Note: See chapter 4 for details of the test.

Assumed data:

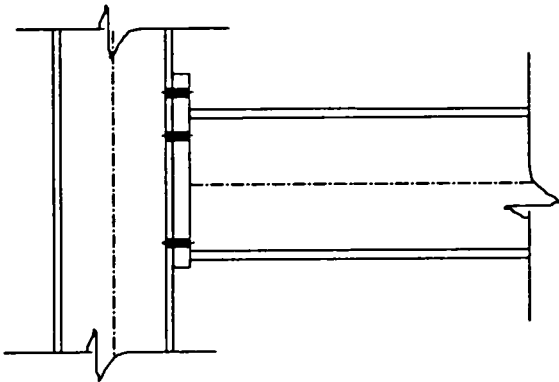
$E=210 \text{ kN/sq. mm.}$ $\sigma_y = 275 \text{ N/mm}^2$
 Col. Area= 2980 mm^2 $k_b = 1175.38 \text{ kN-m/rad}$ and $k_c = 235.08 \text{ kN-m/rad}$

Column No.	Secant Conn. Stiffness k_j^{10} (kN-m/rad)	$\beta = \frac{k_j^{10}}{k_b}$	$\beta^* = \frac{2.3}{3+2}$	$C^* = \beta^* \times k_b$	G_{top}	G_{bot}	k_e	Predicted Load(kN)	$\frac{\text{Test load}}{\text{Predicted Load}}$
3	1382.13	1.18	0.74	869.8	10	1.0	0.86	627.1	1.00
6	1382.13	1.18	0.74	869.8	0.54	1.0	0.74	677.0	1.05

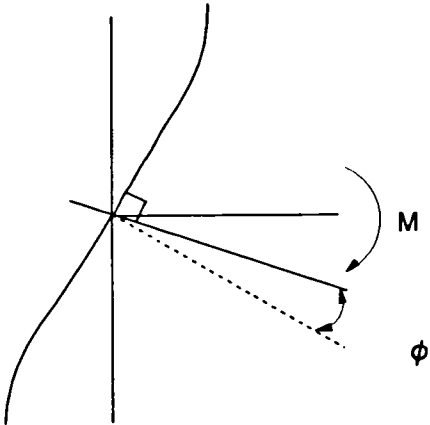
Table 7.18 Comparison of the frame test load (minor axis) with the predicted load by G-factor approach using k_j^{10} , connection stiffness.

Column No.	Secant Conn. Stiffness k_j^{10} (kN-m/rad)	$\beta = \frac{k_j^{10}}{k_b}$	$\beta^* = \frac{3}{3+4}$	$C^* = \beta^* \times k_b$	k_{top}	k_{bot}	k_e	Predicted Load(kN)	$\frac{\text{Test load}}{\text{Predicted Load}}$
3	1382.13	1.18	0.23	270.3	1.0	0.0	0.7	692.0	0.91
6	1382.13	1.18	0.23	270.3	0.78	0.0	0.66	706.0	1.00

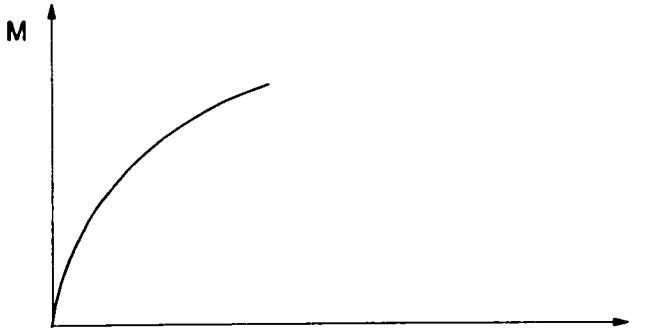
Table 7.19 Comparison of the frame test load (minor axis) with the predicted load by BS 5950 effective length chart using k_j^{10} connection stiffness.



a) Connection



b) Model



c) Moment-rotation characteristic

Figure 7.1 Connection moment and rotation.

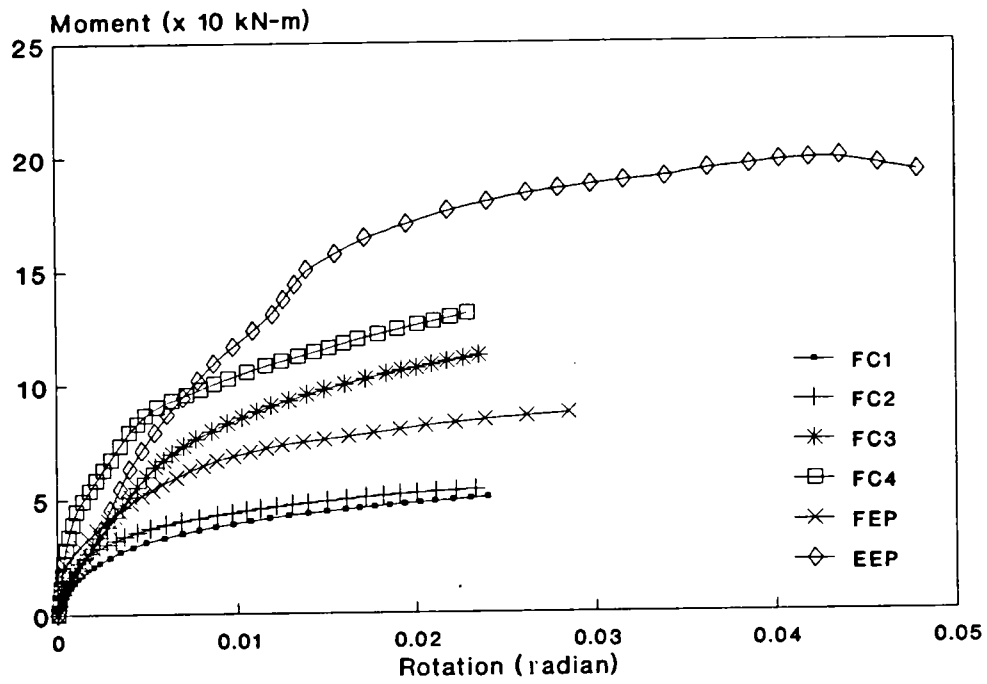


Figure 7.2 M- ϕ relationships for connections of tables 7.1 and 7.2.

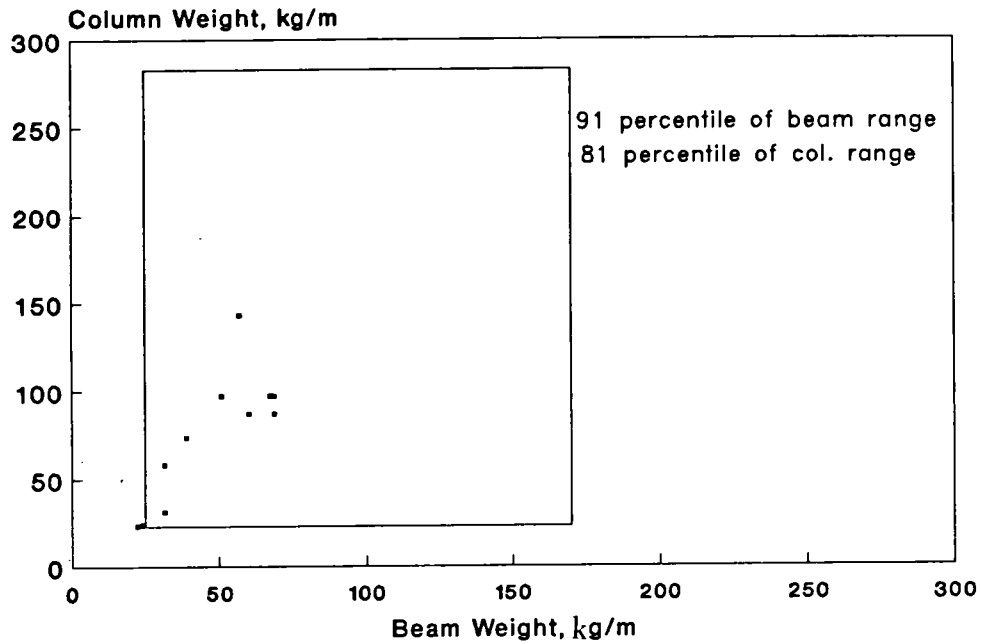


Figure 7.3 (a) Available $M - \phi$ data for flange cleat connections.

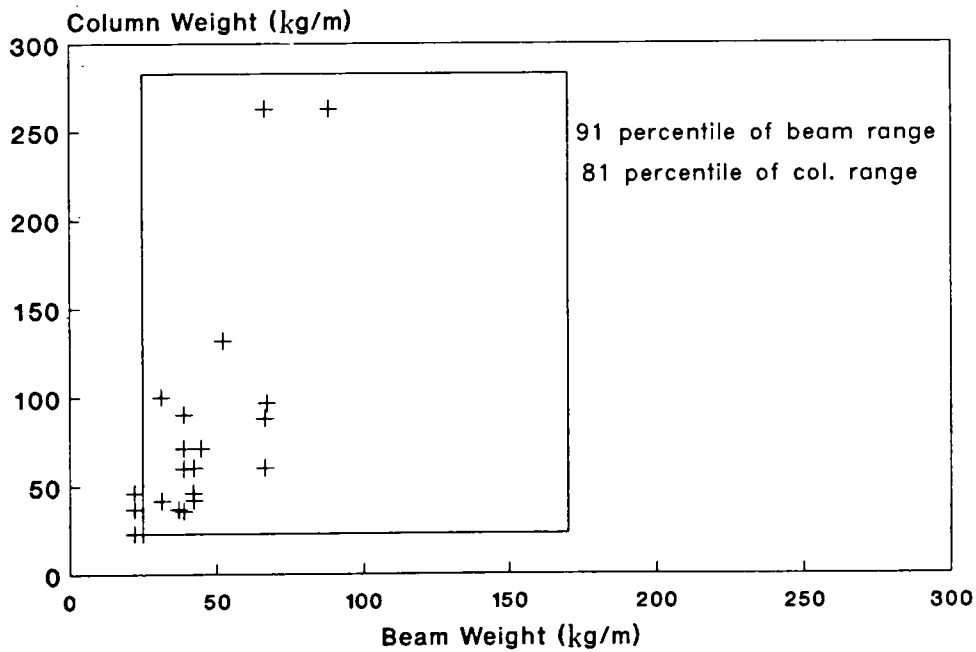


Figure 7.3 (b) Available $M - \phi$ data for flush end plate connections.

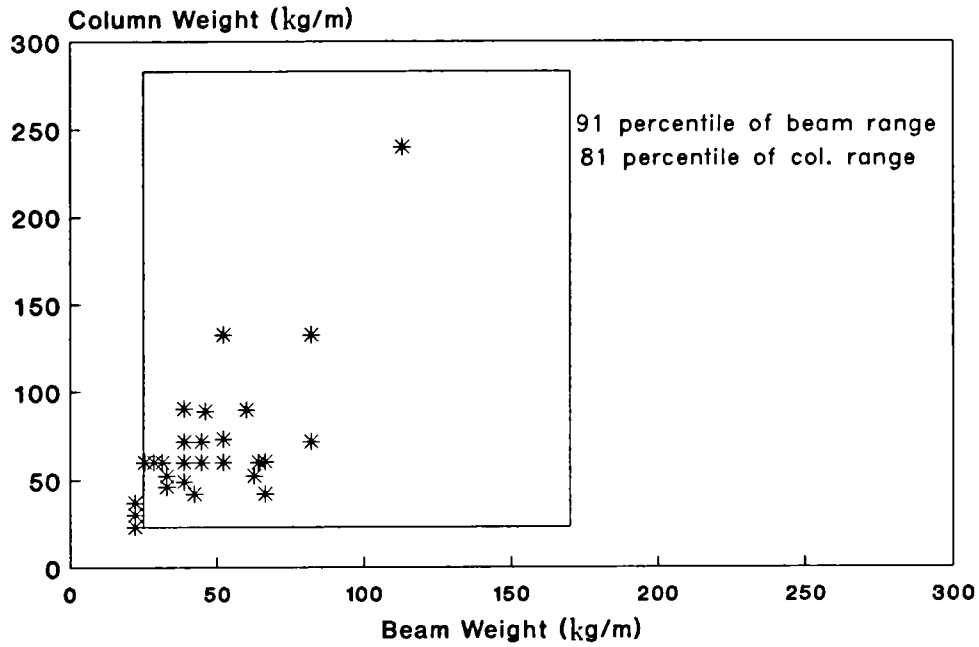


Figure 7.3 (c) Available $M - \phi$ data for extended end plate connections.

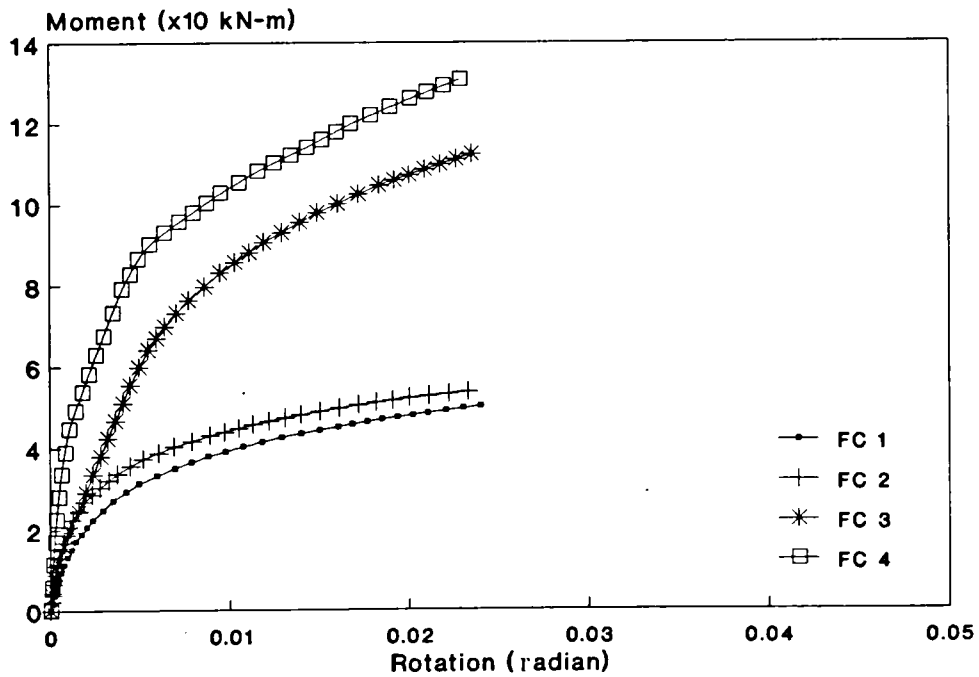


Figure 7.4 $M - \phi$ relationship for the four flange cleat connection of table 7.2.

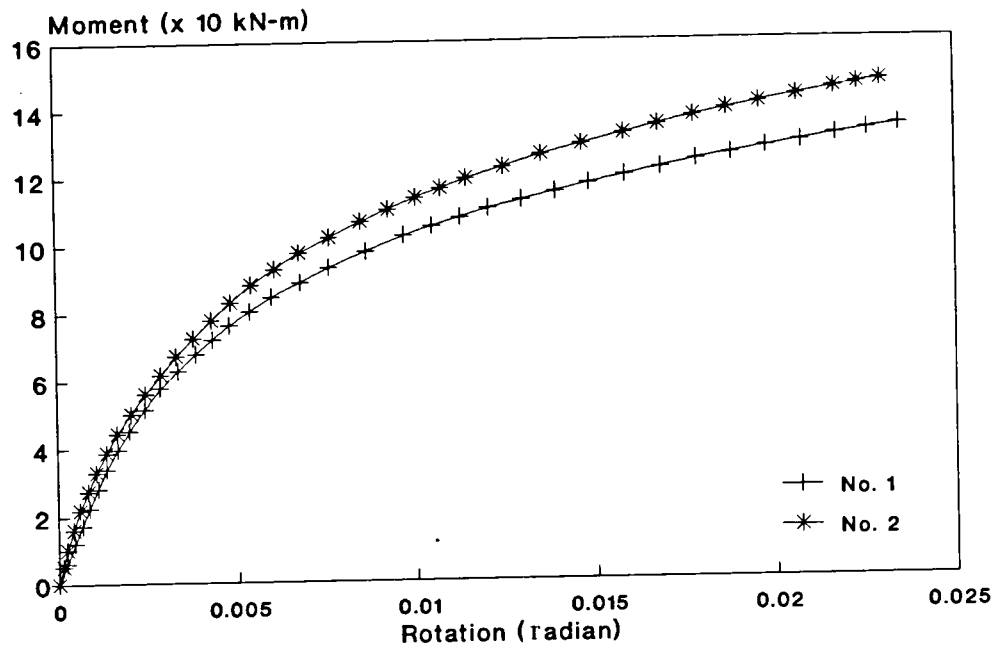


Figure 7.5 $M - \phi$ relationship for the two flange cleat connection of table 7.3.

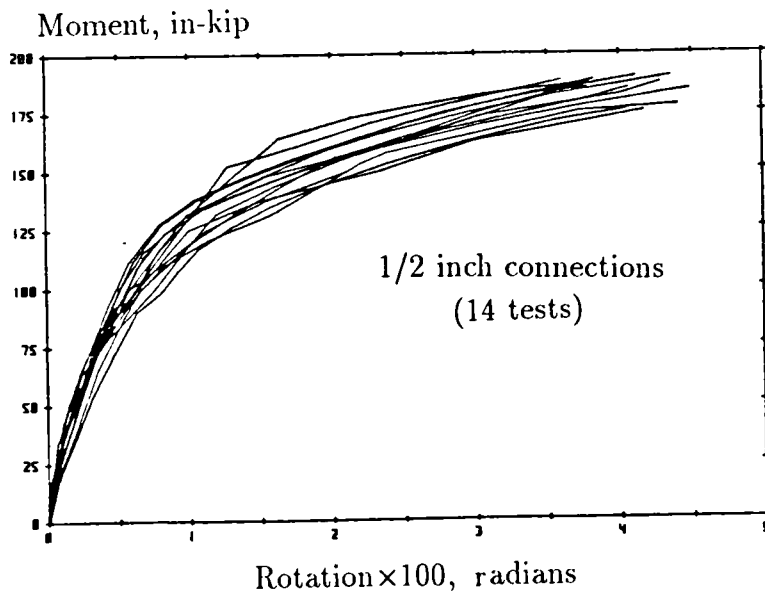


Figure 7.6 Range of variation observed in replicated connection test results [110].

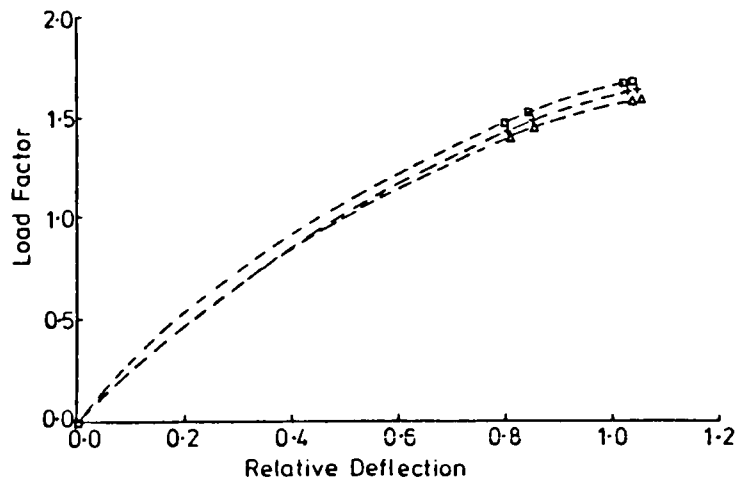


Figure 7.7 Effect of 10% shift in $M - \phi$ characteristic on beam response [8].

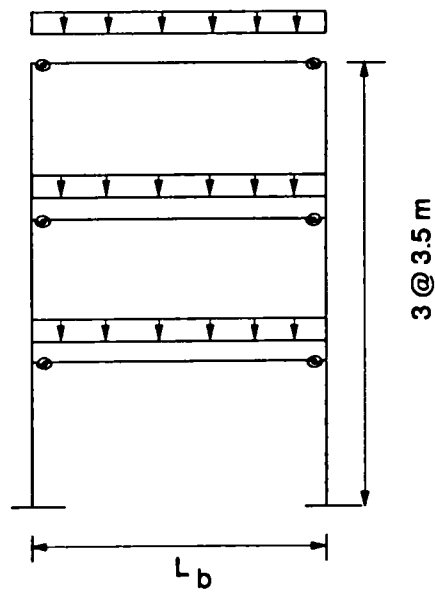


Figure 7.8 Frame considered for parametric study.

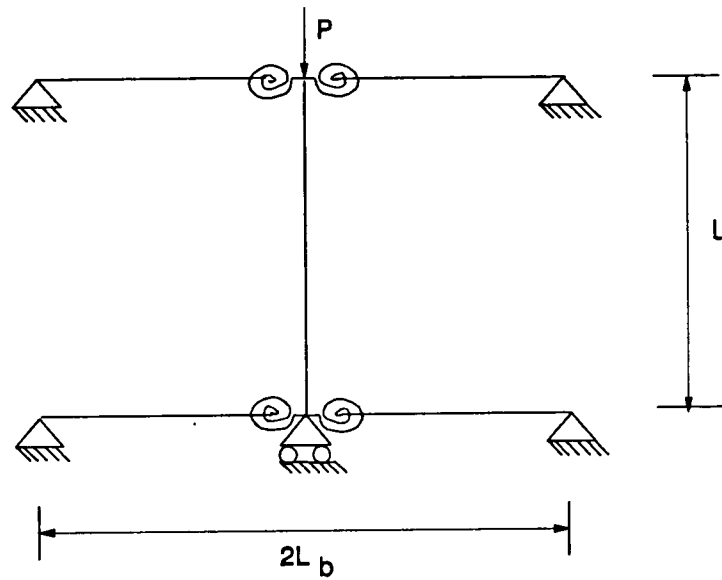


Figure 7.9 (a) I-shaped subassembly used for column strength determination.

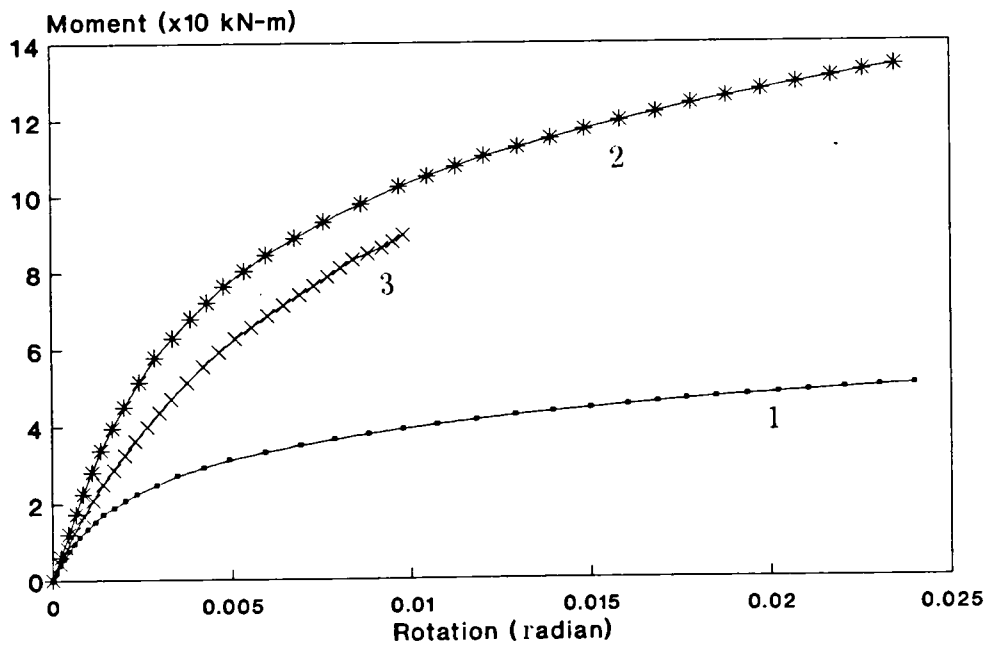


Figure 7.9 (b) Connection $M - \phi$ behaviour considered for the subassembly of figure 7.9(a).

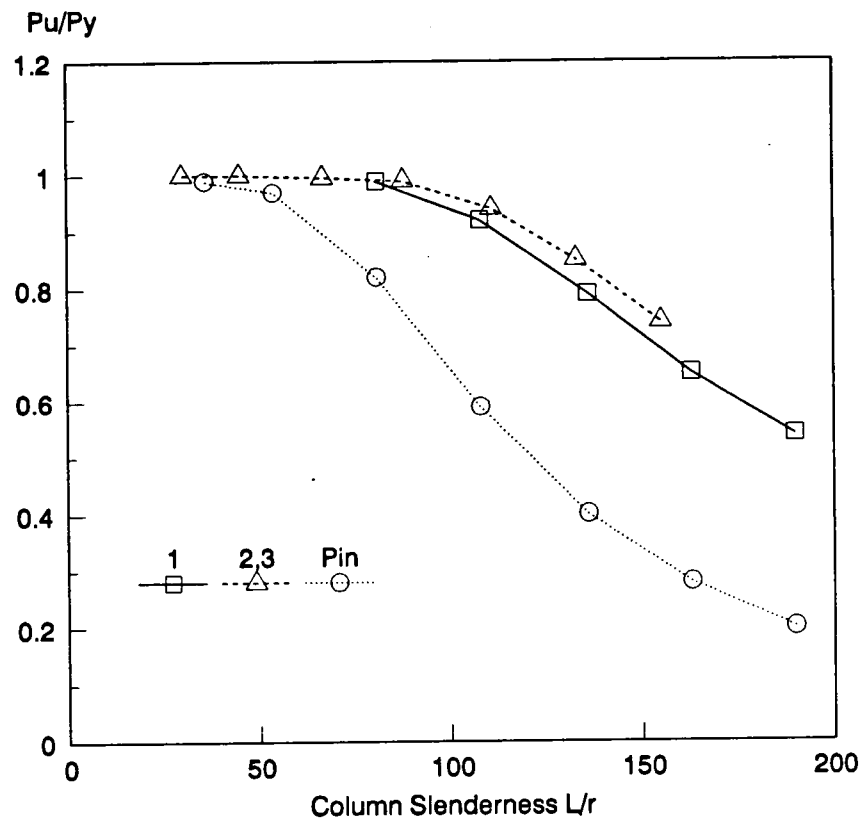


Figure 7.9 (c) Column strength curve for the different connections of figure 7.9(b).

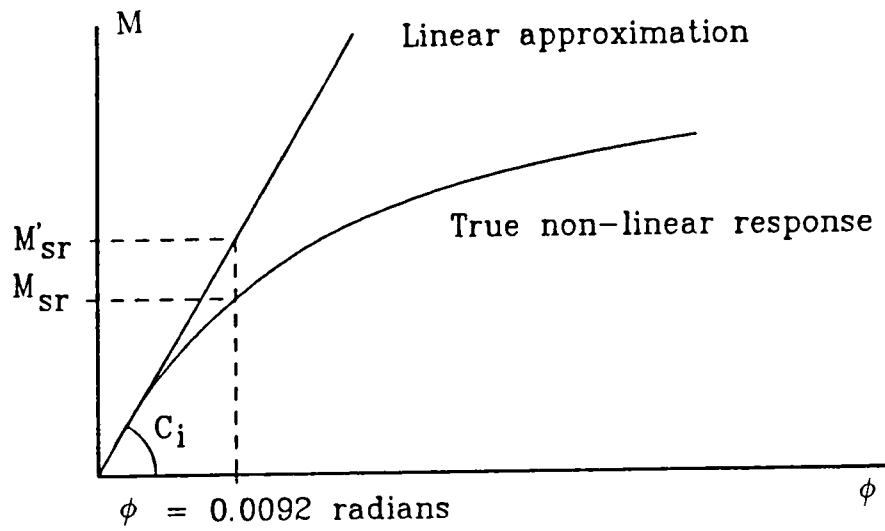


Figure 7.10 Observation of the semi-rigid moment for a given rotation when using the linear initial tangent stiffness.

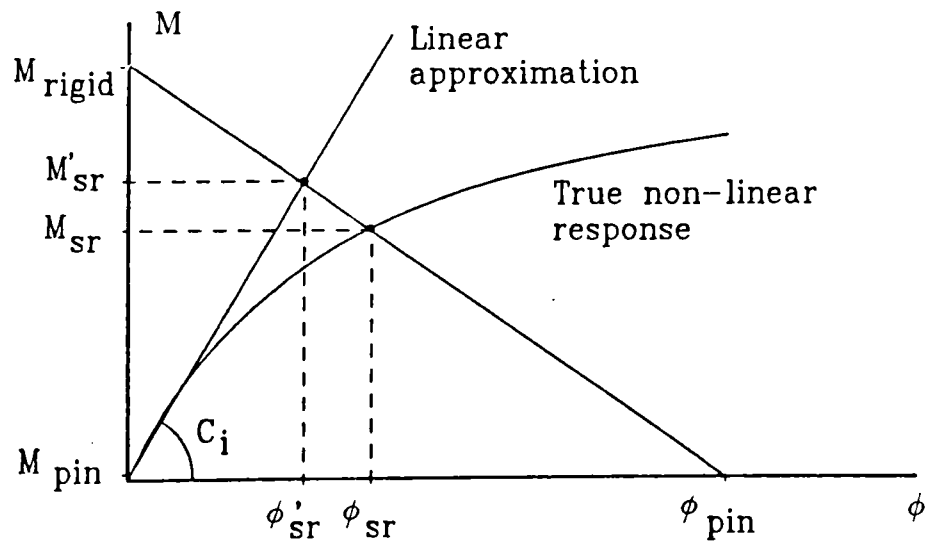


Figure 7.11 Variation of estimated response by a beam line approach for a nonlinear connection $M - \phi$ behaviour and the linear initial tangent stiffness approximation.

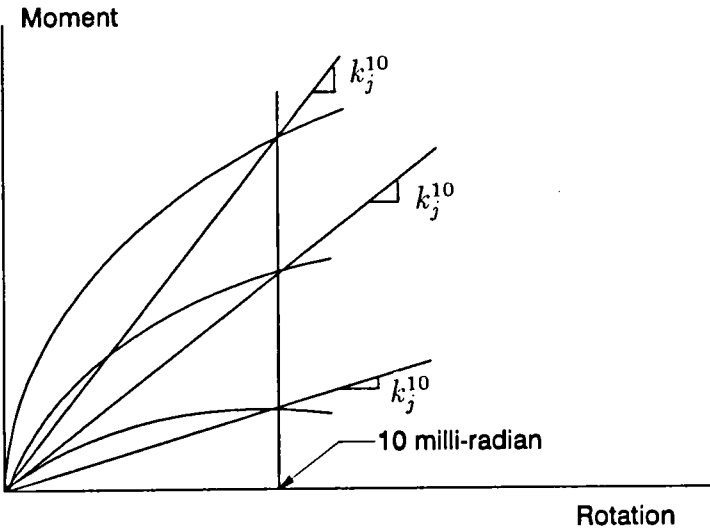


Figure 7.12 Secant stiffness based on fixed rotation level.

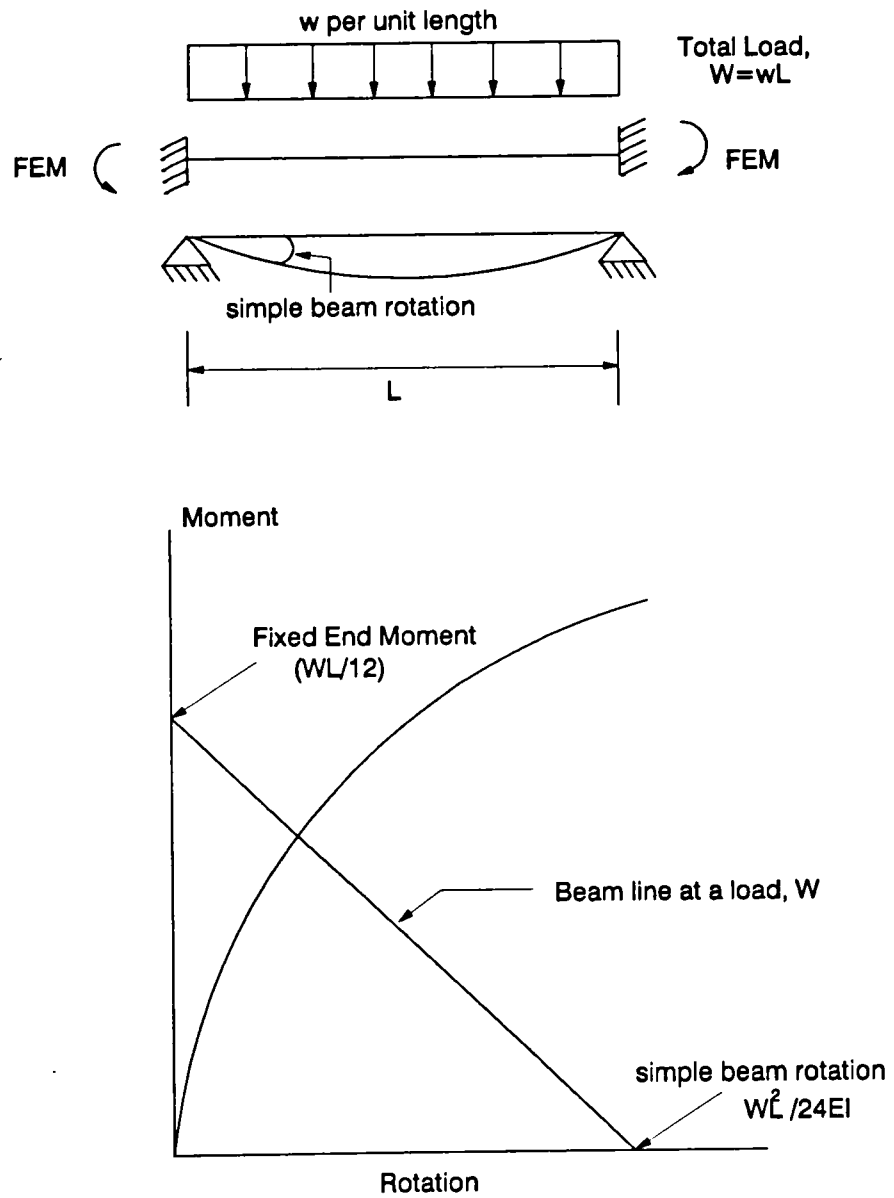


Figure 7.13 The beam line concept.

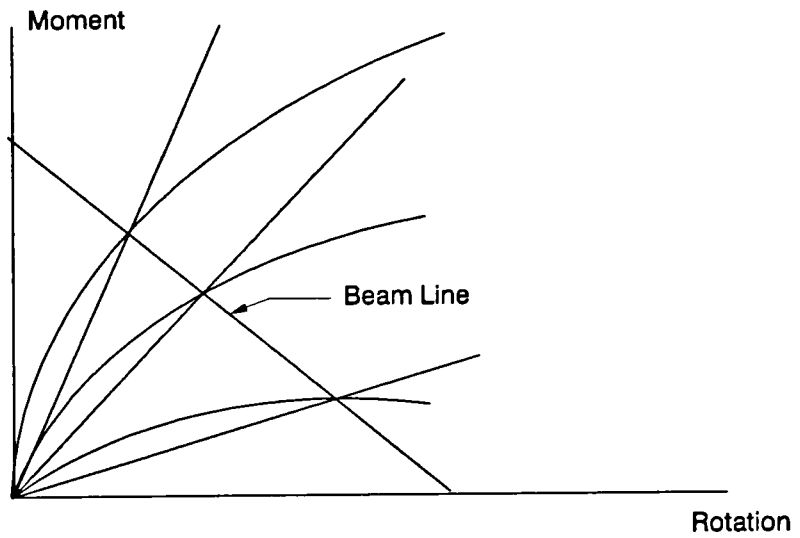


Figure 7.14 Secant stiffnesses based on beam-line.

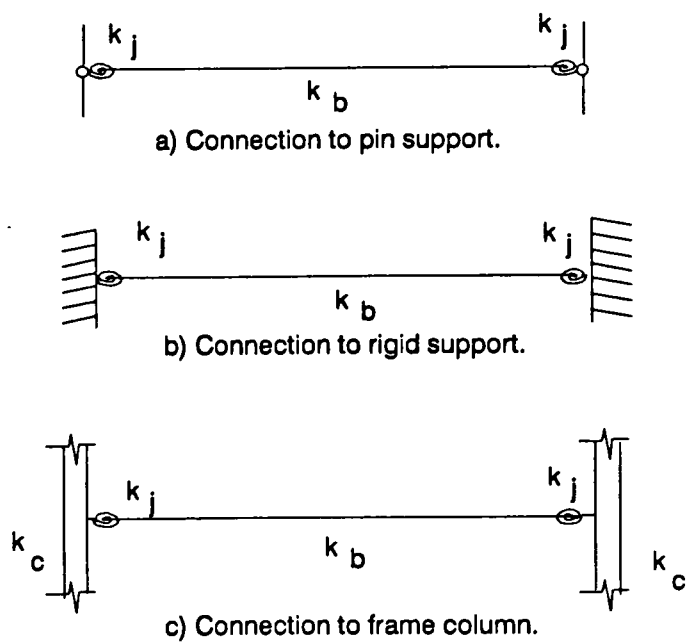


Figure 7.15 Semi-rigid connection to different support arrangements.

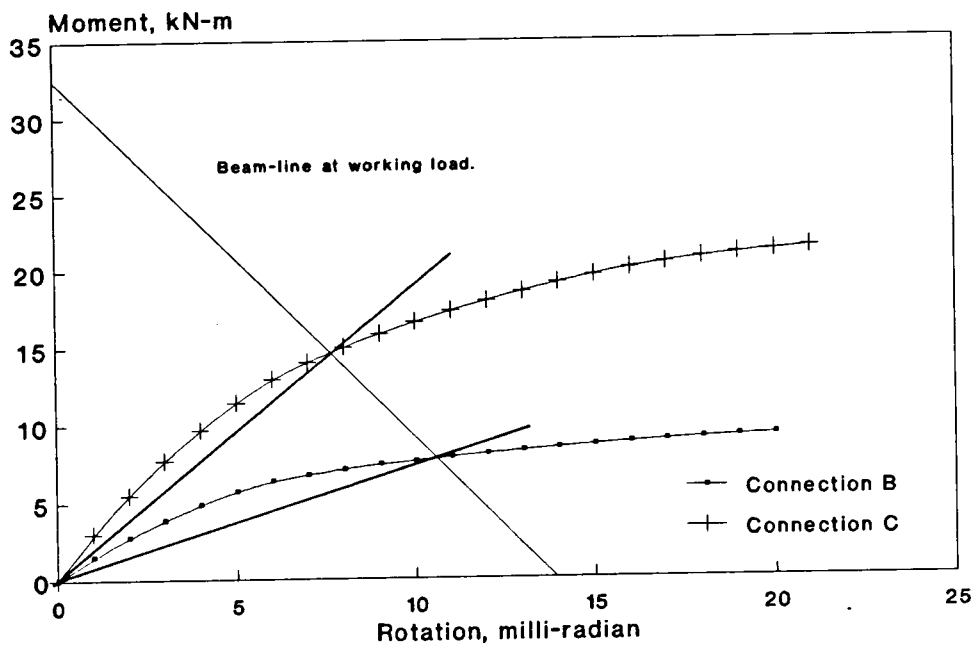
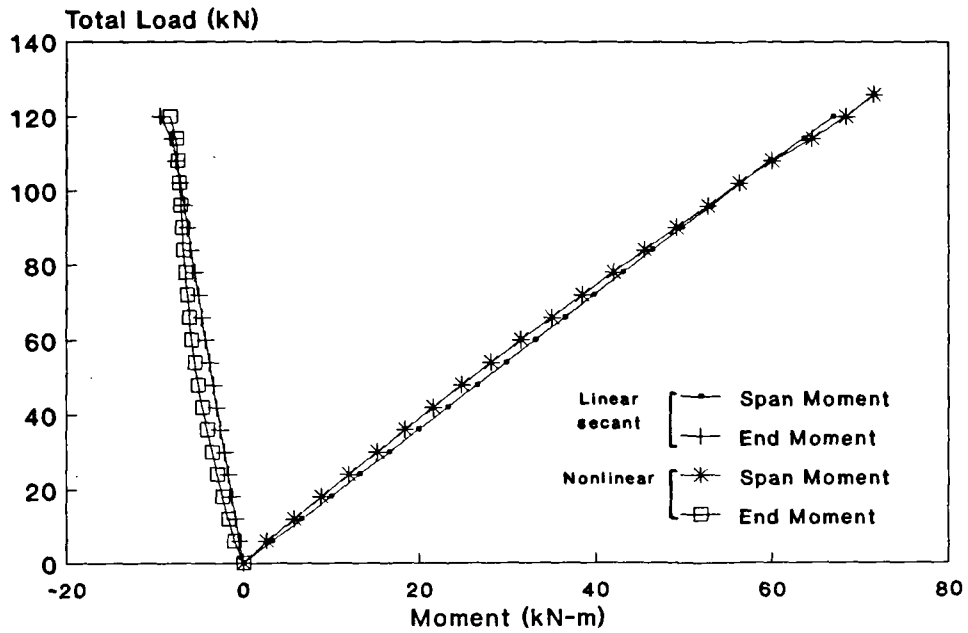
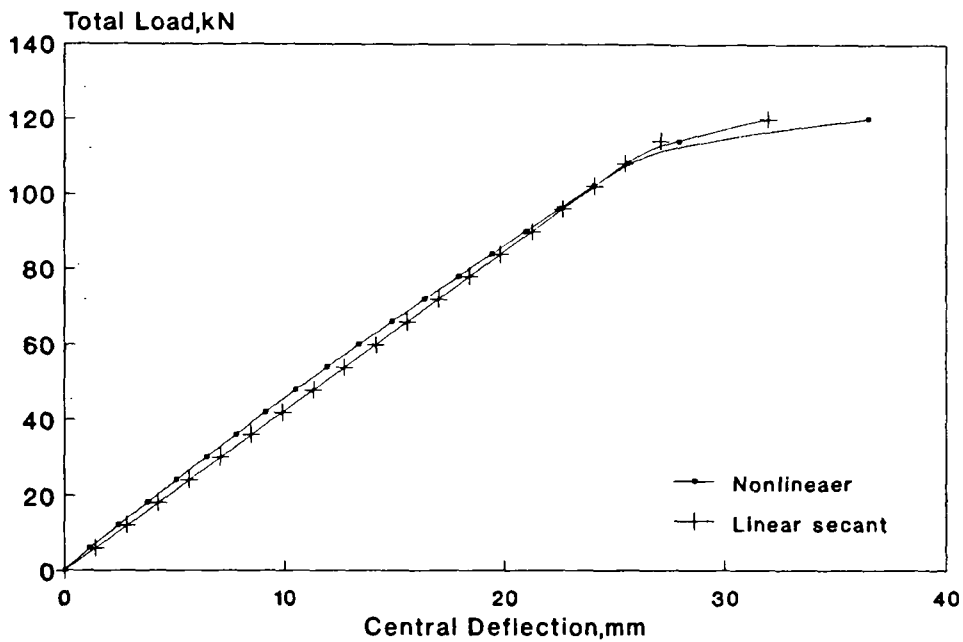


Figure 7.16 Secant stiffness representation of the connection 'B' and 'C' – based on beam line.

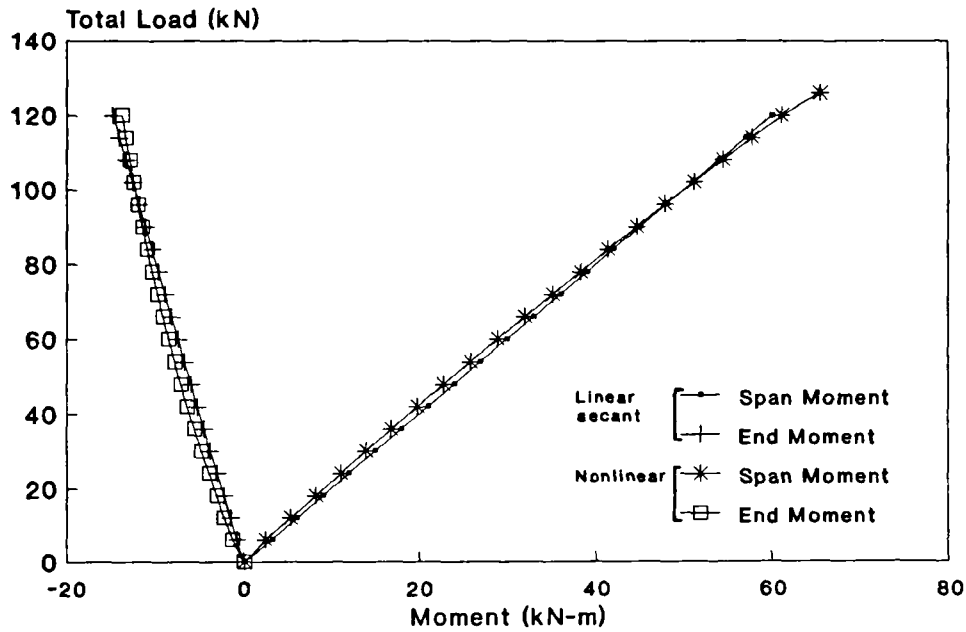


(a) Load-moment relationship.

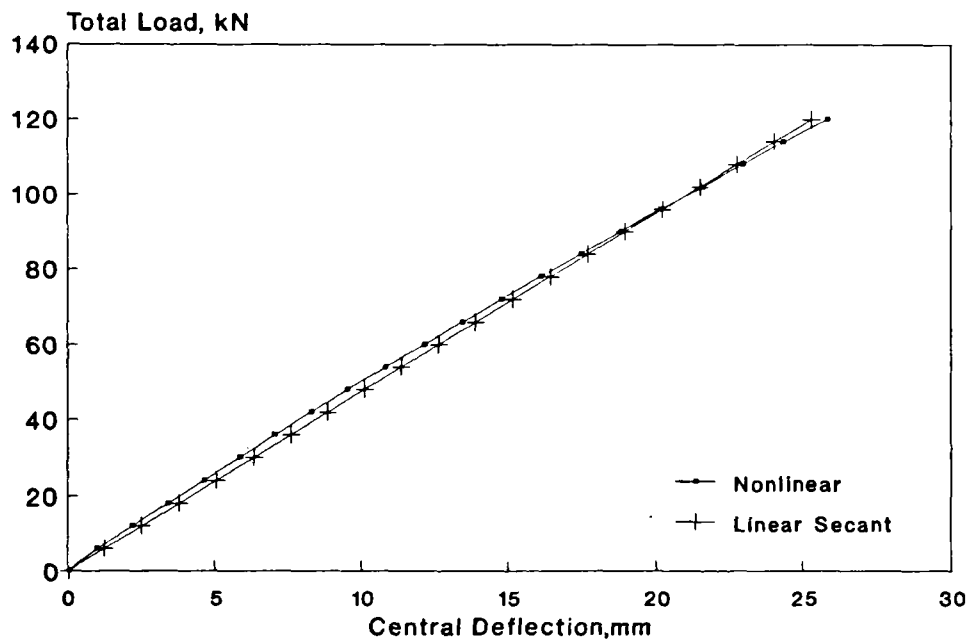


(b) Load-deflection relationship.

Figure 7.17 Effect of using a secant linear representation of the nonlinear connection behaviour for connection B of figure 7.16.



(a) Load-moment relationship.



(b) Load-deflection relationship.

Figure 7.18 Effect of using a secant linear representation of the nonlinear connection behaviour for connection C of figure 7.16.

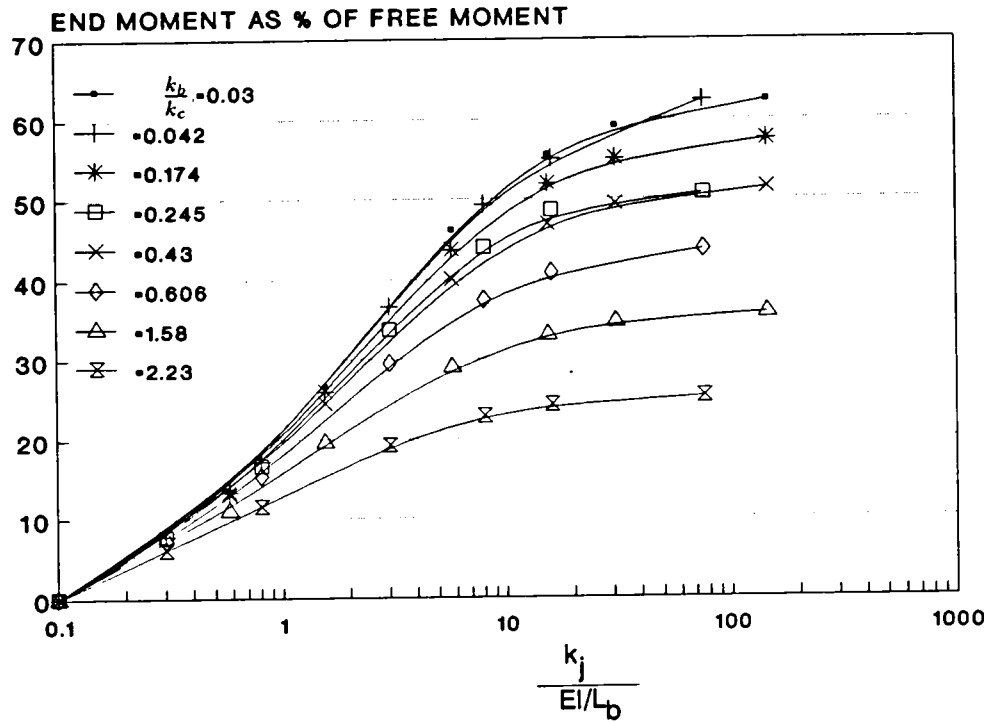


Figure 7.19 Effect of beam-column-connection stiffness on the effectiveness of semi-rigid behaviour.

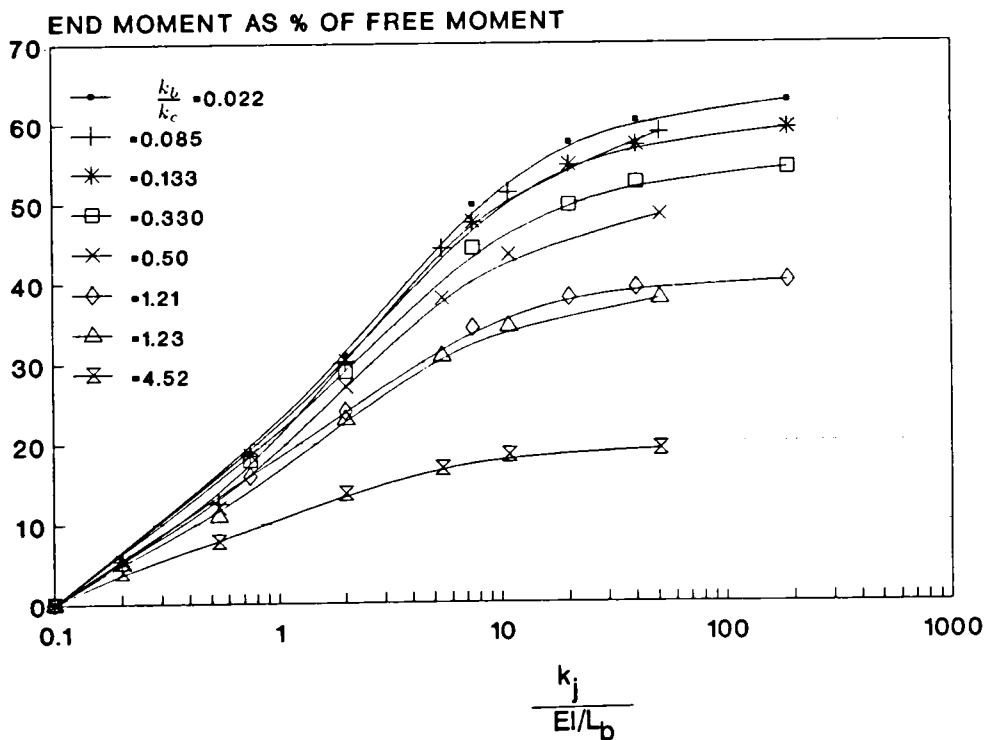


Figure 7.20 Effect of beam-column-connection stiffness on the effectiveness of semi-rigid behaviour.

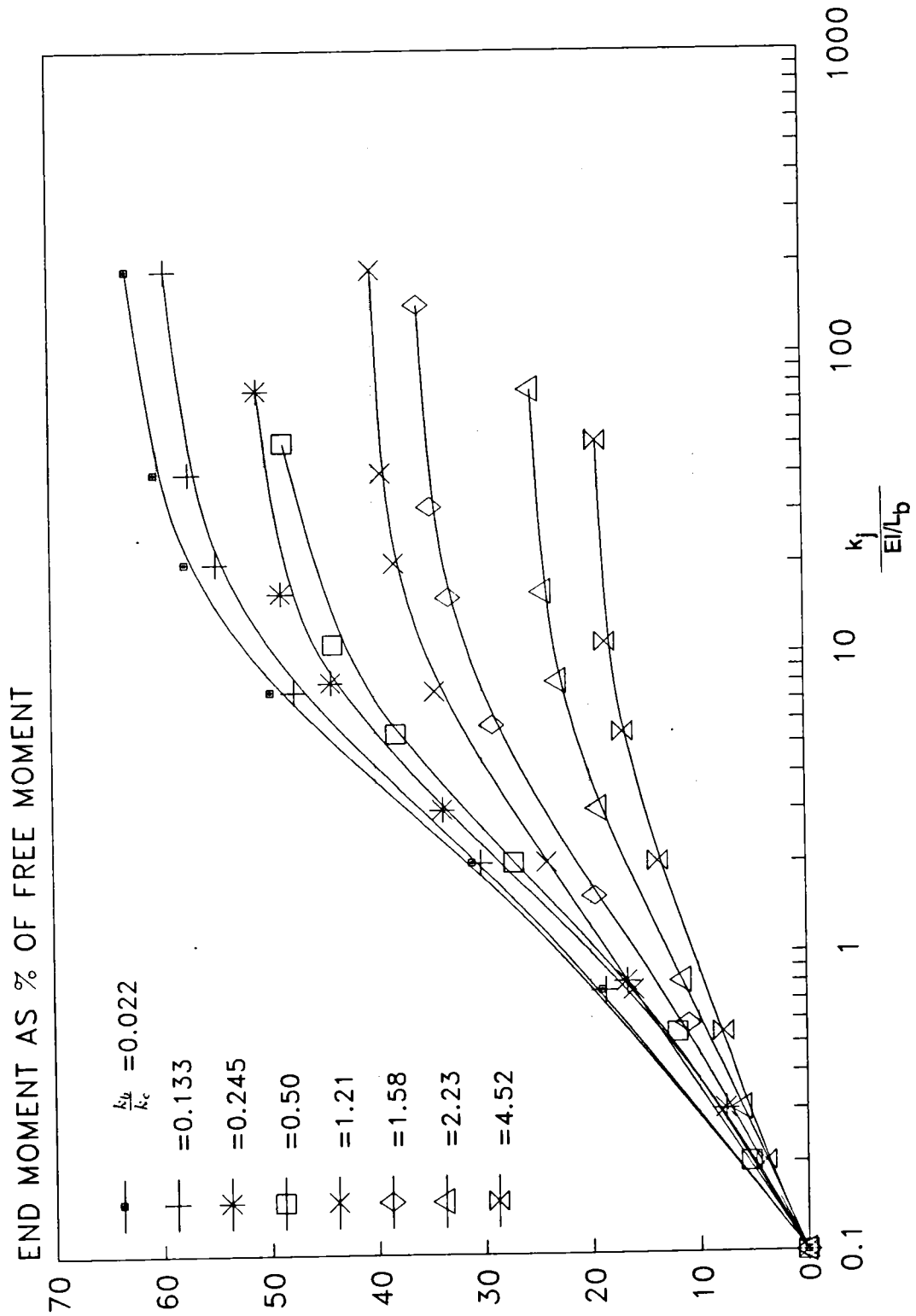
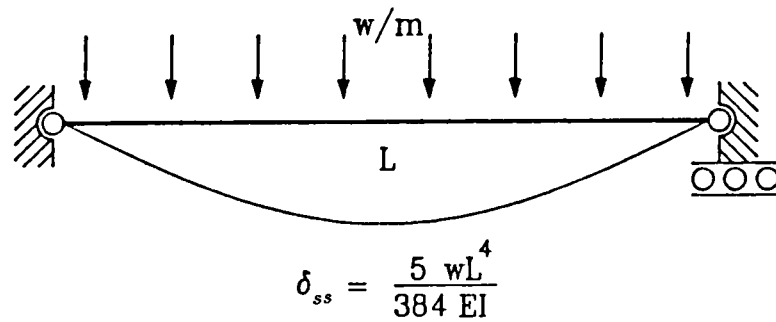
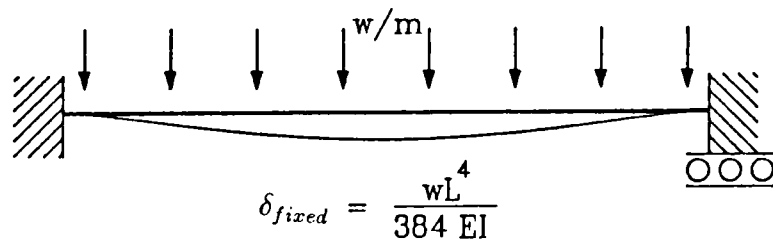


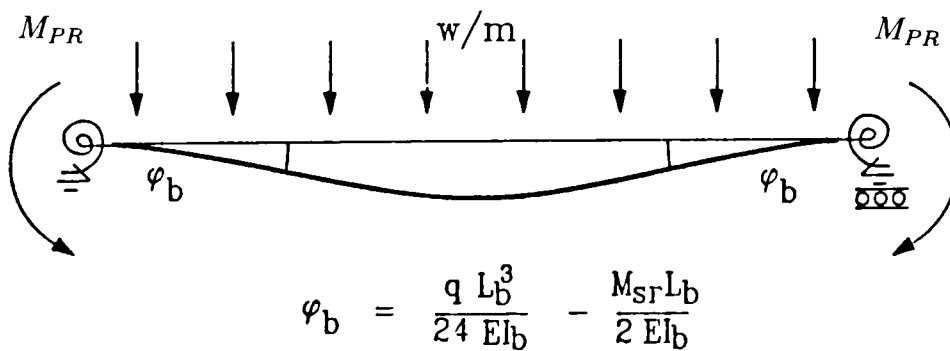
Figure 7.21 Effect of beam-column-connection stiffness on the effectiveness of semi-rigid behaviour.



(a) Simply supported beam



(b) Fixed supported beam



(c) Beam with semi-rigid ends

Figure 7.22 Beam deformation for different support conditions.

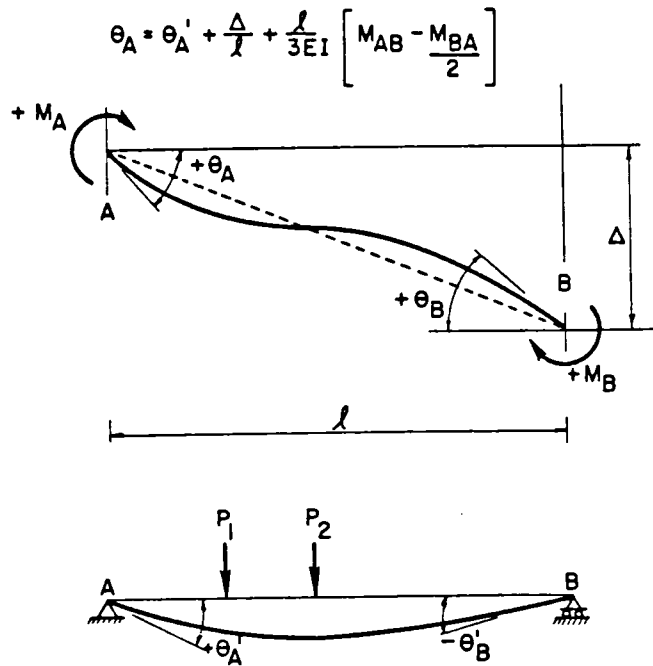


Figure 7.23(a) Nomenclatures for slope-deflection equation.

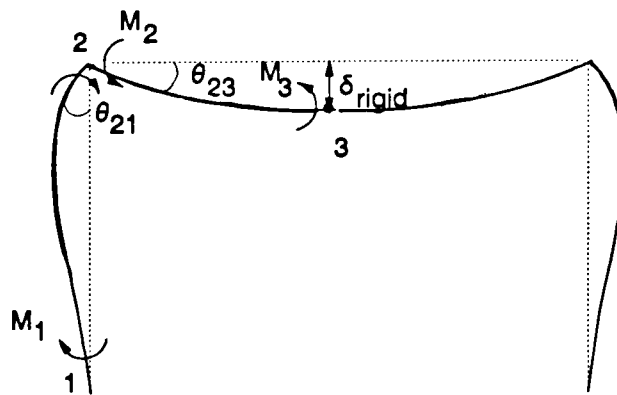


Figure 7.23(b) Rigid frame joint behaviour for the calculation δ_{rigid}

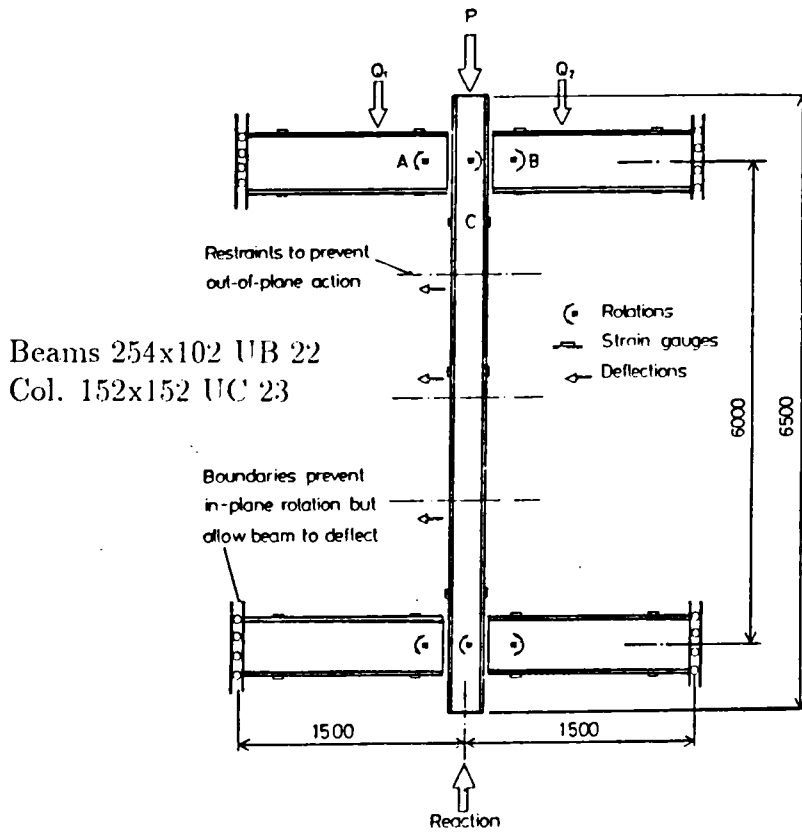


Figure 7.24 I-shaped subassembly tested by Davison [57].

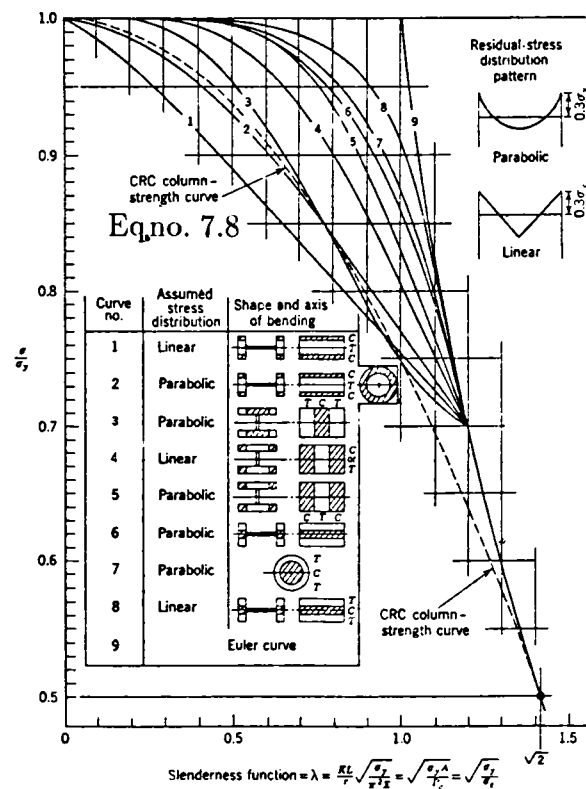


Figure 7.25 CRC column strength curve [93].

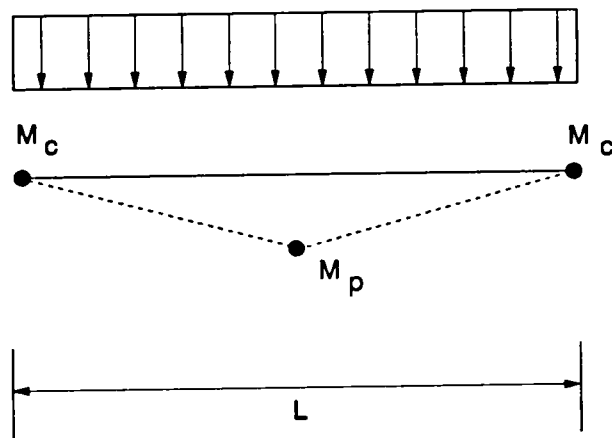


Figure 7.26 Beam mechanism for semi-rigidly connected beam.

Chapter 8

Conclusions and Recommendations

This thesis has reported the development and validation of a computer program and its subsequent use for the behavioural studies of semi-rigidly connected steel frames. Based on a tangent stiffness formulation, this finite element program includes the secondary effects of initial stresses, initial strains and also includes nonlinear connection behaviour in both monotonic and cyclic load situations. The behavioural study of a number of frames has been conducted and the general behavioural patterns for non-sway frames have been identified. Simplified methods for the estimation of design forces in semi-rigid frame have been proposed. Although the computer program developed here has been validated against experimental evidences in both non-sway and sway cases, this present work is mainly limited to non-sway cases. More extensive studies are needed for the development of design approaches for sway cases as well. It is believed that a computer program such as the present one can be utilised for such studies.

This chapter presents a concise itemised summary of the significant conclusions from the present study. Some aspects of relevant future research are also identified here.

8.1 Summary of Conclusions

An existing formulation for a semi-rigid beam-column element has been successfully implemented for a full two dimensional frame analysis. Since the formulation does not treat the semi-rigid joint as a separate element, rather a modified stiffness of normal beam-column element is used to include the effect of semi-rigidity, it gives considerable advantage in reducing the number of unknown variables leading to savings in CPU time. The gradual spread of yield over the cross section is taken into account by dividing the cross-section into sub-elements and, within the limitations of simple beam theory, any elastic-plastic constitutive relationship including the effect of strain-hardening can be assigned. The effect of axial force and the initial geometry are included by means of the $[K_G]$ and $[K_L]$ matrices. A cubic B-spline representation of the connection $M-\phi$ behaviour is used in the analysis. A trilinearized $M-\phi$ characteristic is used to model the connection response under cyclic loading history. The joint-offset, which is an important aspect of the analysis of semi-rigid frames with columns in major axis bending is also included. Material and geometrical imperfections can both be handled by the present program.

Comparison with the available analytical and experimental results have shown that the performance of the present program is quite satisfactory in predicting the load-deflection response as well as the failure load.

The verification of the predicted response in the sway mode, as presented in chapter 5, serves two purposes – firstly it facilitates its intended purpose of verifying the computer program under complicated cyclic loading history and secondly it highlights several important aspects of semi-rigid frame behaviour associated with this particular loading type. These are summarized here:

1. The cyclic response of a semi-rigid frame is adequately modelled by a set of trilinearized connection parameters obtained from a monotonic $M-\phi$ characteristic of the connection behaviour.
2. Symmetric cyclic loading produces symmetric loops of load-deflection response and, because the nonlinear connection behaviour has been represented by a multilinear relationship, the predicted response follows a distinct linear range but still predicts deflections close to the actual ones.
3. For the range of frames and connections considered in chapter 5, it was observed that, within the allowable sway deflection limit of $h/300$, representation of the connection by a linear stiffness would produce satisfactory results for most practical purposes.
4. Repeated cycles of loads were found to be very stable with the semi-rigid frames. Despite loading level high enough to produce deflections many times the allowable limit, incremental deflections were virtually non-existent.

However, these conclusions are based solely on the frames considered in this study, any generalization of these conclusions must await a similar study on relatively slender frames.

A limited parametric study has been conducted on non-sway semi-rigid frames. The influence of frame geometry, various loading types, connection stiffnesses, and imperfection sensitivity on the performance of semi-rigid frames has been studied. Relevant conclusions are drawn at the end of chapter 6, only the most significant conclusions are mentioned here.

1. Semi-rigid frames are not susceptible to significant loss of strength due to the presence of imperfections and the presence of both geometric and material imperfections together is not synergistic.
2. The exact sequence of the application of beam load and the column load, in general, does not appear to have any significant influence on the load carrying capacity of the semi-rigid frames.
3. The codified concept of using a fixed eccentricity for the beam end shear to estimate the columns end moment could, in some cases, result in a gross underestimation of the column moment which is dependent on the stiffnesses of the beam, the column and the connections.
4. For non-sway frames, the upper-bound of connection rotation at or near failure can be taken as 12 milli radian for most frames of reasonable practical dimensions. However, for some stiffer connections failure rotations less than 5 milli radian have been observed.
5. The phenomenon of moment shedding in columns occurs as a result of loss of stiffness of a column by plastification or due to the application of column load after a certain level of beam loadings. However, it was found that this need not be a design consideration since the rate of decrease in moment in framed columns was found to be very insignificant.

As already mentioned, the main goal of this research work was to develop simplified design methods for semi-rigid frames. The main bottlenecks to the development of such methods have been discussed in chapter 7 and some simplified approaches to address the problem have been proposed for the design of non-sway semi-rigid frames. To this end the major conclusions are summarised below:

1. The available connection $M-\phi$ test data cover only a narrow range of the beam and column sizes used in practice.
2. The range of variation in the connection performances that is likely to occur in replicated connections has, from a practical viewpoint, inconsequential effect on the actual behaviour of the structure.
3. A lower bound linear representation of the connection stiffness, by means of a secant stiffness based on the beam line approach was found to predict a satisfactory structural response when compared to those produced by the true nonlinear connection behaviour at working load.
4. Any attempt of classifying the joint as rigid, semi-rigid or pin, must take the consideration of the column, the beam and the connection stiffnesses together.
5. A set of non-dimensionalized curves have been prepared which would facilitate estimation of beam end-moments in non-sway semi-rigid beams under uniformly distributed load.
6. Based on the behavioural studies of chapter 6, a formula originally suggested by McCormic [115] has been generalized by the author for use in determining the elastic force distribution around a non-sway semi-rigid frame.

A method of estimating elastic deflection of semi-rigidly connected beams has also been proposed. Illustrative examples are shown and results compared with those obtained from rigorous analysis. Generally satisfactory agreements were found.

7. It has been shown in chapter 6 that the actual disturbing moments in the columns does not correspond with that assumed in the so called 'simple' design approach of the British code in which it is assumed that the beam end shear acts at the centre of stiff bearing subject to a minimum of 100 mm from the column face. It was found that the disturbing moment at the column in the elastic range, can be simply taken as the sum of the beam end moment and the moment produced by beam end reaction acting at the column face.
8. An existing method of determining the column capacity by the effective length approach has been employed using the secant representation of the semi-rigid connection behaviour. A number of cases have been considered by both the AISC G-factor approach and by the BS5950 effective length chart. It was found that the secant representation provided a dependable prediction of the column capacity when compared with several full scale test results.

8.2 Recommendations for Future Work

The main-emphasis in this research project was to develop a well validated research tool. The capabilities developed and the degree of correlation which has been established demonstrates its usefulness as a powerful analytical tool. To-

wards the main objective of developing a thorough design approach for semi-rigid frames some proposals have been put forward, although further studies are required to bridge the gaps in available information and to raise the confidence in using the semi-rigid design concept by the practising engineers. A number of aspects which deserve further research have been highlighted throughout this thesis; those together with a possible future extension of the present work are summarised in this section.

During the verification stages of this work it was felt that test programs intended to provide data for verifying analytical methods should be designed to correspond^{to} the analytical model as closely as possible – keeping in mind the limitations of modelling every single detail of test conditions. It must be noted that modelling of an arbitrary frame is extraordinarily difficult. Proper documentation of the test conditions is equally important as the reporting of the results.

The conclusions drawn in this thesis regarding the behaviour of semi-rigid frames under cyclic load needs to be generalised by studying the similar effects on relatively slender frames. It is also worth noting that the adopted connection model assumption of elastic unloading up to a length of twice the proportional limit moment showed some discrepancy with the test response and it appears that this, in fact, depends on the location of the point of load reversal. Further studies are needed to clarify this behaviour and then the connection model can be improved.

The connection behaviour in terms of $M-\phi$ response for a broad realistic range is lacking. Researchers intending to carry out test schemes should address this aspect while designing their experimental programme. To aid the elimination of this gap avoiding expensive experimental studies – attempts should be made to

the development of a mathematical tool to predict $M-\phi$ behaviour of apparently similar connections but connected to different beam to column sizes.

The non-dimensionalised design charts as presented in chapter 7 (figure 7.21) can be further improved by replacing the multiple curves by a single curve by choosing a suitable function involving k_b , k_c and k_j in the abscissa (see figure 8.1). An extensive parametric study on other aspects of semi-rigid design needs to be carried out using the present program which will facilitate development of thoroughly validated design approaches.

One possible extension of the present computer program is to develop the formulation for 3-D response of semi-rigid frames. With the achievement of the present level of validation this seems to be a very encouraging prospect. However, the availability of relevant $M-\phi$ characteristics will be an important consideration in this respect.

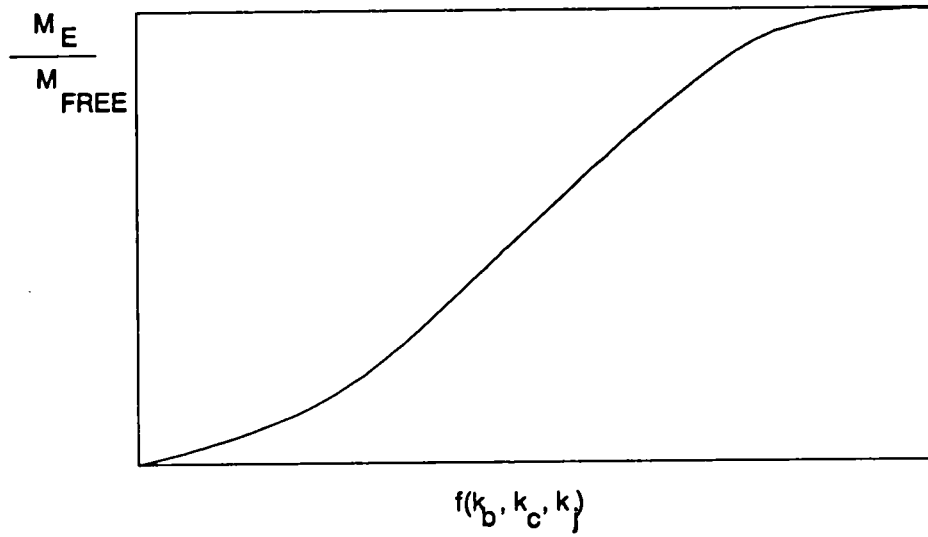


Figure 8.1 Design chart format for semi-rigid beams.

References

- [1] British Standard Institute, BS 5950; Part I : Structural Use of Steelwork in Buildings, London, 1985.
- [2] American Institute of Steel Construction, Manual of Steel Construction, 8th edition, 1980.
- [3] Bjorhovde,R., 'Effect of End Restraint on Column Strength — Practical Applications', Engineering Journal, AISC, Vol.21, No.1, 1984, pp. 1-13.
- [4] Jones,S.W., Kirby,P.A. and Nethercot,D.A., 'Effect of Semi-Rigid Connection on Steel Column Strength', Journal of Constructional Steel Research, Vol. 1, No.1, Sept. 1980, pp.38-46.
- [5] Lewitt,C.W., Chesson,E. and Munse,W.H., 'Restraint Characteristics of Flexible Riveted and Bolted Beam-to-Column Connections', University of Illinois Engineering Experiment Station Bulletin No. 500, Urbana, Ill., Jan. 1969.
- [6] Steel Structure Research Committee, Second Report, Department of Scientific and Industrial Research, HMSO, London, 1934

- [7] Maxwell,S.M., Howlett,J.H., Jenkins,W.M. and Bose, B., 'A Realistic Approach to the Performance and Applications of Semi-Rigid Joints in Steel Structures', *Joints in Structural Steelwork*, edited by Howlett, J.H., Jenkins,W.H., Stainsby,R.,London, Pentech Press, 1981, pp.2.71-2.98.
- [8] Nethercot,D.A., Davison, J.B. and Kirby, P.A., 'Connection Flexibility and Beam Design in Non-sway Frames', *Engineering Journal, AISC*, Vol. 25, No.3, 1988, pp.99-108.
- [9] Roberts, E.H., 'Semi-Rigid Design using Variable Stiffness Method of Column Design', *Joints in Structural Steelwork*, edited by Howlett,J.H.,Jenkins,W.M. and Stainsy,R., London, Pentech Press, 1981, pp.5.36-5.49.
- [10] Wilson, W.M. and Moore, H.F., 'Tests to Determine the Rigidity of Riveted Joints in Steel Structures', *University of Illinois, Engineering Experiment Station Bulletin No. 104, Urbana,Ill.,1917.*
- [11] Jones, S.W., 'Semi-Rigid Connections and their Influence on Steel Column Behaviour', *Ph.D. Thesis, University of Sheffield, 1980.*
- [12] Rifai, A.M., 'Behaviour of Columns in Sub-Frames with Semi-Rigid Joints', *Ph.D. Thesis, University of Sheffield, 1987.*
- [13] Poggi,C. and Corradi,L.,'A Finite Element Model for the Analysis of Flexibly Connected Steel Frames.' *International Journal of Numerical Methods in Engineering*. Vol.260, 1988, pp.2239-2254.
- [14] Nethercot, D.A., 'Joint Action and the Design of Steel Frames', *The Structural Engineer*, Vol. 63 A, No.12, 1985, pp. 371-379.

- [15] Nethercot, D.A. and Chen, W.F., 'Effects of Connections on Column', Steel Beam-to-Column Connections—Special Issue, Journal of Constructional Steel Research, 1988.
- [16] Nethercot, D.A., and Zandonini, R., 'Methods of Prediction of Joint Behaviour: Beam to Column Connections', Structural Connections: Stability and Strength, ed. by Narayanan, R., Elsevier Applied Science, London, 1989, pp. 23-62.
- [17] Johnston, B. and Mount, E.H., 'Analysis of Building Frames with Semi-Rigid Connections', Trans., ASCE, Vol. 107, 1942, pp.993-1019.
- [18] Ackroyd, M.H., 'Nonlinear Inelastic Stability of Flexibly-Connected Plane Steel Frames', Ph.D. Thesis, Department of Civil, Environmental and Architectural Engineering, University of Colorado, Boulder, Co, USA, 1979.
- [19] Goverdhan, A.V., 'A Collection of Experimental Moment-Rotation Curves and Evaluation of Prediction equations for Semi-Rigid Connections', M. S. Thesis, Vanderbilt University, Nashville, TN, USA, Dec.1983.
- [20] Lui, E.M., 'Effect of Connection Flexibility and Panel Zone Deformation on the Behaviour of Plane Steel Frames', Ph.D. Thesis, School of Civil Engineering, Purdue University, West Lafayette, Indiana, May 1985.
- [21] Shukla, S., 'Static Response of Plane Steel frames with Nonlinear Semi-Rigid Connections', M. S. Thesis, Vanderbilt University, Nashville, TN, USA, August 1986.
- [22] Cosenza, E., De Luca, A. and Faella, C., 'Nonlinear Behaviour of Framed Structures with Semi-Rigid Joints' *Costruzioni Metalliche*, No.4, 1984, pp. 199-211.

- [23] Lee, S.L., 'Large Deformation Elastic-Plastic Stability Analysis of Plane Frames with Partially Restrained Connections', M.S. Thesis, Vanderbilt University, Nashville, TN, USA, Dec. 1987.
- [24] Allen, H.G. and Bulson, D.S., *Background to Buckling*, McGraw-Hill, New York, 1980, pp.269-272.
- [25] Monforton, G.R. and Wu, T.S., 'Matrix Analysis of Semi-Rigid Connected Frames', *J. Struct. Div. ASCE*, Vol. 89, ST6, Dec. 1963, pp. 13-41.
- [26] Wang, C.K., *Intermediate Structural Analysis*, McGraw-Hill, New York, 1983.
- [27] Anderson, D. and Lok, T.S., 'Elastic Analysis of Semi-Rigid Steel Frames', Research Report No. CE/17; University of Warwick, January 1985.
- [28] Chen, W.F., and Lui, E.M., 'Effect of Joint Flexibility on the Behaviour of Steel Frames', Report No. CE-STR-85-22, School of Civil Engineering, Purdue University, West Lafayette, Indiana, 1985.
- [29] Poggi, C. and Zandonini, R., 'Behaviour and Strength of Steel Frames with Semi-Rigid Connections', Session on Connection Flexibility and Steel Frames, ASCE Convention, Detroit, Oct. 1985.
- [30] Corradi, L., and Poggi, C., 'An Analysis Procedure for Nonlinear Elastic Plastic Frames Accounting for the Spread of Local Plasticity', *Costruzioni Metalliche*, 1, pp. 1-14, 1985.
- [31] Galambos, T.V., *Structural Members and Frames*. Prentice-Hall, New York, 1968.

- [32] Davison, J.B., 'Strength of Beam-column in Flexibly Connected Steel Frames', Ph.D. Thesis , University of Sheffield, 1987.
- [33] Anderson, D. and Benterkia, Z., 'Analysis of Semi-Rigid Steel Frames and Criteria for their Design', J. of Constructional Steel Research, Vol. 18, No. 3, 1991, pp 227-237.
- [34] Majid, K.I. and Anderson, D., 'The Computer Analysis of Large Multi-Storey Framed Structures', The Structural Engineer, Vol. 46, 1968, pp.357-365.
- [35] Ackroyd, M.H. and Gerstle, K.H., 'Strength of Flexibly-Connected Steel Frames', Engineering Structures, Vol. 5, 1983, pp. 31-37.
- [36] Gerstle, K.H., 'Effect of Connections on Frames', Journal of Constructional Steel Research, Vol. 10, 1988, pp.241-267.
- [37] Shen, Z.Y. and Lu, L.W., 'Analysis of Initially Crooked End Restrained Steel Columns', Journal of Constructional Steel Research, Vol. 3, No.1, 1983, pp.10-18.
- [38] Sugimoto, H. and Chen, W.F., 'Small End Restraint Effect on Strength of H-Columns', Journal of Structural Division, ASCE, Vol. 108, pt-1, March 1982, pp. 661-681.
- [39] Berguist, D.J., 'Tests on Column Restrained by Beams with Simple Connections', Report No. 1, American Iron and Steel Institute project No. 189, Dept. of Civil Engineering, The University of Texas, Austin, Texas, Jan. 1977.

- [40] Jones, S.W., Kirby, P.A. and Nethercot, D.A., 'Columns with Semi-Rigid Joints', *Journal of Structural Division, ASCE*, Vol. No.108, No-ST 2, Feb. 1982, pp. 361-372.
- [41] Grestle, K.H., 'Flexibly Connected Steel Frames', *Steel Framed Structures: Stability and Strength*, edited by Narayanan, R., Elsevier Applied Science Publishers, 1985, pp.205-239.
- [42] Davison, J.B., Zandonini, R., Nethercot, D.A. and Poggi, C., 'Analytical and Experimental Studies of Semi-Rigidly Connected Braced Steel Frames', *Structural Steel Research Council Annual Technical Session, Minneapolis*, 1988.
- [43] Davison, J.B., Kirby, P.A. and Nethercot, D.A., 'Semi-Rigid Connections in Isolation and in Frame', *State-of-the Art Workshop on Connections, Strength and Design of Steel Structures, Cachan, France, May 1987*, pp.195-202.
- [44] Davison, J.B., Kirby, P.A. and Nethercot, D.A., 'Rotational Stiffness Characteristics of Steel Beam-to-Column Connections', *Journal of the Constructional Steel Research*, Vol. 8, 1987, pp.17-54.
- [45] Kirby, P.A., Davison, J.B. and Nethercot, D.A., 'Large Scale Tests on Column Subassemblages and Frames', *State-of-the Art Workshop on Connections, Strength and Design of Steel Structures, Cachan, France, May 1987*, pp.291-299.
- [46] Jones, S.W., Kirby, P.A. and Nethercot, D.A., 'Effect of Semi-Rigid Connection on Steel Column Strength', *Journal of Constructional Steel Research*, Vol. 1, No.1, Sept. 1980, pp.38-36.

- [47] Ackroyd, M.H., Bjorhovde, R., "Discussions on 'Effects of Semi-Rigid Connections on Steel Column Strength' by Jones, S.W., Kirby, P.A., and Nethercot, D.A.", *Journal of Constructional Steel Research*, Vol. 1, No.3, May 1981, pp.48-51.
- [48] Razzaq, Z. and Chang, J.G., 'Partially Restrained Imperfect Columns', *Proc. Conference on Joints in Structural Steelwork*, Pentech Press Ltd., Teesside, England, April, 1981.
- [49] Vinnakotta, S., 'Planar Strength of Restrained Beam-Columns', *Journal of Structural Divison, Proc. ASCE*, Vol. 108, No.ST 11, Nov. 1982, pp.2496-2516.
- [50] Simitises, G.J. and Vlahinos, S.A., 'Stability Analysis of a Semi-Rigidly Connected Simple Frame', *Journal of Constructional Steel Research*, Vol. 2, No.3, Sept. 1982, pp.29-32.
- [51] Anderson, D., Bijlaard, F., Nethercot, D.A., and Zandonini, R., 'Analysis and Design of Steel Frames with Semi-Rigid Connections', *IABSE Surverys S-39/87*, 1987.
- [52] Ackroyd, M.H., and Gerstle, K.H., 'Behaviour of Type 2 Steel Frames', *J. Structural Div., ASCE*, Vol. 108, No. 7, 1982, pp. 1541-1556.
- [53] Wood, R.H., 'Effective Lengths of Columns in Multistorey Buildings', *The Structural Engineer*, Vol. 52, No. 7, July 1974, pp.235-244.
- [54] Baker, J.F., 'A Note on the Effective Length of a Piller Forming Part of a Continuous Member in a Building Frame', 2nd Report, *Steel Structures Research Committee, DSIR, HMSO*, 1934, pp. 200-318.

- [55] Taylor, J.C., 'Semi-Rigid Beam Connections: Effects on Column Design : B/20 Code Method', *Joints in Structural Steelwork*, edited by Howlett, J.H., Jenkins, W.M., and Stainsby, R., London, Pentech Press, 1981, pp 5.50-5.57.
- [56] Chapuis, J. and Galambos, T.V., 'Restrained Crooked Aluminium Columns', *Journal of Structural Divison, ASCE*, Vol. 108, March 1982, pp. 511-524.
- [57] Davison, J.B., Kirby, P.A. and Nethercot, D.A., 'Column Behaviour in PR Construction: Experimental Behaviour', *Journal of Structural Divison, ASCE*, Vol. 113, No.9, August, 1986, pp.2032-2050.
- [58] Lui, E.M. and Chen, W.F., 'Strength of H-Columns with Small End Restraints', *The Structural Engineer*, Vol. 61 B, No.1, Mar.,1983, pp.17-26.
- [59] Galambos, T.V., "Discussion of 'Small End Restraint Effect on Strength of H-Columns' by Chen et al *Journal of Structural Divison, ASCE*, Vol. 108, PT-1, Mar,1982, pp.661-681," *Journal of Structural Divison,ASCE*,Vol. 109, No.ST 4 , Apr. 1982, pp. 1067-1977.
- [60] Johnston, B.G. ed. *SSRC Guide to Stability Design Criteria for Metal Structures*, 3rd ed, Wiley-Interscience, NY, 1976.
- [61] Yura, J.A., 'The Effective Length of Column in Unbraced Frames', *Engineering Journal, AISC*, Vol. 8, No.2, Chicago,Ill., Apr. 1971, pp. 37-42.
- [62] De Falco, F., and Marino, F.J., 'Column Stability in Type-2 Construction', *Engineering Journal, AISC*, Vol. 3, No.2, Apr., 1966, pp. 67-71.
- [63] Driscoll,G.C. , 'Effective Length of Columns with Semi-Rigid Connections', *Engineering Journal, AISC*,Vol. 13, No.4, 1976, pp.108-115.

- [64] Zienkiewicz, O.C., *The Finite Element Method*, McGraw-Hill, 3rd Edition, London, 1977.
- [65] Chen, W.F. and Atsuta, T., *Theory of Beam-Column, Volume 2: Space Behaviour and Design*, McGraw-Hill, NY, 1977.
- [66] Nethercot, D. A., 'Residual Stresses and Their Influences upon the Lateral Buckling of Rolled Steel Beams', *The Structural Engineer*, Vol. 52, No.3, March 1974, pp. 89-96.
- [67] Lee, S.L., and Basu, P.K., 'Secant Method for Nonlinear Semi-Rigid Frames', *Journal of Constructional Steel Research*, Vol. 14, No.4, 1989, pp. 273-299.
- [68] Chen, W.F. and Lui, E.M., *Structural Stability – Theory and Implementation*, Elsevier Science Publishing Co., Inc., N.Y.,1987.
- [69] Galambos, T.V. ed. *Guide to Stability Design Criteria for Metal Structures*, 4th ed, John Wiley & Sons publishers, N.Y.,1988.
- [70] Young, B.W., 'Residual Stress in Hot-Rolled Sections', Report CUED/C-Struct./TR.8, Dept. of Engineering, University of Cambridge, 1971.
- [71] Huber, A.W. and Beedle L.S., 'Residual Stress and Compressive Strength of Steel', *Welding Journal*, Vol. 33, 1954, Res. Sup., pp. 589-s
- [72] *European Recommendations for Steel Construction*, European Convention for Constructional Steelwork, Brussels,1978.
- [73] *Eurocode 3: Common Unified Code of Practice for Steel Structures*. Commission of the European Communities, Rapport EUR 8849, Brussels,1984.

- [74] Beaulieu, D., 'The Destabilizing Forces caused by Gravity Loads Acting on Initially Out-of-Plumb Members in Structures', Ph.D. Thesis, Department of Civil Engineering, University of Alberta, 1977.
- [75] Linder, J., 'Ungewollte Schiefstellungen Von Stahlstützen', IABSE 12th Congress, Vancouver, 1984.
- [76] Cosenza, E., De Luca, A. and Faella, C., 'Inelastic Buckling of Semi-Rigid Sway Frames', Structural Connections: Stability and Strength, ed. by Narayanan, R., Elsevier Applied Science, London, 1989, pp.297-333.
- [77] Moncarz, P.D., and Gerstle, K.H., 'Steel Frames with Nonlinear Connections', Journal of Structural Div., ASCE, Vol. 107, No. ST8, August, 1981, pp. 1427-1441.
- [78] Popov, E.P. and Pinkney, R.B., 'Cyclic Yield Reversal in Steel Building Connections', Jnl. of Structural Div., ASCE, Vol. 95, No. ST3, March 1969, pp. 327-353.
- [79] Marley, M.J., 'Analysis and Tests of Flexibly Connected Steel Frames', Report to AISI, University of Colorado, Boulder, USA, March, 1982.
- [80] Marley, M.J., 'Comparison of Analytical and Measured Flexibly Connected Frame Responses', M. S. Thesis, University of Colorado, Boulder, 1981.
- [81] Rao, S.S., The Finite Element Method in Engineering, Pergamon Press, Oxford, 1982.
- [82] Numerical and Algorithm Group Ltd., Fortran Library Manual, Volume 3, April, 1990.

- [83] Ahmed, I., 'Manual for the Semi-Rigid Analysis Program', Department of Civil & Structural Engineering, The University of Sheffield, under preparation.
- [84] Owen, D.R.J. and Hinton, E., *Finite Element in Plasticity: Theory and Practice*, Pineridge Press Limited, Swansea, U.K., 1980.
- [85] Tebedge, N. and Tall, L., 'Linear Stability Analysis of Beam-Columns', *Journal of the Structural Division, ASCE*, Vol. 99, No. ST12, Proc. paper 10232, December, 1973, pp. 2439-2457.
- [86] El-Zanaty, M., Murray, D.W., and Bjorhovde, R., 'Inelastic Behaviour of Multistorey Steel Frames', *Structural Engineering Report No. 83*, Department of Civil Engineering, University of Alberta, Canada, April, 1980.
- [87] Mugisa, D.R., 'An Assessment of Experimental Full-Scale Steel Frame Test Data', M.Sc. Thesis, Dept. of Civil & Structural Engineering, The University of Sheffield, Sept., 1988.
- [88] Gibbons, C., Nethercot, D.A. and Kirby, P.A., 'The Experimental Behaviour of Semi-Rigid Connections in Braced Steel Frames', *ASCE Structures Congress X, Connection for Metal Structures*, April, 13-15, 1992, San Antonio, Texas.
- [89] Stelmack, T.W., 'Analytical and Experimental Response of Flexibly Connected Steel Frames', M.S. Thesis, Department of Civil, Environmental, Architectural Engineering, The University of Colorado, Boulder, 1982.
- [90] Moncarz, P.D., 'Effects of Nonlinear Connection in Steel Frames', M.S. Thesis, University of Colorado, Boulder, 1976.

- [91] Wang, Y.C., 'Semi-Rigid Action in Steel Frame Structures: Databank of M- ϕ Test Results', ECCS Agreement No. 7210 SA/819, Department of Civil & Structural Engineering, University of Sheffield, 1990.
- [92] Beedle, L.S., and Tall, L., 'Basic Column Strength', Trans. ASCE, Vol. 127, Part II, 1962.
- [93] Johnston, B.G. edited The Column Research Council Guide to Design Criteria for Metal Compression Members, 2nd edition, John Wiley & Sons Inc. NY. 1966.
- [94] Ackroyd, M.H., 'Simplified Frame Design of Type PR Construction', AISC Engineering Journal, 4th Quater, 1987, pp.141-146.
- [95] Poggi, C., and Zandonini, R., 'A Finite Element for the Analysis of Semi-Rigid Frames', Connections in Steel Structures – Proceedings of the International Workshop 1987, ed. by Bjorhovde, R., Cachan, France; Elsevier Applied Science, London, 1988, pp.238-247.
- [96] Chen, W.F., 'Analysis of Steel Frames with Flexible Joints', Structural Connections: Stability and Strength, ed. by Narayanan, R., Elsevier Applied Science, London, 1989, pp. 335-444.
- [97] Rifai, A.M., Nethercot, D.A., and Kirby, P.A., 'Stability of Column Sub-assemblages with Semi-Rigid Connections', Stability of Steel Structures—Proceedings of the Regional Colloquium of Stability of Steel Structures 1986, ed. by Ivanyi, M., Vol-1, Tihany, Hungary, 1988. pp. 443-450.
- [98] Eurocode 3, Design of Steel Structures: Part 1, General Rules and Rules for Buildings, prepared for the Commission of the European Community, Edited Draft, Issue 3, April, 1990.

- [99] Jones, S.W., Kirby, P.A., and Nethercot, D.A., 'The Analysis of Frames with Semi-Rigid Connections – A State of the Art Report', *Journal of Constructional Steel Research*, Vol. 3, No.2, 1983. pp.2-13.
- [100] Kirby, P.A., Zandonini, R., and Davison, J.B., 'Experimental Determination of Moment Rotation Response of Semi-Rigid Beam-to-Column Joints', *Structural Steel Research Council Annual Technical Session*, Minneapolis, 1988.
- [101] Sommer, W.H., 'Behaviour of Welded header Plate Connections', M.S. Thesis, University of Toronto, Ontario, 1969.
- [102] Frye, M.J., and Morris, G.A., 'Analysis of Flexibly Connected Steel Frames', *Canadian Journal of Civil Engineers*, No.3, Sept., 1975, pp. 280-291.
- [103] Nethercot, D.A., 'Utilisation of Experimentally Obtained Connection Data in Assessing the Performance of Steel Frames', *Connection Flexibility and Steel Frames*, ed. by Chen., W.F., ASCE,1985.
- [104] Kishi, N., and Chen, W.F., 'Data Base on Steel Beam-to-Column Connections', CE-STR-86-26, School of Civil Engineering, Purdue University, Lafayette, Indiana, 1986.
- [105] SSRC, Task Group 25, 'Connection Bibliography', Third Draft, March, 1987.
- [106] Prescott, A.T., 'The Performance of End-Plate Connection in Steel Structure and their Influence on Overall Structural Behaviour', Ph.D. Thesis, Civil Engineering Division, Hatfield Polytechnic, July,1987.

- [107] Johnston, N.D., and Walpole, W.R., 'Bolted End-Plate Beam-to-Column Connections under Earthquake Type Loading', Research Report 81-7, Dept. of Civil Engineering, University of Canterbury. New Zealand, 1981.
- [108] Hechtmann, R.A., and Johnston, B.G., 'Riveted Semi-Rigid Beam-to-Column Building Connections', Progress Report No.1, AISC Research at Lehigh University, 1947.
- [109] Moore, D. B., 'Beam-to-Column Steelwork Connections – Trends in UK Practice', Building Research Establishment, Doc. No. BRE/86/2/3, July, 1990.
- [110] Stelmack, T.W., Marley, M.J., and Gerstle, K.H., 'Analysis and Tests of Flexibly Connected Steel Frames', Journal of Struc. Engineering, ASCE, Vol. 112, No.7, July, 1986, pp.1573-1588.
- [111] Gerstle, K.H., and Cook, N.E., 'Practical Analysis of Flexibly Connected Building Frames', Personal Communication.
- [112] Gibbons, C., 'The Strength of Biaxially Loaded Beam-Column in Flexibly Connected Steel Frames', Ph.D. Thesis, Vol. 1, Department of Civil & Structural Engineering, The University of Sheffield, December, 1990.
- [113] Zoetemaier, P., 'Influence of Joint Characteristics on Structural Response of Frames', Structural Connections: Stability and Strength, ed. by Narayanan, R., Elsevier Applied Science, London, 1989, pp. 121-152.
- [114] Harvard Graphics, Software Publishing Corporation, USA, 1990.
- [115] McCormick, M.M., 'Standard Connections Manual', BHP Melb. Res. Lab. Report. MRL. 39/1, March, 1974.

- [116] Joint Committee of WRC and ASCE, Plastic Design in Steel – A Guide and Commentary, 2nd ed. ASCE Manuals and Reports on Engineering Practice No.41, New York, 1971.
- [117] Baker, J.F., The Steel Skeleton Vol. 1 – Elastic Behaviour and Design, Cambridge University Press, 1959.
- [118] Julian, O.G., and Lawrence, L.S., ‘Notes on J and L Nomograms for Determination of Effective Lengths’, Unpublished Report.
- [119] Bleich, F., Buckling Strength of Metal Structures, Engineering Soc. Monograph, McGraw-Hill, New York, 1952.
- [120] Bijlaard, F.S.K., ‘Requirement for Welded and Bolted Beam-to-Column Connections in Non-Sway Frames’, Joints in Structural Steelwork, ed. by Howlett, J.H., Jenkins, W.H., Stainsby, R., London, Pentech Press, 1981, pp. 2.119-2.137

Appendix A

Additional Details of Comparisons with SUF Tests

Following the presentation of the comparison of the predicted response from the present program with the Sheffield University Frame (SUF) test results some additional information which has been referred to in chapter 4 is given in this appendix.

Scan No.	Total Load per Beam (kN)				
	B-2	B-3	B-4	B-5	B-6
1	0.0	0.0	0.0	0.0	0.0
2	8.72	8.01	8.78	8.82	8.81
3	18.88	18.09	19.08	19.50	19.60
4	29.02	28.21	29.29	30.17	30.35
5	39.18	38.39	39.52	40.86	40.89
6	52.36	51.60	52.77	54.71	54.37
7	59.51	58.76	59.93	54.69	61.63
8	73.93	73.24	74.46	54.68	76.36
9	79.317	78.64	79.84	54.7	81.81
10	90.02	89.36	90.61	54.69	92.70
11	100.73	100.02	101.34	54.68	103.54
12	117.0	116.21	117.70	54.71	119.98

Table A.1 Loading history in the beams of the test SUF1 [32].

Scan No.	Total Load per Beam (kN)					
	B-1	B-2	B-3	B-4	B-5	B-6
1	0.0	0.0	0.0	0.0	0.0	0.0
2	9.33	8.53	8.60	8.63	8.91	8.58
3	19.91	18.70	18.74	18.81	19.62	19.11
4	30.47	28.88	28.91	29.04	30.32	29.69
5	41.02	39.05	39.07	39.26	41.01	40.09
6	54.66	52.26	52.26	52.51	54.87	53.53
7	62.08	59.49	59.49	59.75	54.93	60.81
8	77.00	73.97	73.94	74.27	54.90	75.45
9	82.5	79.37	79.36	79.63	54.9	80.87
10	93.58	90.10	90.05	90.46	54.89	91.74
11	104.58	100.85	100.69	101.28	54.89	102.57
12	121.31	117.13	116.81	117.61	54.88	118.93

Table A.2 Loading history in the beams of the test SUF2 [32].

Step No.	Total Load per Beam (kN)					
	B-1	B-2	B-3	B-4	B-5	B-6
1	0.0	0.0	0.0	0.0	0.0	0.0
2	9.0	9.0	9.0	9.0	9.0	9.0
3	18.0	18.0	18.0	18.0	18.0	18.0
4	27.0	27.0	27.0	27.0	27.0	27.0
5	36.0	36.0	36.0	36.0	36.0	36.0
6	45.0	45.0	45.0	45.0	45.0	45.0
7	54.0	54.0	54.0	54.0	54.0	54.0
8	61.50	61.5	61.5	61.5	54.0	61.5
9	69.0	69.0	69.0	69.0	54.0	69.0
10	76.5	76.5	76.5	76.5	54.0	76.5
11	84.0	84.0	84.0	84.0	54.0	84.0
12	91.50	91.5	91.5	91.5	54.0	91.5
13	99.0	99.0	99.0	99.0	54.0	99.0
14	103.5	103.5	103.5	103.5	54.0	103.5
15	108.0	108.0	108.0	108.0	54.0	108.0
16	112.5	112.5	112.5	112.5	54.0	112.5
17	117.0	117.0	117.0	117.0	54.0	117.0

Table A.3 Loading history in the beams of the analytical models of SUF1 and SUF2 (B-1 is only for SUF2).

Member Desig.	Specmn. ref.	D mm	B mm	T_w mm	T_f mm	A cm^2	I_x cm^4	I_y cm^4
Colm.	C13	153.31	156.45	6.47	6.95	31.38	1339.4	445.5
	C14	153.32	156.45	6.52	6.89	31.27	1331.9	441.6
	C15	153.03	156.58	6.25	6.89	30.89	1321.3	442.7
	C16	153.01	155.94	6.10	6.65	29.87	1277.9	422.1
	C17	153.91	154.33	5.97	6.70	29.68	1287.0	412.3
	C18	153.62	156.58	6.68	6.86	31.44	1337.8	440.8
Beam	B17	254.30	103.87	6.39	6.84	30.22	3001.8	129.0
	B18	254.25	103.95	6.40	6.83	30.24	3000.5	129.1
	B19	254.53	103.78	6.01	6.80	29.23	2950.5	127.9
	B21	254.20	103.61	6.04	6.80	29.26	2941.8	127.2
	B22	254.70	103.47	6.16	6.77	29.50	2957.5	126.2
	B23	254.50	103.87	6.18	6.91	29.87	3002.5	130.3
	B24	254.50	104.40	6.19	6.91	29.97	3014.9	132.3
	B25	254.50	103.90	6.24	6.90	30.00	3007.3	130.2
	B26	254.20	103.34	6.15	6.80	29.49	2948.9	126.3
	B27	251.10	103.29	5.89	6.73	28.72	2895.4	124.8
	B28	254.20	102.98	6.03	6.76	29.07	2916.3	124.2

Table A.4 Sectional properties of the members of the test frames [32].

Member Desig.	Specmn ref.	Static yield stress (N/mm^2)	Stub column test results
Colm.	C13A	269.43	$\sigma_y=295N/mm^2$ $E=277kN/mm^2$
	C13B	243.66	
	C13C	222.42	
	C14A	268.33	$\sigma_y=295N/mm^2$ $E=222kN/mm^2$
	C14B	255.13	
	C14C	266.50	
	C15A	271.28	$\sigma_y=300N/mm^2$ $E=210kN/mm^2$
	C15B	261.01	
	C15C	254.56	
	C16A	294.72	$\sigma_y=304N/mm^2$ $E=202kN/mm^2$
	C16C	302.78	
	C17A	288.86	$\sigma_y=300/mm^2$ $E=207kN/mm^2$
	C17C	297.84	
	C18A	278.71	
	C18B	277.43	
Beam	B17A	280.60	
	B17B	259.53	
	B17C	262.74	
	B18A	283.01	
	B18B	258.54	
	B18C	260.75	
	B19B	269.25	
	B19C	269.30	

Table A.5 Material properties of the members of the test frames [32].

Member Desig.	Specmn ref.	Static yield stress (N/mm^2)	Stub column test results
	B20A	283.37	
	B20B	266.42	
	B20C	264.60	
	B21B	272.63	
	B21C	266.30	
	B22A	286.85	
	B22B	244.21	
	B22C	270.63	
	B23A	311.15	
	B23B	287.26	
	B23C	287.73	
	B24A	313.34	
	B24B	289.03	
	B24C	298.57	
	B25A	311.78	
	B25B	282.96	
	B25C	293.23	
	B26A	291.44	
	B26B	279.07	
	B26C	292.03	
	B27A	286.96	
	B27B	286.29	
	B27C	287.38	
	B28A	289.43	
	B28B	276.62	
	B28C	297.44	

Table A.5 Material properties of the members of the test frames (continued from previous page).

Appendix B

Worked Design Examples

A simplified design approach for non-sway semi-rigid frames have been presented in chapter 7. The approach uses a secant representation of the connection behaviour based on beam-line at the appropriate load level. In this appendix 4 examples are worked out for two different frame configuration with two different connection types and two different loading conditions.

Design Example 1

Given the structure of figure B.1

Load $P=50$ kN each acting at the quarter points of each beam.

Connections are all of type B, whose moment-rotation response is as shown in figure 7.16

$$\frac{EI_b}{L} = 11,6865 \text{ kN} - \text{cm/rad.}$$

$$\frac{EI_c}{h} = 6,4842 \text{ kN} - \text{cm/rad.}$$

$k_j = 54674kN - cm/rad$ (secant stiffness by beam-line at the specified load)

Top Floor

$$\begin{aligned}
 k_b &= \frac{3EI_b}{L} & k_c &= \frac{6EI_c}{h} \\
 M_E^e &= \frac{M^F}{\left(1 + \frac{k_b}{k_c} + \frac{k_b}{k_j}\right)} \\
 &= \frac{46.85 \times 1.5}{8.31} \\
 &= 8.45kN - m
 \end{aligned}$$

Intermediate Floors

$$\begin{aligned}
 k_b &= \frac{3EI_b}{L} & k_c &= \frac{12EI_c}{h} \\
 M_E^e &= \frac{70.3}{7.86} \\
 &= 8.94kN - m
 \end{aligned}$$

The beam centre moment can be obtained from simple statics and the column moments are obtained as sum of the beam end moment and the moment due to the beam end shear acting along the flange of the column (i.e. with $D/2$ eccentricity from the column centre-line, D being the column depth). The moment at the fixed base of the column can be approximately taken as one half of the value of the moment at the top end of the same column. The results of this approxiamte method are compared with that of the rigorous analysis in figure B.2

Design Example 2

The structure of figure B.1 but with storey heights of 3.5 m is subjected to uniformly distributed load of 19.2 kN/m.

$$\frac{EI_b}{L} = 116865 \text{ kN} - \text{cm/rad}$$

$$\frac{EI_c}{h} = 74106 \text{ kN} - \text{cm/rad}$$

$$k_j = 66071.0 \text{ kN} - \text{cm/rad}$$

Top Floor

$$\begin{aligned} k_b &= \frac{3EI_b}{L} & k_c &= \frac{6EI_c}{h} \\ M_E^e &= \frac{M^F}{1 + \frac{k_b}{k_c} + \frac{k_b}{k_j}} \\ &= \frac{60}{7.09} \\ &= 8.46 \text{ kN} - \text{m} \end{aligned}$$

Intermediate Floors

$$\begin{aligned} k_b &= \frac{3EI_b}{L} & k_c &= \frac{12EI_c}{h} \\ M_E^e &= \frac{60.0}{6.7} \\ &= 8.41 \text{ kN} - \text{m} \end{aligned}$$

Results of this example are again compared with those obtained from the rigorous analysis in figure B.3.

Design Example 3

The structure of figure B.4 is 50 kN concentrated load at the quarter points of each beam. The connections are all of type C (see figure 7.16).

$$\frac{EI_b}{L} = 116865 \text{ kN} - \text{cm/rad}$$

$$\frac{EI_c}{h} = 74106 \text{ kN} - \text{cm/rad}$$

$$k_j = 150122.9 \text{ kN} - \text{cm/rad}$$

Top Floor

External End:

$$k_b = \frac{2EI_b}{L} \quad k_c = \frac{6EI_c}{h}$$

$$M_E^e = \frac{M^F}{1 + \frac{k_b}{k_c} + \frac{k_b}{k_j}}$$

$$= \frac{46.85}{3.08}$$

$$= 15.21 \text{ kN} - \text{m}$$

Internal End:

$$k_b = \frac{3EI_b}{L} \quad k_c = \frac{6EI_c}{h}$$

$$M_E^i = \frac{M^F}{1 + \frac{k_b}{k_c} + \frac{k_b}{k_j}}$$

$$= \frac{70.3}{4.12}$$

$$= 17.0 \text{ kN} - \text{m}$$

Intermediate Floors

External End:

$$\begin{aligned}
 k_b &= \frac{2EI_b}{L} & k_c &= \frac{12EI_c}{h} \\
 M_E^c &= \frac{46.85}{2.82} \\
 &= 16.3kN - m
 \end{aligned}$$

Internal End:

$$\begin{aligned}
 k_b &= \frac{3EI_b}{L} & k_c &= \frac{12EI_c}{h} \\
 M_E^i &= \frac{M^F}{1 + \frac{k_b}{k_c} + \frac{k_b}{k_j}} \\
 &= \frac{70.3}{3.73} \\
 &= 18.85kN - m
 \end{aligned}$$

Moments at other beam locations are found by statics and column moments are calculated by as per example 1. Results of this example are shown in figure B.5 where it has been compared with those obtained from the rigorous analysis.

Design Example 4

The same structure of example 3 is subjected to uniformly distributed load of 21kN/m.

$$\frac{EI_c}{h} = 74106kN - cm/rad$$

$$\frac{EI_b}{L} = 116865kN - cm/rad$$

$$k_j = 167200kN - cm/rad$$

Top Floor

External End:

$$\begin{aligned}
 k_b &= \frac{2EI_b}{L} & k_c &= \frac{6EI_c}{h} \\
 M_E^e &= \frac{M^F}{1 + \frac{k_b}{k_c} + \frac{k_b}{k_j}} \\
 &= \frac{41.13}{2.92} \\
 &= 14.0kN - m
 \end{aligned}$$

Internal End:

$$\begin{aligned}
 k_b &= \frac{3EI_b}{L} & k_c &= \frac{6EI_c}{h} \\
 M_E^i &= \frac{M^F}{1 + \frac{k_b}{k_c} + \frac{k_b}{k_j}} \\
 &= \frac{61.7}{3.88} \\
 &= 15.90kN - m
 \end{aligned}$$

Intermediate Floors

External End:

$$\begin{aligned}
 k_b &= \frac{2EI_b}{L} & k_c &= \frac{12EI_c}{h} \\
 M_E^e &= \frac{41.30}{2.66} \\
 &= 15.46kN - m
 \end{aligned}$$

Internal End:

$$k_b = \frac{3EI_b}{L} \quad k_c = \frac{12EI_c}{h}$$

$$\begin{aligned}M_E^i &= \frac{M^F}{1 + \frac{k_b}{k_c} + \frac{k_b}{k_j}} \\&= \frac{61.7}{3.49} \\&= 17.68kN - m\end{aligned}$$

The bending moments for this example are shown in figure B.6 where they have been compared with those obtained from the rigorous analysis.

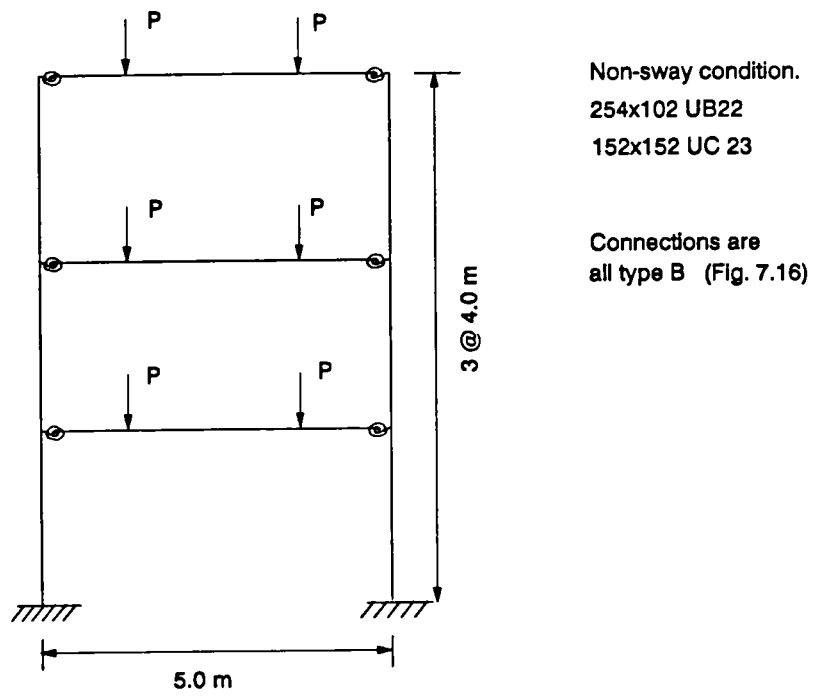


Figure B.1 Frame considered for example 1.

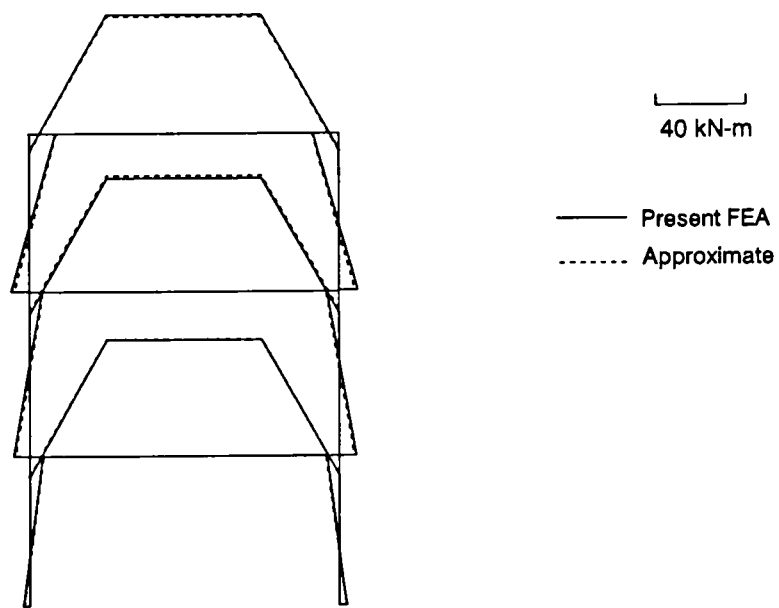


Figure B.2 Bending moment diagram for example 1.

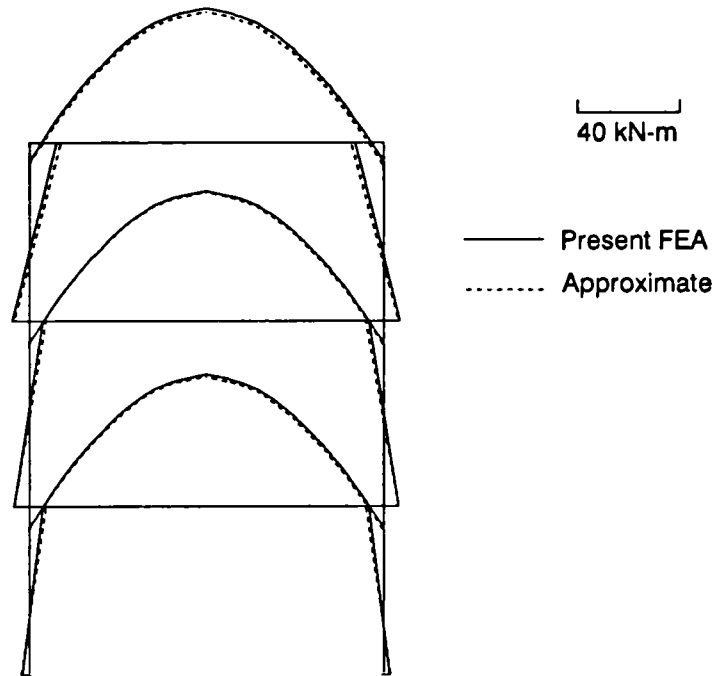


Figure B.3 Bending moment diagram for example 2.

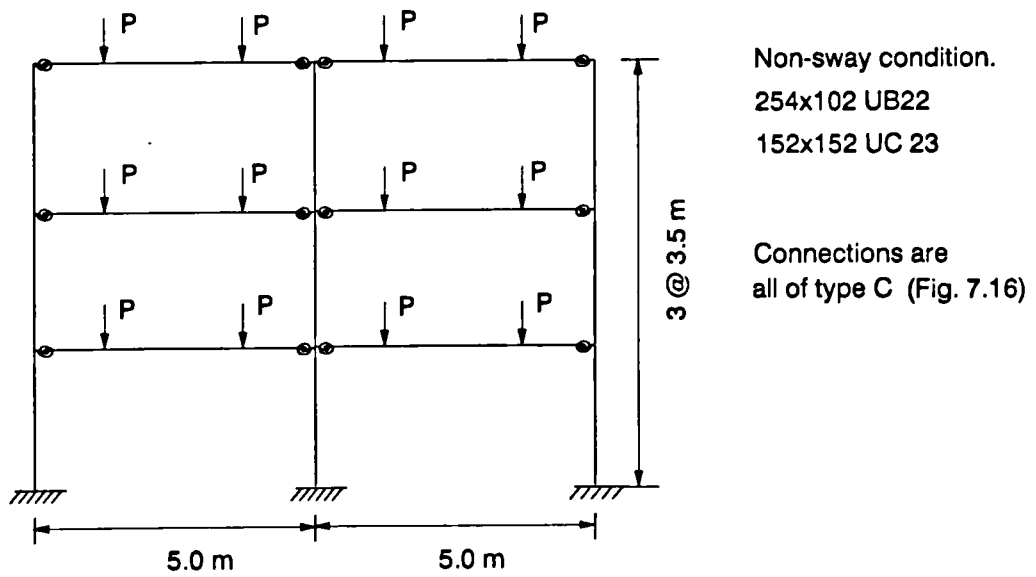


Figure B.4 Frame considered for example 3.

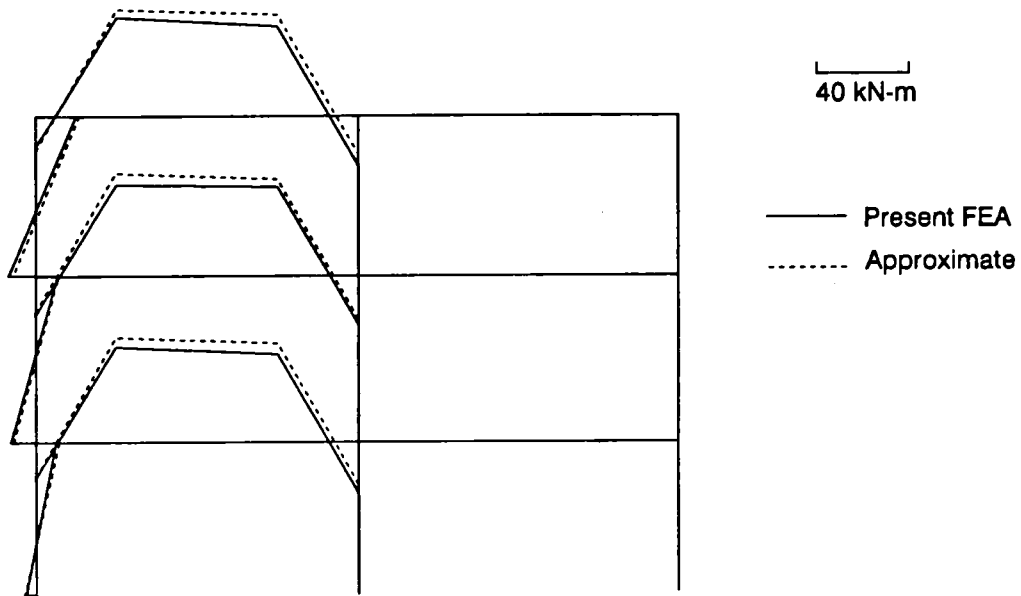


Figure B.5 Bending moment diagram for example 3.

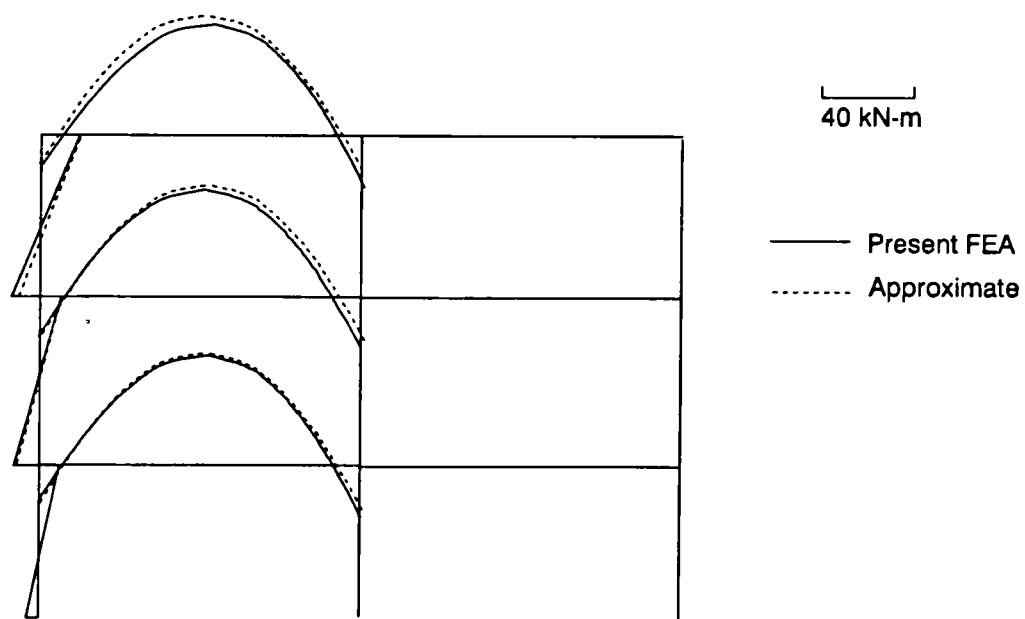


Figure B.6 Bending moment diagram for example 4.